William & Mary
CHARTERED 1693

W&M ScholarWorks

Dissertations, Theses, and Masters Projects

Theses, Dissertations, & Master Projects

2023

Empirical Valuation Of Primary And Alternative Nursery Habitats For The Blue Crab Callinectes Sapidus In Chesapeake Bay

Alexander C. Hyman
William & Mary - Virginia Institute of Marine Science, achyman@ufl.edu

Follow this and additional works at: https://scholarworks.wm.edu/etd

 Part of the Aquaculture and Fisheries Commons, and the Ecology and Evolutionary Biology Commons

Recommended Citation

Hyman, Alexander C., "Empirical Valuation Of Primary And Alternative Nursery Habitats For The Blue Crab Callinectes Sapidus In Chesapeake Bay" (2023). *Dissertations, Theses, and Masters Projects.* William & Mary. Paper 1697552696.
https://dx.doi.org/10.25773/v5-67a4-wq53

This Dissertation is brought to you for free and open access by the Theses, Dissertations, & Master Projects at W&M ScholarWorks. It has been accepted for inclusion in Dissertations, Theses, and Masters Projects by an authorized administrator of W&M ScholarWorks. For more information, please contact scholarworks@wm.edu.

Empirical valuation of primary and alternative nursery habitats for the blue crab *Callinectes sapidus* in Chesapeake Bay

---

A Dissertation

Presented to

The Faculty of the School of Marine Science

The College of William and Mary in Virginia

In Partial Fulfillment

of the Requirements for the Degree of

Doctor of Philosophy

---

by

A. Challen Hyman

August 2023

APPROVAL PAGE

This Dissertation is submitted in partial fulfillment of
the requirements for the degree of

Doctor of Philosophy

Alexander Challen Hyman

Approved by the Committee, August 2023

Romuald N. Lipcius, Ph.D.
Committee Chairman/Adviser

Grace S. Chiu, Ph.D.
Adviser

Mary Fabrizio, Ph.D.

Christopher Patrick, Ph.D.

David Eggleston, Ph.D.
North Carolina State University
Raleigh, North Carolina

TABLE OF CONTENTS

ACKNOWLEDGMENTS

This dissertation could not have been possible without the dedication of several amazing individuals. First and foremost, I extend my immense gratitude to Drs. Grace S. Chiu and Romuald N. Lipcius. Dr. Chiu's tremendous patience, dedication, and devotion to her students has been unparalleled in my experience in academia, especially in the final months of this endeavor. On more than one occasion, Dr. Chiu dedicated her time and energy to creating entire classes, both formal and informal, to advance my quantitative skill sets. I will be forever grateful for the quality of education she has provided me. I similarly thank Dr. Lipcius for his immense insight on blue crab biology and ecology, his willingness to expose me to numerous professional development experiences, and the high degree of confidence and independence he confers to his students. Dr. Lipcius encourages his students to participate in a variety of activities usually reserved for more senior scientists, which has greatly expanded my professional network and lent me immense insight into the world beyond graduate school, for which I am similarly immensely grateful. I greatly appreciate the support of my committee, Drs. Mary Fabrizio, Christopher Patrick, and David Eggleston. Their insight and guidance have greatly improved the quality of this dissertation, and my development as a scientist. I also extend my immense gratitude to Dr. Jeff Shields, for his advice, recommendations, and experience.

The staff and students of the Marine Conservation Biology and Community Ecology laboratories (Mike Seebo, Katie Knick, Alison Smith, and Gabrielle Saluta, Shantelle Landry, Alex Schneider, Natalia Schoenberg, Jainita Patel, and Nihal Guennouni) were instrumental in the design, implementation, and sample processing of my field projects. They helped collect 1000s of samples for my dissertation during my time at VIMS, and this work quite literally would not have been possible without them. I would also like to thank Cole Miller, Alex Pomroy, and Jiakun "Andy" Li for their help in the lab and field. Cindy Forrester, Linda Schaffner, and Jennifer Hay also deserve the immense gratitude from any student graduating from VIMS for their vigilance in keeping students (such as myself) on track throughout our time as students.

As Isaac Newton once wrote, "If I have seen further, it is by standing on the shoulders of giants". The giant in this case is Gina Ralph, a brilliant former student of the Marine Conservation Biology Lab whose work was instrumental in guiding my own questions on juvenile blue crab ecology. Without her diligent, earlier work, or her advice during my time as a student, my own work would have surely floundered.

Most importantly, none of this would have been possible without my friends and family. First, my parents, Mark Hyman and Cheryl Flax-Hyman, and little sister McKenna Hyman never once stopped believing in and encouraging me throughout these last few years. I am also grateful to my non-VIMS family in Williamsburg: Eli Knittle; Victoria Fong; Sayed Muhammed Wajih Hassan; and Anna Caputo, as well as my close friends outside Virginia: Douglas Brown, Mason Armstrong, Chet Seaman, Alli Cauvin, Crews Chambers, Chris Cerjan, Blake Wagner, Scott Steckroth, Ray Spradlin, and Joe Dunham for keeping me

laughing and in good spirits during the hardest periods of graduate school. I am also indebted to two amazing mentors, Dr.s Dana Stephens and Savanna Barry, for training me and guiding me prior to my time at VIMS. My experiences at VIMS were only complete because of my fellow graduate students. With this in mind, I sincerely thank Alex Smith, Michelle Woods, Kayla Martinez-Soto, Alex Marquardt, Kaitlyn O'Brien, Shannon Smith, and many other students and friends for keeping me sane throughout my time here.

Finally, I would like to acknowledge William & Mary Research Computing for providing computational resources and technical support that have contributed to the results reported within Chapter 1. URL: `https://www.wm.edu/it/rc`.

To my mother and father, Cheryl Flax-Hyman and Mark Hyman, who never stopped cheering for me, encouraging me, and challenging me to give my all. I am forever grateful for your love and guidance.

LIST OF TABLES

LIST OF FIGURES

ABSTRACT

The blue crab (*Callinectes sapidus*) is a commercially and ecologically important species found along the Atlantic coast of North and South America. These crustaceans play a critical role in coastal ecosystems, serving as both predators and prey in the food web. The blue crab supports a major fishery in Chesapeake Bay, where the species is a cultural icon. Juvenile blue crabs, the smallest and most vulnerable size classes of individuals, are reliant upon structurally complex habitats. Population dynamics of this species are therefore influenced by spatiotemporally fluctuating environmental variables, such as habitat availability. Understanding blue crab ecology is essential for managing their populations sustainably and maintaining the health of their habitats. The primary aim of this dissertation was to quantitatively evaluate the contributions of several widely distributed habitats to blue crab population dynamics in Chesapeake Bay. Empirical valuation of nursery habitat effects on blue crab population dynamics can (i) estimate the optimal extent of habitat required for the long-term sustainability of blue crab fisheries, (ii) quantify how changes in habitat extent will affect blue crab populations, such as alterations due to climate change, and (iii) inform ecosystem-based fisheries management (EBFM) decisions, as a complement to stock assessments. Here, I present four separate but interrelated studies examining habitat-specific demographic rates at multiple spatial and temporal scales. These studies involved a combination of survey data, mensurative and manipulative field experiments, and complex population dynamics models. Chapter 1 evaluates nursery habitat contributions to blue crab population dynamics by examining relationships between juvenile blue crab distributions and multiple environmental variables in three tributaries—the York, James, and Rappahannock rivers—at broad spatial (regional) and temporal (decadal) scales using fisheries-independent survey data and digitized GIS maps of habitat distributions. Chapter 2 examines fine-scale spatiotemporal (i.e., 10s of km^2 over biweekly intervals) variation and ontogenetic shifts in juvenile blue crab densities in salt marsh edge, seagrass, shallow detrital habitat, and unstructured habitat under a suite of physical and biological parameters in the York River. Chapter 3 expands on these findings to examine the mechanistic basis for ontogenetic habitat shifts by evaluating differential abundance and survival of juvenile blue crabs across three size classes in salt marsh edge, seagrass, and unstructured sand habitat, with specific attention to effects of refuge, turbidity, and postlarval supply. Finally, Chapter 4 integrates population-scale indices of abundance from two major fisheries-independent surveys with time-series of habitat data to assess the influence of seagrass species on blue crab population dynamics at the scale of Chesapeake Bay.

Empirical valuation of primary and alternative nursery habitats for the blue crab *Callinectes sapidus* in Chesapeake Bay

Chapter 1

Spatiotemporal modeling of nursery habitat using Bayesian inference: environmental drivers of juvenile blue crab abundance

Abstract

Nursery grounds are favorable for growth and survival of juvenile fish and crustaceans through abundant food resources and refugia, and enhance secondary production of populations. While small-scale studies remain important tools to assess nursery value of habitats, targeted applications that unify survey data over large spatiotemporal scales are vital to generalize inference of nursery function, identify highly productive regions, and inform management strategies. Using 21 years of GIS and spatiotemporally indexed field survey data on potential nursery habitats, we constructed five Bayesian models with

varying spatiotemporal dependence structures to infer nursery habitat value for juveniles of the blue crab C. sapidus within three tributaries in lower Chesapeake Bay. Out-of-sample predictions of juvenile counts from a fully nonseparable spatiotemporal model outperformed predictions from simpler models. Salt marsh surface area, turbidity, and their interaction showed the strongest associations (and positively) with abundance. Relative seagrass area, previously emphasized as the most valuable nursery in small spatial-scale studies, was not associated with abundance. Hence, we argue that salt marshes should be considered a key nursery habitat for blue crabs, even amidst extensive seagrass beds. Moreover, identification of nurseries should be based on investigations at broad spatiotemporal scales incorporating multiple potential nursery habitats, and on rigorously addressing spatiotemporal dependence.

1.1 Introduction

A key element of ecosystem-based fishery management (EBFM) is the incorporation of habitat (e.g., EFH, “Essential Fish Habitat”) into management, conservation and restoration decisions [139]. However, quantitative assessments of the production value of habitats have only recently been attempted [216, 188, 226, 16, 21]; see [102] for a review. In particular, nursery habitats can enhance growth and survival of juvenile fish and crustaceans in diverse marine and estuarine ecosystems [8, 67, 128, 140, 109, 143, 160] through the provision of food resources and refugia. Hence, linking nursery habitat quantity and quality to population dynamics and EBFM of exploited species has been emphasized [188, 216, 226, 16, 102, 21].

Unfortunately, quantification of habitat value has been uncommon due to the considerable logistical difficulties associated with field experiments [8]. Until recently, comparison of potential nurseries relied primarily on examination of specific habitat types (e.g., sea grass,

oyster reef, marsh) as single units disconnected from adjacent habitats [140]. However, estuaries are complex habitat mosaics that include physical, biotic, and chemical components interacting at multiple spatial and temporal scales [149], and as such, these connections must be considered. Operational definitions of nurseries must be expanded to consider multiple structured and unstructured habitat types, as well as environmental characteristics within a region [140]. Furthermore, inference on nursery habitat value is complicated in that habitat preferences of many marine and estuarine species change with ontogeny, such that early-life stages frequently inhabit different habitats than older juveniles or adults [89, 141, 44]. Quantitative assessments of nursery function and fisheries production must therefore move beyond comparisons between specific habitat types [140, 191, 109] and be considered within the context of ontogeny [103], especially for organisms with complex life cycles [103, 43, 44].

While ecological studies often quantify nursery function at fine temporal and spatial scales, few are conducted at the scales relevant to the population [208]. Small-scale studies on the importance of structured habitats as nurseries may not scale up to the population level. For example, high local juvenile density or survival in small-scale studies [8] may not translate to high secondary production in a population if per-unit-area productivity of a potential nursery habitat is negated by the small area of a habitat in the seascape [35, 140]. For robust evaluation of nursery habitats at sub-population or population scales, small-scale field studies should be complemented with analyses of large-scale field data, especially when informing decision-making within the context of EBFM.

The blue crab *Callinectes sapidus*, which supports valuable fisheries along the Western Atlantic and Gulf of Mexico coasts [144], is a model organism for quantifying value of structured habitats under spatially and temporally varying environmental characteristics. Like many exploited marine species, the blue crab utilizes a range of nursery habitats

and exhibits ontogenetic shifts in habitat utilization [154, 70, 103, 188, 44]. Postlarvae settle in structured habitats, such as seagrass, where they metamorphose to the first juvenile instar [120] and either remain or exhibit density-dependent secondary dispersal to alternative structured habitats [45, 46, 88]. After reaching 20-25 mm carapace width (CW), they emigrate to unstructured soft-bottom habitats [105, 186], but also continue to use structured habitats for foraging, molting, and mating [70, 103]. For the blue crab, [70] and [103] reviewed the extensive evidence for the value of specific nursery habitats, such as seagrass, using the definition of nursery habitat as areas with elevated per-unit-area density, survival and growth.

Two aspects of the blue crab's life history are particularly useful in quantifying value of nursery habitats. First, size-specific habitat use and dispersal patterns of the blue crab through ontogeny are well understood [103, 70]. Second, male and immature female blue crabs larger than 20 mm carapace width (CW) exhibit high site fidelity and low emigration rates during summer and fall at spatial scales less than a few kilometers [230, 36, 71, 86]. Hence, abundance of juvenile blue crabs larger than 20 mm CW can be used to identify areas of high productivity, and facilitate quantitative comparisons of the relative contribution of multiple nursery habitats in the seascape to the population.

Here, we exploited the differential habitat utilization of pre- and post-dispersal juvenile blue crabs to infer relative nursery value of various habitats associated with specific environmental characteristics. We constructed statistical spatiotemporal models to examine geographic heterogeneity in post-dispersal juvenile blue crab abundance and to infer variation in nursery habitat value within and across estuaries in lower Chesapeake Bay, Virginia. Specifically, we used temporal extensions of conditional autoregressive (CAR) spatial models to assess the effects of environmental factors on abundance of juvenile blue crabs at the tributary and regional scales simultaneously. Using local abundance of

post-dispersal sized (20-40 mm CW) juvenile blue crabs as an indicator for local production, our objectives were to 1) evaluate relationships between nursery habitat distribution and local productivity at regional scales ($\geq$ 100 km^2), and 2) identify geographic areas with consistently high abundance and productivity.

1.2 Study design

1.2.1 Study Area

The three large tributaries analyzed in this study–the James, York, and Rappahannock Rivers–discharge into the lower portion of western Chesapeake Bay and serve as nursery, foraging and spawning habitats for many marine and estuarine species (Fig. 1.1). The tributaries are partially mixed, coastal plain subestuaries with depths generally between 5 to 10 m along the axes, but with deeper portions ($>$20 m) near the mouths [196]. Each tributary contains a range of seagrass and salt marsh configurations. Seagrasses, primarily eelgrass *Zostera marina* and widgeon grass *Ruppia maritima*, vary from large, continuous meadows to areas with few small patches of variable shoot densities [77]. Salt marshes, dominated by smooth cordgrass *Spartina alterniflora*, span extensive sections of the shorelines of each tributary, although areal coverage of marsh patches varies spatially among and within individual tributaries.

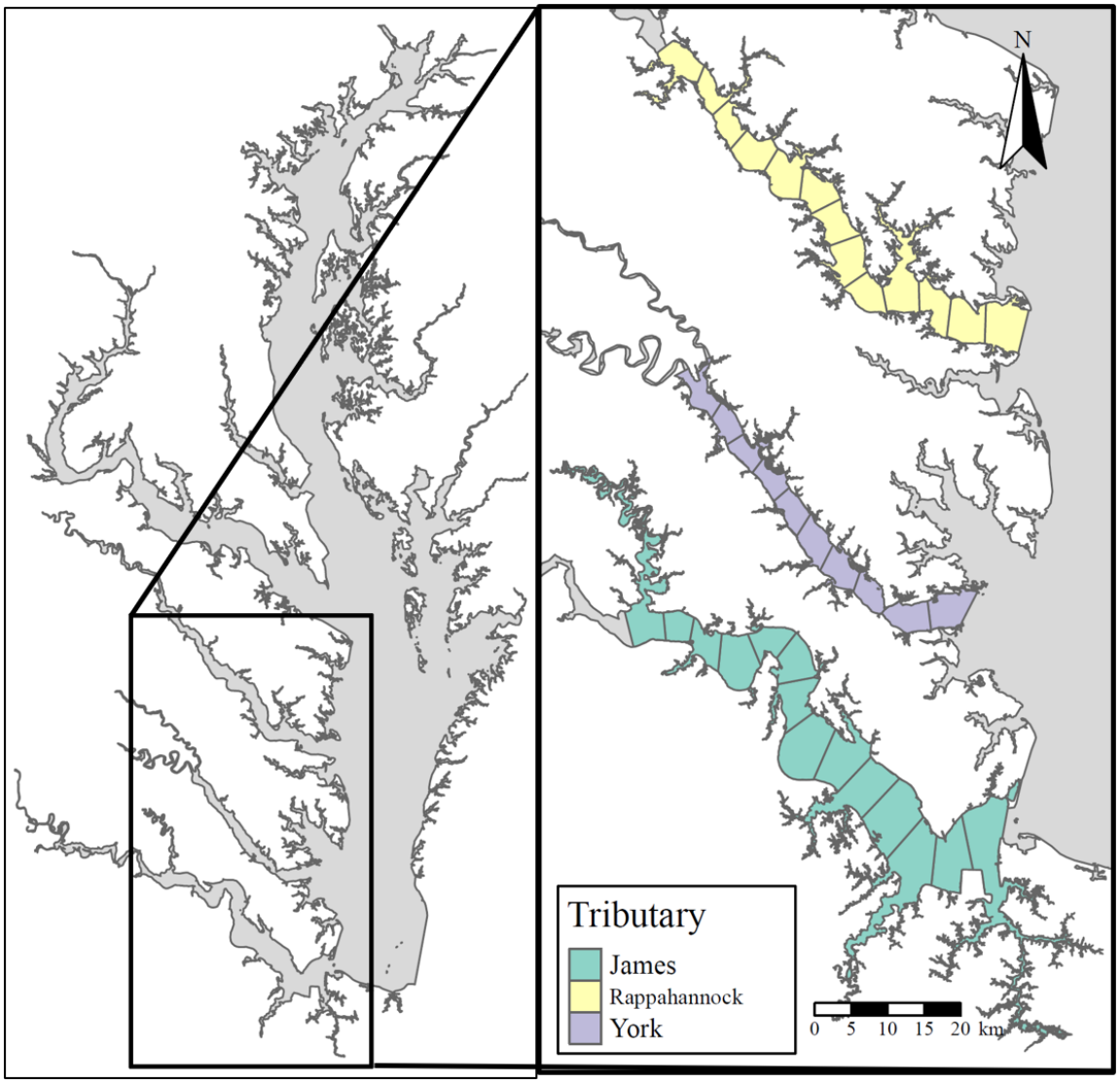

Figure 1.1: Map of Rappahannock, James, and York rivers with tributary sections (areal units) superimposed. See Section 1.2.3 and Appendix A.2 for the definition of areal units within tributaries.

1.2.2 Predictors of Abundance and Productivity

Seven environmental variables (herein, predictors) were initially considered as potential determinants of local productivity for juvenile blue crabs, and are described below. Additional

details on variable definition and associated regression coefficients are in Section 1.2.3, Table 1.1, and Appendix A.1. We did not include salinity as a predictor due to substantial collinearity with turbidity and location along the river axis.

Table 1.1: Descriptions of predictors used in all initial models

Predictor	**Regression** Coefficient	**Description**
—	β_0	(Intercept of model)
Tow distance (log)	O	Offset term relating juvenile blue crab abundance to surface area river sections
Turbidity	$\beta_{\text{Turbidity}}$	Mean water cloudiness measured as the negative value of the Secchi disk depth (m) for the kth river section in the tth year
Seagrass (relative area)	β_{Seagrass}	$\frac{(\text{SAV area})_{kt}}{(\text{Section area})_k}$ = Total area of SAV in section k at time t divided by the area of section k
Marsh (relative area)	β_{Marsh}	$\frac{(\text{Marsh area})_{kt}}{(\text{Section area})_k}$ = Total area of salt marsh in section k at time t divided by the area of section k
Marsh $\times$ Turbidity	$\beta_{\text{Marsh}\times\text{Turbidity}}$	Interaction term between marsh relative area and turbidity.
Predator abundance (log-count)	β_{Predator}	Log-transformed counts, in section k at time t, of predator abundance between 100 and 300 mm in total length (fish) or CW (adult blue crabs) from the 10 most common predators of small juvenile blue crabs (see Table 1.2)
Management (post 2008)	$\beta_{\text{Management}}$	Effect of Chesapeake Bay blue crab management changes enacted in 2008
Rappahannock	$\beta_{\text{Rappahannock}}$	Tributary-specific effect of the Rappahannock River relative to the James River (baseline)
York	β_{York}	Tributary-specific effect of the York River relative to the James River (baseline)

Seagrass

Historically, emphasis was placed on seagrass meadows as the preferred nursery for small (i.e., $<$30 mm CW) juvenile blue crabs [154, 159, 77, 171] due to the high densities of juvenile crabs and settlement of postlarvae [148, 222, 215] in seagrass meadows over alternative structured and unstructured substrates [154, 105]. Effects of seagrass area

are likely influenced by the spatial extent of the river section. Thus, we defined a relative seagrass area metric by dividing the area of seagrass cover within each river section in each year by the area of that section to yield a relative seagrass area metric (i.e., percent area covered, PAC). Hereafter, we refer to the spatiotemporal unit representing a given river section in each year as a section-year.

Marsh

Salt marshes may serve as nursery habitat for juvenile blue crabs, particularly in locations where seagrass is absent or declining [84, 12, 86]. In the Gulf of Mexico, juvenile blue crab abundance is high in both seagrass and salt marsh habitats [205, 175, 66]. In tethering experiments, survival of juveniles was comparable between the two habitats, both of which had higher survival than in unstructured habitat [189]. Similar to seagrass, we defined a relative marsh area metric for each section-year.

Turbidity

Strong turbidity gradients exist in each tributary [142, 93, 98, 48]. Dissolved and particulate suspended solids are imported from surrounding watersheds to tributaries via terrestrial runoff. In contrast, seawater from estuarine mouths is relatively clear. Divergence in turbidity is apparent when comparing marine (i.e., polyhaline) to mesohaline and oligohaline, highly turbid upriver areas, where water clarity is frequently driven by allochthonous inputs and sediments from the surrounding watershed. The estuarine turbidity maximum (ETM), a region of elevated suspended solid concentrations and reduced light availability, occurs near the limit of salt intrusion in each tributary, where turbidity peaks [181].

Turbidity may provide juvenile blue crabs with protection from visual predators [32, 113] and from cannibalism by larger congeners [146] through a reduction in light intensity.

Upriver unstructured habitat is turbid, whereas similar habitat downriver has lower turbidity, such that upriver unstructured habitat can also serve as an effective nursery [105, 186]. Hence, mean turbidity per section-year was included as a continuous covariate.

Marsh-Turbidity Interaction

Whereas seagrass meadows do not occur in high-turbidity areas due to light requirements, extensive salt marshes are present in both high- and low-turbidity regions of the tributaries. As such, turbidity may modify the effectiveness of structured salt marsh habitat as nursery for juvenile crabs by decreasing predatory foraging efficiency through both low visibility (turbidity) and structural impediments (marsh grass). For this reason, the interaction between marsh area and turbidity was included in the analysis. We recognize that there may be confounding variables with turbidity, such as location along the upriver-downriver gradient and resources such as prey availability. Hence, our interpretations will be limited to a association between crab abundance and turbidity.

Predation

Although physical refuges can reduce predator foraging success, predator density may also determine survival [130]. For example, high abundances of juvenile blue crabs in low salinity regions have been linked to low predator abundance in those regions [165]. Predators for each section-year were determined from the literature and abundances of the 10 most important predators of small juvenile blue crabs, including larger conspecifics (Table 1.2), were obtained from the Virginia Institute of Marine Science Juvenile Fish and Blue Crab Trawl Survey (hereafter VIMS Trawl Survey) [206]. Predator densities were estimated for individuals between 100 and 300 mm in total fish length (or CW for blue crabs), with the lower bound defining the smallest size able to capture and consume small juvenile

blue crabs [182], and the upper bound representing animals which would be expected to consume smaller juvenile blue crabs.

Table 1.2: List of predator species considered in predation abundance variable

Common name	Species name	Source
Blue crab (adult)	*Callinectes sapidus*	[70, 14]
Striped Bass	*Morone saxatilis*	[70, 103, 15]
Red Drum	*Sciaenops ocellatus*	[70, 61, 15]
Silver Perch	*Bairdiella chrysoura*	[61]
Weakfish	*Cynoscion regalis*	[15]
Atlantic Croaker	*Micropogonias undulates*	[61, 15]
Northern Puffer	*Sphoeroides maculatus*	[14]
Striped Burrfish	*Chilomycterus schoepfi*	[14]
Blue Catfish	*Ictalurus furcatus*	[184]
Oyster Toadfish	*Opsanus tau*	[14]

Tributary

The three tributaries in our study vary in geography, morphology, and hydrology. Average discharge is relatively high in the James River (194 $m^3\ s^{-1}$) and lower in the Rappahannock and York Rivers (47 m $m^3\ s^{-1}$ and 31 $m^3\ s^{-1}$, respectively) [29]. Additionally, the three tributaries are positioned along a latitudinal gradient in Chesapeake Bay, with the Rappahannock River being northernmost, the James River southernmost and closest to the Bay mouth, and the York River intermediate. Finally, these tributaries vary substantially in surface area [29]. The James River is the largest at 513.0 km^2, the York River is the smallest at 162.5 km^2, and the Rappahannock River is intermediate at 307.5 km^2 [196]. Variation in these physical characteristics may affect blue crab abundance and thus, tributary was considered as a predictor in the model.

Management

Early in the 1990s the blue crab spawning stock in Chesapeake Bay declined by 80% [106], and average annual female abundance dropped 50% from 172 million crabs in 1989-1993 to 86 million crabs in 1994-2007 [117]. As a consequence, larval abundance and postlarval recruitment were lower by approximately 1 order of magnitude [106]. The sharp decline resulted in a range of management and recovery actions implemented from 2001 through 2008, including establishment of an extensive spawning sanctuary that encompassed about 75% of the spawning grounds in Chesapeake Bay [104, 107, 94]. Most notably, severe fishery reductions were implemented in 2008 by the three management agencies, which included the Virginia Marine Resources Commission, Potomac River Fisheries Commission, and Maryland Department of Natural Resources (MDNR), leading to a 34% reduction in female landings across Maryland and Virginia [117] and triggering population recovery in subsequent years. Since 2008, annual female abundance rebounded to pre-1994 levels, and stabilized at an average of 161 million crabs during 2008-2019 [117]. We included management status (before and after 2008, with 2009 being the first recruitment period after management change) as a categorical predictor to capture potential effects on juvenile blue crab abundance due to increases in female blue crab abundance in response to regulatory changes that were implemented in 2008. However, we also realize that the effects of management may be interactive with those of other factors (e.g., management may increase abundance in marsh habitats but not in unvegetated areas), and thus we interpret the results for the additive effect of management with caution.

1.2.3 Sampling and Data Processing

Juvenile blue crab and predator abundance data were obtained from the fisheries-independent VIMS Trawl Survey [206]. Beginning in March 1996 and continuing to the present, stratified-

random and fixed-site sampling has been conducted monthly in the James, York, and Rappahannock Rivers using consistent gear, research vessel, and methodology. Secchi disk measurements, a proxy for turbidity, are collected immediately following each trawl tow. This sampling design provided a monthly time series of juvenile blue crab and predator catch data as well as water quality data (temperature, turbidity) in each tributary. The maximum size of predators (300 mm fish total length or crab carapace width) represent the sizes that are reliably captured by the VIMS Trawl Survey [206].

GIS data on submersed aquatic vegetation (SAV) and salt marsh distributions were used as explanatory habitat variables. SAV polygons digitized from annual aerial photographs were obtained from the VIMS SAV program, while polygons of salt marsh distributions were obtained from the Shoreline and Tidal Marsh Inventory dataset from the VIMS Center for Coastal Resource Management.

The spatiotemporally varying samples from the VIMS Trawl Survey were aggregated to annually indexed areal units for the period 1996 to 2017. We limited the months considered for each year to April–December to avoid bias in crab distributions associated with winter dormancy [70]. First, each tributary was divided along its axis into sections approximately five km in length resulting in $K = K_1 + K_2 + K_3 = 37$ total areal units, or sections ($K_1 = 14$ for James, $K_2 = 13$ for Rappahannock, and $K_3 = 10$ for York), which excluded one polygon at the mouth of the James representing the first five km because no samples were collected in this region by the trawl survey (Fig. 1.1). Areal unit definitions are discussed in Appendix A.2. For each kth areal unit within each tth year (i.e., (k, t)th section-year), blue crab catch and tow distance (m) information were summed to derive values of total abundance and total tow distance. Secchi disk depth and $\log_e$-transformed predator abundance values were averaged within each (k, t). Finally, marsh and seagrass area within each section-year divided by the total area of each section were used as a relative habitat area metric for

each structurally complex habitat. The aggregated trawl data resulted in 814 section-year observations. All but one of the 814 section-years contained trawl tows, and the exception was from 2017. This aggregation resulted in values of relevant response and predictor variables for each river section k in each year t.

1.3 Model Development and Specification

The spatiotemporal structure of the data in this study required complex modeling because sampling sites did not represent independent replicates. The study region covered three tributaries, each comprised of a set of $k = 1, ..., K_g$ non-overlapping areal units (sections), $g = 1, 2, 3$, and data were recorded for each section for $t = 1, ..., T$ consecutive time periods ($T = 21$ years over 1996–2016, due to the 2017 data being withheld for out-of-sample cross validation; see Section 4.2.7). A multilevel (hierarchical) spatiotemporal Bayesian model framework for discrete responses (count data) was used to evaluate the effects of predictors while simultaneously accounting for spatiotemporal dependence. We used temporal extensions of conditional autoregressive (CAR) models [220] to examine spatiotemporal patterns in the abundance of juvenile blue crabs among potential nursery areas. To determine the necessary model complexity to capture spatial and temporal patterns in juvenile blue crab abundance, we constructed five model variants with various spatiotemporal dependence structures. Specifically, we compared models that i) ignored spatial and temporal autocorrelation, ii) considered exclusively spatial autocorrelation, iii) considered separable (i.e., non-interacting) spatial and temporal autocorrelation (split into (3a) and (3b)) and iv) considered fully non-separable (i.e., interacting) spatiotemporal autocorrelation.

1.3.1 Model 1

The simplest model considered in this study was a Poisson generalized linear mixed-effects model with a random effect for all river sections $k = 1, ..., K$:

$$
\begin{aligned}
Y_{kt}|\mu_{kt} &\sim \text{Pois}(\mu_{kt}) \\
\ln(\mu_{kt}) &= \sum_{i=0}^{p} x_{kti}\beta_i + O_{kt} + \theta_k \\
\theta_k|\sigma^2_\theta &\sim N(0, \sigma^2_\theta) \\
\beta_i &\sim N(0, 100) \\
\sigma^2_\theta &\sim \text{inverse-Gamma}(1, 1)
\end{aligned}
\tag{1.1}
$$

The response data, juvenile crab counts, are denoted by Y_{kt}, for the kth section in year t. Tow distances, known offsets that have been log-transformed, are denoted by O_{kt}. An offset variable is one that is treated like a regression covariate whose slope parameter is fixed at 1. Offset variables are most often used to scale the modeling of the mean structure when the response variable is expected to be proportional to the offset term. A vector of predictors (see Table 1.1), $x_{kt} = (1, x_{kt1}, ..., x_{ktp})$ is denoted for each (k, t), and includes $x_{kt0} = 1$ which corresponds to the intercept term. Model 1 included an independent and identically distributed (i.i.d.) random effect, θ_k. This parameter was normally distributed and accounted for section-specific variation only and did not consider spatial autocorrelation among neighboring sections or temporal autocorrelation within a given section through time. All fixed-effect regression coefficients were given a normal prior distribution with mean 0 and variance 100. The random-effect variance σ^2_θ was given an inverse-Gamma$(1, 1)$ hyperprior, which is reasonably diffuse to reflect the lack of information about the parameter.

1.3.2 Model 2

This model considered the effects of spatial autocorrelation among neighboring river sections through the substitution of i.i.d. θ_k with conditionally autoregressive (CAR) Φ_k [218]:

$$
\begin{aligned}
Y_{kt}|\mu_{kt} &\sim \text{Pois}(\mu_{kt}) \\
\ln(\mu_{kt}) &= \sum_{i=0}^{p} x_{kti}\beta_i + O_{kt} + \Phi_k \\
\Phi|\Sigma &\sim \text{MVN}(0, \Sigma) \\
\Sigma &= \sigma_\Phi^2 (D - \lambda W)^{-1} \\
\beta_i &\sim N(0, 100) \\
\lambda &\sim \text{U}(0, 1) \\
\sigma_\Phi^2 &\sim \text{inverse-Gamma}(1, 1)
\end{aligned}
\tag{1.2}
$$

where the joint probability distribution of $\Phi = (\Phi_1, ..., \Phi_K)$ is specified as a multivariate normal distribution with a mean vector of 0s and variance-covariance matrix Σ. The Σ matrix describes spatial correlation based on the neighborhood structure specified by a $K \times K$ adjacency matrix, W, and an autocorrelation parameter λ, which controls the degree of spatial autocorrelation among neighboring sections across the entire region of study. We employed a binary weighting scheme for W where $w_{k,k'} = 0$ for all (k, k') unless areal units $k \neq k'$ share a common border. The influence of neighboring sections on a given section was standardized by subtracting λW from D, a diagonal matrix where $D_{k,k}$ is the number of neighbors for section k. This specification effectively scaled spatial dependence by the number of neighbors for each section while avoiding model unidentifiability of the intrinsic CAR (ICAR) structure [23]. The parameter λ was constrained between 0 and 1 (hence,

non-negative) through a uniform prior. This spatial dependence structure was assumed to be homoscedastic through the variance parameter σ^2_Φ, again with an inverse-Gamma$(1,1)$ hyperprior. The regression coefficients were given the same prior distributions as before.

1.3.3 Model 3

Models 3a and 3b considered separable spatial and temporal dependence [220] by expanding on Model 2 through the addition of an autoregressive temporal autocorrelation structure of order 1, i.e., $AR(1)$, at two spatial resolutions. The model equations below for 3a and 3b hold for all k and t. Model 3a included an autocorrelated normally distributed error term η_t, with $\eta = (\eta_1, ..., \eta_T)$ and a global temporal autocorrelation parameter, ρ, and variance σ^2_η, where ρ is given a uniform prior distribution between 0 and 1, (again, non-negative) and the remaining model parameters are given the same prior distributions as before.

$$
\begin{aligned}
Y_{kt}|\mu_{kt} &\sim \text{Pois}(\mu_{kt}) \qquad (1.3a)\\
\ln(\mu_{kt}) &= \sum_{i=0}^{p} x_{kti}\beta_i + O_{kt} + \Phi_k + \eta_t\\
\Phi|\Sigma &\sim \text{MVN}(0, \Sigma)\\
\Sigma &= \sigma^2_\Phi (D - \lambda W)^{-1}\\
\eta_t|\rho, \eta_{t-1}, \sigma^2_\eta &\sim \text{N}(\rho\eta_{t-1}, \sigma^2_\eta) \quad \text{for all } t = 2, 3, ..., T\\
\beta_i &\sim N(0, 100)\\
\lambda, \rho &\sim \text{U}(0, 1)\\
\sigma^2_\Phi, \sigma^2_\eta &\sim \text{inverse-Gamma}(1, 1)
\end{aligned}
$$

In contrast, Model 3b stipulated tributary-specific temporal autocorrelation for $g = 1, 2, 3$:

$$
\begin{aligned}
Y_{ktg}|\mu_{ktg} &\sim \text{Pois}(\mu_{ktg}) \qquad (1.3b)\\
\ln(\mu_{ktg}) &= \sum_{i=0}^{p} x_{kti}\beta_i + O_{kt} + \Phi_k + \eta_{gt}\\
\Phi|\Sigma &\sim \text{MVN}(0, \Sigma)\\
\Sigma &= \sigma_\Phi^2 (D - \lambda W)^{-1}\\
\eta_{gt}|\rho_g, \eta_{g,t-1}, \sigma_\eta^2 &\sim \text{N}(\rho_g \eta_{g,t-1}, \sigma_\eta^2) \quad \text{for all } t = 2, 3, ..., T\\
\text{logit}(\rho_g) &= \text{logit}(P) + r_g\\
r_3 &= -r_1 - r_2\\
\beta_i &\sim N(0, 100)\\
\lambda, P &\sim \text{U}(0, 1)\\
\sigma_\Phi^2, \sigma_\eta^2 &\sim \text{inverse-Gamma}(1, 1)\\
r_1, r_2 &\sim \text{N}(0, 0.25)
\end{aligned}
$$

Here, η_{gt} is the normally distributed AR(1) error term for year t and tributary g, with a local temporal autocorrelation parameter ρ_g and global variance σ_η^2. the complete set is denoted by $\eta = (\eta_1, \eta_2, \eta_3)$, where $\eta_g = (\eta_{g1}, \eta_{g2}, ..., \eta_{gT})$. Here, each ρ_g on the logit scale is modeled as the logit of a global temporal autocorrelation parameter P plus a tributary-specific offset r_g, subject to the sum-to-zero constraint $\sum_{i=1}^{3} r_g = 0$. Two of the r_gs are given normal priors of $N(0, 0.25)$ which reflect a compromise between the lack of pre-existing knowledge about these parameters and a desire to constrain the distributions from unrealistic extremes (Fig. A1)[56]. The inverse-logit transformation, $\text{logit}^{-1}(u) = \frac{e^u}{1+e^u}$ for any real number u (here, $u = \text{logit}(\rho_g)$), constrains ρ_g between 0 and 1. Similarly, P is given a uniform prior between 0 and 1. The remaining model parameters were given the

same prior distributions as before.

1.3.4 Model 4

For the final model, we considered a non-separable spatiotemporal random effect. The spatiotemporal structure includes a multivariate first-order autoregressive process with a first-order spatial CAR structure. The data level and linear predictor of the resulting hierarchical model are:

$$Y_{kt}|\mu_{kt} \sim \text{Pois}(\mu_{kt}) \qquad \text{and} \qquad \ln(\mu_{kt}) = \sum_{i=0}^{p} x_{kti}\beta_i + O_{kt} + \Phi_{kt}.$$

Here, the Φ_{kt} term is the random effect associated with section k in year t, with the complete set denoted by $\Phi = (\Phi_1, ..., \Phi_T)$, where each $\Phi_t = (\Phi_{1t}, ..., \Phi_{Kt})$ is the tth map of spatial random effects.

$$\begin{aligned}
&\Phi_1|\Sigma \sim \text{MVN}(0, \Sigma) \\
&\quad \Sigma = \sigma^2_\Phi (D - \lambda W)^{-1} \\
&\Phi_t|\rho, \Phi_{t-1}, \Sigma \sim \text{MVN}(\rho\Phi_{t-1}, \Sigma), \text{ when } t > 1 \\
&\quad \Sigma = \sigma^2_\Phi (D - \lambda W)^{-1} \\
&\qquad \beta_i \sim N(0, 100) \\
&\qquad \sigma^2_\Phi \sim \text{inverse-Gamma(1,1)} \\
&\qquad \lambda, \rho \sim \text{U}(0, 1).
\end{aligned} \tag{1.4}$$

The spatiotemporal autocorrelation structure is stipulated by replacing η_t in Model 3a

with the entire Φ_t map, an approach employed by previous work [179], and represents the spatiotemporal pattern in the mean response with a single set of spatially and temporally autocorrelated random effects. The Φ_t map follows a multivariate autoregressive process of order one. Thus, in year $t = 1$, the Φ_1 map assumes a strictly CAR structure. However, when $t > 1$, temporal autocorrelation is induced by explicitly allowing Φ_t to have conditional mean equal to $\rho\Phi_{t-1}$.

The regression coefficients, autocorrelation parameters, and variance parameters were given the same prior distributions as before.

1.4 Model Implementation and Validation

For each model, Bayesian inference required numerical approximation of the joint posterior distribution of all model parameters including the vectors of random effects θ, Φ, and η. To this end, we implemented the above models using the Stan programming language for Bayesian inference to generate Markov chain Monte Carlo (MCMC) samples from the posterior [57]. For each model, we ran four parallel Markov chains, each with 15,000 iterations for the warm-up/adaptive phase (and subsequently discarded as burn-in), and another 15,000 iterations as posterior samples (i.e., 60,000 draws in total for posterior inference). Convergence of the chains was determined both by visual inspection of trace plots (e.g., Fig. B2) and through inspection of the split $\hat{R}$ statistic. All sampled parameters had an $\hat{R}$ value less than 1.01, indicating chain convergence [57]. Covariates and interactions whose regression coefficients had credible intervals (CIs) that excluded 0 at a credible level of 80% (i.e., reasonably high for hierarchical Bayesian inference) were considered scientifically relevant to juvenile blue crab abundance. All CIs referenced here are highest posterior density intervals (HPDIs) [115].

Model validation and relative predictive performance were assessed using out-of-sample

cross validation (CV), whereby a subset of the full data was used to train models, and the trained models were then used to predict the withheld data. Given the spatiotemporal dependence structures within our model, common CV procedures, such as leave-one-out (LOO), are difficult to interpret if the goal is to assess predictive performance, because withheld observations depend on other observations from different time periods and different spatial units in addition to the dependence on the model parameters [19]. For example, withholding random observations in time-series models will still allow information from the future to influence predictions of the past. Instead, we employed the leave-future-out (LFO) CV approach to evaluate predictive performance through withholding future samples [18]. Thus, prior to CV analysis, the data from the final year of the study, 2017, were excluded from the models. Then, the above Models 1–4 were fitted to the reduced dataset for both model inference (whose results appear under Section 1.5) as well as CV. For CV, 80% Bayesian prediction intervals were computed from the posterior predictive distributions of the excluded values, as a forecasting exercise. The final step of CV analysis was to compare the excluded blue crab count values to the forecast prediction intervals. Note that due to missing data in one of the sections in 2017 (see Section 1.5.1), CV was only possible for $n = 36$ sections.

1.5 Results

1.5.1 Data Summary

In total, 75,103 juvenile blue crabs between 20-40 mm CW were captured between 1996 and 2017 from April to December in the York, James, and Rappahannock Rivers. The highest abundances of juvenile blue crabs occurred in upriver locations of each tributary (Fig. 1.2a, 1.3a). Relative seagrass area was highest in the York River and lowest in the

James River (Table 1.3). Relative marsh area and turbidity were highest in the York River and lowest in the Rappahannock River (Table 1.3). Within each tributary, turbidity generally increased with distance upriver.

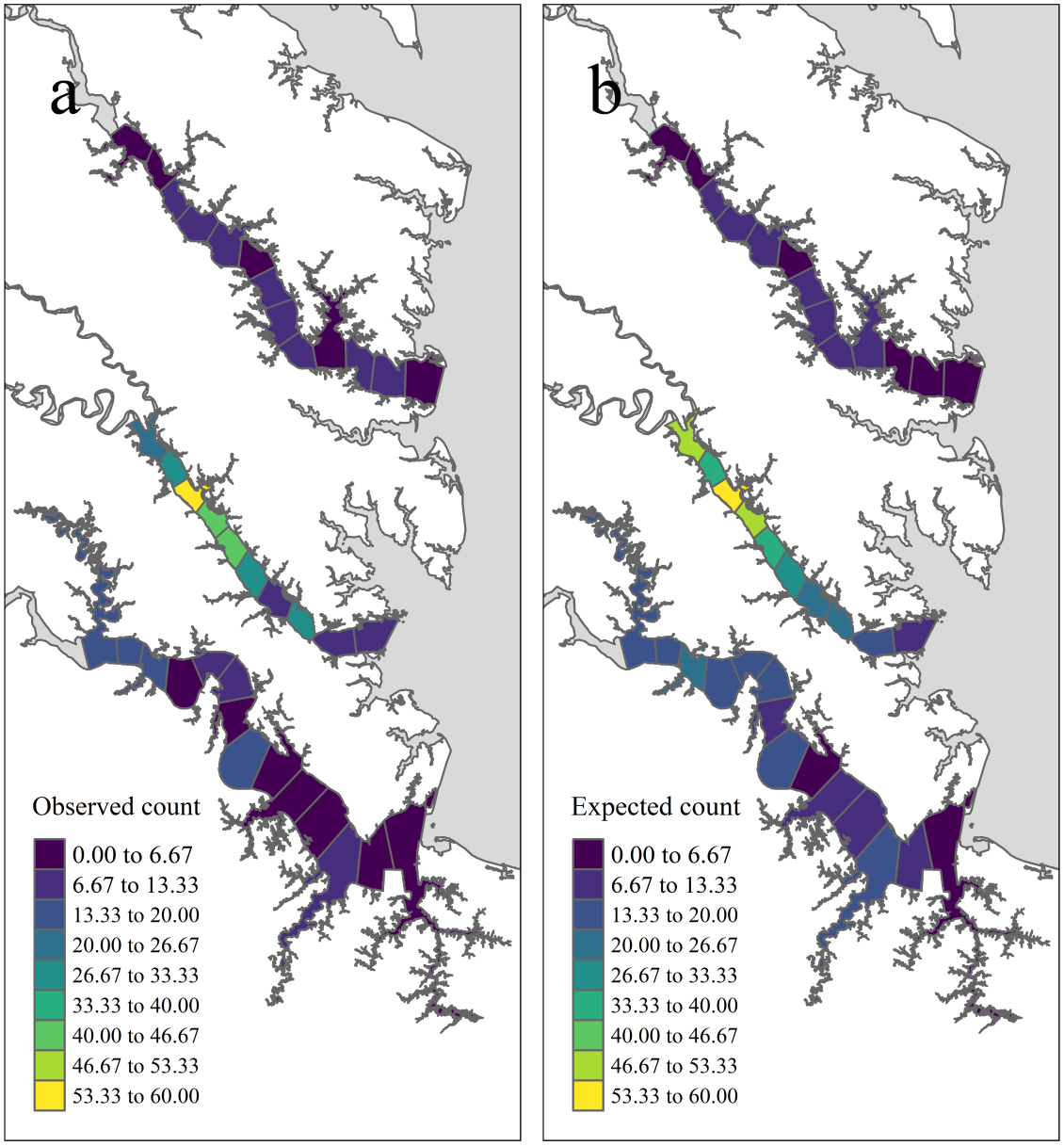

Figure 1.2: Temporally aggregated observed and expected juvenile blue crab abundance in each tributary section based on inter-annual grand means of model quantities from years 2009-2017 and management after 2008 (see Section 1.5.3 for definitions). Panel (**a**) shows the mean observed juvenile blue crab abundance ($\overline{y}_{k+}$), while Panel (**b**) shows the pseudo-posterior median of the expected abundance on the count scale ($\overline{\mu}_{k+}$).

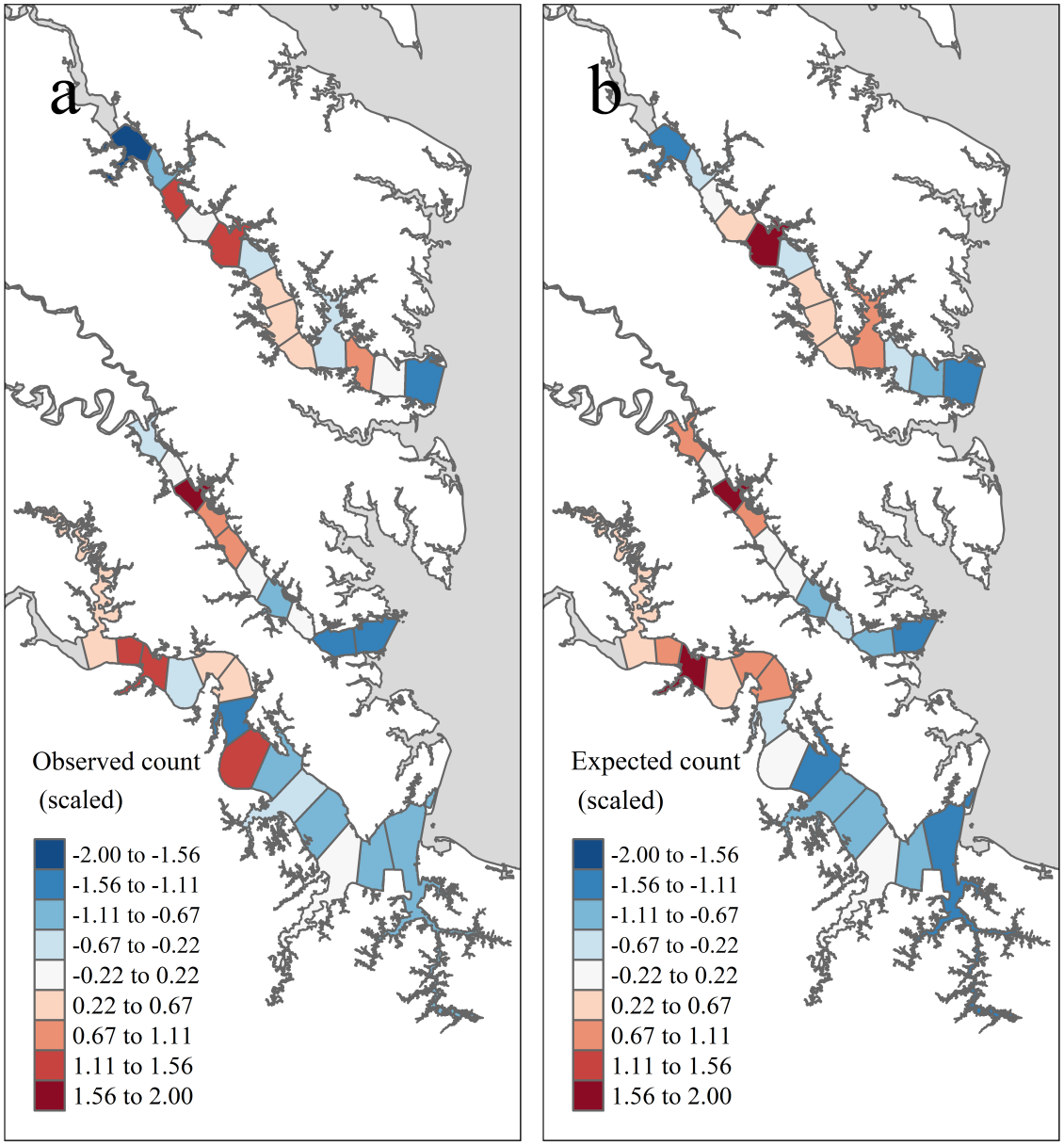

Figure 1.3: Temporally aggregated observed and expected juvenile blue crab abundance in each tributary section based on inter-annual grand means of model quantities from years 2009-2017 and management after 2008 (see Section 1.5.3 for definitions), standardized within tributary. Panel (**a**) shows the tributary-specific standardized values of $\overline{y}_{k+}$ (mean observed juvenile blue crab abundance), while Panel (**b**) shows the tributary-specific standardized values of $\overline{\mu}_{k+}$ (pseudo-posterior median of the expected abundance on the count scale).

Table 1.3: Mean (minimum–maximum) section-year values for Secchi disk depth, salinity, relative seagrass area (RSA), relative marsh area (RMA), and predator abundance for each tributary. Values were calculated from data collected over a 22-year period (1996–2017).

Tributary	Secchi	Salinity	RSA	RMA	Predator abundance
James	0.77	11.13	0	0.15	287.52
	(0.29–1.59)	(0.5–22.12)	(0–0.08)	(0.02–0.36)	(0–2838)
Rappahannock	1.1	12.74	0.01	0.08	147.32
	(0.26–2.34)	(2.73–19.39)	(0–0.09)	(0.01–0.38)	(0–2154)
York	0.78	15.85	0.02	0.23	383.62
	(0.38–1.57)	(6.81–22.24)	(0–0.17)	(0.01–0.48)	(2–2381)

1.5.2 Model Selection and Validation

Cross validation indicated that the non-separable spatiotemporal model, Model 4, best described patterns in juvenile blue crab abundance. The 80% posterior prediction intervals from Model 4 contained 81.1% of withheld 2017 data, while Model 1 (random effect only), Model 2 (spatial-only CAR model) , Model 3a (spatial CAR model with separable, global AR(1) term), and Model 3b (spatial CAR model with separable, tributary-specific AR(1) term) captured 21.6, 18.9, 43.2, and 70.3% of withheld data, respectively (Fig. 4.5). A full description of model validation and predictive performance is provided in Appendix A.3. Hereafter, inferences are made from Model 4 only.

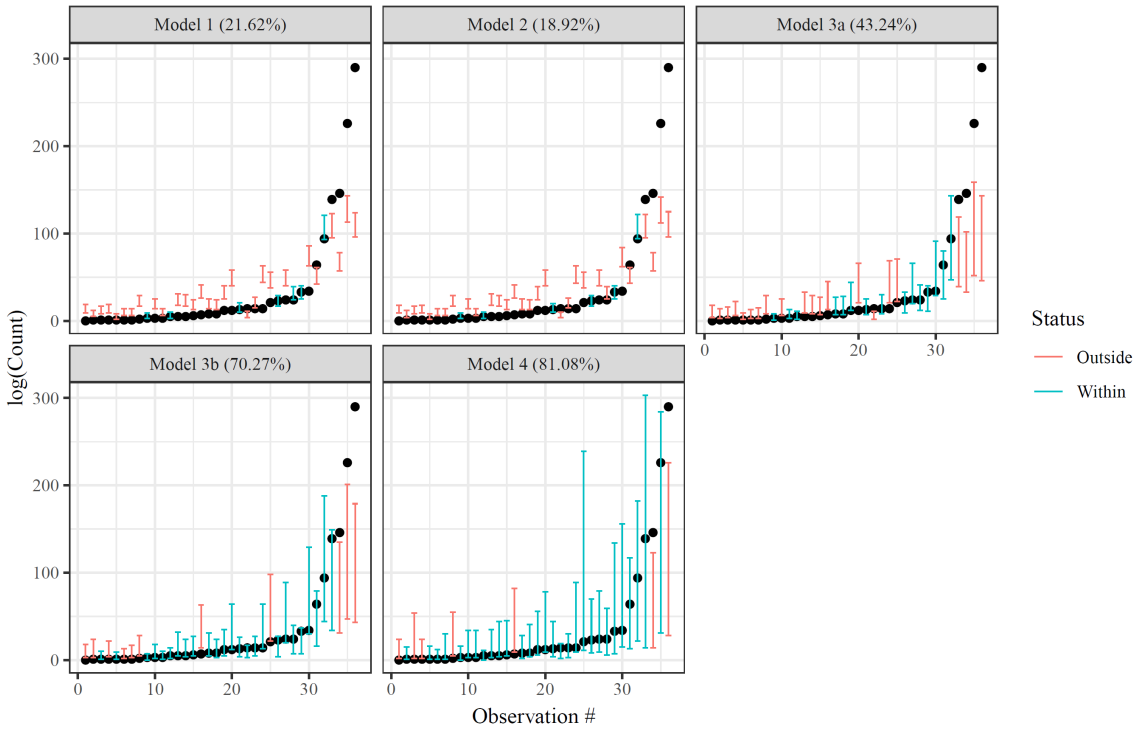

Figure 1.4: Leave-future-out cross validation results for Models 1–4. Bars denote nominal 80% Bayesian prediction intervals derived from posterior predictive distributions, while dots depict observed crab counts for 2017. Red bars indicate an observed value is outside the prediction interval, while blue bars indicate an observed value is within the prediction interval. Actual coverage percentages of prediction intervals (= % of blue) appear in the panel headings.

1.5.3 Implications of Prioritized Areas for Conservation

Using posterior distributions derived from Model 4, we aggregated over time and made spatial-only predictions of juvenile blue crab abundance to identify areas of high abundance. For continuous predictors, data were aggregated for each section over 2009–2017 to obtain inter-annual grand means, i.e., $\overline{x}_{k+i} = \sum_{t=1}^{T} x_{kti}/T$ for continuous predictor variable x_{kti}, where $T = 9$ for all sections except $T = 8$ for the section with no trawl data in 2017. The same aggregation was applied respectively to the log-transformed tow distance

offset term O_{kt} and each dth posterior draw for the spatiotemporal random-effect term $\Phi_{kt}^{(d)}$ to define $\overline{O}_{k+}$ and $\overline{\Phi}_{k+}^{(d)}$. Thus, for abundance, $\overline{\mu}_{k+}^{(d)}$ denotes a temporally aggregated posterior draw of the expected abundance from replacing μ_{kt} of Model 4 with $\overline{\mu}_{k+}^{(d)}$ that was computed using $\overline{x}_{k+i}, \overline{O}_{k+}$, and $\overline{\Phi}_{k+}^{(d)}$; the set $\{\overline{\mu}_{k+}^{(1)}, \overline{\mu}_{k+}^{(2)}, ...\overline{\mu}_{k+}^{(60000)}\}$ for each k forms a *pseudo-posterior distribution* of the temporally aggregated expected abundance $\overline{\mu}_{k+}$ for spatial section k. (A true posterior distribution would require fitting a spatial-only version of Model 4 that directly models temporally averaged counts $\overline{y}_{k+}$.) We limited spatial-only comparisons to 2009–2017 due to the change in management following 2008, which was a categorical predictor and could not be reasonably averaged over time. In addition to inspecting the $n = 37$ values of pseudo-posterior median for $\overline{\mu}_{k+}$ ($k = 1, ..., n$), we computed tributary-specific standardized values (centered and scaled to have unit variance) of the pseudo-posterior medians of $\overline{\mu}_{k+}$ to determine regions of locally high and low abundance relative to each tributary. Resulting sections with predictions corresponding to higher average relative juvenile blue crab abundance were interpreted as more productive within tributary, whereas sections with predictions corresponding to lower average relative juvenile blue crab abundance were interpreted as less productive within tributary.

According to pseudo-posterior medians of $\overline{\mu}_{k+}$, upriver sections of tributaries consistently harbored highest crab abundances (Figs. 1.2b and 1.3b). In particular, upriver sections in the York River were very high, with a pseudo-posterior median of 30–60 crabs per 1000 m towed. Upriver sections in the James River had a pseudo-posterior median of 13–26 crabs per 1000 m towed, whereas those in the Rappahannock River were much lower at 0–13 crabs per 1000 m towed. Pseudo-posterior medians for $\overline{\mu}_{k+}$ were generally consistent with observed juvenile blue crab abundances $\overline{y}_{k+}$ in each section from 2009–2017 (Figs. 1.2 and 1.3).

1.5.4 Drivers of Juvenile Blue Crab Abundance

Based on posterior distributions of Model 4 parameters, tributary, turbidity, relative marsh area, and relative marsh area $\times$ turbidity were relevant drivers of juvenile blue crab abundance. All tributaries differed in average juvenile blue crab abundances, with posterior probabilities $P(\beta_{\text{York}} > \beta_{\text{James}}|\text{data}) > 0.99$, $P(\beta_{\text{York}} > \beta_{\text{Rappahannock}}|\text{data}) > 0.99$, and $P(\beta_{\text{James}} > \beta_{\text{Rappahannock}}|\text{data}) = 0.99$. Turbidity, marsh, and their interaction positively influenced juvenile blue crab abundance — posterior medians (and 80% CIs) were: $\beta_{\text{Turbidity}}$ = 0.48 (0.20–0.77), β_{Marsh} = 2.55 (1.07–4.01), and $\beta_{\text{Marsh x Turbidity}}$ = 3.42 (1.34–5.49). Regression coefficients β_{Seagrass}, β_{Predator}, and $\beta_{\text{Management}}$ had respective 80% CIs that included 0. Supporting posterior summaries and graphics are in Table 1.4 and Fig. C2.

Table 1.4: Posterior summary statistics (median and 80% CIS) of regression coefficients β as well as autocorrelation parameters λ (spatial) and ρ (temporal) from Model 4. For regression coefficients, the symbol "*" indicates the 80% CI does not contain 0

Parameter	10%	50%	90%
β_0*	-4.66	-4.33	-3.99
$\beta_{\text{Turbidity}}$*	0.20	0.48	0.77
β_{Seagrass}	-4.44	-1.24	1.88
β_{Marsh} *	1.07	2.55	4.01
$\beta_{\text{Marsh}\times\text{Turbidity}}$*	1.34	3.42	5.49
β_{Predator}	-0.00	0.04	0.09
$\beta_{\text{Management}}$	-0.08	0.09	0.27
$\beta_{\text{Rappahannock}}$*	-0.56	-0.34	-0.13
β_{York}*	0.53	0.74	0.97
λ	0.48	0.55	0.61
ρ	0.05	0.11	0.16

Conditional effects plots (Figs. 1.5 and 1.6) were used to visualize the relationship between juvenile blue crab abundance and predictors relative marsh area and turbidity. For conditional effects plots, we considered the function $\mu_{\text{cond}}(x_{\text{Turbidity}}, x_{\text{Marsh}}) = x_{\text{Turbidity}}\beta_{\text{Turbidity}} + x_{\text{Marsh}}\beta_{\text{Marsh}} + x_{\text{Marsh}}x_{\text{Turbidity}}\beta_{\text{Marsh}\times\text{Turbidity}} + \beta_{\text{Management}} + \ln(1000)$, which

re-expresses the juvenile blue crab expected abundance μ_{kt} as a function of $x_{\text{Turbidity}}$ and x_{Marsh} as the only varying predictors, while all other continuous predictor variables were held at 0 and the tow offset term was held at 1000 m, while categorical variables were held at the James River (tributary) and post 2009 period. The relationship between each varying predictor and μ_{cond} was plotted (along with credible bands) with the other varying predictor held at fixed percentiles (1, 20, 40, 60, 80, and 99%) to visualize interaction effects. Relative marsh area influenced juvenile blue crab abundance negatively at low turbidities (i.e., ≤ -0.81 = median) and positively at high turbidities (i.e., ≥ -0.81 = median) (Fig. 1.5). In contrast, turbidity influenced crab abundance positively at both low and high relative marsh area values, with the strength of the relationship between turbidity and abundance growing progressively stronger at high relative marsh area values (Fig. 1.6).

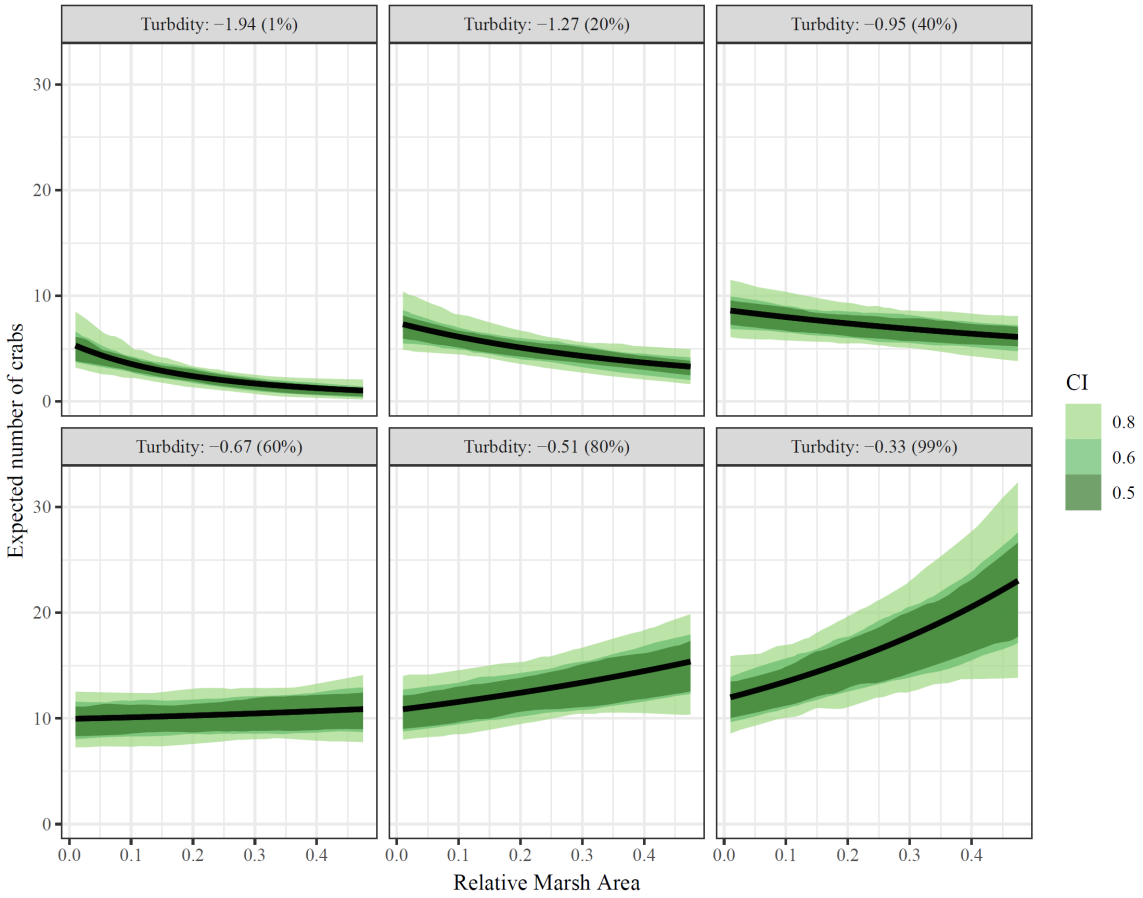

Figure 1.5: Conditional effects plots depicting relationship between juvenile blue crab abundance per 1000 m towed (μ_{cond}) vs relative marsh area (RMA) at turbidity values corresponding to 1, 20, 40, 60, 80, and 99% percentiles to visualize interaction effects between relative marsh area and turbidity on crab abundance. All other continuous variables were held at 0 and categorical variables at the James River (tributary) and post 2008 (management). Colored bands indicate credible bands of μ_{cond}. (See Section 1.5.4 for definitions.)

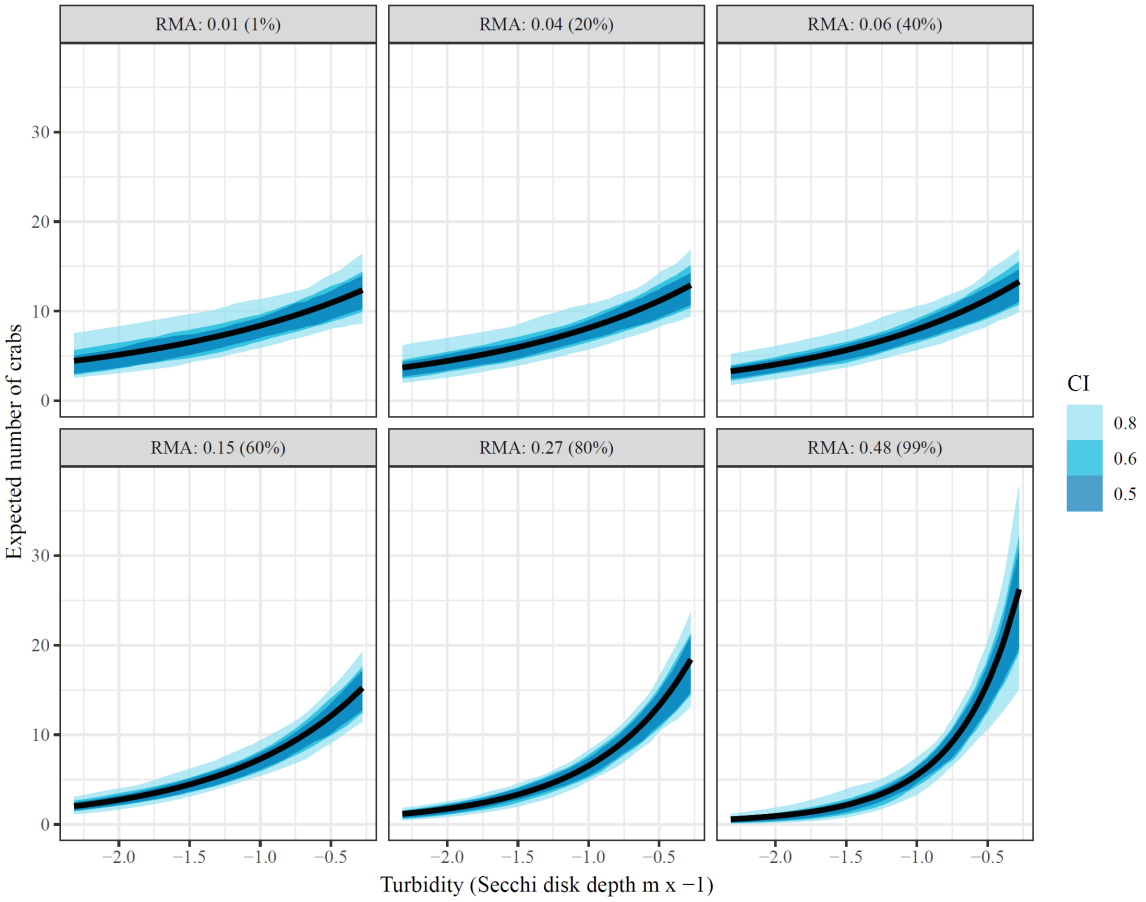

Figure 1.6: Conditional effects plots depicting relationship between juvenile blue crab abundance per 1000 m towed (μ_{cond}) vs turbidity at relative marsh area (RMA) values corresponding to 1, 20, 40, 60, 80, and 99% percentiles to visualize interaction effects between relative marsh area and turbidity on crab abundance. All other continuous variables were held at 0 and categorical variables at the James River (tributary) and post 2008 (management). Colored bands indicate credible bands of μ_{cond}. (See Section 1.5.4 for definitions.)

1.5.5 Spatiotemporal Dependence

The posterior distribution of λ indicated that substantial spatial dependence existed within the data (Fig. C3). Posterior distributions of λ and ρ yielded medians (80% CIs) of 0.61 (0.55–0.68) and 0.14 (0.08–0.19), respectively. Although the magnitude of ρ was small,

this non-separable spatiotemporal model, when compared to simpler models, gave leave-future-out 80% Bayesian prediction intervals that had the highest coverage of the withheld 2017 data, and the coverage was close to its nominal 80% (Fig. 4.5). Moreover, among the competing models the spatiotemporal structure was strong enough that posteriors of the fixed□effect coefficients changed markedly when spatially and spatiotemporally structured random effects were included (Fig. C4).

1.6 Discussion

Abundance of juvenile blue crabs varied spatially both within and among the three tributaries, James, York and Rappahannock Rivers. Within all tributaries, abundance of juvenile blue crabs consistently peaked in upriver sections. Given the limited mobility of juvenile blue crabs $<$60 mm CW, we interpret high 20–40 mm CW abundance in upriver areas as reflective of highly productive nursery habitats, as previously hypothesized for the York River [105, 186]. Moreover, juvenile blue crab abundance was associated with specific environmental characteristics, especially with high turbidity and extensive marsh area near the turbidity maximum of each tributary. These findings offer an initial quantification of multiple environmental components of highly productive nursery locations within the seascape paradigm for juvenile blue crabs in lower Chesapeake Bay.

1.6.1 Environmental Determinants of Juvenile Blue Crab Abundance

Availability of marsh habitat and high turbidity were the most important predictors of juvenile blue crab abundance, which was strongly and positively related to turbidity, and increased with the availability of salt marsh habitat relative to geographic area. However, the substantial interaction between marsh habitat and turbidity required that inferences on

the relationship between marsh habitat or turbidity and juvenile blue crab abundance be made within the context of the other factor.

In areas characterized by low turbidity (i.e., mean Secchi depth $>$1 m), the effect of marsh habitat ranged from negligible to negative. Conversely, in locations of high turbidity (i.e., mean Secchi depth $<$1 m), juvenile blue crab abundance was positively associated with availability of marsh habitat. About half of the section-years considered in our study were characterized by high turbidity where marsh availability was positively related to crab abundance. Turbidity and crab abundance were always related positively, and this relationship grew stronger (steeper slope) as marsh area increased in a river section.

While relative area of adjacent marsh habitat was positively related to juvenile blue crab abundance, other potential nursery habitats were weakly associated with crab abundance. Specifically, relative seagrass area was not associated with juvenile crab abundance. This was particularly surprising for seagrass, which has long been considered the preferred nursery habitat for small juvenile blue crabs [154, 103]. We propose that the lack of association between juvenile blue crab abundance and these habitat types reflects differences between nursery habitat contributions per unit area ([proposed by [8]) versus effective nursery habitat and total contribution to the adult segment of the population (proposed by[35]). At the tributary spatial scale of our study, the areal extent of marsh habitat relative to the area of river sections was much greater than that of seagrass meadows, particularly in the York and James Rivers. Moreover, section-years harboring seagrass meadows (such as in downriver York and midriver-downriver Rappahannock sections) were not associated with high juvenile blue crab abundance. Consequently, at the tributary scale, the potentially high production of juvenile blue crabs per unit area expected in river sections with seagrass meadows was likely obfuscated by the broad areal extent of marsh habitat in other sections. Furthermore, in downriver sections where seagrass was present, a substantial fraction of

juveniles 20–40 mm CW may have remained in seagrass where they were not susceptible to capture by the trawl [154, 105, 186, 171].

Predator abundance was not related to juvenile blue crab abundance. The apparent lack of an effect of predator abundance on juvenile blue crab abundance may reflect high refuge capacity of crab nurseries or increased availability of alternative prey in locations harboring high blue crab abundance [105]. Moreover, finfish predators are highly mobile and not likely to remain in a specific section. Regardless, our findings suggest that abundances of juvenile blue crabs at the regional scale are largely driven by bottom-up controls rather than top-down controls, which is consistent with studies of blue crab abundance in highly turbid, upriver localities harboring expansive marsh habitat [187, 165, 186].

Finally, juvenile blue crab abundance differed substantially among the three tributaries. These spatial patterns in abundance likely reflected tributary-specific characteristics that we did not consider in our models (e.g., differences in flow, bathymetry, total area, geographic position relative to the mouth of the Chesapeake Bay, or land-use patterns). Ultimately, spatial variation in juvenile blue crab abundance among tributaries indicates that tributaries in the Chesapeake Bay are not equal as nursery areas for the blue crab population, and that further studies should quantify tributary-specific production to the population.

1.6.2 Effect of Management

Changes in management of the blue crab population in the Chesapeake Bay after 2009 were positively associated with juvenile blue crab abundance, but not strongly, in contrast to the findings of other studies [117, 100]. One explanation for this result is the potential effect of cannibalism by larger juveniles and adults on small juveniles, which might negate positive effects of increased recruitment from a larger spawning stock [106]. More likely, the effect of management may depend upon specific habitats, especially those where juveniles

are abundant, such as in habitats with expansive marshes. Other sections where juveniles are not as abundant, such as unvegetated habitat, may not be able to support higher levels of recruitment, which would confound singular interpretation of management. Targeted analyses of the effects of management in specific habitats are ongoing to resolve this issue.

1.6.3 Prioritized Areas for Conservation

An objective of this study was to assist management to prioritize and direct restoration and conservation efforts of the blue crab within Chesapeake Bay as well as other blue crab stocks along its geographic range. Although previous focus of blue crab nursery studies was on seagrass meadows [169], salt marshes and certain unstructured, high turbidity habitats appear more valuable at the tributary and regional scales due to their extensive areal cover. Our best fitting model indicates that expansive salt marshes in highly turbid upriver locations are highly productive nurseries for this ecologically and economically exploited species. As a result, a major recommendation of this paper is the inclusion of these habitats in future conservation targets.

1.6.4 Relevance

The EFH provisions of the Magnuson-Stevens Act directs fishery management councils to utilize the best available science to describe and identify EFH for federally managed species and protect them to the extent practicable [139]. The highest level of EFH information is level 4: production rates by habitat type; yet level 4 EFH information is largely unavailable for most commercially harvested species, particularly at spatial and temporal scales needed for effective fisheries management. This lack of level 4 EFH information is currently limiting the inclusion of habitat effects in stock assessments and in ecosystem-based fisheries management plans [60]. Furthermore, area-based estimates of nursery habitat value may

inform decision-making related to protected area management and habitat restoration, by allowing the per unit area contribution of protected or restored habitat to be quantified [233].

Understanding the relative contribution of both structured habitats and other environmental factors on the productivity of a given area is important, as many conditions resulting in such productivity are diminishing. Some structured nursery habitats are declining, especially *Z. marina* eelgrass beds due to direct and indirect anthropogenic influences such as land-use change and long-term warming of Chesapeake Bay [156, 137, 158]. Similarly, salt marshes have been reduced by coastal development and shoreline hardening [193].

Scientists and managers have generally assumed that when structured habitats are degraded, the services they provide such as nursery habitat for valuable marine species are lost [163]. Therefore, state and federal agencies have long invested in coastal habitat conservation and restoration to recover lost production. However, these investments have often preceded the availability of, and thus would be enhanced by the development of, rigorous analytical tools capable of quantifying the ecosystem services expected from conservation actions and habitat restoration efforts. While standalone small-scale studies have been and remain important tools to initially assess nursery value of structured habitats and other environmental factors, targeted comprehensive applications of survey data collected over broad spatial and temporal scales are a vital complement to generalize inference of nursery function, highlight highly productive regions, and inform regional management strategies.

Chapter 2

Ontogenetic Patterns in Juvenile Blue Crab Density: Effects of Habitat and Turbidity in a Chesapeake Bay Tributary

Abstract

Nursery habitats are characterized by favorable conditions for juveniles, such as higher food availability and lower predation risk, and disproportionately contribute more individuals per unit area to adult segments of the population compared to other habitats. However, nursery habitat inference is complicated by changes in habitat preferences with ontogeny; individuals in early-life stages frequently inhabit different habitats than older juveniles or adults. In this study, we quantified juvenile blue crab density of two size classes based on carapace width (CW) across multiple juvenile habitats at various locations within an

estuarine seascape over the blue crab recruitment season. We examined four habitat types—unstructured sand, seagrass meadows, salt marsh edge (SME), and shallow detrital habitat (SDH). Results indicated that although densities of small juvenile blue crabs ($\leq$ 15 mm CW) were highest in seagrass, abundances of larger juveniles (16–30 mm CW) were highest in SME. Meanwhile, densities of large juvenile blue crabs in SME were greater than those of small juveniles, suggesting immigration to this habitat. Finally, turbidity was positively correlated with densities of both sizes classes, although it was unclear whether this was due to top-down (refuge) or bottom-up (food availability) mechanisms. Observed patterns in size-specific habitat utilization may result from changing requirements of juvenile blue crabs with size as animals minimize mortality-to-growth ratios. Taken together with previous work and patterns observed in SME, these findings emphasize the role of salt marsh habitat within juvenile blue crab ontogeny and underscore the need to quantify and preserve the complete chain of habitats used by juveniles before they enter adult populations.

2.1 Introduction

Nursery habitats are critically important for fishes and invertebrates. Under the Nursery Role Hypothesis [8], nursery habitats are characterized by favorable conditions for juveniles, such as higher food availability and lower predation risk, and disproportionately contribute more individuals per unit area to adult segments of the population compared to other habitats [8, 67, 128, 58]. Hence, nursery habitat availability is a major driver of commercially exploited fisheries population dynamics. Consequently, a major research focus in fisheries science and estuarine ecology is identification of nursery habitats for commercially exploited fish and invertebrate species both to prioritize conservation and restoration efforts as well as to guide management decisions [188, 216].

Nursery status is often evaluated through four factors: juvenile density, growth, survival, and connectivity between juvenile and adult habitats [8]. As the contribution of juveniles to adult segments of the population arises from combinations of these four factors, these metrics are generally higher in nursery habitats compared to other candidate nursery habitats [67, 128]. However, nursery habitat research typically focuses on one or two of the first three factors due to financial and methodological limitations [2, 188, 216, 109, 102].

The Nursery Role Hypothesis maintains that comparisons among all, or at least most, juvenile habitats are required prior to conferring nursery status of a habitat for a given species [8, 35, 109]. Juveniles tend to utilize structurally complex habitats as nurseries in early life stages in part because of their superior refuge capacity [67, 128, 95]. The relative value of a given structurally complex habitat as a nursery may be dependent on availability of other habitats with similar characteristics. For example, submersed aquatic vegetation (SAV) or intertidal emergent vegetation (e.g. salt marshes) may seem less important as nurseries in regions where alternative structurally complex habitats are present and accessible [140, 109]. However, many studies investigating nursery habitats only consider binary comparisons such as a structured habitat and an unstructured control (see review by [27]), which can severely limit inference.

Characteristics of nominal nursery habitats (e.g. seagrass meadows or salt marshes) may fluctuate across space and time. The nursery function of these habitats can vary depending on the position within the seascape or season due to the influence of latent environmental, biological, or anthropogenic factors [140, 191, 109]. For example, predator composition and density vary seasonally in temperate estuaries [41], and may alter habitat use of prey [30, 54, 31, 28]. Moreover, spatial position within the seascape may modify a habitat's suitability as a nursery, such as when habitats are positioned close to the site of larval ingress [201] or in areas with low predation pressure [165]. Assessments of

habitats conducted over short temporal intervals or only in one spatial location may miss such phenomena and lead to spurious conclusions about nursery status [109]. Hence, these dynamic processes require careful consideration to ensure inferences on habitat comparisons are robust. Moreover, indirect comparisons of multiple habitats via meta-analyses and literature reviews of multiple studies – each considering different combinations of potential nursery habitats – are hindered by the potential influence of confounding, spatiotemporally fluctuating latent variables [82]. Thus, robust evaluation of nursery habitat requires that studies consider as many habitats concomitantly as possible, as well as other influential environmental factors.

Assessment of nursery habitat value is complicated by changes in habitat preferences with ontogeny. Individuals in early-life stages frequently inhabit different habitats than older juveniles or adults [89, 141, 44]. Ontogenetic habitat shifts from one nursery to another can minimize mortality-to-growth ratios [223], and juvenile survival increases with size [164] such that larger juveniles can exploit habitats with less structural refuge and higher food availability [34, 105, 186, 141]. Consequently, juveniles may utilize different habitats as they grow to minimize mortality-to-growth ratios. Failure to consider these shifts may lead investigators to prioritize only a subset of habitats critical for maintaining healthy population abundances, while neglecting habitats that may be preferred by different stages [192, 191, 140]. Quantitative assessments of nursery function must therefore consider nursery roles within the context of ontogeny, especially for organisms with complex life cycles [103, 43, 188, 216, 109, 44]. Partitioning juveniles into multiple size classes and assessing each class concomitantly allows researchers to detect shifts in habitat utilization as juveniles grow and identify stage-specific nursery habitats throughout ontogeny [140, 111, 5, 1]. It is especially important to identify all nurseries used through ontogeny for commercially exploited species with complex life histories so that these habitats can be

conserved and related fisheries remain sustainable.

The blue crab *Callinectes sapidus* is an commercially exploited species that relies on structurally complex nursery habitats through ontogeny. The blue crab opportunistically utilizes many habitats in early life stages, including seagrass (e.g. eelgrass *Zostera marina* and widgeon grass *Ruppia maritima* meadows in the Chesapeake Bay), *Spartina alterniflora* salt marshes, and coarse woody debris (see [103] for a review). After re-invading estuaries from the continental shelf, blue crab postlarvae settle into structurally complex nursery habitats, such as seagrass meadows, and rapidly metamorphosize into first instar (j1) juveniles [43, 44]. Although some early (j1–j5) juveniles emigrate from initial settlement locations to avoid adverse density-dependent effects associated with conspecifics [45, 13, 172], many remain to exploit the high refuge quality afforded by primary nursery grounds. As juveniles outgrow the mouth-gape sizes of smaller predators, they emigrate to other habitats with lower quality refuge but more abundant preferred prey (e.g. *Macoma balthica*; [187, 105, 186]).

Several studies have posited different size thresholds for when emigration out of primary nursery grounds unfolds. A mesocosm experiment examining the effects of simulated *S. alternaflora* shoots on survival estimated that juvenile blue crabs may shift their habitat preferences at sizes as small as 12 mm carapace width (CW), when they could achieve a size refuge from smaller predators abundant within salt marsh habitats (e.g. *Fundulus heteroclitus*; [155]). Subsequent field studies maintained that juveniles begin emigrating from seagrass meadows to utilize unstructured and salt marsh habitats only after reaching 25–30 mm CW [164, 105, 88, 82]. Notably, these hypotheses are not mutually exclusive. Salt marsh habitat may represent an intermediate nursery – one with marginally lower refuge quality than seagrass but higher food availability [187, 186] – before juveniles emigrate to unstructured or alternative nursery habitats [201, 131, 169, 228].

Secondary production from a habitat is the common currency used to quantify the value of different habitats [163]. Small-scale studies previously demonstrated that blue crab production from salt marshes was substantial in the Gulf of Mexico [205, 232] and Chesapeake Bay [26, 25]. Recently, large-scale spatiotemporal analyses of juvenile blue crab habitats emphasized the roles of salt marsh and high-turbidity habitats in addition to seagrass meadows in promoting secondary production [82]. Spatially explicit analyses of relative secondary production are useful for assessing potential nursery capacity of large regions [53, 9, 171]. For example, by exploiting ontogenetic shifts in habitat usage, such as juveniles emigrating from nursery habitats to unstructured adult habitats, broad-scale studies can highlight productive areas which can be prioritized for conservation [82]. However, evaluation of nursery habitats at broad scales may miss important processes operating at smaller scales. In addition, broad-scale studies are unable to ascertain which aspects of a habitat promote secondary production. For example, although turbid salt marsh habitat is positively associated with juvenile blue crab density at large spatial and temporal scales [82], it is unclear if such production is more closely linked to vegetative structure (i.e. *Spartina* shoots; [86, 83]), or to structurally complex detritus along erosional marsh shorelines [45, 46]. As small-scale studies are uniquely suited for capturing these processes, it is important to employ this approach in concert with broad-scale studies to determine: (1) which habitats are associated with high juvenile density; (2) which habitat characteristics are important in promoting juvenile density, and (3) which environmental variables modify habitat suitability.

In this study, we modeled juvenile blue crab abundance of two size classes (herein small: $\leq$15 mm CW, and large: 16–30 mm CW) in multiple juvenile habitats at various locations within an estuarine seascape during the blue crab late summer-fall recruitment season. Building on previous work [82], we sought to complement large-scale spatiotemporal analy-

ses with mensurative experiments [210] at local spatial (i.e. 10s of kilometers) and temporal (i.e. biweekly) scales within the York River, a tributary of Chesapeake Bay. Specifically, we wanted to determine the effects of habitat, spatial position, and environmental factors on juvenile blue crab density. To accomplish this, we developed multiple models (labeled g_i) with different combinations of spatial position, habitat, and turbidity as independent variables. We describe and justify the models and corresponding independent variables in Appendix B.1.

2.2 Habitats considered

We examined four habitat types—unstructured sand, seagrass meadows, salt marsh edge, and shallow detrital habitat. Seagrass meadows (herein, seagrass) are regarded as preferred nursery for juvenile blue crabs [154, 159, 77, 75, 171] due to disproportionately high densities and survival of small juvenile crabs (i.e. $<$30 mm CW) in seagrass meadows relative to other potential nursery habitats [154, 164, 105]. Meanwhile, salt marshes serve as alternative nursery habitat for juvenile blue crabs in locations where seagrass is absent or declining [49, 84, 12, 86]. In Gulf of Mexico and some Chesapeake Bay nursery habitats, juvenile blue crab density was high in both seagrass and salt marsh habitats [205, 175, 66, 82]. Salt marshes may afford refuge through structurally complex shoots and rhizomes (i.e. salt marsh edge; SME; [86, 123]). In addition, detritus exported from the vegetated marsh surface accumulates in adjacent tidal marsh creeks. This “shallow detrital habitat” (SDH) is associated with eroding peat and can harbor high densities of juvenile blue crabs [45, 46, 219]. Finally, unstructured sand habitat (herein, sand) constitutes the most abundant shallow habitat in Chesapeake Bay, but is characterized by relatively low predation refuge [105] and serves as a control to assess nursery value of seagrass and salt marsh habitats for juvenile blue crabs [66, 105, 189].

2.3 Methods

2.3.1 Study Area

Field work was conducted in the York River, a tributary in the lower portion of western Chesapeake Bay between August and November, 2020. The river is morphometrically characterized by depths generally between 5 to 10 m along the axes, but with deeper portions (>20 m) near the mouth [196]. In addition, This system contains a range of seagrass, salt marsh, and unstructured sand habitat configurations ideally suited for investigating the relative importance of multiple habitat types [77, 105]. Seagrasses, primarily eelgrass (*Zostera marina*) and Widgeon grass (*Ruppia maritima*), vary from large, continuous meadows to areas with few small patches of variable shoot densities [77]. Salt marshes, dominated by smooth cordgrass (*Spartina alterniflora*), span extensive sections of the shorelines, although areal coverage of marsh patches varies spatially along the shorelines. Secchi disk depth values, a proxy for turbidity, range from 0.5–1.5 m at the mouth of the system and 0–0.5 m upriver near the confluence of the Pamunkey and Mattaponi tributaries. For a more detailed description of physiochemical variables, see Table B1. The river was divided into 3 approximately evenly split strata (nearly 17 km each) for a lack of an obvious stratification strategy, constituting downriver, midriver, and upriver strata (Fig. 3.1).

Figure 2.1: Map of the York River displaying sampling sites colored by habitat type. Salt marsh edge sites are a subset of shallow detrital habitat sites.

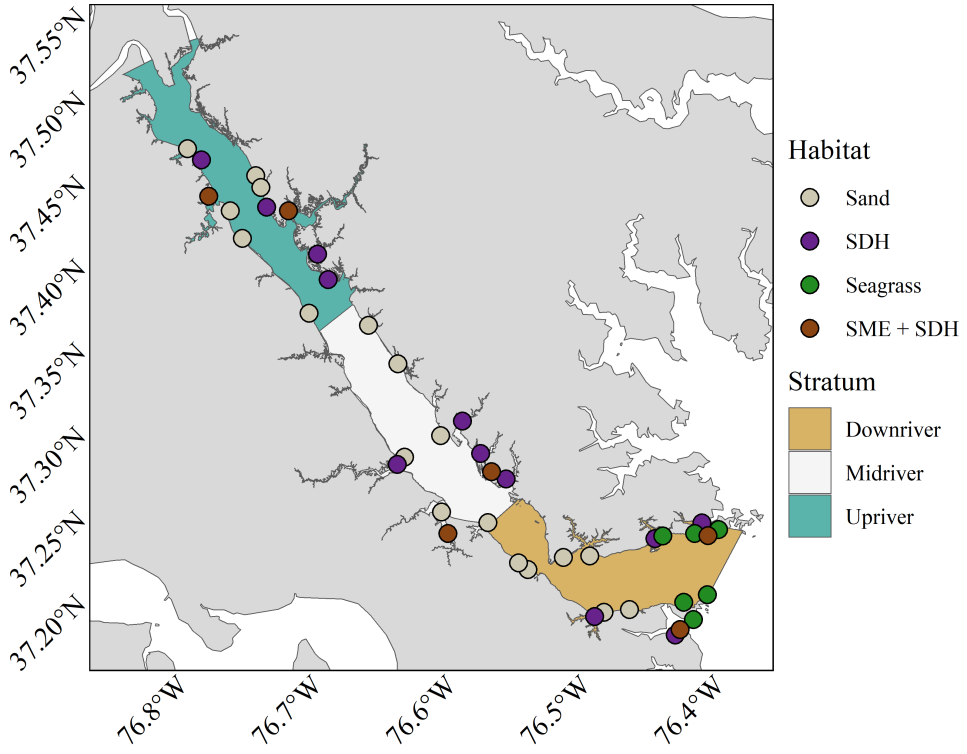

2.3.2 Sampling design

Site selection was achieved via a random sampling algorithm. Selection involved (1) extracting geographic coordinates for the entire shoreline of the York River, (2) subsetting coordinates by habitat type and stratum, and (3) randomly selecting a prespecified number of stations for each habitat within each stratum. Six SDH and sand stations were selected in each stratum, while two SME stations were randomly selected from the six SDH sites in each stratum. Finally, six seagrass stations were randomly selected from the downriver stratum, as seagrass is absent in midriver or upriver strata (Fig. 3.1). The number of sites per habitat in each stratum were the maximum logistically feasible to sample in a day given

time constraints and tidal considerations.

Between August and November 2020, juvenile blue crabs were sampled in seagrass, SME, SDH, and sand at biweekly intervals. Four sampling trips were conducted to sample all four habitats. The first three sampling trips – targeting seagrass, SDH, and sand – were conducted August 24th–27th (Trip 1), September 15th–22nd (Trip 2), and October 5th–8th (Trip 3). SME was also sampled on trips 2 and 3, as well as Trip 4, which occurred October 19th–23rd. Hence, there is confounding between trip 4 and SME habitat, otherwise exploratory data analyses did not indicate interactions between habitat and trip. This culminated in a total of 144 samples (Table B2), although five samples were later expunged due to missing predictor values (i.e. Secchi disk depth) in seagrass (two) and SDH (three).

Each habitat was sampled using gear and methodologies corresponding to habitat-specific structure and bottom types. All gear types used 3-mm mesh netting to ensure that size-specific catchability was consistent after accounting for differences in gear efficiency. SDH and sand stations were sampled ± 3 h of high tide via benthic scrapes towed for 20 m along tidal salt marsh creek and beach shorelines, respectively [170]. Meanwhile, SME stations were sampled using modified flume nets set at flood tide and collected at ebb tide (Fig. B1) [116]. At seagrass stations, a 1.68-m^2 drop-cylinder and a 10-cm diam PVC suction pipe attached to a sampling pump, modified from [154], were employed to collect juvenile blue crabs [154, 171, 77, 66]. Seagrass stations were suctioned within the drop-cylinders for 6 min continuously. For sand, SDH, and SME stations, immature juvenile crabs were counted, measured *in situ* and released. The contents of each seagrass suction sample were frozen for storage and subsequently examined for juvenile blue crabs, double-checked, and all crabs counted and measured. Physicochemical variables salinity, temperature, and turbidity were recorded using a YSI data sonde (for salinity and temperature) and a Secchi disk (water clarity, the inverse of turbidity) at each station on

each trip.

2.3.3 Analyses

2.3.3.1 Basic model structure

All data analyses, transformations, and visualizations were carried out using the R programming language for statistical computing [167]. Relationships between both small and large juvenile blue crab abundance and environmental variables were evaluated using multivariate negative binomial linear mixed-effects models within a Bayesian framework. The predictor variables for juvenile abundance include habitat (seagrass, SME, SDH, and sand), spatial stratum (downriver, midriver, and upriver), and turbidity.

Transformations to turbidity values were applied prior to their inclusion in abundance models. Here, ln turbidity was defined as the natural log transformation of Secchi-disk depth, multiplied by -1 ($T = -\ln$ Secchi). The natural log transformation was applied based on the assumption that a threshold exists in water transparency. Assuming that effects of turbidity on juvenile abundance reflect refuge from visually oriented predators (top-down control), small changes in water transparency when water is relatively clear are not expected to substantially affect juvenile abundance as much as small changes in water transparency when water is turbid (e.g. predation rates by summer flounder on mysid shrimp; [78]). Similarly, if associations between juvenile abundance and turbidity are related to elevated food availability near the estuarine turbidity maximum, juveniles would presumably remain more sensitive to fluctuations in turbidity at high values compared to clearer waters. Multiplying the variable by -1 facilitates inference on turbidity, instead of water transparency (inverse).

For the s^{th} site on trip t in habitat h, the Bayesian model for juvenile blue crab abundance of size class i is expressed as:

$$
\begin{aligned}
y_{hsti} | \mu_{hsti}, \phi_i &\sim \text{NB}(\mu_{hsti}, \phi_i) \\
\ln(\mu_{hsti}) &= X_{hst}\beta_i + \theta_{hsi} + A_h + E_h \\
\beta_i &= [\beta_{i1}, \beta_{i2}, \ldots, \beta_{ip}] \\
\begin{bmatrix} \theta_{hs1} \\ \theta_{hs2} \end{bmatrix} | \Sigma &\sim \text{MVN}(0, \Sigma) \\
\Sigma &= \begin{bmatrix} \sigma_1^2 & \rho\sigma_1\sigma_2 \\ \rho\sigma_1\sigma_2 & \sigma_2^2 \end{bmatrix} \\
\frac{1}{2}\ln\left(\frac{1+\rho}{1-\rho}\right) &\sim \text{N}(0, 0.9^2) \\
\beta_{ik} &\sim N(0,1) \text{ for } k = 1, \ldots, p \\
E_{sand}, E_{SDH} &\sim N(-1.20, 0.18) \\
E_{SME} &\sim N(-0.083, 0.02) \\
E_{seagrass} &\sim N(-0.13, 0.02) \\
\sigma_1^2, \sigma_2^2, \phi_1, \phi_2 &\sim \text{inverse-Gamma}(1,1)
\end{aligned}
$$

where $NB(\mu_{hsti}, \phi_i)$ denotes a negative binomial type II distribution with mean μ_{hsti}, while ϕ_i controls the over-dispersion for each size class such that $E[y_{hsti}] = \mu_{hsti}$ and VAR$[y_{hsti}] = \mu_{hsti} + \frac{\mu_{hsti}^2}{\phi_i}$. The response variables, juvenile crab counts for size classes, are denoted y_{hsti} where $i = 1$ denotes the small size class ($\leq$ 15 mm) and $i = 2$ denotes the large size class (16–30 mm). Total area sampled (seagrass = 1.68 m^2, SME = 1 m^2, SDH and sand = 20 m^2) is included as an offset term A_h. Here, θ_{hs} denotes a site-specific random effect following a multivariate normal (MVN) distribution with mean 0 and covariance Σ. The covariance matrix is composed of σ_i^2 along the diagonal denoting variance for size class i and ρ describing the correlation between size classes at a given site. A normal prior was applied to Fisher-transformed ρ to constrain values between -1 and 1. In addition,

due to varying requirements as a function of size, each size class was not expected to respond equally to predictor variables X_{hst} (habitat, turbidity, spatial position, and relevant interaction terms, see Appendix B.1 for details). Hence, β_i refer to regression coefficients for each size class i associated with X_{hst}. Measurements of both the abundances of size classes and predictors X_{hst} were taken at the site-trip spatiotemporal resolution, such that predictors were not specific to any one size class i but to all sizes classes at a given site-trip. Informative prior distributions for gear efficiency E_h were supplied based on gear efficiencies from literature (seagrass, SDH, and sand) and from the fall pilot study (SME), converted to the ln-scale (see Appendix B.2 for details). This incorporated increased uncertainty into habitat-specific estimates.

Bayesian inference required numerical approximation of the joint posterior distribution of all model parameters including the vectors of random effects. To this end, we implemented the model using the Stan programming language for Bayesian inference to generate Markov chain Monte Carlo (MCMC) samples from the posterior [57]. For each model, we ran four parallel Markov chains, each with 5,000 iterations for the warm-up/adaptive phase, and another 5,000 iterations as posterior samples (i.e. 20,000 draws in total for posterior inference). Convergence of the chains was determined both by visual inspection of trace plots (e.g. Fig B2) and through inspection of the split $\hat{R}$ statistic. All sampled parameters had an $\hat{R}$ value less than 1.01, indicating chain convergence [57]. We considered covariates and interactions whose posterior distributions indicated a positive or negative effect with $\geq$ 80% posterior probability, as scientifically relevant to juvenile blue crab abundance [92]. All CIs referenced here are the highest posterior density intervals [115].

Estimated log-pointwise predictive density (ELPD) and related Δ_{ELPD} values were used to evaluate the degree of predictive power for each model among the set of statistical models g_i [217]. The ELPD is a statistical concept used in model evaluation and comparison. It

measures the accuracy of a probabilistic model's predictions by estimating the log likelihood of the observed data given the model structure and coefficient estimates. Values of ELPD are widely employed to measure out-of sample predictive accuracy, while Δ_{ELPD} values refer to the difference in ELPD between a given model and the model with the best ELPD in the set. Values of ELPD and Δ_{ELPD} were estimated using the Widely-Applicable Information Criterion (WAIC) [221, 57, 217]. Both WAIC and ELPD were estimated using the `loo` package. When two models had comparable Δ_{ELPD} values (i.e. ≤ 4), the simpler model was chosen as the more appropriate model under the principle of parsimony [194].

2.3.3.2 Alternative model structures

In our design, the downriver stratum was partially confounded with seagrass habitat, as seagrass is present only at the mouth of the York River (Fig. 3.1)[82]. As a consequence, under this design it is not easily discernible whether spatial stratum interacted with seagrass habitat. To ensure that seagrass habitat and spatial stratum did not interact and influence results, we constructed two additional models – one with only SME, SDH, and sand across all strata and a second with all four habitats only in the downriver stratum – and compared the results to our best-fitting model, g_1. Posterior distributions of main effects (where present across models) strongly overlapped, indicating that interactions between spatial stratum and habitat were unlikely when other predictors were considered (Fig. B3).

2.3.3.3 Conditional effects

Conditional effects plots were used to visualize the relationship between response variables (juvenile blue crab abundance) and meaningful predictors both among habitats within a size class and within habitats between size classes. Herein, we refer to "conditional effects" as the effects of a given predictor (either continuous or categorical) while holding

all random effects at 0 and fixing co-varying predictors. Specifically, we held ln turbidity at 0 to estimate habitat conditional effects and held habitat effects at the reference (i.e. sand; h = 1). Conditional effects were used to conceptualize mean effects of each level in a given categorical variable. Hence conditional linear contrast statements were used to determine whether differences in abundances among habitats were statistically meaningful. For the h^{th} habitat (where $h > 1$), we considered pairwise difference between habitats $\beta_{hi} - \beta_{1i}$, where β_{1i} is the reference intercept (sand). Meanwhile, for comparisons of within-habitat abundances between $\leq$ 15 (i.e. $i = 15$) and 16–30 mm ($i = 30$) size classes, for the h^{th} habitat, we considered the contrast $\beta_{h,15} - \beta_{h,30}$.

2.4 Results

We collected and measured 1,004 juvenile blue crabs $\leq$ 30 mm CW from 139 samples. A complete summary of all physicochemical variables and crab sizes is detailed in Table B1, while a histogram of crab sizes is provided in Figure B4. Herein, all abundance values for size classes refer to abundance per square meter, and are referred to as density.

2.4.1 Model selection

The best fitting model was g_5, which posited juvenile blue crab abundance as a function of habitat, turbidity, stratum, and a habitat-turbidity interaction. However, all models had comparable ELPD values ($\Delta_{ELPD} \leq 4$ for all models except g_4) and overlapping standard errors (Table 2.1), indicating relative statistical equivalence. Hence, we chose the simplest model g_1, with habitat and turbidity additive, as the best model under the principle of parsimony. Hereafter, inferences are based on model g_1.

Table 2.1: Model selection results from five Bayesian multivariate negative binomial regression models (g_i) using ln turbidity (**T**), habitat (**H**), and stratum (**S**) as predictors of juvenile blue crab abundance. Models are presented in order of predictive power based on collected data. **WAIC**: the Widely-Applicable Information Criterion; **ELPD$_{\text{WAIC}}$**: the estimated log-pointwise density calculated from WAIC; $\Delta_{\textbf{ELPD}}$: the relative difference between the ELPD of any model and the best model in the set; SE$_{\Delta_{\text{ELPD}}}$: standard error for the pairwise differences in ELPD between the best model and any given model; **pWAIC**: estimated effective number of parameters. The selected model (g_1) values are presented in bold font. Model justifications are in Appendix B.1

Model: Fixed effects in mean structure	WAIC	ELPD$_{\text{WAIC}}$	Δ_{ELPD}	SE$_{\Delta_{\text{ELPD}}}$	p$_{\text{WAIC}}$
g_5: H + T + S + (H x T)	1049.76	-524.88	0.00	0.00	37.03
g_1: H + T	**1050.46**	**-525.23**	**-0.35**	**3.31**	**36.92**
g_2: H + T + (H x T)	1050.60	-525.30	-0.42	1.67	37.36
g_3: H + T + S	1050.76	-525.38	-0.50	3.17	37.13
g_4: H + T + S + (H x S)	1058.09	-529.04	-4.16	3.71	40.43

2.4.2 Habitat effects

2.4.2.1 Small ($\leq$15 mm) size class

Small juvenile blue crab density was highest in seagrass (13.83 per m^2 on the count scale), followed by SME (4.70), SDH (0.62), and sand (0.35) (Table 3.6; Figs. 2.2 and B5). For pairwise linear contrasts among habitats, the posterior probability that a given contrast was positive all exceeded 90%, indicating that differences in the expected density of small juvenile crabs among habitats were statistically meaningful (Table 2.3 and Fig. B6).

Table 2.2: Posterior summary statistics (median and 80% CI) of habitat and turbidity effects for the small ($\leq$15 mm CW) juvenile size class based on model g_1 . Habitat values represent the expected small juvenile density in a given habitat (abundance per m^2), holding random effects and ln turbidity at 0. Meanwhile, the last column reflects the effect (i.e. regression coefficient) of ln turbidity on small juvenile density, irrespective of habitat. Values are supplied on both the model (ln) and count scales.

Scale	Quantile	Sand	Seagrass	SME	SDH	ln **Turbidity**
Model	10%	-2.02	1.24	0.38	-1.54	-0.06
	50%	-1.06	2.63	1.55	-0.48	0.18
	90%	-0.10	3.94	2.66	0.58	0.43
Count	10%	0.13	3.47	1.47	0.21	0.94
	50%	0.35	13.83	4.70	0.62	1.20
	90%	0.91	51.39	14.30	1.78	1.54

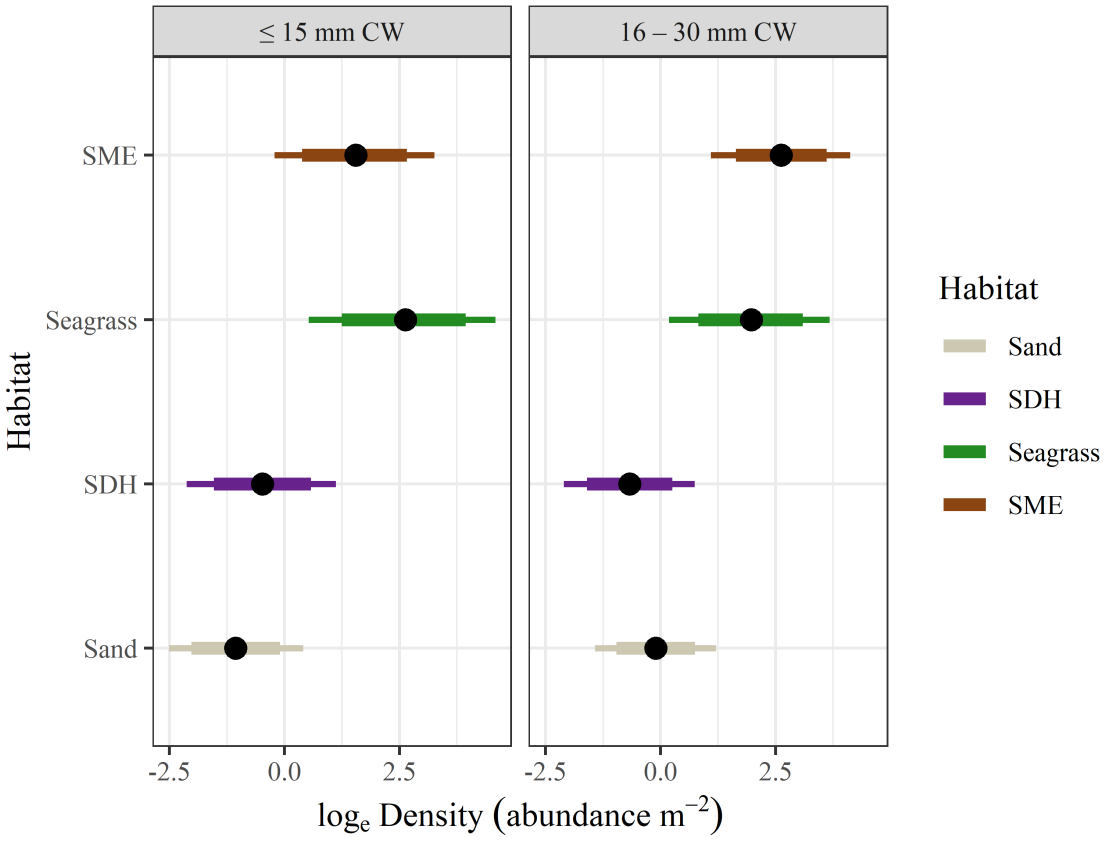

Figure 2.2: Posterior distributions of habitat-specific conditional ln expected densities (holding random effects and ln turbdity at 0), from model g_1 for both small ($\leq$15 mm CW; left column) and large (16–30 mm CW; right column) size classes. Dots denote posterior median expected values, while thick bars represent 80% Bayesian CIS and thin bars denote 95% Bayesian CIS.

Table 2.3: Within-size class linear contrast depicting differences in expected juvenile blue crab density between habitats from Model g_1 (model scale), holding random effects and ln turbidity at 0. Percentages indicate 80% CI and median of differences in effect sizes, while the final two columns list the probability of a positive or negative effect.

Size Class	Contrast	10%	50%	90%	Pr $>$ 0	Pr $<$ 0
Small	SDH – Sand	0.05	0.59	1.09	0.92	0.08
	Seagrass – Sand	2.83	3.70	4.47	$\approx$ 1.00	$\approx$ 0.00
	Seagrass – SDH	2.33	3.11	3.83	$\approx$ 1.00	$\approx$ 0.00
	Seagrass – SME	0.28	1.10	1.85	0.95	0.05
	SME – Sand	1.94	2.60	3.24	$\approx$ 1.00	$\approx$ 0.00
	SME – SDH	1.52	2.01	2.51	$\approx$ 1.00	$\approx$ 0.00
Large	SDH – Sand	-0.97	-0.56	-0.17	0.03	0.97
	Seagrass – Sand	1.44	2.08	2.68	$\approx$ 1.00	$\approx$ 0.00
	Seagrass – SDH	2.02	2.64	3.23	$\approx$ 1.00	$\approx$ 0.00
	Seagrass – SME	-1.27	-0.65	-0.07	0.07	0.93
	SME – Sand	2.21	2.73	3.24	$\approx$ 1.00	$\approx$ 0.00
	SME – SDH	2.84	3.29	3.76	$\approx$ 1.00	$\approx$ 0.00

2.4.2.2 Large (16-30 mm) size class

In contrast to the smaller size class, density of the large size class was highest in SME (13.80), followed by seagrass (7.19), sand (0.90), and SDH (0.51) (Table 3.8; Fig. 2.2). For pairwise linear contrasts among habitats SME–SDH, SME–sand, seagrass–SDH, and seagrass–sand, the posterior probability that a given contrast was positive exceeded 90%. Meanwhile, for pairwise linear contrasts among habitats seagrass–SME and SDH–sand, the posterior probability that a given contrast was negative exceeded 90%. Taken together, these results indicated that differences in the expected ln density of small juvenile crabs among habitats were statistically meaningful (Table 2.3 and Fig. B6).

Pairwise linear contrasts among habitats yielded posterior probabilities that a given contrast was positive or negative all exceeded 90%, indicating that differences in the expected density of large juvenile crabs among habitats were statistically meaningful (Table 2.3 and Fig. B7).

Table 2.4: Posterior summary statistics (median and 80% CI) of habitat and turbidity effects for the large (16–30 mm CW) juvenile size class based on model g_1. Habitat values represent the conditional expected large juvenile density in a given habitat (see Section 3.5). Meanwhile, the last column reflects the effect (i.e. regression coefficient) of ln turbidity on large juvenile density, irrespective of habitat. Values are supplied on both the model (ln) and count scales.

Scale	Quantile	Sand	Seagrass	SME	SDH	ln **Turbidity**
Model	10%	-0.96	0.82	1.64	-1.60	0.07
	50%	-0.11	1.97	2.62	-0.67	0.29
	90%	0.75	3.10	3.61	0.26	0.51
Count	10%	0.38	2.27	5.16	0.20	1.07
	50%	0.90	7.19	13.80	0.51	1.33
	90%	2.12	22.09	37.00	1.29	1.67

2.4.2.3 Comparisons among size classes

Within-habitat linear contrasts between small and large size classes indicated changes in habitat utilization with size. Moving from small to large size classes, utilization decreased in seagrass meadows, increased in both SME and sand, and did not change appreciably in SDH. The probability of seagrass harboring fewer large crabs than small crabs was 70%, indicating weak-moderate support but failing to meet our threshold for relevance. Meanwhile, the probability that SME and sand harbored more large individuals than small individuals were both 85% (Table 2.5; Fig. B8). Conversely, contrasts among size classes for SDH were distributed evenly across both negative and positive values, indicating considerable uncertainty and no discernible size effect.

Table 2.5: Within-habitat linear contrasts depicting differences in expected juvenile blue crab density between small and large size class (see Section 3.5) Positive values indicate increases in expected density as animals grow from $\leq$15 to 16 – 30 mm, while negative values indicate decreases in expected density. The first three rows indicate 80% CI and median values, while the final two rows list the probability of a positive or negative effect.

Quantile	Sand	Seagrass	SME	SDH
10%	-0.24	-2.22	-0.26	-1.46
50%	0.94	-0.66	1.07	-0.21
90%	2.17	0.95	2.47	1.12
Probability				
Pr $>$ 0	0.85	0.30	0.85	0.42
Pr $<$ 0	0.15	0.70	0.15	0.58

2.4.3 Turbidity effects

Turbidity was positively associated with juvenile density, though the effect of turbidity was stronger for large juveniles. Posterior distributions of regression coefficients for ln turbidity indicated a broadly positive effect for both small and large size classes. The probability that the effect sizes of turbidity were positive were 83% and 96% for small and large juveniles, respectively (Tables 3.6 and 3.8; Fig. 2.3 right of red line).

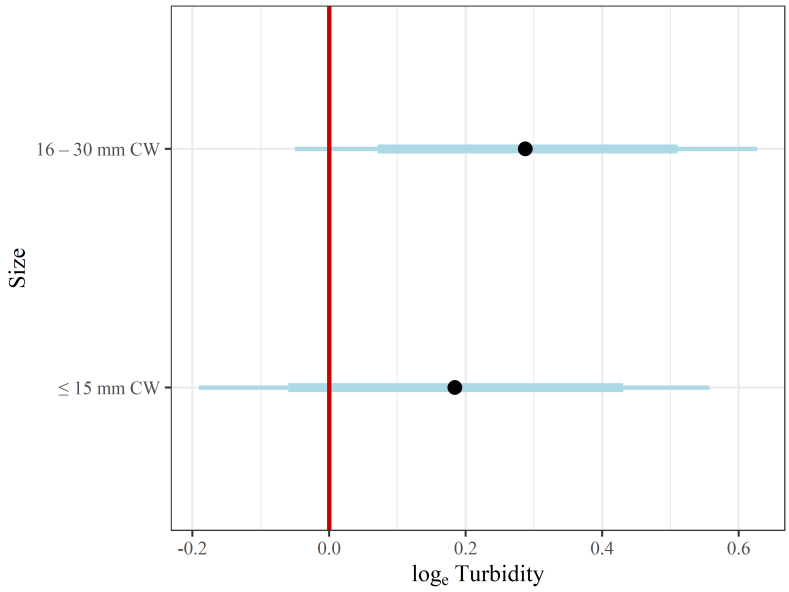

Figure 2.3: Posterior summaries (median and CIs) for ln turbidity regression coefficients for small (≤15 mm CW) and large (16–30 mm CW) size classes. Dots denote posterior median difference in expected values, while thick bars represent 80% Bayesian CIS and thin bars denote 95% Bayesian CIS. The red line denotes 0.

2.4.4 Correlation between size classes

The posterior distribution of ρ suggested that substantial dependence existed among size classes (Fig. 2.4). The posterior distribution of ρ yielded median of 0.90 (80% CI: 0.71–0.97), which indicated strong positive associations between size classes.

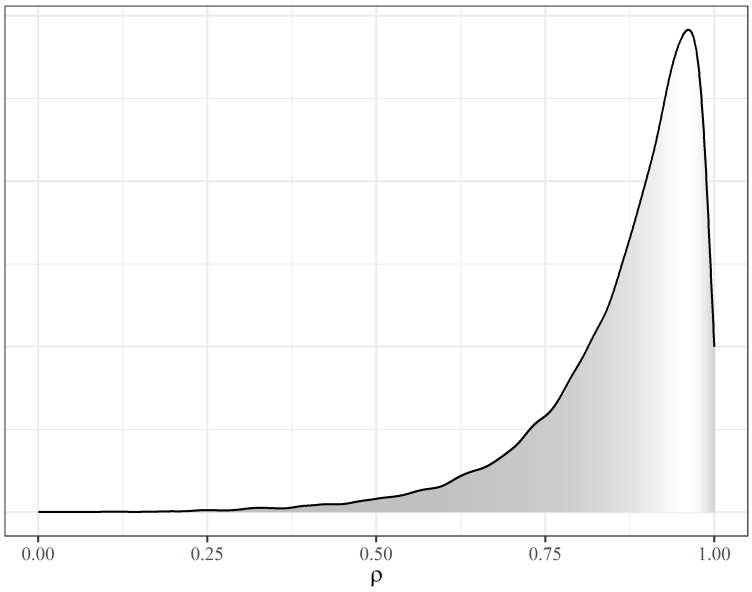

Figure 2.4: Posterior distribution for the correlation parameter ρ between small and large juvenile size classes.

2.5 Discussion

This study presents model-based evidence of differential habitat utilization among juvenile blue crab early-life stages and suggests the current paradigm surrounding blue crab early life history requires revision. Subsetting young-of-year juveniles into finer-scale size classes enabled us to observe shifts in density between small and large size classes among habitats, particularly from seagrass to SME. Our results are consistent with previous work emphasizing seagrass as an important nursery for the smallest juveniles (e.g. [103]), and suggest that SME represents a possible intermediate nursery habitat following initial emigration from seagrass beds but before occupying unstructured habitat commonly utilized by adults [105]. After accounting for habitat-specific differences in density, turbidity was positively related with both small and large juveniles. However, our models could not address whether this effect is due to top-down (predation) or bottom-up (food availability) controls. Although more evidence (i.e., comparisons of survival and growth) is required to ascertain the exact role of structured marsh habitat in juvenile blue crab ecology, we posit that both seagrass and SME habitats are important in maintaining adult populations and serve as nurseries for different size classes of juveniles.

2.5.1 Size-specific habitat effects

Small juvenile blue crab density was highest in structurally complex seagrass and SME habitats. In our study, seagrass meadows harbored the highest densities of small juvenile crabs, which is consistent with previous work emphasizing this habitat as the preferred nursery for small juveniles [154, 159, 77, 171, 219]. We also observed that SME harbored high densities of small juveniles per square meter relative to sand and SDH, although SME densities remained much lower than those estimated in seagrass. Postlarvae re-invading

Chesapeake Bay likely encounter seagrass beds and other SAV such as the non-native macroalga *Gracilaria vermiculophylla* and preferentially choose these habitats for initial settlement [201, 215, 88, 228]. However, heterogeneity in hydrodynamic conditions can cause a substantial proportion of ingressing postlarvae to miss structurally complex SAV habitats [201]. Although somewhat less suitable than SAV, SME provides an alternative nursery habitat. In addition, a proportion of early juveniles in SAV emigrate to alternative substrates to avoid adverse density-dependent effects [45, 172, 13]. High densities of juveniles observed in salt marshes at all spatial locations within the tributary likely reflect a combination of these two processes.

In contrast, small juvenile densities in SDH and sand were less than 1 m^{-2}, suggesting that these habitats were relatively unproductive. Although food availability can be high in sand, occupation by smaller juveniles in this habitat is likely discouraged by low structural refuge. High densities of small juveniles were reported inhabiting SDH in North Carolina estuaries [45, 46, 219]. We estimated far lower small juvenile densities in similar habitat in the York River. It is unclear why SDH is an attractive habitat for small juveniles in other locations but not within the York River, although differences in gear type or hydrodynamics associated with wind-driven vs tidally-driven estuaries may be responsible for these discrepancies. Specifically, logistical issues related to benthic scrapes may make this gear type inefficient when assessing abundance in SDH. Unlike sand, SDH is characterized by pitted surfaces and complex material, such that this gear type may be much less efficient in this habitat than efficiency estimates would indicate. As a result, we caution that our abundance estimates may be overly conservative, and stress that additional studies using gear better suited to sample SDH (e.g. kick-net sampling; [219]) are required to validate our estimates.

Our estimated habitat-specific abundance patterns changed notably between small and

large juveniles. Whereas small juveniles were more abundant in seagrass meadows than in SME, this pattern reversed among large juveniles. Moreover, large juveniles were more abundant in SME and less abundant in seagrass relative to small juveniles. Decreases in habitat-specific density of large juveniles with size are understood as being due to mortality or emigration of small juveniles. Mortality and emigration may explain decreases in juvenile abundance between small and large size classes, but the degree to which these processes affect density is not clear. In contrast, increases in the density of large juveniles in SME are indicative of a possible shift in habitat utilization concurrent with losses due to mortality and emigration, and consequently the preference of SME for this size class may be understated.

Patterns in size-specific habitat utilization observed here likely result from changing requirements of juvenile blue crabs with size. Seagrass meadows afford high survival to newly settled juveniles, particularly from smaller predators, due to the small interstitial spaces between shoots and rhizomes. In contrast, emergent salt marsh vegetation has higher interstitial space between shoots, allowing small predators such as the mummichog (*Fundulus heteroclitus*) to navigate and forage within the inundated marsh surface [155]. In the absence of juvenile density-dependent effects, smaller juveniles may prefer seagrass meadows because of the lower mortality risk when compared to salt marshes. However, upon reaching 10–15 mm CW, juvenile blue crabs outgrow the mouth-gape sizes of many smaller predators, making salt marsh habitats favorable [155, 211]. Furthermore, marsh shoots are dense enough to prevent larger predators from foraging effectively [87, 123]. Salt marshes additionally harbor abundant detrital material, bivalves, and other invertebrates, which are consumed by juveniles to accelerate growth [186]. The combination of lower mortality risk from small predators and high food availability is consistent with mechanisms driving ontogenetic shifts in many marine species [223, 34], and accounts for shifts in utilization from seagrass to SME as juveniles grow.

Similar to patterns we observed in SME, sand utilization also increased among large juveniles. Estimated densities of large juveniles in sand were nearly triple those of smaller juveniles, although in both size classes, abundance in sand was much lower than in seagrass and SME. These findings are consistent with the current paradigm that as juveniles reach 20–30 mm CW, they reach a size refuge from a broader suite of predators and are free to increasingly exploit unstructured habitat with less refuge but high food availability [105, 186].

Taken together with previous work and patterns observed in SME [105, 86, 82], our findings suggest that the existing paradigm of ontogenetic shift in juvenile blue crab habitat utilization requires revision. Although previous evidence supports shifts in blue crab habitat utilization at sizes exceeding 25 mm CW, our results suggest that juvenile blue crabs begin to emigrate from seagrass meadows to salt marsh habitat near 15 mm CW, before progressing to unstructured habitats at larger sizes (i.e. 25–55 mm CW) [105]. Emigration to SME at smaller sizes would also explain patterns at larger spatial and temporal scales [82], whereby density of juvenile blue crabs 20–40 mm CW was positively correlated with salt marsh habitat availability, especially in turbid areas. Although low densities of juveniles $>$30 mm CW prevented us from evaluating their habitat use of salt marsh, the present findings and related inferences would benefit from studies that consider additional size classes beyond those included here (e.g. $\leq$ 15, 16–30, and 31–45 mm CW size classes) to assess whether larger juveniles remain near marsh habitat or emigrate to other unstructured habitats.

2.5.2 Turbidity

In our study, juvenile blue crab abundance was positively associated with turbidity in both size classes. In addition, the association between turbidity and abundance of large juvenile

was stronger than that of small juveniles. High turbidity may increase juvenile abundance through both bottom-up and top-down controls. First, turbidity is positively associated with preferred food items of juvenile blue crabs: thin-shelled infaunal bivalves including the soft-shell clam *Mya arenaria* and Baltic clam *Macoma balthica* [187, 186]. These species constitute a substantial proportion of juvenile blue crab diets and they aggregate near estuarine turbidity maxima within Chesapeake Bay tributaries [187]. Turbid upriver unstructured habitats are associated with higher juvenile blue crab growth rates than those in downriver habitats [186]. Hence, association between turbidity and juvenile blue crab abundance may be a proxy for high prey abundance and bottom-up control. Second, turbidity may provide protection to juveniles from visual predators through a reduction in detectability [32, 4, 113], and it may also reduce cannibalism by larger congeners [146]. However, many estuarine-dependent predators possess adaptations to forage using chemo-tactile sensors in low-visibility environments characteristic of estuaries, and as a result it is unlikely that high turbidity provides more than a partial refuge from predation (e.g. summer flounder *Paralichthys dentatus*, blue catfish *Ictalurus furcatus*, adult blue crabs *callinectes sapidus*; [79, 59, 70]). Whether the association between turbidity and juvenile abundance is due to the former mechanism, the latter, or a combination of both is not addressed here and requires further research.

2.6 Conclusions and future work

Juveniles of marine fish and invertebrates encounter a diverse portfolio of habitats within the estuarine seascape. Habitat characteristics and environmental heterogeneity engender variability in vital rates. The attractiveness of a particular habitat to juveniles is dependent on size or life stage due to changing requirements as juveniles grow [223, 34, 105, 88]. These shifts in habitat utilization can occur at small sizes [140]. The relatively short duration

of occupancy, coupled with the tendency of studies to assess juvenile habitat requirements in aggregate (i.e. assessing the needs of immature animals without regard to size-classes), may cause researchers to underestimate the importance of transient habitats essential to juvenile organisms at specific life stages [140]. As requirements of juveniles may change most rapidly in their earliest life stages, it is imperative that fine-scale changes in habitat utilization be identified.

Our results both underscore the value of salt marsh habitat for small blue crab juveniles and is consistent with the hypothesis that salt marshes represent a valuable intermediate nursery habitat as larger juveniles move from seagrass meadows to unstructured bottom through ontogeny [223, 34, 105]. Loss of salt marsh habitat may thus impose a bottleneck in population dynamics as small juveniles emigrate from seagrass beds.

Although juvenile abundance is a key metric when assessing the nursery function of salt marsh habitat, its role in population dynamics requires assessment of secondary production to the adult segment of a population by the use of additional metrics including survival, growth, and juvenile-adult linkage [8]. For example, high juvenile abundance will not necessarily translate into high secondary production if survival of juveniles to adulthood is low. Further studies using additional metrics concomitantly, such as growth and survival, would help to clarify the role of salt marsh nursery habitats at the population level for blue crabs.

2.7 Caveats and limitations

Our study comes with several important caveats that should be considered when interpreting the inferences drawn from our results. First, although we included gear efficiency for each habitat concerning juvenile blue crabs in our design, it is essential to note that there might be differences in gear efficiencies for different size classes. Unfortunately, data on gear

efficiency as a function of juvenile blue crab size are currently unavailable. Thus, a major assumption of our work is that efficiency for both size classes is comparable. To ensure the robustness of our findings, future research should explore the viability of this assumption.

Second, our primary focus was on structurally complex habitats, but it is crucial to recognize that the vast majority of the York River consists of unstructured sand. Despite the low juvenile density in such areas, unstructured sand contributes significantly to adult populations in aggregate [105, 169], aligning with the effective juvenile habitat hypothesis [35]. While our current study primarily examines ontogenetic patterns in juvenile blue crab habitat shifts, it would be a mistake to overlook the substantial contribution of unstructured sand at population scales.

Third, it is important to acknowledge that our study was not replicated spatially in other tributaries within Chesapeake Bay, nor was it replicated temporally at an annual scale. This lack of replication raises questions about the generalizability of our findings. Unfortunately, logistical constraints prevented us from expanding the replication beyond the York River on a biweekly temporal scale. Although our results appear to align with findings from a broad-scale study that examined salt marsh utilization patterns for larger juveniles across multiple tributaries in Chesapeake Bay [82], we emphasize the need for future studies to replicate these investigations across multiple size classes and locations within Chesapeake Bay to ensure the reliability of our conclusions.

Finally, it is crucial to reiterate the uncertainty surrounding SDH due to gear limitations and logistical challenges. While we made efforts to sample this habitat, there is a strong possibility that it plays a significant nursery role similar to observations described in other systems. Hence, future research should focus on evaluating the nursery role of shallow detrital habitats in Chesapeake Bay.

In summary, we acknowledge these limitations and emphasize the need for further

research to confirm and strengthen the validity of our findings on ontogenetic juvenile blue crab habitat shifts.

Chapter 3

Model-based evaluation of critical nursery habitats for juvenile blue crabs through ontogeny: abundance and survival in seagrass, salt marsh, and unstructured bottom

Abstract

Ontogenetic nursery habitat shifts refer to the dynamic changes in habitat preferences exhibited by juvenile organisms as they progress through different stages of their life cycle. During early developmental phases, juveniles often seek specific nursery habitats that offer optimal conditions for survival, such as protection from predators. However, juvenile marine and estuarine organisms commonly use multiple habitats as nurseries at

different life stages to satisfy shifting resource requirements, such as preferences for higher food availability over refugia at larger sizes. It is important to identify and conserve all habitats used by a species through ontogeny. To this end, we conducted manipulative and mensurative field experiments to evaluate two nursery metrics, abundance and survival, for juvenile blue crabs across multiple size classes and habitats, including structurally complex habitats — seagrass meadows and salt marshes — and unstructured habitat (sand flats) in the York River, Chesapeake Bay. We also considered effects of site-specific spatial orientation within the York River, seasonality, physicochemical variables, and postlarval influx. Our results showed that abundance was higher in both seagrass meadows and salt marshes relative to unstructured sand, and positively associated with turbidity and post-larval abundance. Notably, seagrass habitats harbored the highest abundances of small ($\leq$15 mm carapace width) juveniles, whereas salt marsh edge harbored the highest abundance of medium (16–30 mm carapace width) and large (31–60 mm carapace width) juveniles. Moreover, survival was positively associated with juvenile size and structurally complex habitats relative to unvegetated controls. Seasonally, survival peaked in April, reached a seasonal minimum in August, and increased throughout fall. Finally, habitat-specific survival was dependent on spatial position: survival was elevated at upriver salt marsh and unstructured sand habitats compared to downriver counterparts. Taken together, abundance and survival results indicate that seagrass meadows are key nurseries primarily for early-stage juveniles, whereas salt marshes are an intermediate nursery habitat for larger individuals, most likely to maximize growth-to-mortality ratios. Our results underscore the need to consider both habitats as critical nurseries for juvenile blue crabs throughout ontogeny.

3.1 Introduction

The population dynamics of marine and estuarine organisms are dependent upon multiple habitats used throughout their life cycles. Specifically, the value of a particular habitat to juveniles is dependent on size- or life-stage due to changing growth and survival requirements [223, 34, 105, 52]. Juveniles possess life-history strategies that maximize energy gains (i.e. growth rates) and minimize predation risk [223, 34]. In many cases, however, there are trade-offs; habitats that offer higher potential growth rates can have greater risks of predation [105]. Juvenile habitat use therefore shifts with transitions between different life stages because of changing resource needs as well as altered predation risk. Initially, the earliest juvenile life stages are the smallest and most vulnerable to predation, and typically prioritize refuge for survival over food availability for growth [88]. As juveniles grow, their probability of survival increases as their size exceeds the mouth gapes of many smaller predatory species [141]. However, to continue growth and development, juveniles must have access to ample food resources.

Literature on nursery habitats has increasingly emphasized the need to consider all critical habitats utilized by a species throughout ontogeny [140]. Prioritizing only a subset of nursery habitats throughout ontogeny may miss bottlenecks at one or more life stages. For example, if initial settlement habitats are conserved, but intermediate habitats used by larger size classes deteriorate, overall population abundance may decrease. Explicitly focusing on vital rates for only a single size class or multiple size classes in aggregate is insufficient for complete nursery inference [192, 191]; multiple size classes must be evaluated concomitantly across candidate habitats to identify the full scope of nursery habitats required to maintain healthy populations [140, 81].

One economically important species which uses multiple nursery habitats during early

life stages is the blue cab, *Callinectes sapidus*. Initially, ingressing postlarvae (herein, megalopae) preferentially settle into seagrass habitats when available, but may use other structurally complex habitats if seagrass meadows are unavailable or competition for space/resources in seagrass is substantial due to high juvenile densities. The current paradigm maintains that juveniles emigrate to unstructured habitat after reaching 30 mm carapace width (CW), upon which individuals reach a size refuge from predation and may exploit abundant food resources in unstructured habitat [103]. However, abundances of 16 – 30 mm CW crabs are higher in salt marshes [169, 176, 81], particularly salt marsh habitat near the estuarine turbidity maximum [82]. These recent findings suggest that salt marsh habitat may serve as an intermediate nursery due to higher food availability, which may be ideal for larger juveniles.

Although the proposed mechanism for these shifts is hypothesized to be changes in the mortality-to-growth ratio, evidence is circumstantial, and several important questions remain. First, previous work did not consider abundance patterns with respect to spatial variation in megalopae supply. Without information on megalopae supply, it is unclear whether juvenile abundance patterns across habitats are a function of habitat quality or simply reflect higher numbers of ingressing postlarval recruits [192]. Second, the refuge function of salt marsh habitat for blue crabs is not well understood. Although previous mesocosm experiments suggest juvenile blue crab survival is higher in salt marshes relative to unstructured habitats [87, 123], there is little field evidence to validate this hypothesis. For example, juvenile survival was equivalent in salt marshes and unstructured habitat in a fragmented salt marsh system in the Gulf of Mexico [189], and no comparable field studies exist to evaluate juvenile survival among multiple structured habitats in mid-Atlantic estuaries. Robust inferences on ontogenetic habitat shifts require information on larval supply, juvenile abundance, and juvenile survival to understand the relative importance of

both initial nursery habitats and intermediate habitats within the estuarine seascape for a given life stage [8, 140].

In this study, we conducted mensurative (abundance) and manipulative (survival) field experiments to investigate juvenile blue crab abundance and survival across multiple nursery habitats and juvenile size classes. Our objectives were to 1) evaluate the extent to which habitat- and size-specific vital rates were consistent with the existing paradigm on juvenile blue crab life history and 2) determine the contribution of multiple structurally complex habitats to juvenile blue crab secondary production at various juvenile stages. These objectives are in light of the fact that ontogenetic shifts in larger size classes of juvenile blue crabs are presently unclear, notwithstanding the well understood principles regarding ontogenetic habit shifts in general ecology [223, 34], and the robust association between the smallest individuals and seagrass meadows[103]. In addition, both megalopae supply and turbidity may influence abundance [45, 46, 201, 82], and turbidity alone may influence survival [4, 78], potentially confounding results if either were excluded. Hence, we concurrently assessed the influence of spatially varying turbidity and megalopal supply through comprehensive field sampling. To address these objectives, we constructed Bayesian hierarchical models to evaluate the effects of two structurally complex habitats – seagrass beds (herein, seagrass) and salt marsh edge (herein, SME) – as well as unstructured sand habitat (as a control; herein, sand) across the seascape of the York River, a tributary of Chesapeake Bay. We focused on three size classes of juveniles: small ($\leq$15 mm CW), medium (16–30 mm CW) and large (31–60 mm CW).

3.2 Methods

3.2.1 Study Area

Blue crab abundance sampling and survival experiments were conducted in the York River, a tributary in the lower portion of western Chesapeake Bay. The tributary contains a wide range of habitat configurations and gradients of environmental variables such as turbidity [81]. In addition, the York River harbors high abundance of juvenile blue crabs spanning multiple size classes [82]. These characteristics make the York River an ideal natural laboratory for nursery habitat comparisons among multiple size classes.

The river was divided into sections based on morphology, constituting downriver, midriver, and upriver strata (Fig. 3.1). This is in contrast to Chapter 2, which arbitrarily divided the system into three approximately equal sections. Here, we used the Coleman Bridge (Lat = 37.2421, Lon = -76.5068) as a logical delineation between downriver and midriver strata due to the large changes in hydrology associated with this area of geographic constriction and may limit megalopae supply to upriver areas [201]. Delineation between midriver and upriver remained consistent with Chapter 2.

Figure 3.1: Map displaying sampling sites for the York River. **A**: abundance sites; **B**: megalopae sites; **C**: survival sites; and **D**: a close-up of seagrass abundance sites sampled in the downriver stratum. Megalopae (i.e. postlarvae) sites are not habitat-specific and are not color-coded by habitat.

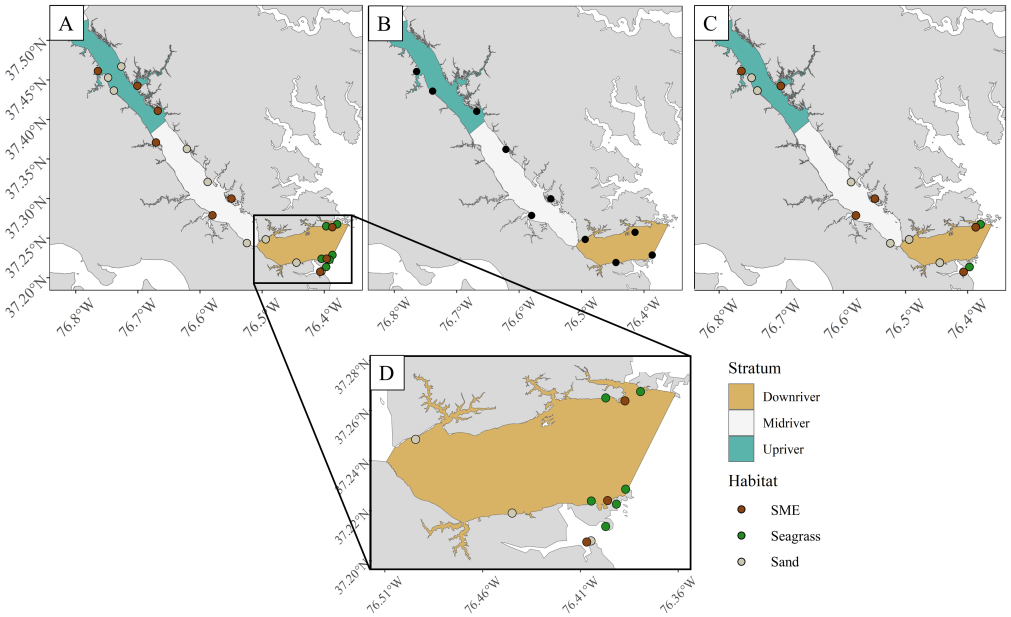

3.2.2 Predictors

We considered six environmental and biological variables (herein, predictors) as potential determinants of abundance and survival for juvenile blue crabs (Tables 3.1 and 3.2). Although most predictors were included in both the abundance and survival models (Sections 3.2.4.1 and 3.2.4.2), some were only included in one or the other model. We justify the inclusion or exclusion of each predictor for a given model in Tables 3.1 and 3.2. We did not include salinity as a predictor in either model due to substantial collinearity with turbidity and location along the river axis. For a detailed description and justification of all predictors, see Appendix C.

Table 3.1: Descriptions and justifications of predictors used in modeling juvenile abundance.

Predictor	Levels (if categorical)	Justification and prediction	References
Habitat	Seagrass SME Sand	Abundance should be higher in structurally complex seagrass and SME relative to sand.	[154, 105, 103, 88, 171, 82, 81]
Stratum	Downriver Midriver Upriver	Spatial position may influence abundance through spatially correlated, unobserved variables.	[165, 105]
Megalopae	continuous	Abundance is initially dictated by postlarval supply.	[46, 66, 65]
Turbidity	continuous	Abundance is positively correlated with turbidity due to higher food availability and refuge afforded by turbid habitat.	[32, 113, 146, 78, 74]

Table 3.2: Descriptions and justifications of predictors used in the juvenile survival model. The categorical variables stratum, habitat, and structure form an incomplete, crossed design and therefore are collapsed into a single categorical variable (Str x Hab x Struc indicates stratum–habitat–structure interaction). For details, see Appendix C.

Predictor	Levels (if categorical)	Justification and prediction	References
Str x Hab x Struc	Downriver seagrass structured Downriver seagrass unstructured Downriver SME structured Downriver SME unstructured Downriver sand Midriver SME structured Midriver SME unstructured Midriver sand Upriver SME structured Upriver SME unstructured Upriver sand	Survival will vary as a function of spatial stratum, habitat, and structure due to differences in spatial and habitat-specific predator assemblages, refuge quality, and alternative prey availability.	[154, 105, 103, 88, 171, 82, 81, 165, 105, 76, 77]
Month	April May June August September October	Juvenile blue crab survival fluctuates seasonally.	[73, 70, 103]
Turbidity	Continuous	Survival is positively correlated with turbidity due to higher refuge afforded by turbid habitat	[146, 78, 74]
Size	Continuous	Survival increases with size. As juvenile blue crabs grow, they are less susceptible to predation as their carapace widens and hardens, spines become more prominent, and aggressive behavior intensifies.	[73, 77, 103, 15]

3.2.3 Field Sampling

All sampling sites were selected from a subset of sites used in the random sampling design from Chapter 2 (Fig. 3.1). Subsampling was due to changes in the primary gear type for sand habitat (i.e. seine hauls instead of boat-mounted scrapes) which reduced the number of samples logistically feasible. Survival sites were also a subset of sites in Chapter 2 for logistical reasons. For juvenile abundance sampling, three SME and sand sites were randomly selected from the six habitat-specific sites in each stratum from Chapter 2. The six seagrass sites used in the downriver stratum were consistent with those employed in Chapter 2 (n_{sites} = 3 x 6 + 6 = 24). In midriver and upriver strata, seagrass was not present and only sand and SME were investigated. Megalopae sampling was used to assess the effect of postlarval supply on juvenile blue crab abundance, particularly for the small size class. Logistical limitations prevented us from sampling megalopae at every abundance site. Therefore, site selection for megalopae sampling and survival assessment was based on a random subsample of the 24 abundance sites. Specifically, three random shoreline sites in the upriver and midriver strata and four sites in the downriver stratum were randomly chosen (n_{sites} = 10). Finally, in the survival study two tethering sites were randomly selected from the three abundance sites for each habitat within each stratum (n_{sites} = 14). Turbidity was recorded a Secchi disk (proxy for inverse of turbidity) at each site on each trip for all three sampling procedures. For a detailed description of sampling effort by study type, habitat, and stratum, see Table C1.

3.2.3.1 Juvenile abundance

Juvenile abundance was sampled at each station in seagrass, SME, and sand at biweekly intervals between August 5th and October 14th, 2021 (5 trips x 24 sites = 120). Juvenile blue crabs in sand sites were sampled using a 5 m seine net (half-circle sweeps), while

SME sites were sampled using modified flume nets [116]. At seagrass sites, a suction sampler was utilized to collect juvenile blue crabs [154, 171, 77, 66]. All gear types used 3 mm^2 mesh. Juvenile crabs were counted and measured for carapace width (see Chapter 2 for additional details on abundance sample processing).

As different sampling methods were employed for the three habitat types, gear efficiency estimates were required to scale abundance estimates for each sample. Efficiency of the suction sampling methodology is estimated at 88% [154], while efficiency tests of the modified flume net design using marked blue crabs in fall of 2020 suggested an estimated efficiency of 92% [81]. Finally, literature suggested efficiency estimates for seine nets targeting juvenile blue crabs varied between 10–50% (mean 30% ;[37]). These efficiency estimates and their associated uncertainties were included as Bayesian prior distributions in juvenile abundance models both to more accurately determine the effects of habitat as well as to incorporate relevant uncertainty into model estimates. For additional details on how gear efficiency was incorporated in the model, see Table 3.3, Section 3.2.4.1, and Chapter 2.

3.2.3.2 Megalopae

Megalopae sampling was used to assess the effects of postlarval supply on juvenile blue crab abundance. Sampling took place at biweekly intervals between July 16th and October 7th, 2021, following new and full moon cycles (7 trips x 10 sites = 70; [214, 43, 44]). Collectors consisted of a hog's hair filter sleeve surrounding an inner PVC cylinder (0.18 m^2; [214, 121]), deployed for approximately 12 h from sunset to sunrise. Upon collection, filters were submersed in fresh water in the field for 1 h to remove megalopae. The filters were then transported to the lab and rinsed again in fresh water three times until no fauna remained. The filter contents were subsequently sieved using 500 micron mesh. Sieve

contents were sorted underneath a magnifying glass for blue crab megalopae, which are distinct in coloration and morphology relative to other local estuarine crustacean larvae [147]. Megalopae were counted and recorded along with local turbidity as described in Appendix **??**.

3.2.3.3 Survival

A tethering experiment was conducted at biweekly intervals between April and November, 2021 with juvenile crabs of 6–50 mm CW (n = 848), using an established tethering technique to assess survival [105]. July was not considered because logistical issues prevented sampling in that month. Tethering was conducted in $<$1 m mean low water to limit the influence of depth [177]. At each site, five crabs were haphazardly selected and tethered in both structured (where present) and unstructured treatments. Within a habitat/treatment, individual tethers were haphazardly spaced $\sim$5 m apart. The size (CW) of each crab was measured to the nearest 0.1 mm using calipers prior to deployment, and deployed for $\sim$24 h. Within SME and seagrass, locations within the delineated habitat which were devoid of vegetation were regarded as “unstructured” and used to compare variation in survival at the patch scale. Unstructured SME habitat was defined as areas devoid of vegetation immediately adjacent to the SME, whereas unstructured seagrass habitat was defined as interstitial barren patches within or immediately adjacent to seagrass beds. In contrast, “structured” SME and seagrass habitat were defined as localities within those habitats where vegetation was present. Within SME and seagrass habitats, crabs were tethered in both structured and unstructured treatments. Only seagrass patches with 100% aerial cover were considered in the structured seagrass treatment, while sand consisted of only an unstructured treatment. Additional details, including assessment of treatment-specific bias, can be found in Appendix C.3.

3.2.4 Analysis

All data analyses, transformations, and visualizations were completed using the R programming language for statistical computing [167] and the Stan probabilistic programming language for Bayesian statistical modeling [199, 198].

3.2.4.1 Abundance

Relationships between abundance and environmental variables for small juvenile blue crabs were modeled using a multivariate negative binomial linear mixed-effects model under a Bayesian framework. Predictor variables for juvenile abundance data included habitat (seagrass, SME, and sand), stratum (downriver, midriver, and upriver), megalopae local abundance four weeks prior to each sampling trip (averaged across stratum), and turbidity. Natural log (ln)-transformations were applied to both turbidity and megalopae abundance prior to analyses (see Appendix **??** for details).

Extending the model from [81], for the s^{th} site on date t in habitat h, the model for juvenile blue crab abundance in the i^{th} size class is expressed as:

$$
\begin{aligned}
y_{hsti} | \mu_{hsti}, \phi_i &\sim \text{NB}(\mu_{hsti}, \phi_i) \\
\ln(\mu_{hsti}) &= x_{hst}^{\top} \beta_i + \theta_{hsi} + A_h \\
\beta_i &= [\beta_{1i}, \beta_{2i}, \ldots, \beta_{pi}]^{\top} \\
\begin{bmatrix} \theta_{hs1} \\ \theta_{hs2} \\ \theta_{hs3} \end{bmatrix} &| \Sigma \sim \text{MVN}(0, \Sigma) \\
\Sigma &= \sigma_{\theta}^2 (D - \lambda W)^{-1} \\
\lambda &\sim \text{U}(-1, 1) \\
\sigma_{\theta}^2, \phi_1, \phi_2, \phi_3 &\sim \text{inverse-Gamma}(1, 1)
\end{aligned}
\tag{3.1}
$$

where $NB(\mu_{hsti}, \phi_i)$ denotes a negative binomial type II distribution with mean μ_{hsti}, while ϕ_i controls the over-dispersion for each size class such that $E[y_{hsti}] = \mu_{hsti}$ and VAR$[y_{hsti}] = \mu_{hsti} + \frac{\mu_{hsti}^2}{\phi_i}$. The response variable, juvenile crab counts for each size class i, is denoted y_{hsti} where $i = 1$ denotes CW $\leq$15 mm, $i = 2$ denotes 16–30 mm, and $i = 3$ denotes 31–60 mm. Total area sampled in habitat h (SME = 1 m^2, seagrass = 1.68 m^2, sand = 9.81 m^2) is included as an offset term A_h. Meanwhile, β_i refers to regression coefficients for each size class i associated with predictors x_{hst}, while $\top$ denotes that the β_i coefficients were transposed. Measurements of both the abundances of size classes and predictors x_{hst} were taken at the site-trip spatiotemporal resolution, such that predictors were not specific to any one size class i but to all sizes classes at a given site-trip. Here, θ_{hsi} denotes a site-specific random effect for a given size class i. The joint probability distribution of $(\theta_{hs1}, \theta_{hs2}, \theta_{hs3})$ is specified as multivariate normal with a mean vector of 0s and variance-covariance matrix Σ. The Σ matrix describes dependence among size classes based on the nearest neighbor structure specified by a 3×3 adjacency matrix, W, and an autocorrelation parameter λ,

which controls the degree of autocorrelation among size classes. We employed a binary weighting scheme for W where $w_{i,i'} = 0$ for all (i, i') unless size classes $i \neq i'$ were adjacent. For example, the smallest size class ($\leq$15 mm CW) and the next largest $i = 2$ (16–30 mm CW) are considered adjacent because increases in size among individuals in $i = 1$ would shift them to $i = 2$, whereas size classes $i = 1$ and $i = 3$ are not considered adjacent because individuals in size class $i = 1$ ($\leq$15 mm CW) would need to move through size class $i = 2$ prior to reaching $i = 3$ (31–60 mm CW). Hence the 3×3 binary adjacency matrix employed here is expressed as:

$$W = \begin{bmatrix} 0, 1, 0 \\ 1, 0, 1 \\ 0, 1, 0 \end{bmatrix}$$

The influence of an adjacent size class on a given size class was standardized by subtracting λW from D, a diagonal matrix where $D_{i,i}$ is the number of neighbors for size class i (1, 2, and 1 for size classes $i = 1,\ 2,$ and 3 respectively). The parameter λ was constrained between -1 and 1 through a uniform prior. This size class dependence structure was assumed to be homoscedastic through the variance parameter σ^2_θ, with an inverse-Gamma$(1, 1)$ hyperprior. A similar parameterization is outlined in [82], although here the nearest neighbor structure refers to covariance among size classes instead of covariance across spatial polygons. Results from [81] suggested that spatial dependence was accounted for by spatial stratum and site random effects.

Initial model priors for fixed-effects coefficients were derived from the posterior inference from Chapter 2, which examined the same sites, habitats, and size classes except for the largest size class $i = 3$. For size class $i = 3$ (31–60 mm CW), supplied prior means were identical to those for size class $i = 2$, while prior variances were scaled by a factor of 4 (model scale) to account for higher prior uncertainty associated with this size class. Descriptions of fixed effects included in the preliminary juvenile abundance model as well

as their corresponding prior distributions are listed in Table 3.3.

Table 3.3: Descriptions of predictor coefficients used in the juvenile abundance model. Prior distributions are on the model (log) scale. All β terms refer to priors of a given coefficient for all three size classes (Small = $\leq$15 mm CW; Medium = 16–30 mm CW; Large = 31–60 mm CW.

Predictor	Regression Coefficient	Description	Prior (Small)	Prior (Medium)	Prior (Large)
—	β_{0i}	Intercept of model (i.e. intercept of the reference, taken to be sand downriver)	N$(-1.10, 0.75)$	N$(-0.11, 0.67)$	N$(-0.11, 2.00)$
Turbidity	β_{1i}	Effect of water cloudiness measured as the negative log transformation of the Secchi disk depth (m) in site s on date t (see Appendix **??** for details)	N$(0.19, 0.19)$	N$(0.29, 0.17)$	N$(0.29, 2.00)$
SME	β_{2i}	Effect of SME relative to the reference	N$(2.59, 0.51)$	N$(2.72, 0.4)$	N$(2.72, 2.00)$
Seagrass	β_{3i}	Effect of seagrass habitat relative to the reference	N$(3.67, 0.64)$	N$(2.07, 0.49)$,	N$(2.07, 2.00)$
Midriver	β_{4i}	Effect of midriver stratum relative to the reference	N$(0, 10)$	N$(0, 10)$	N$(0, 10)$
Upriver	β_{5i}	Effect of upriver stratum relative to the reference	N$(1.20, 10)$	N$(1.2, 10)$	N$(1.2, 10)$
Megalopae	β_{6i}	Effect of ln(average megalopae abundance + 1) in a given stratum corresponding to site s four weeks prior to the t^{th} date (see Appendix **??** for details)	N$(0, 10)$	N$(0, 10)$	N$(0, 10)$
Suction efficiency	β_{7i}	Suction efficiency parameter for juvenile blue crab abundance in seagrass	N$(-0.13, 0.02)$	N$(-0.13, 0.02)$	N$(-0.13, 0.02)$
Flume efficiency	β_{8i}	Flume efficiency parameter for juvenile blue crab abundance in SME	N$(-0.08, 0.02)$	N$(-0.08, 0.02)$	N$(-0.08, 0.02)$
Seine efficiency	β_{7i}	Seine efficiency parameter for juvenile blue crab abundance in sand	N$(-1.27, 0.41)$	N$(-1.27, 0.41)$	N$(-1.27, 0.41)$
Area (log)	A	Offset term relating juvenile blue crab abundance to surface area of gear used to sample habitat h	—	—	—

3.2.4.2 Survival

Crab survival, recorded as 1 (alive) or 0 (eaten), was analyzed for probability of survival using a hierarchical logistic regression mixed-effects model. Within stratum, unstructured treatments among habitats (seagrass, SME, and sand for downriver or SME and sand otherwise) were compared to isolate effects of differing predation pressure and refuge. Within a given stratum and within SME and seagrass habitats (where present), nearby structured and unstructured treatments were compared to facilitate inference on the effect of structure while controlling for differences in predation pressure. Due to the nature of our sampling design, we approximated nonlinear effects of seasonality by using month as a categorical fixed effect.

For the j^{th} tether trial in the s^{th} site on date t, the model for juvenile blue crab survival is expressed as:

$$
\begin{aligned}
y_{stj}|\pi_{st} &\sim \text{Bernoulli}(\pi_{st}) \\
\text{logit}(\pi_{st}) &= x_{st}^{\top}\beta + \theta_s + \eta_{st} \\
\theta_s|\sigma_\theta^2 &\sim N(0, \sigma_\theta^2) \\
\eta_{st}|\sigma_\eta^2 &\sim \text{N}(0, \sigma_\eta^2) \\
\beta_i &\sim N(0, 10) \\
\sigma_\theta^2, \sigma_\eta^2 &\sim \text{inverse-Gamma}(1, 1).
\end{aligned}
\tag{3.2}
$$

The response, binary juvenile crab survival y_{stj} for the j^{th} tethering trial, is distributed as a Bernoulli random variable with probability of survival, π_{st}. Tethering trials entailed

repeatedly using the same sites, which may introduce site-specific bias. Moreover, 5 m spacing of individual tethers within a site may not have been sufficient to guarantee independence [6]. Hence, θ_s and η_{st} denote site-specific and site within trip-specific random effects, respectively. All regression coefficients were assigned diffuse priors ($N(0, 10)$). Descriptions of the fixed effects for the preliminary juvenile blue crab survival model can be found in Table 3.4.

Table 3.4: Descriptions of regression coefficients used in the juvenile survival model. The categorical variables stratum, habitat, and structure form an incomplete, crossed design and therefore are collapsed into a single categorical variable. For details, see Appendix **??**.

Predictor	**Regression Coefficient**	**Description**
—	β_0	Intercept of model (i.e. the reference intercept, taken to be the intercept for sand downriver in April)
Turbidity	β_1	Effect of water cloudiness measured as the negative log transformation of the Secchi disk depth (m) in site s on date t (see Appendix **??** for details)
Carapace width	β_2	Effect of crab width (mm)
May	β_3	Effect of May relative to the reference
June	β_4	Effect of June relative to the reference
August	β_5	Effect of August relative to the reference
September	β_6	Effect of September relative to the reference
October	β_7	Effect of October relative to the reference
Downriver SME structured	β_8	Effect of downriver structured SME relative to the reference
Midriver SME structured	β_9	Effect of midriver structured SME relative to the reference
Upriver SME structured	β_{10}	Effect of upriver structured SME relative to the reference
Downriver SME unstructured	β_{11}	Effect of downriver unstructured SME relative to the reference
Midriver SME unstructured	β_{12}	Effect of midriver unstructured SME relative to the reference
Upriver SME unstructured	β_{13}	Effect of upriver unstructured SME relative to the reference
Downriver seagrass structured	β_{14}	Effect of downriver structured seagrass relative to the reference
Downriver seagrass structured	β_{15}	Effect of downriver unstructured seagrass relative to the reference
Midriver sand	β_{16}	Effect of midriver sand relative to the reference
Upriver sand	β_{17}	Effect of upriver sand relative to the reference

3.2.5 Model implementation and validation

For each model, Bayesian inference required numerical approximation of the joint posterior distribution of all model parameters including the vectors of random effects. To this end, we implemented the above models using the Stan programming language for Bayesian inference to generate Hamiltonian Monte Carlo (HMC) samples from the posterior [57]. For each model, we ran four parallel Markov chains, each with 5,000 iterations for the warm-up/adaptive phase, and another 5,000 iterations as posterior samples (i.e. 20,000 draws in total for posterior inference). Convergence of the chains was determined both by visual inspection of trace plots (e.g. Fig. D3) and through inspection of the split $\hat{R}$ statistic. All sampled parameters had an $\hat{R}$ value less than 1.01, suggesting chain convergence [57]. Covariates and interactions whose regression coefficients had Bayesian confidence intervals (CIs) that excluded 0 at a confidence level of 80% were considered scientifically relevant to juvenile blue crab abundance and survival. All CIs referenced here are highest posterior density intervals [115].

3.2.6 Conditional inference

Conditional means and conditional effects plots were used to assess the relationship between response variables (juvenile blue crab abundance and survival) and meaningful predictors both among habitats within a size class and within habitats between size classes. Herein, we refer to "conditional" as holding all random effects at 0 and fixing co-varying predictors. For a detailed description of the estimation procedure for each conditional quantity, see Table 3.5. Conditional effects for categorical terms are reported using posterior median values and 80% CIs, while the relationship between the conditional mean ($\mu_{\text{cond}_{vi}}$ or π_{cond_v}) and each continuous predictor (x_{vi} or x_v) was plotted with posterior medians as well as 50%, 60%, and 80% credible bands.

Table 3.5: Descriptions of conditional means and conditional effects derived from the abundance and survival models.

Model	Term	Description	Equation
Abundance	$\mu_{\text{cond}_{hi}}$	The expected number of crabs in size class i in habitat h, with random effects fixed at 0, ln turbidity and ln megalopae fixed at 0, and stratum taken to be downriver (reference).	$exp(\beta_{0i})$ for h $=$ reference $exp(\beta_{hi} + \beta_{0i})$ for h $>$ reference
	$\mu_{\text{cond}_{vi}}(x_{vi})$	The expected number of crabs in size class i as a function of continuous predictor x_{vi}, with random effects fixed at 0, all other continuous predictors fixed at 0, and categorical terms fixed at the reference (i.e. downriver sand).	$exp(\beta_{0i} + \beta_{vi}x_{vi})$
	$\eta_{\text{cond}_{hi}}$	The ln $\mu_{cond_{hi}}$ (i.e. the linear predictor).	β_{0i} for h $=$ reference $\beta_{hi} + \beta_{0i}$ for h $>$ reference
	L_{hi-mi}	The linear contrast between habitat h and habitat m for size class i	$\eta_{cond_{hi}} - \eta_{cond_{mi}}$
Survival	π_{cond_j}	The probability of survival at categorical level j, with random effects fixed at 0, ln turbidity fixed at 0, and crab width fixed at 22.4 mm (i.e. average crab size in study). When j denotes a stratum-habitat-structure combination, month is held at April. When j denotes a month, stratum-habitat-structure is fixed at downriver sand.	$expit(\beta_0)$ for j $=$ reference $expit(\beta_j + \beta_0)$ for j $>$ reference
	γ_{cond_j}	The linear predictor (logit π_{cond_j})	β_0 for j $=$ reference $\beta_j + \beta_0$ for j $>$ reference
	W_{j-r}	The linear contrast between levels j and r.	$\gamma_{cond_j} - \gamma_{cond_r}$
	$\pi_{\text{cond}_v}(x_v)$	The probability of survival as a function of continuous predictor x_v, with random effects fixed at 0, all other continuous predictors fixed at 0 (except crab CW, fixed at 1 mm to show increased contrast in survival probabilities), and categorical terms fixed at the reference.	$expit(\beta_0 + \beta_v x_v)$

3.3 Results

3.3.1 Abundance

3.3.1.1 Patterns in abundance among small-sized ($\leq$15 mm) juveniles

Habitat was an important driver of small juvenile blue crab abundance (Table 3.6; Fig. C2). Among habitats, the estimate (i.e. posterior median) of the conditional mean ($\mu_{\text{cond}_{h,15}}$, Table 3.5) for small juvenile blue crab abundance was highest in seagrass, followed by SME and sand (Table 3.6; Fig. 3.2, left panel). Linear contrasts ($L_{h,15-m,15}$) between habitats for small juvenile blue crabs all yielded 80% Bayesian CIs that excluded 0, indicating that differences in the expected number of small juvenile crabs among habitats were statistically meaningful (Fig. 3.3, left panel). Herein, we use the term “indicate” to refer to inferences with strong statistical support (see section 3.2.5).

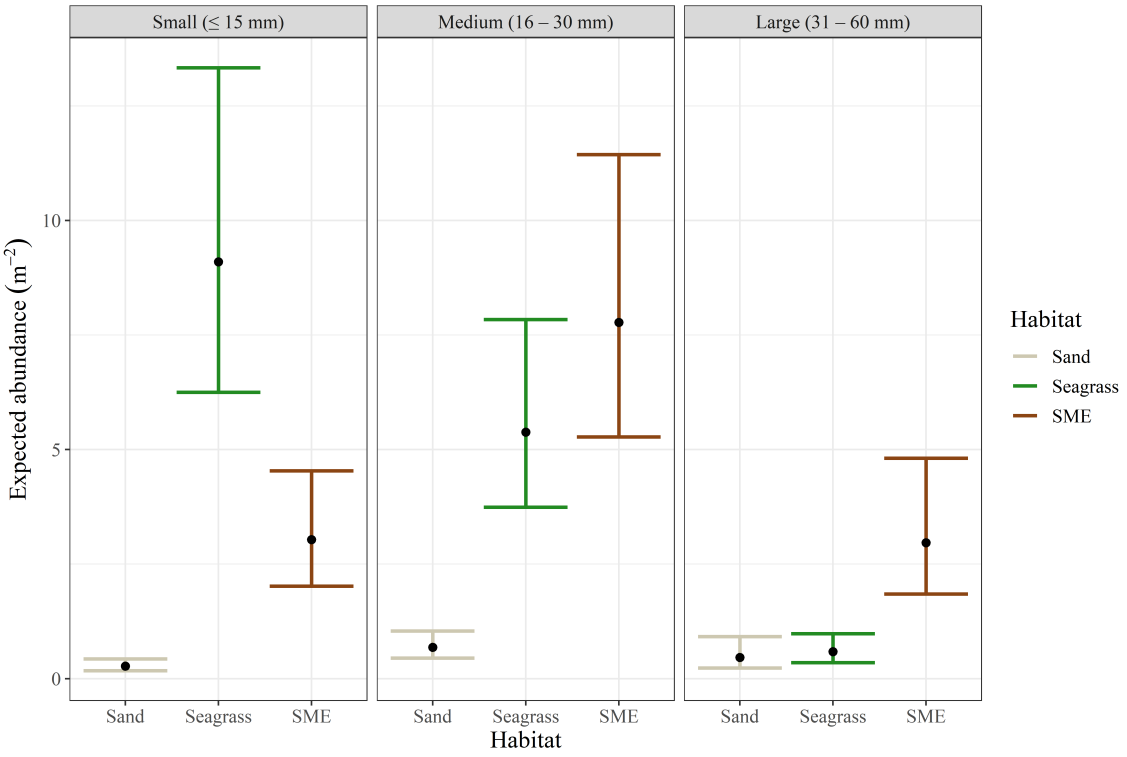

Figure 3.2: Posterior median and 80% CI for $\mu_{\text{cond}_{hi}}$ of habitat for small ($\leq$15 mm CW; left column), medium (16–30 mm CW; middle column), and large (31–60 mm CW; right column) size classes.

Table 3.6: Posterior summary statistics (median and 80% CIs) for the small ($\leq$15 mm CW) juvenile size class. Values under the habitat columns refer to $\eta_{\text{cond}_{h,15}}$ (model scale) and $\mu_{\text{cond}_{h,15}}$ (count scale) and should be interpreted as the expected small juvenile abundance in a given habitat at a given site with 0 ln turbidity and 0 ln megalopae. Values under the ln turbidity and ln megalopae columns reflect abundance model slope terms (β) for those continuous predictors with categorical terms held at the reference (i.e. downriver sand). Stratum effects were not statistically meaningful for any size class and are not reported here.

Scale	**Quantile**	**Sand**	**Seagrass**	**SME**	ln **Turbidity**	ln **Megalopae**
Model	10%	-1.75	1.84	0.70	0.06	0.01
	50%	-1.31	2.20	1.10	0.27	0.12
	90%	-0.84	2.58	1.51	0.47	0.24
Count	10%	0.17	6.27	2.01	1.06	1.01
	50%	0.27	9.06	3.02	1.31	1.13
	90%	0.43	13.16	4.52	1.61	1.27

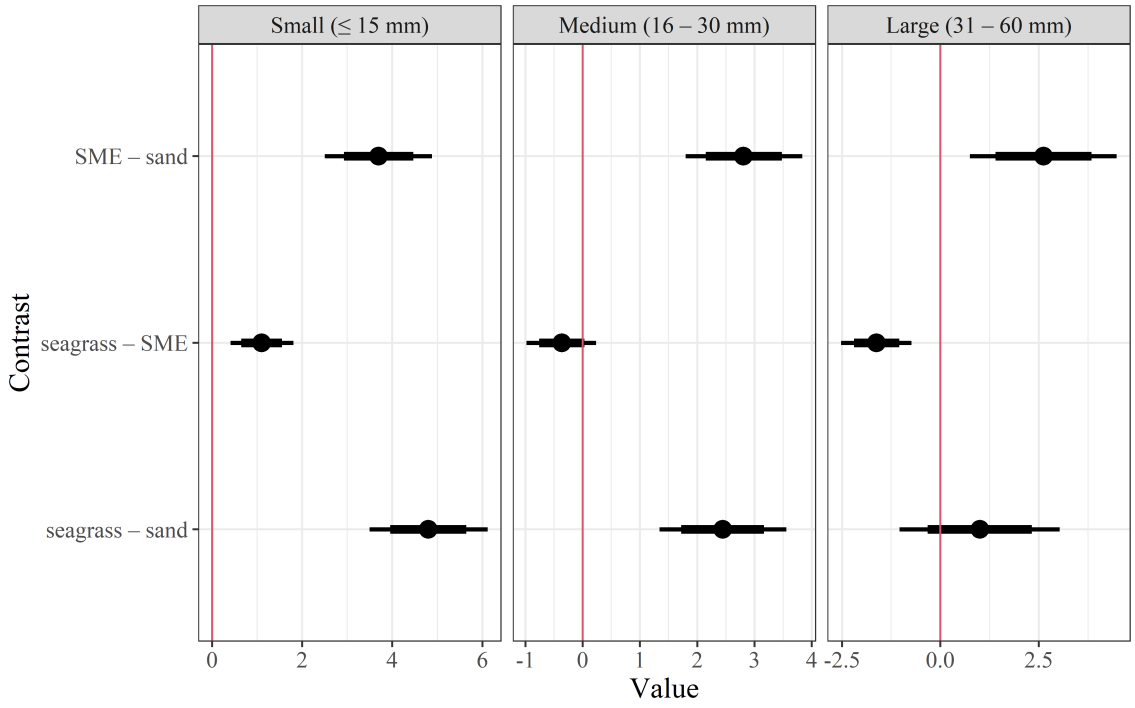

Figure 3.3: Linear contrast statements (L_{hi-mi}) depicting conditional differences in expected juvenile blue crab abundance between habitats by size class. Dots denote posterior median difference in expected values, while thick bars represent 80% Bayesian CIs and thin bars denote 95% Bayesian CIs. The red vertical line denotes 0.

Turbidity and megalopae abundance were both positively associated with small juvenile blue crab abundance – 80% CIs of both (model scale) are above 0 (Table 3.6 and Fig. C2). Conversely, effects of midriver and upriver strata relative to the downriver stratum (reference) were not meaningfully different (Fig. C2). Expected small juvenile abundance increased with both average megalopae per collector (back-transformed from ln (megalopae +1) and ln turbidity (Figs. 3.4A and 3.4B).

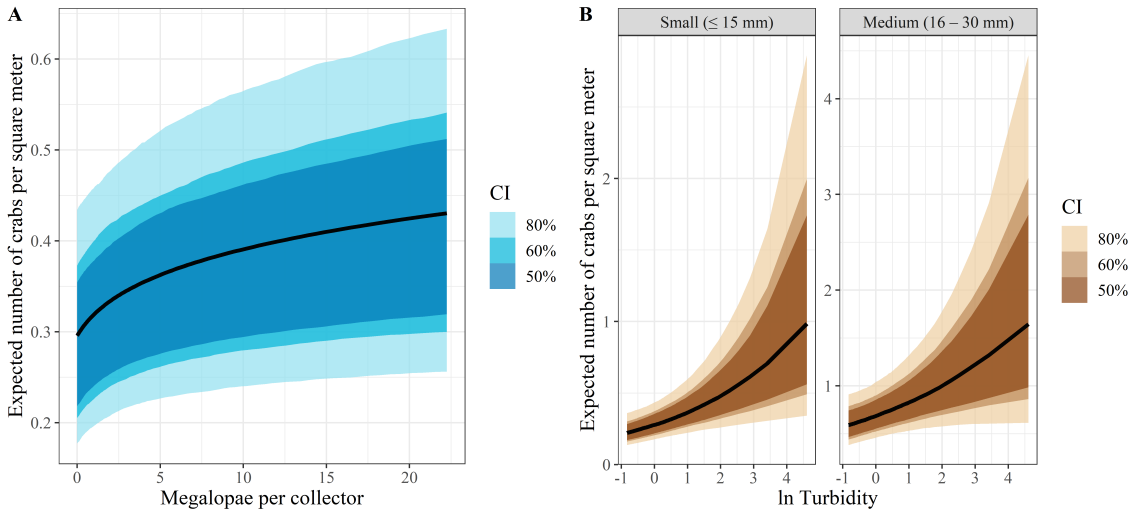

Figure 3.4: Conditional relationships between expected juvenile blue crab abundance ($\mu_{\text{cond}_{vi}}(x_v)$) as a function of **A**) average megalopae abundance per collector and **B**) ln turbidity. The response value for **A**) is the expected number for small size class, while the response values for **B**) include both small (left) and medium (right) size classes. Colored bands indicate credible bands ranging from 50% (0.5) to 80% (0.8) credibility.

3.3.1.2 Patterns in abundance among medium-sized (16–30 mm) juveniles

Habitat and turbidity were both relevant drivers of abundances of medium-sized juvenile blue crabs (Fig. C3). Based on the posterior median of $\mu_{\text{cond}_{hi}}$ (Table 3.5), unlike the smaller size class, medium-sized juveniles were most abundant in SME, followed by seagrass and sand (Table 3.7; Fig. 3.2). Similar to small juveniles, linear contrasts ($L_{h,30-m,30}$) among habitats for juveniles in the medium size class indicated that differences in the expected number of medium-sized juvenile crabs among habitats were statistically meaningful, although the linear contrast between seagrass and SME was marginally meaningful (i.e. 80% CI = -0.76 to 0.031; Fig. 3.3, middle panel). Turbidity was also positively associated with medium-sized juvenile abundance (Table 3.7 and Fig. C3). However, posterior distributions of coefficients for both megalopae and spatial strata indicated that these predictors were

not meaningful in predicting abundances of medium-sized juveniles (Fig. C3).

Table 3.7: Posterior summary statistics (median and 80% CIs) for the medium (16–30 mm CW) juvenile size class. Values under the habitat columns refer to $\eta_{\text{cond}_{h,30}}$ (model scale) and $\mu_{\text{cond}_{h,30}}$ (count scale) and should be interpreted as the expected small juvenile abundance in a given habitat at a given site with 0 ln turbidity and 0 ln megalopae. Values under the ln turbidity and ln megalopae columns reflect abundance model slope terms (β) for those continuous predictors with categorical terms held at the reference (i.e. downriver sand). Stratum effects were not statistically meaningful for any size class and are not reported here.

Scale	Quantile	Sand	Seagrass	SME	ln **Turbidity**	ln **Megalopae**
Model	10%	-0.79	1.32	1.67	0.00	-0.15
	50%	-0.38	1.68	2.05	0.19	-0.03
	90%	0.05	2.05	2.43	0.38	0.11
Count	10%	0.46	3.73	5.32	1.00	0.86
	50%	0.68	5.36	7.74	1.21	0.97
	90%	1.05	7.75	11.40	1.46	1.11

3.3.1.3 Patterns in abundance among large (31–60 mm) size class

Habitat was the only predictor that was statistically informative of abundances among the largest size class of juvenile blue crabs (Fig. C4). The posterior median of large juvenile conditional abundance ($\mu_{\text{cond}_{h,60}}$) was highest in SME habitat, and lower in sand and seagrass (Table 3.8; Fig. 3.2). 80% CIs for linear contrasts between both SME and seagrass as well as SME and sand excluded 0, although that between seagrass and sand included 0 (Fig. 3.3). This indicated that SME was associated with higher abundances of large juveniles relative to seagrass and sand, which harbored equivalent abundances of large juveniles. Posterior distributions for coefficients of turbidity, megalopae, and strata indicated these variables did not statistically influence large juvenile blue crab abundance (Fig. C4).

Table 3.8: Posterior summary statistics (median and 80% CIs) for the large (31–60 mm CW) juvenile size class. Values under the habitat columns refer to $\eta_{\text{cond}_{h,60}}$ (model scale) and $\mu_{\text{cond}_{h,60}}$ (count scale) and should be interpreted as the expected small juvenile abundance in a given habitat at a given site with 0 ln turbidity and 0 ln megalopae. Values under the ln turbidity and ln megalopae columns reflect abundance model slope terms (β) for those continuous predictors with categorical terms held at the reference (i.e. downriver sand). Stratum effects were not statistically meaningful for any size class and are not reported here.

Scale	Quantile	Sand	Seagrass	SME	ln **Turbidity**	ln **Megalopae**
Model	10%	-1.41	-1.03	0.62	-0.71	-0.23
	50%	-0.75	-0.53	1.10	-0.23	-0.08
	90%	-0.06	-0.05	1.58	0.25	0.07
Count	10%	0.24	0.36	1.87	0.49	0.80
	50%	0.47	0.59	3.01	0.80	0.93
	90%	0.94	0.96	4.84	1.28	1.07

3.3.2 Survival

Stratum-habitat-structure, turbidity, month, and carapace width were relevant drivers of juvenile blue crab survival (Table 3.9 and Fig. C5). Among stratum-habitat-structure combinations, the posterior median of the conditional probability of juvenile blue crab survival (π_{cond_j}, Table 3.5) was highest in downriver seagrass structured, followed by midriver and upriver SME structured habitat (Fig. 3.5). The stratum-habitat-structure combination with the lowest posterior median conditional probability of survival was downriver seagrass unstructured .

Table 3.9: Posterior summary statistics (median and 80% CIs) of regression coefficients β from the survival model. Effects of categorical predictors should be interpreted as relative to the reference (downriver sand in April). See Table 3.4 for descriptions of predictors. Values in bold font indicate that the coefficient of a given parameter is statistically meaningful.

Coefficient corresponding to	10%	50%	90%
Intercept	-0.09	1.04	2.29
ln Turbidity	-0.01	0.29	0.60
CW	**0.03**	**0.04**	**0.06**
May	**-2.75**	**-1.83**	**-1.02**
June	**-3.93**	**-2.97**	**-2.12**
August	**-4.17**	**-3.28**	**-2.49**
September	**-3.69**	**-2.78**	**-1.99**
October	**-2.70**	**-1.82**	**-1.05**
Downriver SME structure	-0.28	0.60	1.45
Midriver SME structure	**0.77**	**1.69**	**2.63**
Upriver SME structure	**1.10**	**2.06**	**3.05**
Downriver SME unstructured	-1.50	-0.60	0.26
Midriver SME unstructured	-0.55	0.36	1.28
Upriver SME unstructured	-0.58	0.38	1.33
Downriver seagrass structure	**1.39**	**2.20**	**3.09**
Downriver seagrass unstructured	**-2.26**	**-1.35**	**-0.42**
Midriver sand	-0.59	0.33	1.25
Upriver sand	-0.72	0.26	1.22

Figure 3.5: Posterior median and 80% CIs of conditional mean (π_{cond_j}) for habitat-structure combinations by river stratum.

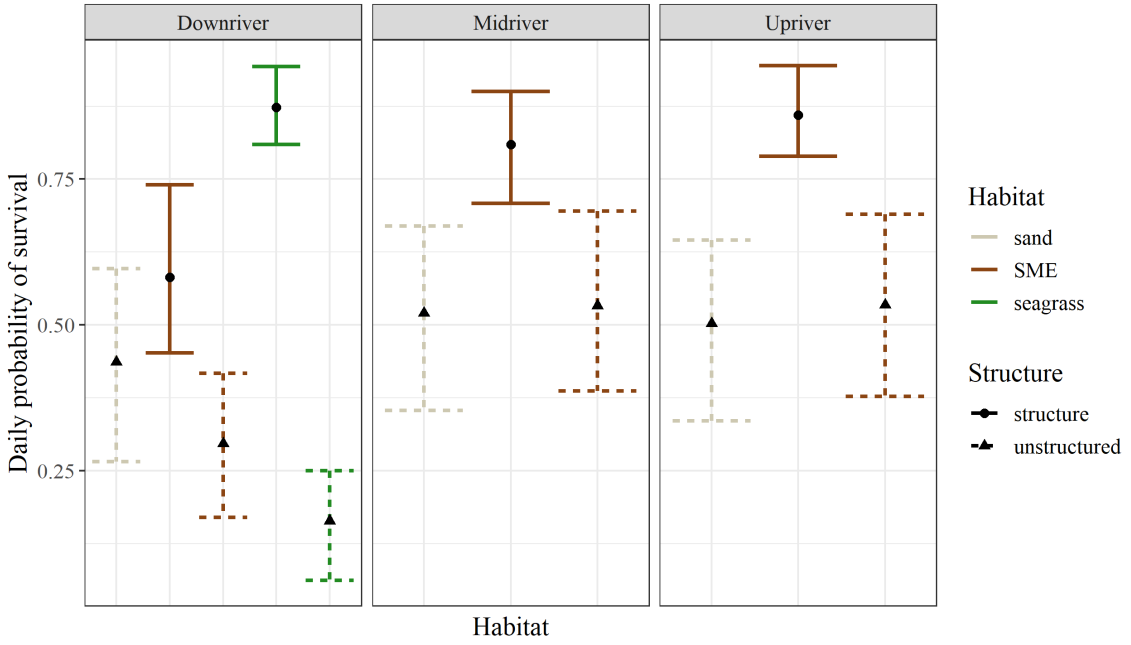

Bayesian 80% CIs of linear contrasts (W_{j-r}) indicated downriver structured seagrass, midriver structured SME, and upriver structured SME indicated that these habitats conferred the highest relative survival to juvenile blue crabs. Linear contrasts between these stratum-habitat-structure levels against all others were positive and excluded 0. This (Table C2). However, linear contrasts among these three stratum-habitat-structure combinations indicated that they conferred equivalent probabilities of survival relative to one another. Moreover, contrasts among sand habitats across all strata indicated that these habitats conferred equivalent survival regardless of location. The posterior median for the conditional probability of survival in SME habitat increased from downriver to midriver and upriver habitats. The 80% CIs of linear contrasts between downriver unstructured seagrass and all other habitats were negative and excluded 0 with the exception of downriver unstruc-

tured SME, which indicated that this habitat conferred the lowest survival among those considered.

Among months considered, the posterior median for the conditional probability of survival (π_{cond_j}) was highest in April and lowest in August (Fig. 3.6). Across months, this probability exhibited a nonlinear pattern in which survival appeared to peak in spring, decline in summer months, and increase again through fall (Fig. 3.6). 80% CIs of linear contrasts between April and all other months were positive and excluded 0, indicating that April conferred the highest survival among months (Fig. C6). Linear contrasts among June–September and June–August indicated these months conferred relatively equivalent survival, although juvenile survival was lower in August than September (Table C2 and Fig. 3.6). Finally, May and October conferred statistically equivalent survival, which was higher than in summer months (June, August, and September) but lower than April (Table C2 and Fig. 3.6).

Figure 3.6: Posterior median and 80% CIs of juvenile blue crab conditional survival probability (π_{cond_j}) in months April, May, June, August, September, and October.

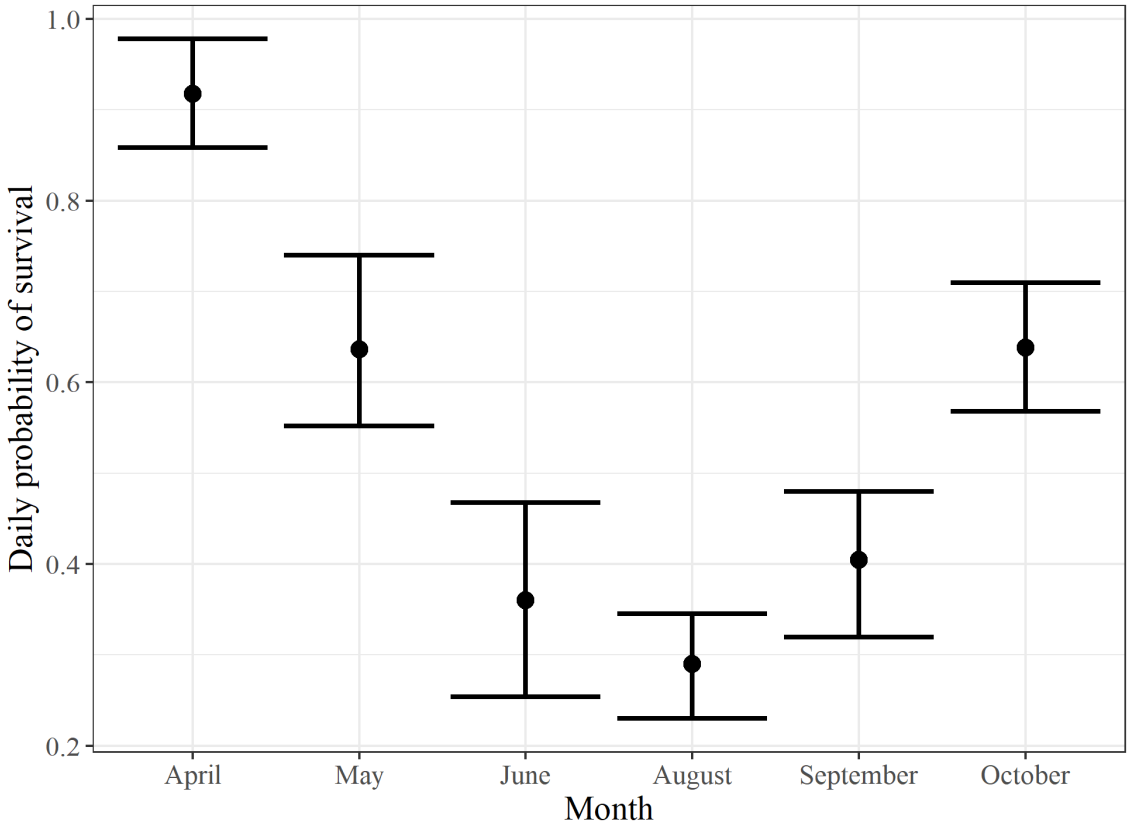

With respect to continuous predictors, the conditional probability of survival ($\pi_{\text{cond}_v}(x_v)$) increased with both carapace width and ln turbidity: the 80% CI for carapace width excluded 0, which indicated CW was statistically important in explaining variation in juvenile blue crab survival. Similarly, the lower limit of the 80% CI for the effect of ln turbidity marginally contained 0 (Table 3.9). Based on the posterior median, the conditional probability of survival increased with ln turbidity, such that for every unit (ln(1 cm)) increase in turbidity, the odds ($\frac{\pi}{1-\pi}$) of survival increased by 33% (Fig. 3.7). Similarly, based on the posterior median, a 1-unit increase in carapace width (1 mm) corresponded with an increase in the

odds of survival by 4% (Fig. 3.7).

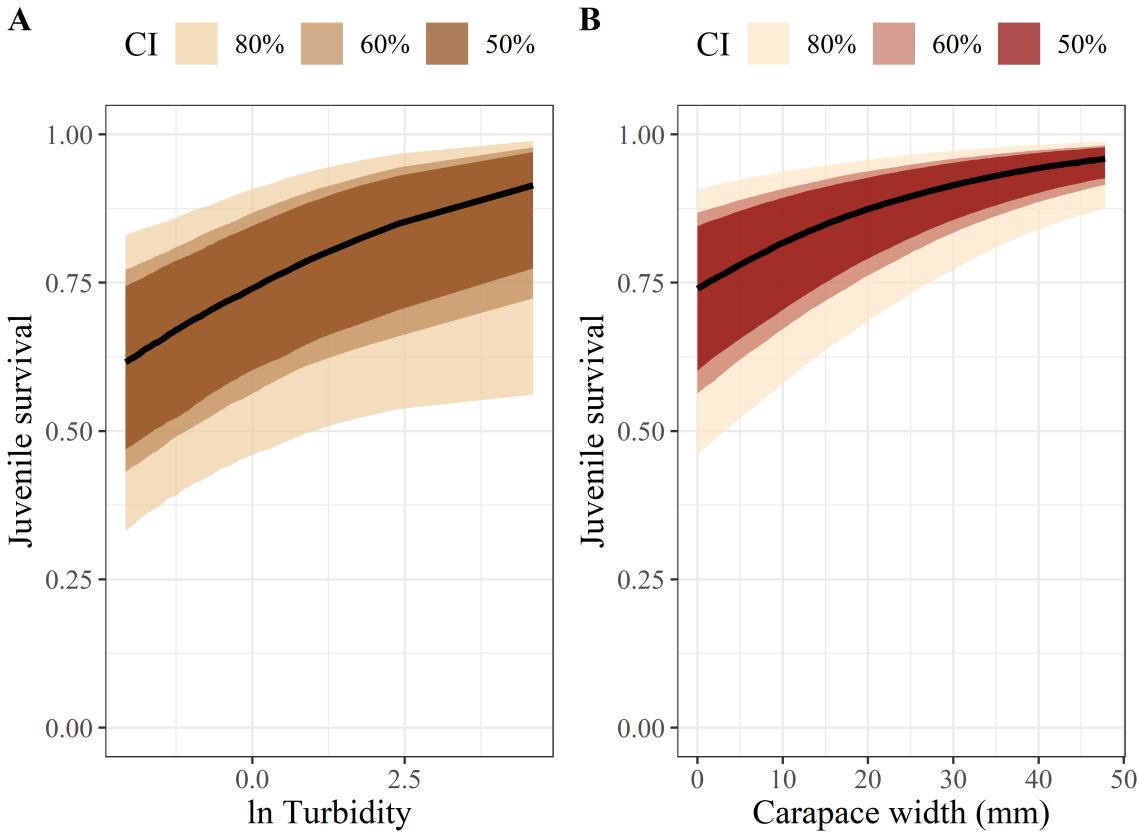

Figure 3.7: Relationships between the conditional probability of juvenile blue crab survival ($\pi_{\text{cond}_v}(x_v)$). Colored regions indicate credible bands.

3.4 Discussion

For a given life stage, habitat-specific abundance and survival are key determinants of a habitat's relative importance within the seascape. Identifying and understanding the biotic and abiotic mechanisms governing these two processes both within and among habitats is critical for accurate estimation of size- and habitat-specific production. In nursery habitats of marine species, evaluation of survival, growth, abundance and ontogenetic habitat

shifts has typically focused on relatively broad size ranges through the juvenile phase. Yet, ontogenetic shifts in habitat use may occur within narrower size ranges. Early-stage ontogenetic shifts have not been well studied in many species and may be important to the conservation and restoration of nursery habitats. Using manipulative and mensurative field experiments, we jointly assessed habitat-specific abundance and survival for multiple size classes of newly recruited juvenile blue crabs to highlight the relative importance of initial and intermediate nursery habitats through ontogeny. We found that habitat-specific utilization rates differed by juvenile size class over a surprisingly narrow range of size, and were related to (1) the structural and biological characteristics of the nominal nursery habitats, (2) spatial gradients of environmental variables within the tributary, and (3) the likely trade-offs between growth and survival through ontogeny .

3.4.1 Habitat-utilization patterns of juvenile blue crabs

3.4.1.1 Small juveniles

Habitat utilization by small ($\leq$15 mm CW) juveniles was a function of habitat, postlarval supply, turbidity, and survival. Small juvenile abundance was positively correlated with megalopal recruitment, whereby small juvenile abundance sharply increased when megalopal abundance was elevated in the previous month and then tapered to an asymptote at the highest densities of megalopae. This phenomenon is consistent with density-dependent processes occurring at this size class. Strong responses to megalopal supply are expected when juvenile densities are low. However, high abundances of megalopae may exceed the carrying capacity of structurally complex nursery habitats [65]. As a result, post-settlement processes such as competition, cannibalism, and density-dependent secondary dispersal increasingly influence small juveniles at higher megalopal abundances [66, 197, 45, 172, 13]

After accounting for variation in abundances due to megalopal supply, small juveniles

were most abundant in seagrass, followed by SME and sand. High abundance of small juveniles in seagrass and SME is consistent with previous research demonstrating that these structured habitats are preferred primary nurseries (seagrass; [154, 159, 77, 171, 88, 219]) as well as alternative nurseries (SME and complex algae;[154, 165, 86, 228, 82, 81]) for this life stage of juveniles. High abundances of small juveniles in structured habitats should be considered within the context of megalopal supply. Megalopae re-enter estuaries from the continental shelf, and therefore the highest concentrations of megalopae occur near the York River mouth and decline farther upriver [201]. Seagrass beds only occur in the downriver portion of the York River and are positioned farther from the shoreline (and thus closer to ingressing megalopae) relative to SME. Seagrass beds are therefore most likely the first structurally complex habitat encountered by immigrating megalopae within the seascape and act as an initial settlement habitat [201]. Moreover, structured seagrass habitat provided the highest relative survival among all habitats considered. Survival also increased with size across habitats, adding further support that the smallest juveniles are most vulnerable to predation pressure [164, 159]. Hence, the spatial orientation of seagrass beds relative to ingressing megalopae, coupled with the survival requirements of small juveniles, renders seagrass beds an adaptive initial settlement habitat.

SME also harbored higher abundances of small juveniles compared to sand habitat, but lower than seagrass habitat. This observation is likely a function of (1) the survival conferred by SME, (2) habitat-specific megalopal encounter probabilities, and (3) density-dependent trade-offs. First, structured SME – particularly structured SME positioned upriver – conferred roughly equivalent survival to juveniles relative to seagrass. In contrast, survival in unstructured SME was lower and roughly equivalent to sand. As access to salt marsh vegetation for aquatic organisms is controlled by marsh flooding and tidal regimes, the importance of marsh structural complexity in governing survival is likely regulated by

hydrology [129]. In Chesapeake Bay, SME utilization is limited by mesotidal inundation profiles characteristic of mid-Atlantic estuaries [129, 38]. Aggregate survival in SME is therefore a combination of the survival conferred by both structured and unstructured components of salt marshes. Indeed, the effectiveness of the flume nets used to capture juveniles in SME relied upon movement of small juveniles from structured salt marsh vegetation to unstructured bottom to remain inundated. Second, although a majority of megalopae encounter seagrass beds, a portion of megalopae miss this habitat and are advected upriver [201]. Here, higher survival conferred by upriver SME relative to nearby sand habitat makes SME an adaptive alternative in the absence of seagrass habitat. Finally, in downriver habitat immediately adjacent to seagrass beds, high juvenile abundance in SME habitat is likely related to density-dependent secondary dispersal of juveniles avoiding competition in seagrass beds [45, 46, 172, 13].

3.4.1.2 Medium-sized juveniles

In contrast to small juveniles, medium-sized (16-30 mm) juveniles were not correlated with megalopal abundance and were more abundant in SME than in seagrass, although abundances remained high in both types of structured habitats. Megalopal abundance was not expected to directly affect medium-sized or large juvenile abundances, as megalopae must transit the small juvenile stage before reaching larger size classes. Preferences of medium-sized juveniles for SME are consistent with recent findings in this system [169, 81] and likely reflect shifting energetic requirements relative to predation pressure [223]. In contrast to smaller juveniles, medium-sized juveniles were less vulnerable to predation. In addition, juvenile blue crab growth rates are higher in upriver unstructured SME due to high availability of preferred prey items [187, 186, 105]. The shift in utilization from seagrass to SME likely reflects changes in predation risk-growth rate tradeoffs and the changing

resource requirements between small and medium-sized juveniles, such that juvenile crabs may derive a growth advantage by dispersing from seagrass beds to SME as they continue to grow [13, 172, 173, 105, 169, 81].

3.4.1.3 Large juveniles

Large (31–60 mm) juveniles were most abundant in SME. In contrast, large juvenile abundances in seagrass and sand were relatively low and equivalent. Densities in SME were six times as high as those in seagrass and sand. The findings that both medium-sized and large juveniles remain in SME is supported by movement patterns across a range of juvenile sizes in salt marsh habitat, which indicates immature blue crabs between 20–60 mm exhibit high site fidelity and low emigration rates within salt marsh tidal creeks [86]. The ontogenetic habitat-shift paradigm [223, 34], coupled with literature on blue crab growth and movement within the seascape-nursery concept offer an explanation for these observed patterns. Although the current understanding of ontogenetic blue crab habitat shifts maintains that larger juveniles exploit unstructured bottom habitat for high food availability, unstructured bottom exists both within marsh-fringed tidal creeks and embayments as well as along shorelines devoid of vegetation. Both of these unstructured habitat types harbor high abundances of preferred prey [187, 186]. Unstructured habitat near salt marshes may be exceptionally productive, harboring higher diversity and abundance of benthic prey relative to comparable unstructured habitat distant from fringing salt marsh vegetation [185]. Accordingly, juveniles of many estuarine species commonly utilize multiple unstructured and structured habitat types for foraging and refuge [140]. The close proximity between the high-refuge, structurally complex salt marsh vegetation and prey-rich adjacent unstructured muddy bottom confers high survival and growth rates to both medium-sized and large juveniles within salt marshes. Although unstructured bottom distant from marsh habitat

likely offers similarly high growth rates, the additional refuge afforded by salt marshes shifts predation risk-growth rate ratios in favor of salt marsh habitat utilization.

3.4.2 Turbidity

Abundance and survival of small and medium-sized juveniles were positively associated with turbidity. This finding agrees with recent evidence detailing positive effects of turbidity over both large [82] and small [81] spatial scales. In addition, the relationship between turbidity and juvenile blue crab abundance was stronger in medium-sized than in small juveniles. The positive association between juvenile blue crab abundance and turbidity may reflect both top-down and bottom-up effects, albeit to varying degrees. First, juvenile blue crabs are positively associated with abundances of preferred prey such as the thin-shelled bivalve *Macoma balthica*, which aggregate in unstructured habitats near estuarine turbidity maxima [187, 186]. Hence, positive associations between juvenile blue crab abundance and turbidity may be a proxy for the bottom-up effect of benthic food availability. Second, the positive association between turbidity and survival implies that turbidity inhibits foraging efficiency among visually-oriented predators [146, 78, 74] which may partially ameliorate predation pressure for juveniles. Although the effect of turbidity on survival was positive, the posterior contained 0 within 80% credible intervals, indicating a relatively high degree of uncertainty. This may be explained by adaptations of estuarine-dependent predators. Although turbidity reduces foraging efficiency of visually-oriented predators, some estuarine-dependent predators rely on chemosensory abilities to forage in low visibility waters [79] and are unlikely to experience major impediments to foraging in highly turbid water. Our results indicate that turbidity is most likely a proxy for food availability (i.e. a bottom-up control) [187, 105, 186], though turbidity may also provide a partial refuge from predation from predators primarily relying on visual foraging. Moreover, in concert with

ontogenetic preferences of larger juveniles for salt marsh habitat, effects of turbidity provide a mechanism for high abundances of 20–40 mm CW juveniles observed in highly turbid salt marsh habitat [82], as this combination of habitat and environmental characteristics would be ideal for minimizing predation risk-growth rate ratios.

3.4.3 Spatiotemporal variation in habitat-specific survival

Within a habitat, juvenile blue crab survival changed across space and time. Seasonally, survival was highest in spring and late fall, and lowest in summer. This curvilinear pattern in survival is consistent with literature on seasonal juvenile blue crab survival rates and corresponds well with patterns in seasonal predation pressure by cannibalistic and piscine blue crab predators [73, 178, 133, 76, 47]. In salt marsh habitat, both structured and unstructured, survival increased from downriver to midriver and upriver habitats. Spatial differences in survival in juvenile blue crabs have been linked to variation in predator communities along estuarine salinity gradients [165], as well as increased alternative prey availability [186, 105]. As our results are consistent under either proposed mechanism, additional work is required to determine the extent to which either mechanism is driving survival patterns.

The high relative survival in upriver and midriver salt marsh habitat conflicts with previous work [189]. A major caveat of these results is the potential confounding between historically low adult blue crab abundance and effects on habitat-specific survival, particularly in midriver and upriver strata. Specifically, adult male population abundances in 2021 were the lowest ever recorded since fisheries-independent monitoring began in 1990 [117, 22]. Adult blue crabs are a substantial source of mortality for juvenile conspecifics [132, 42, 70, 103, 15]. In particular, adult male blue crabs concentrate upriver near estuarine turbidity maxima where salt marsh edge survival was highest [72]. Hence, it is conceivable that higher survival

probabilities in upriver and midriver SME were positively influenced by relatively low adult male blue crab predation pressure, and hence salt marsh edge relative survival may be overstated. Hence, we caution broader interpretability of these results, and stress that our results should be replicated once adult male populations rebound to ensure that these patterns are robust.

In contrast to survival, abundance of juvenile blue crabs did not vary spatially once we accounted for two co-varying environmental variables: megalopal abundance and turbidity. Both of these variables exhibited strong spatial gradients across the tributary axis (i.e. downriver to upriver). Hence, spatial variation in juvenile blue crab abundance is likely predominantly controlled by these environmental variables. Although megalopal supply declined precipitously with distance upriver, juvenile blue crab abundances remained high even in the upriver stratum. This highlights the role of density-dependent secondary dispersal [45, 172, 13]. High initial settlement of juveniles in downriver structured habitats may exceed habitat carrying capacities, such that juveniles emigrate to upriver habitats to avoid adverse density-dependent effects.

3.4.4 Within-habitat variation in survival

Within seagrass and SME, survival varied markedly among structured and unstructured treatments. In all cases, survival was higher in structurally complex vegetation within seagrass and SME. This finding was particularly notable in seagrass, which conferred the highest survival among all habitats considered in its structured treatments and the lowest survival within its unstructured treatment. These patterns are consistent with the general predation-refuge paradigm associated with structurally complex habitats and edge effects [161, 195] and highlights a need for researchers to carefully define the degree of spatial separation between vegetated treatments and unstructured controls in survival studies [103].

The higher refuge value of structurally complex habitats makes them attractive for vulnerable prey. Although the structural complexity of seagrass and salt marsh shoots provides high refuge value, it is also attractive to predators due to the higher availability of food resources [195]. Within structured portions of these habitats, higher predation pressure is offset by high refugia. However, interstitial patches devoid of vegetation are characterized by equivalent predation pressure as in adjacent structured patches but without the associated refuge, leading to disproportionately higher mortality. These effects underscore the need to separate unstructured controls and vegetated treatments by considerable distances to avoid confounding predation pressure and refuge capacity [103].

These findings have additional implications for intertidal habitats such as salt marshes. As SME remains inundated for only a portion of the full tidal cycle, small juveniles must leave the vegetated marsh surface to adjacent unstructured habitat at low tide [38], while larger juveniles and adults may remain in tidal pools to opportunistically forage [85]. Although survival in adjacent unstructured habitat in these locations maybe be higher than in similar deeper habitat [177], these areas nevertheless provide lower refuge quality relative to structured habitat [180]. Aggregate survival in SME may therefore be an average in survival across structured and unstructured patches of a nursery habitat, based on accessibility dictated by hydrology and tidal regimes.

3.4.5 Ontogenetic habitat shifts for the juvenile blue crab: a revised paradigm

Placed within the context of previous work, our results indicate that the current paradigm of juvenile blue crab ontogenetic habitat utilization requires revision. Here, we propose a revised conceptual model describing differences in juvenile blue crab habitat use at different size classes (Fig. 3.8). Initially, ingressing megalopae predominantly settle into seagrass beds or other SAV until $\sim$15 mm CW [154, 81, 88], although small juveniles may utilize

salt marsh vegetation as an alternative nursery if they do not encounter downriver SAV as megalopae [201] or after emigrating from seagrass to avoid adverse density-dependent effects [45, 46, 172, 13]. Once juveniles reach $\sim$15 mm CW, they begin dispersing to SME and tidal marsh creek habitats with increasing frequency to exploit the higher food availability (and higher growth rates) associated with these habitats. Juveniles may also exploit refugia associated with salt marsh vegetation, particularly when molting [180, 103, 70]. The higher food availability in upriver salt marsh habitat near the estuarine turbidity maximum appears particularly valuable for juveniles $\geq$20 mm [82]. By 31-60 mm CW, most juveniles reside in salt marsh habitats before maturing.

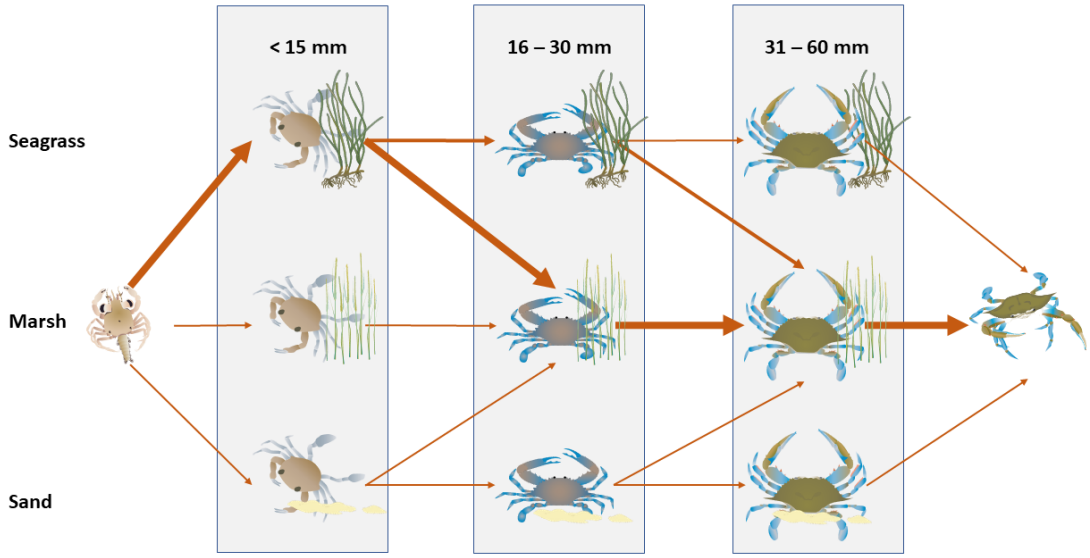

Figure 3.8: Conceptual diagram of revised juvenile blue crab ontogenetic habitat shifts. Arrows depict transitions between habitats with increases in size. Arrow widths denote abundance contributions of individuals between habitats. Images were derived from the University of Maryland Center for Environmental Science Integrated and Application Network

Similar ontogenetic habitat shifts were posited by [103], which maintained that the size

refuge obtained by juveniles at approximately 30 mm allowed individuals to exploit the high food availability afforded by upriver unstructured habitats. The new conceptual model advanced here illustrates the intermediate refuge value of both unstructured as well as structured salt marsh habitat in conferring high survival and growth rates.

3.4.6 Caveats and limitations

While this study provides valuable insights on the ontogenetic mechanisms governing blue crab habitat shifts, there are several important caveats that must be considered. First, our abundance study focused solely on shallow water habitats. Although previous evidence suggested that juveniles predominantly inhabit shallow waters to avoid larger piscine predators [177], it is conceivable that larger juveniles, having reached a size refuge from predators, may have shifted to deeper water habitats which were not included in our experimental design. Consequently, while our findings offer compelling evidence of ontogenetic habitat shifts from seagrass to salt marsh habitats among small and medium-sized juveniles, there remains greater uncertainty regarding shifts (or lack thereof) between medium-sized and large juveniles. To bolster the robustness of our results, we emphasize the need for additional sampling in deeper-water unstructured sand habitats further from the river shoreline.

Second, although our measurements of megalopae abundance were taken at regular intervals (biweekly) along the river axis, we did not conduct shorter frequency (i.e. daily) measurements. Hydrodynamic modeling suggests that megalopae may take several days to reach upriver locations distant from the river mouth [201]. Therefore, repeated sampling over multiple days, preferably near the time of the new and/or full moon, would offer more concrete insights into the relationship between river location and maximum megalopae supply.

Finally, as mentioned earlier, we observed surprisingly high survival rates of juveniles in midriver and upriver salt marsh edge habitats, which appear to differ from previous findings in other systems. As such, we urge further investigation to determine whether this pattern persists or if it is influenced by local and/or ephemeral processes. Additional research in this area is crucial to validate and understand these results more comprehensively.

3.4.7 Relevance

Our results expand upon previous work documenting patterns of habitat utilization in juvenile blue crabs [105, 81] to include more size classes and provide a plausible mechanism – trade-offs between growth and survival – underlying ontogenetic habitat shifts. Our findings indicate that shifts in habitat utilization from seagrass beds occur at earlier size intervals than previously thought and emphasize the role of structured salt marsh habitat as a critical nursery to juveniles within 16-60 mm size ranges.

Our results also add to a growing body of research highlighting a need to preserve both seagrass beds and salt marsh habitat to preserve the complete chain of habitats used by juvenile blue crabs before entering adult habitats [86, 82, 81]. Seagrass and salt marsh declines have received considerable attention in Chesapeake Bay [137, 183]. Eelgrass (*Zostera marina*) beds are declining due to direct and indirect anthropogenic influences such as land-use change and long-term warming of Chesapeake Bay [156, 137, 158]. Similarly, salt marshes have been reduced by coastal development and shoreline hardening [193] as well as sea level rise [91, 183]. Although losses in blue crab secondary production associated with seagrass declines has received considerable attention [76, 77, 131, 171, 88], effects of salt marsh loss on blue crab population dynamics remains a major data gap for Chesapeake Bay and other mid-Atlantic estuaries. Moreover, ratios of marsh-migration to marsh-erosion associated with sea level rise are spatiotemporally variable, and higher rates

of salt marsh loss are expected in upriver regions such as within the York River [183], which are potentially the most valuable for later-stage juvenile blue crabs. Additional empirical and mechanistic modeling is required to estimate how shifting seagrass and salt marsh distributions, as well as novel nursery habitats such as algal patches, will affect blue crab population dynamics both within Chesapeake Bay specifically and among Northwestern Atlantic estuaries generally.

Chapter 4

A state space approach to modeling blue crab population dynamics of Chesapeake Bay: influence of seagrass availability on juvenile survival

Abstract

Nursery habitats enhance growth and survival of juvenile fish and invertebrates by providing abundant food resources and refugia, and can significantly augment secondary production of exploited species and their fisheries. The quality of nursery habitats therefore influences success of fisheries management and conservation efforts. Although the importance of nursery habitats to marine and estuarine species has been documented widely, the

quantitative value of these habitats in population dynamics at spatial and temporal scales relevant to management has only recently been emphasized and documented for a few species. Hence, a need exists to quantify the relative value of nursery habitats to population dynamics of exploited species. One particularly useful approach to population dynamics modeling is the use of state-space models in fisheries stock assessment where data are noisy or incomplete. These models can provide more precise estimates of population size and growth rates while also incorporating environmental effects, which can inform ecosystem-based management decisions. Using multiple sources of juvenile and adult indices of abundance, in concert with spatiotemporal data on seagrass (habitat) extent, we developed a 2-stage state-space model of the effects of seagrass habitat distribution on blue crab, *Callinectes sapidus*, population dynamics. Despite the well-understood importance of seagrass meadows on juvenile blue crab vital rates, and by extension its influence on adult population dynamics, traditional population models of the blue crab have primarily emphasized generalized stock-recruit relationships, fishing mortality, and population-level vital rates without consideration of habitat-specific effects or multiple sources of uncertainty. We found that seagrass availability, specifically that of *Zostera marina* increased carrying capacity of the blue crab population, and that maximum sustainable yield was overestimated when seagrass cover was excluded as a covariate. Taken together, our results indicate that fisheries managers should consider habitat (e.g. seagrass) availability within blue crab population dynamics models to set more realistic harvest and seagrass conservation targets.

4.1 Introduction

Fisheries are critical components of marine and estuarine ecosystems and constitute a major source of both food security and income for coastal communities. However, the

vast majority of global marine fish and invertebrate stocks are either fully or over-exploited [118], which has far-reaching effects on both coastal communities and marine ecosystems [17]. Furthermore, anthropogenic stressors like habitat loss/fragmentation, climate change, and pollution further exacerbate the degradation of ecosystems and negatively impact fish stocks [62, 200]. Attempts to manage fisheries and rebuild stocks globally have had mixed success, and there has been increasing recognition of the need to incorporate ecosystem considerations into management frameworks [99, 40].

One vital requirement for the success and sustainability of fisheries is the quantity and quality of juvenile habitats. In particular, nursery habitats contribute disproportionately to fisheries productivity. A habitat is considered a nursery if it contributes more juveniles per unit area to adult populations relative to other candidate habitats, which may be due to higher relative survival and/or growth [8]. Generally, nurseries support greater secondary production via enhanced density, growth, and/or survival of juveniles [8, 67, 128, 35, 143, 140, 109, 160] through the provision of food resources and refugia.

Despite the importance of these habitats to fisheries, the quantitative contribution of these habitats to populations at spatial and temporal scales relevant to fisheries management has only recently been emphasized and documented for a few species [216, 188, 226, 16, 102, 21]. Without this information, management frameworks may not account for environmental processes that reduce juvenile survival and growth – such as habitat loss. Resulting habitat management failures may lead to degradation, fragmentation, and loss of nursery habitat, which directly affects fisheries by lowering population productivity, either by reducing resiliency, lowering the carrying capacity of an ecosystem harboring an important fishery, or both [209, 229, 203, 216]. These potential negative impacts to commercially exploited species' population dynamics have important implications for fisheries reference points, management interventions, and long-term sustainability of the fishery [216]. In

contrast, effective management of nursery habitats, including conservation and restoration measures, can help maintain the integrity and functionality of these critical habitats, ensuring the presence of essential nursery habitat for juvenile fish and invertebrates [234].

The expansion of traditional population modeling approaches to rigorously link habitat availability to fisheries production can provide important insights with relevance to fisheries management [102]. These approaches can explicitly incorporate nursery habitat effects either by leveraging vital rates derived from small-scale studies [51, 131, 114, 212] or directly estimating effects of habitat on vital rates through inclusion of environmental covariates into stochastic population models fit to observed field data [39, 114, 127]. Further, using Bayesian inferential frameworks, fisheries population models can robustly integrate nursery habitat characteristics and their effects on vital rates by initially using estimates from small-scale, reductionist studies as prior distributions (when available) and subsequently evaluating habitat-specific vital rates at the population level by fitting models to population survey data [122].

In this study, we constructed multiple population dynamics models to demonstrate the effects of nursery habitat on fisheries using the blue crab *Callinectes sapidus* population in Chesapeake Bay as a case study. The blue crab fishery is both currently and historically one of the most valuable fisheries in Chesapeake Bay. Blue crabs undergo complex ontogenetic changes in habitat utilization, with seagrass meadows serving as the preferred nursery habitat for the smallest and most vulnerable juvenile stages. [103, 70]. However, seagrass meadows in Chesapeake Bay are threatened by climate change and nutrient pollution [156, 137, 158, 68]. To model the effects of seagrass habitat on blue crab population dynamics, we employed a state-space model framework to incorporate data on both abundance indices from multiple fisheries-independent surveys and annual seagrass cover information. Specifically, we constructed five state-space models with different

configurations of seagrass effects, specifically looking at availability of *Zostera marina* and *Ruppia maritima*. Additionally, by using published seagrass species-specific distribution trajectories modeled under different management actions, we established a clear and direct connection between water quality management and blue crab population abundance. Our research is particularly insightful when comparing the results to models that exclude seagrass covariates, highlighting the critical role of seagrass in shaping the outcomes of ecosystems generally and fisheries management strategies specifically.

4.2 Methods

4.2.1 Study fishery and area

We focus on the Chesapeake Bay blue crab *Callinectes sapidus* stock from 1990–2022. Chesapeake Bay harbors the largest blue crab fishery along the Atlantic coast. The blue crab population in Chesapeake Bay has fluctuated considerably over the 33 years since an annual bay-wide population surveys were established. From 1990 to 2007, the blue crab spawning stock in Chesapeake Bay declined by 80% [106, 117]. In response to these trends, severe fishery reductions, including the closure of the winter dredge fishery, were implemented in 2008 by the three management agencies operating within Chesapeake Bay: the Virginia Marine Resources Commission (VMRC); Potomac River Fisheries Commission (PRFC); and Maryland Department of Natural Resources (MDNR) [22]. Although estimates of population abundance and fishery exploitation between 2009–2016 suggested that the population had begun to recovered from over-exploitation, annual adult female abundances have fluctuated substantially between very low and high levels since 2017 [22]. Meanwhile, juvenile abundances in 2021 and 2022 were the lowest on record [101]. The absence of a sustained, population-level response to management interventions in 2008 suggests

that fishing pressure is not the sole driver of blue crab abundance. Further recovery of the Chesapeake Bay blue crab population may be dependent upon seagrass quality and availability during recruitment [131, 171], the role of which has yet to be quantified at the population level.

4.2.2 Life cycle

The current understanding of the blue crab life cycle underlies the proposed state-space model framework (Fig. 4.1). Consistent with many estuarine invertebrate species, the blue crab has a complex life history. After mating, mature females migrate to high-salinity entrances of estuaries in late spring/early summer to brood. Once hatched, zoeae (larvae) are advected from the estuary into adjacent marine waters along the continental shelf [44]. Following three to four weeks of development and seven to eight larval molts, zoeae molt to become megalopae (postlarvae) and subsequently re-invade estuaries and coastal systems between late summer and mid-fall via wave or tidally driven currents and eventually settle into nursery habitats before rapidly metamorphosing to first-instar recruits [103]. Recruits must subsequently survive through fall, which is a function of fluctuating environmental variables such as habitat, predation pressure, and population size [70, 103]. Surviving recruits then overwinter as juveniles and mature over the following year.

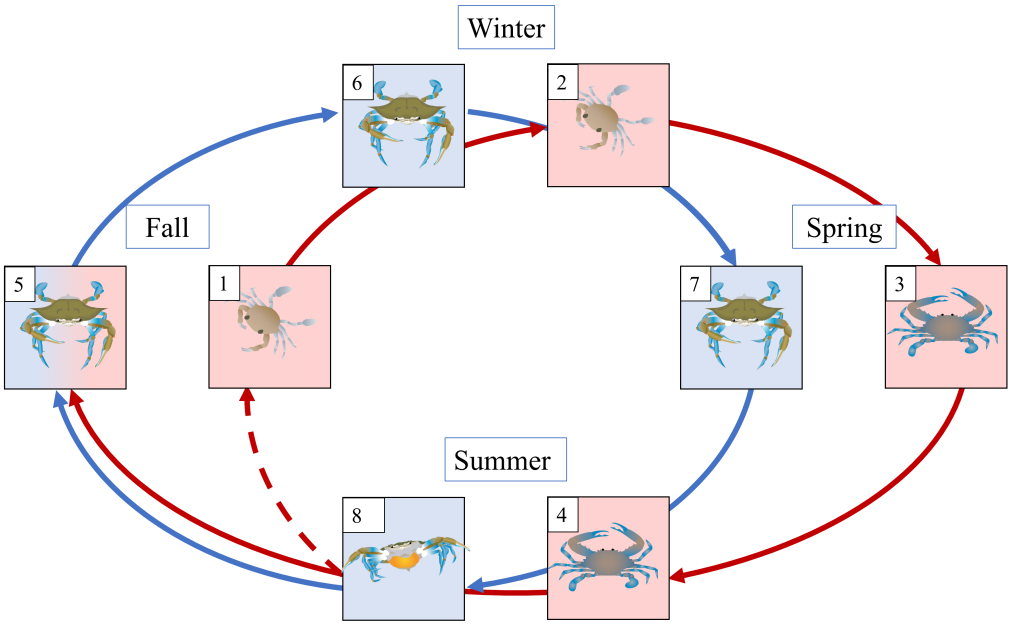

Figure 4.1: Life cycle diagram of the blue crab population with two stages. Blue boxes denote adult stages in each season, while red boxes denote juvenile states. Similarly, blue and red arrows denote transitions between stages at different times of year for adults and juveniles, respectively. The dashed red line denotes offspring produced by adults in summer. The life cycle begins with juveniles recruiting to nursery habitat in fall (1). Juveniles then overwinter (2) and gradually grow to larger size classes over the following spring (3) and fall (4), before maturing after approximately one year (5). Adults subsequently overwinter (6) before mating in spring (7) and reproducing in summer (8). Surviving adults remain in the adult stage (5–8) until death. Blue crab symbols were obtained through the University of Maryland Center for Environmental Science Integrated Application Network (UMCES IAN) Image Library.

4.2.3 Environmental covariates considered

The blue crab is reliant on abundant nursery habitat distributions during its early life stages [103]. In particular, seagrass meadows represent a critically important nursery habitat for the smallest and most vulnerable juvenile stages [154, 159, 164, 77, 171], although other nursery habitats such as fringing salt marsh appear critically important to larger juveniles [105, 186, 86, 82, 81, 81]. Juvenile blue crab growth and survival are both

enhanced in seagrass meadows [159, 164, 76, 77], and juvenile blue crab densities are frequently orders of magnitude higher in seagrass meadows relative to unstructured sand habitat [154, 171, 81]. Despite the well-understood importance of seagrass meadows on juvenile blue crab vital rates, and by extension their influence on adult population dynamics, traditional population models of blue crabs have primarily emphasized generalized stock-recruit relationships, fishing mortality, and population-level vital rates without consideration of habitat-specific effects, particularly at the population scale [124, 125, 106, 126]. Moreover, more recent efforts to estimate the influence of seagrass habitat on blue crab population dynamics [131, 169, 227] relied primarily on parameter estimates derived from small- scale studies and did not fit population dynamics models to observed estimates of juvenile and adult abundance at the population scale. As observed relationships between environmental variables and population abundances may decouple when assessed at multiple spatial and temporal scales [82], the effect of seagrass availability on blue crab population dynamics at the population level remains an open question.

Trends in seagrass aerial cover in Chesapeake Bay appear species-specific, and future blue crab population sizes may depend on whether the nursery quality conferred by seagrass meadows are equivalent across seagrass species. Although recent reductions in nutrient loads have led to general recoveries of some seagrass beds in Chesapeake Bay [96], future projections depict long term declines in the historically dominant seagrass species, eelgrass *Zostera marina* due to increasing thermal stress associated with anthropogenic climate change [137, 225, 68]. In contrast, projections of a co-occurring seagrass species, *Ruppia maritima* are less influenced by projected water temperature shifts and instead will depend on whether additional nutrient reduction measures are undertaken [68]. It is unclear how the Chesapeake Bay blue crab population will respond to changes in differential trajectories of various seagrass species. Limited evidence suggests that juvenile densities

may be higher in *R. maritima* than *Z. marina* [157, 219], perhaps due to higher structural complexity associated with *R. maritima* shoots [219]. Moreover, even among seagrass monocultures, meadows are not homogeneous, and evidence suggests that seagrass shoot density influences juvenile abundance and survival [76, 77, 14], which may impact carrying capacity [131]. Hence, we considered multiple seagrass habitat covariate configurations of varying complexities ranging from no seagrass effect to separable *Z. marina* and *R. maritima* density-weighted cover effects (see Section 4.2.5).

4.2.4 Sampling and data processing

4.2.4.1 Indices of abundance and catch data

Blue crab indices of abundance were developed from two fishery-independent surveys employing stratified random sampling designs: the Virginia Institute of Marine Science Juvenile Fish and Blue Crab Trawl Survey (herein; VIMS Trawl Survey)[207], and the Winter Dredge Survey (WDS;Fig. 4.2)[101]. Herein, all instances of juveniles refer to animals $\leq$60 mm carapace width (CW), while adults refer to animals $>$60 mm CW. Beginning in March 1989 and continuing to the present, the VIMS Trawl Survey has conducted spatially stratified-random and fixed-site monthly sampling in the mainstem Virginia portion of Chesapeake Bay using consistent gear and methodology. In addition, the VIMS Trawl Survey has employed similar methodology in Virginia tributaries (i.e. the York, James, and Rappahannock rivers) since 1996. Meanwhile, the WDS has been operating in Chesapeake Bay using a stratified random sampling design (with a different spatial strata design for the entire bay) since its inception in 1990. In contrast to the monthly resolution of the VIMS Trawl Survey, the WDS is conducted annually each year between November and March at 1,500 randomly selected sampling stations throughout the Maryland and Virginia waters. The WDS employs a crab dredge and targets both adult and juvenile crab populations

during winter while crabs are dormant and buried in the sediment to increase gear efficiency [190].

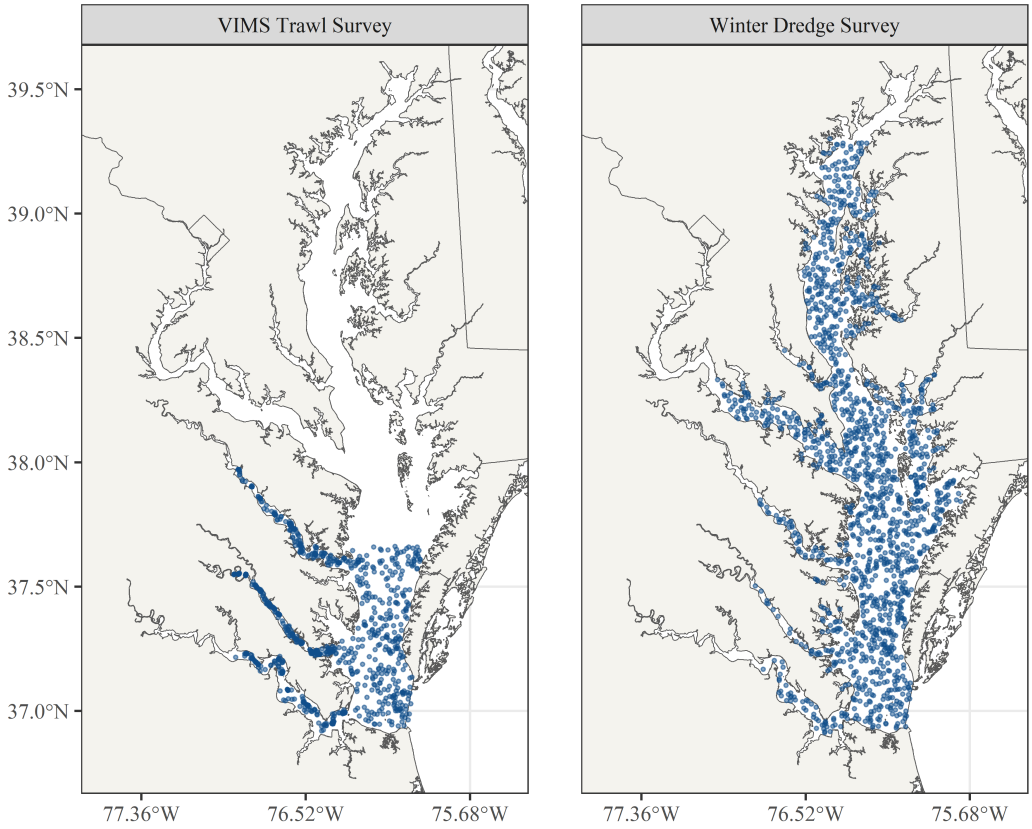

Figure 4.2: Maps describing the sampling distribution of the VIMS Trawl Survey and Winter Dredge Survey. Points denote 2022 sampling.

Juvenile and adult indices of abundance and corresponding uncertainty estimates were developed based on the stratified-random survey design employed by VIMS Trawl Survey with a finite-population correction, as follows. For a given stage l (where $l = J$ for juveniles and $l = A$ for adults) in the VIMS Trawl Survey in year t, the index of abundance $\hat{O}_{lt}$ and associated variance $\sigma^2_{\hat{O}_{lt}}$ are calculated as:

$$\hat{O}_{lt} = \sum_{s=1}^{H} \bar{y}_{slt} \cdot W_s \tag{4.1}$$

$$\bar{y}_{slt} = \frac{\sum_{g=1}^{n_{st}} y_{sglt}}{n_{st}}$$

$$\sigma^2_{\hat{O}_{lt}} = \sum_{s=1}^{M} \left(W_s\right)^2 \cdot \frac{v_{slt}}{n_{st}} \cdot \left(1 - \frac{n_{st}}{N_s}\right)$$

The expected value for an index of abundance for a given state $\hat{O}_{lt}$ in year t is the sum of $\bar{y}_{slt}$ (the mean number of crabs in stage l caught per tow in stratum s in year t), multiplied by the stratum weight W_s for all H strata. $\bar{y}_{slt}$ is the sum of y_{sglt} (the number of animals from stage l collected in the g^{th} trawl tow collected from the s^{th} stratum in year t) divided by n_{st} (the number of samples in the s^{th} stratum in year t). Meanwhile, $W_s = \frac{N_s}{N}$ is the stratum weight, where N_s is the total number of spatially explicit grid cells (here using a 1000 m x 1000 m lattice) in a stratum [63, 231, 207] and N is the total number of cells such that $N = N_1, +N_2 + ... + N_H$. Finally, the index variance, $\sigma^2_{\hat{O}_{lt}}$, is expressed as the sum of stratum weights W_s squared and subsequently multiplied by v_{slt}, the sample variance in abundances of stage l for randomly selected tows in stratum s in year t and scaled by a finite population correction factor [90].

For each year, we considered trawl survey tows collected between April and June (i.e. when water is warm enough to facilitate relatively high catchability in bottom trawl tows), leading to an average of 169 trawl samples each year, with a standard deviation 56. This information was used to develop VIMS Trawl Survey indices of abundance for temporally indexed juvenile and adult indices of abundance and associated time-varying, state-specific observation error. Although the VIMS Trawl Survey has employed consistent gear and methodology across all sampled regions for nearly 30 years, a vessel change

in 2015 was associated with reduced catchability of adult and juvenile blue crabs [207]. As a consequence, we only considered VIMS Trawl Survey estimates from 1990–2014 for adults and 1996–2014 for juveniles. Meanwhile, temporally indexed WDS juvenile and adult indices of abundance and time-varying juvenile and adult observation error were calculated using similar methodology and corrected for adult catchability [190], and were supplied by MDNR [126, 22]. Both VIMS Trawl Survey and WDS indices of abundance and observation errors were estimated at spatial scales of 1 m^2. Hence, all indices and observation errors were multiplied by 1.16×10^{10}, the total surface of Chesapeake Bay in units of m^2, to relate observations to the spatial scale of the blue crab population in Chesapeake Bay. We note that for the VIMS Trawl Survey, this is a strong assumption; abundances of blue crabs – particularly juveniles – may not be equally distributed across Maryland and Virginia waters. Finally, estimates of bay-wide total annual female catch (number of animals) were supplied by MDNR.

4.2.4.2 Seagrass data

Estimates of seagrass availability were derived from GIS data on submersed aquatic vegetation (SAV) obtained from the Virginia Institute of Marine Science SAV Monitoring Program, as follows. First, *R. maritima* and *Z. marina* beds were identified from a ground observation dataset consisting of *in situ* presence/absence field surveys of SAV species collected throughout the bay by both researchers and citizen scientists [153]. To quantify annual total aerial SAV cover, as well as annual density-weighted SAV cover in identified *R. maritima* and *Z. marina* beds, annual aerial imagery was analyzed from 1984–2022 [68], although only data from 1990–2022 were considered in this modeling effort. Juvenile blue crabs primarily settle in the southern portion of Chesapeake Bay (i.e. lower Bay) during the fall recruitment period [213, 64] and do not reach Maryland waters until the

following summer, at which point they have achieved sizes less vulnerable to predation [72]. On the western shore, postlarvae and recruits occur as far as the Potomac River, while incoming currents advect postlarvae and young juveniles farther north along the eastern shore (*R. Lipcius pers comm*)[214]. Consequently, we chose to consider only SAV from the Chesapeake Bay mouth to the Potomac River (latitude: 38.063, longitude: -76.322) on the western shore, and SAV between the Bay mouth and Fishing Creek (latitude: 38.315, longitude: -76.205) on the eastern shore (Fig. 4.3).

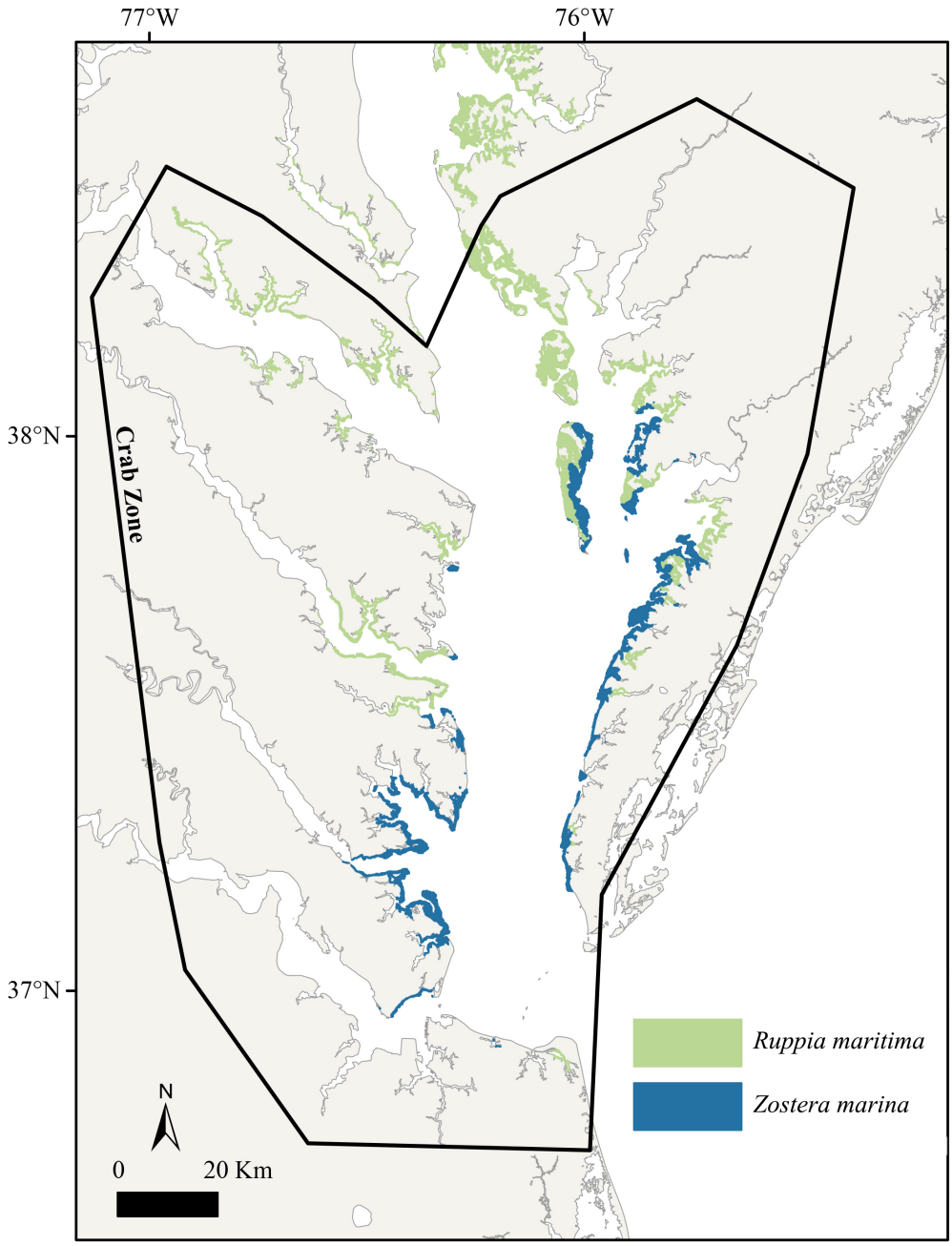

Figure 4.3: Seagrass meadow coverage of *Z. marina* (blue) and *R. maritima* (green) of Chesapeake Bay in 2019. The black polygon denotes the boundary of seagrass considered in the blue crab state-space model framework.

For each year, density-weighted aerial cover was calculated by a previous publication [68] for each species-complex (i.e. *R. maritima* monoculture, *Z. marina* monoculture, and mixed species beds). Digitized SAV polygons were assigned by by the Virginia Institute of Marine Science Restoration and Mapping Program (herein, VIMS SAV Program) a density score of 1–4, indicating densities of 0–10%, 11–40%, 41–70%, and 71–100% cover, respectively. Using these data, we took the mean aerial cover (0.05, 0.25, 0.55 and 0.85) for each density score and applied a weighted sum of total cover for a given species-complex in a given year to obtain density-weighted area estimates (in thousands of hectares). In the absence of an obvious assignment scheme, we divided the areas of mixed-species beds for each year by two and added the area values to corresponding total and density-weighted area estimates of *R. maritima* and *Z. marina*. Finally, we calculated total seagrass density-weighted area for each year as the sum of respective *R. maritima* and *Z. marina* areas (see Appendix D.1 for details).

We used future seagrass projections for each seagrass species developed by the VIMS SAV Program (https://www.vims.edu/research/units/programs/sav/predicting-sav/index.php) to simulate conditional catch at maximum sustainable yield (C_{MSY}) under various climate change and nutrient management scenarios. The scenarios include “no climate change”, “no further reduction”, and “nutrient reductions”. The “no climate change” scenario” is a hypothetical scenario in which climate change does not continue to occur and no nutrient reductions were undertaken as part of the Chesapeake Bay Watershed Implementation Plan (WIP) and established Total Maximum Daily Loads (TMDLs) of dissolved nitrogen and phosphorous. The “no further reductions” follows a semi-plausible assumption where, after 2017, no further nutrient reductions are enacted. Finally, the “nutrient reductions” scenario assumes watershed managers will continue agreed nutrient reductions according to the WIP and established TMDLs.

4.2.5 Model structure

Based on blue crab life history (Fig. 4.1), we constructed five state-space models to evaluate the effects of seagrass quantity on blue crab population dynamics using a Bayesian framework. State-space models present a flexible framework which can incorporate environmental effects as well as uncertainty inherent in estimating population abundance, particularly when considering biomathematical models (e.g. Ricker or Beverton-Holt density-dependence). State-space models are Markov hidden process models that enable separation of process error – stochastic changes in the population over time – and observation error – uncertainty associated with estimates of population size arising from random sampling of commercially exploited populations [3]. State-space models express unobserved states (i.e. abundances of different stages or ages, subject to process error) at time t through a probabilistic function of (1) the states at time $t-1$ and (2) the observations (subject to sampling error) of each state at time t. The additional complexity of state-space approaches, although computationally expensive, reduces bias in parameter estimates relative to regression-based approaches which assume either perfect state observations (i.e. process error only) or perfect model structure (i.e. observation error only) at all time-steps [202]. Hence, state-space models are an improvement from traditional regression approaches that employ well-established mechanistic (process) models while allowing for rigorous statistical inference of model quantities. State-space frameworks have been successfully used to assess vital rates in both age- and stage-structured populations [204, 50, 174, 20], and more recently have expanded to include environmental effects [39, 114, 166, 127].

All state-space models considered here were predicated on a two-stage population structure consisting of immature juvenile (here defined as $\leq$60 mm CW) and mature adult (>60 mm CW) abundance at each year t, denoted J_t and A_t, respectively. For simplicity,

we chose to focus only on juvenile and mature female blue crab abundances and assumed that fecundity was predominantly a function of female spawning stock. Our models are structured as follows. For a given year t, juvenile abundance is a function of the mature female abundance at year $t-1$. Meanwhile, mature female abundance in year t is a function of mature female abundance at year $t-1$, juvenile abundance at time $t-1$, fishing mortality F_{t-1}, and natural mortality M (fixed at 0.9 for both states, see below). For each year, we assumed a log-normal process error structure for both juvenile and adult states. Juvenile and adult states in year t were related to observed indices of abundance for juveniles and adults at year t from multiple fisheries-independent surveys (see Section 4.2.4.1). We assumed that observation errors associated with juvenile and adult states were normally distributed with supplied indices of abundance and corresponding variances derived from stratified random sampling designs with finite population corrections. Indices of abundance $\hat{O}_{lit}$ and related observation error $\sigma_{\hat{O}_{lit}}$ were calculated from the VIMS Trawl Survey using raw data from equation 4.1, while WDS indices and observation error were supplied by MDNR. Finally, fishing mortality in year t was related to observed catch in year t using Baranov's catch equation [7]. Here, we assume that C_t, observed commercial catch at year t, is an imprecise but unbiased estimate of the true catch in year t. We therefore specified that model estimates of catch calculated using Baranov's catch equation be related to observed catch through a normal distribution with a standard deviation of 10^7, yielding coefficients of variation between 5% and 17% among all years. This choice of catch error was the smallest possible while still facilitating model convergence and estimated catch corresponded well with reported values (Fig. D1). Moreover, the majority of coefficients of variation specified here were comparable to coefficients of variation estimated by the previous benchmark stock assessment from 1990 to 2010 (the last year of the assessment), although values estimated by the previous assessment were slightly larger (min: 8%; max:

22%; Fig. D2) [126]. Hence, the complete set of model equations is expressed as:

$$
\begin{aligned}
\ln(J_t) &= \ln\left(\frac{\alpha A_{t-1}}{1+\beta_{t-1}A_{t-1}}\right) + \epsilon_{Jt} \qquad (4.2)\\
\ln(A_t) &= \ln(A_{t-1}+J_{t-1}) - (F_{t-1}+M) + \epsilon_{At}\\
C_t &\sim N\left(\frac{\frac{F_t}{F_t+M}\left(1-e^{-(F_t+M)}\right)(A_t+J_t)}{D_t}, 10^7\right)\\
\hat{O}_{Jit} &\sim N(q_{Ji}J_t, \sigma_{\hat{O}_{Jit}})\\
\hat{O}_{Ait} &\sim N(q_{Ai}A_t, \sigma_{\hat{O}_{Ait}})\\
\beta_t &= e^{\gamma_0+X_t\gamma}\\
\epsilon_{lt} &\sim N(0,\sigma_l)\\
D_t &= D_o \qquad \text{if } t = 1990, 1991, ..., 2008\\
D_t &= 1 \qquad \text{if } t = 2009, 2010, ..., 2022
\end{aligned}
$$

Here, $\hat{O}_{lit}$ denotes the i^{th} index of abundance (where $i = D$ for WDS and $i = V$ for VIMS Trawl Survey) for stage l (where $l = J$ for juveniles and $l = A$ for adults), with standard deviation $\sigma_{\hat{O}_{lit}}$. Catchability coefficients relating index of abundance i at the population level to state l is denoted q_{li}. Adult WDS indices of abundance were already corrected for catchability across multiple vessels sampling Virginia and Maryland waters using estimates derived from a previous study leveraging 10 years of efficiency data [190]. As a result, we assumed $q_{AD} = 1$. However, recent evidence suggests that the survey design of the WDS results in systematic under-sampling of juveniles, with catchability rates estimated between 0.14 and 0.24 [169]. Moreover, catchability of juvenile and adult stages in VIMS Trawl Survey are unknown. Hence, we specified prior distributions for q_{JD}, q_{AV}, and q_{JV} (see Appendix D.2 and Table D1). Finally D_t is a scaling parameter to account for dredge

fishery mortality not accounted for in reported catch values i.e. animals destroyed as part of the dredging process that were not landed) [124]. The dredge fishery was closed in 2008, and as a result for all years prior to 2009, we set $D_t = D_o$, where D_o is an estimated parameter used to scale catch data, while for all years later than or equal to 2009, we set $D_t = 1$. Hence, A_t, J_t, F_t, and D_t are state variables; α, γ_0, q_{Ji}, q_{Ai}, σ_l are coefficients and dispersion parameters; and C_t, $\hat{O}_{Jit}$, and $\hat{O}_{Ait}$ are imperfect observations of functions of state variables.

Model results based on simulated data with known parameter values resulted in nonsensical inference when catchability coefficients and natural mortality M were both estimated, indicating that the model was unidentifiable. Hence, we chose to fix M in all models and estimate fishing mortality and catchability coefficients [112]. A comparison of direct and indirect estimates of annual natural mortality suggested that M ranges from $0.7 - 1.1$ for large juvenile and adult blue crabs [69]. Here, we fixed M at the median value, 0.9 [69, 126].

Density dependence was imposed using a Beverton-Holt stock-recruit relationship, which presumes that density-dependent juvenile mortality in year t is primarily a function of cohort size [10]. Here, α is the productivity parameter at low spawning stock size (i.e. the product of per capita female births, density-independent larval/postlarval survival, and density-independent juvenile survival) [124, 125, 131]. Meanwhile, β_t denotes the effect of density dependence, such that the carrying capacity of juveniles in the system at time t is $\frac{\alpha}{\beta_t}$. Different models were predicated on various hypothesized relationships between juvenile survival and seagrass quality and quantity (Table 4.1). Specifically, we postulated that juvenile survival would be a function of either (1) a seagrass-invariant carrying capacity (i.e. no seagrass effect), (2) total seagrass density-weighted aerial cover without consideration of seagrass species, (3) *Z. marina* density-weighted seagrass aerial cover, (4) *R. maritima*

density-weighted seagrass aerial cover, or (5) *Z. marina* and *R. maritima* separate density-weighted aerial cover (i.e. two environmental covariates). Following the approach by a recent study including environmental covariates in state-space frameworks [127], we related density dependence to environmental covariate (here, seagrass predictors) using a log linear function such that $\beta_t = e^{\gamma_0 + X_t\gamma}$ where γ_0 denotes the seagrass-independent density-dependence effect, X_t is a design matrix of one or more seagrass predictors at year t, and γ is a vector of coefficients (see Table 4.1). Altogether, the unknown model parameters to be estimated are $\alpha, \gamma_0, \gamma, \sigma_J, \sigma_A, D_o, J_t, A_t,$ and F_t. Prior distributions for all non-temporal parameters are detailed in Appendix D.2 and Table D1.

Table 4.1: Descriptions and justifications of five expressions (g_k) of juvenile density dependence as a function of seagrass cover.

Model	Hypothesis	Justification
g_1: $\beta_t = e^{\gamma_0}$	Juvenile density-dependence is solely a function of seagrass-independent component γ_0.	Juvenile blue crabs are highly opportunistic and may utilize a diverse suite of structurally complex habitats when seagrass is not present[165, 86, 88].
g_2: $\beta_t = e^{\gamma_0+\gamma_1\hat{G}_t}$	Juvenile density-dependence is a function of a seagrass-independent component and a total density-weighted seagrass cover $\hat{G}_t$ with coefficient γ_1 without consideration of species composition.	Juvenile blue crabs grow faster, survive at higher rates, and are more abundant in seagrass meadows compared to unstructured habitat, such that bay-wide carrying capacity increases with higher seagrass availability [154, 76, 77, 103, 70, 171, 14].
g_3: $\beta_t = e^{\gamma_0+\gamma_2\hat{\xi}_{zt}}$	Juvenile density-dependence is a function of a seagrass-independent component and a *Z. marina* cover component $\hat{\xi}_{zt}$ with coefficient γ_2.	*Z. marina* may provide superior habitat characteristics for juvenile blue crabs, supporting their growth, survival, and overall fitness. For instance, *Z. marina* beds offer high structural complexity, which provides refuge and protection for young crabs against predation. Additionally, *Z. marina* beds exhibit greater biomass and higher primary productivity than *R. maritima*, providing a more food-rich environment for juveniles, such as higher abundances and diversities of prey species, such as amphipods and polychaetes. Finally, the spatial location of *Z. marina* beds in the lower Bay may make this habitat more attractive to postlarvae re-entering the estuary, as it may be encountered first [152, 224, 80, 103].
g_4: $\beta_t = e^{\gamma_0+\gamma_3\hat{\xi}_{rt}}$	Juvenile density-dependence is a function of a seagrass-independent component and a *R. maritima* cover component $\hat{\xi}_{rt}$ with coefficient γ_3.	*R. maritima* shoots and blades are smaller and more complex than *Z. marina*, corresponding to higher structural complexity. As a result, juvenile blue crab carrying capacity may be more closely related to distributions of *R. maritima* than that of *Z. marina* [157].
g_5: $\beta_t = e^{\gamma_0+\gamma_4\hat{\xi}_{zt}+\gamma_5\hat{\xi}_{rt}}$	Juvenile density-dependence is a function of a seagrass-independent component and species-specific seagrass cover for *Z. marina* and *R. maritima* ($\hat{\xi}_{zt}$ and $\hat{\xi}_{rt}$, respectively) with coefficients γ_3 and γ_4.	Structural characteristics and spatial orientation of both *Z. marina* and *R. maritima* may result in significantly different but positive effects on juvenile blue crab carrying capacity (see above sources)

4.2.6 Model implementation

All data analyses, transformations, and visualizations were completed using the R programming language for statistical computing [167] and the Stan probabilistic programming language for Bayesian statistical modeling [199, 198]. We used Bayesian inference to approximate the joint posterior distribution of all model parameters for each model. To this end, we utilized the Stan programming language with Hamiltonian Monte Carlo (HMC) estimation to generate samples from the joint posterior distribution [57]. Each model was subjected to a warm-up/adaptive phase consisting of 5,000 iterations in a single Markov chain, followed by an additional 5,000 iterations to obtain posterior samples. We assessed chain convergence by examining trace plots and the split $\hat{R}$ statistic (e.g. Fig. D3). In all cases, the $\hat{R}$ values for all unknown quantities in the model were below 1.01, indicating convergence of the chains for all models [57]. Reported effect sizes were calculated based on 80% Bayesian confidence intervals. All confidence intervals referenced here are the highest posterior density intervals [115].

4.2.7 Model selection

Relative model performance was assessed using a one-step-ahead prediction leave-future-out cross validation (1-SAP LFO-CV) approach to evaluate predictive performance through withholding future observations [18]. We created 22 truncated datasets with terminal years 2000 to 2021. We subsequently re-fit each model to each artificially truncated dataset and predicted the juvenile and adult abundances for the year immediately following the terminal year. The final step of 1-SAP LFO-CV analysis was to compare the forecasted predictions and associated uncertainty to excluded juvenile and adult blue crab indices of abundance (i.e. 2001 to 2022, one year after terminal year). To this end, we used estimated log-pointwise predictive density (ELPD) to evaluate out-of-sample predictive

accuracy for each model [217]. For a given index i of abundance for a given stage l in year t ($\hat{O}_{lit}$), conditioned on all previous observations from all states and indices (denoted $Y_{1:t-1} = \{\hat{O}_{AD1:t-1}, \hat{O}_{AV1:t-1}, \hat{O}_{JD1:t-1}, \hat{O}_{JV1:t-1}\}$ for brevity) and the joint posterior distribution $p(\theta|Y_{1:t-1})$ of the vector of all parameters θ, the ELPD_{LFO} for the m^{th} model is:

$$
\begin{aligned}
ELPD_m &= \sum_{l=\{J,A\}} \sum_{i=\{V,D\}} \sum_{t=1991}^{2021} \ln p(\hat{O}_{lit}|Y_{1:t-1}) \qquad \text{for } n = 2000, 2001, ..., 2021 \qquad (4.3) \\
&= \sum_{l=\{J,A\}} \sum_{i=\{V,D\}} \sum_{t=1991}^{2021} \ln \int p(\hat{O}_{lit}|Y_{1:t-1}) p(\theta|Y_{1:t-1}) d\theta \\
&\approx \sum_{l=\{J,A\}} \sum_{i=\{V,D\}} \sum_{t=1991}^{2021} \ln \frac{1}{S} \sum_{s=1}^{S} p(\hat{O}_{lit}|Y_{1:t-1}, \theta^{(s)}_{1:t-1})
\end{aligned}
$$

where here s denotes a given posterior predictive draw among a total of S. Models were evaluated using Δ_{ELPD} values: the difference in ELPD_{LFO} between a given model and the model with the best (i.e. largest) ELPD_{LFO} in the set, as well as $\text{SE}_{\Delta\text{ELPD}}$, the standard error for the pairwise differences in ELPD between the best model and any given model. We assume that a normal approximation adequately describes the pairwise differences (i.e. Δ_{ELPD} values).

Models with large Δ_{ELPD} values (i.e. > 4 and $> 1.96 \times \text{SE}_{\Delta\text{ELPD}}$; [194]) were considered inferior relative to the best fitting model. When two models had comparable Δ_{ELPD} values (i.e. ≤ 4 and$\leq 1.96 \times \text{SE}_{\Delta\text{ELPD}}$; [194]), the simpler model was chosen under the principle of parsimony.

4.2.8 Goodness of fit

Goodness of fit for the highest-performing model was assessed through CV. For each reduced dataset ending in $t = 2000, 2001, 2002, \ldots 2021$, we computed 80% and 95%

posterior predictive intervals for each index of abundance the following year ($t+1$). For CV, we compared each forecasted posterior predictive interval to the corresponding observed index of abundance at time $t+1$, as a forecasting exercise. Goodness of fit was determined based on the observed coverage. (i.e. the proportion of excluded values which were successfully captured by their respective 80% and 95% prediction intervals). For example, a model yielding an observed coverage differing greatly from the nominal Bayesian predictive credible level of 80% or 95% may indicate underfitting/overfitting.

4.2.9 Simulation-based projections

After fitting the five models, we chose the best performing model using 1-SAP LFO-CV. Based on the best performing model, we conditionally projected multiple counterfactual scenarios to illustrate the effect of seagrass covariates on blue crab population dynamics and to approximate maximum sustainable yield (MSY) curves under each seagrass management scenario. Using observed past seagrass cover as well as mean seagrass projections for years 2023–2060 (both taken from VIMS SAV Program), we employed numerical simulations to generate these conditional counterfactual plots and projection-based MSY estimates. Conditional counterfactual projections were made by 1) setting starting values to the 2022 state estimates (i.e. the entire posterior distributions for adults and juveniles in 2022, conditioned on holding process error values at 0, 2) fixing catch at harvest estimates from 2022 (67 million individuals), and 3) fixing density-weighted *Z. marina* cover for all years 2023–2060 at maximum, median, and minimum values observed from 1990–2022. For all mathematical formulas and detailed descriptions of counterfactual plots, see Appendix D.1. For projection-based MSY estimates, again using observed past seagrass cover (1990 – 2022) as well as mean seagrass projections for years 2023–2060, we employed numerical simulations with starting values at 5×10^8 for both juvenile and adult

states (i.e. reasonably high to assume unexploited conditions). For each exploitation rate $u = 0.0, 0.05, 0.1, \ldots 1$, we projected the population forward 100 iterations using posterior draws of model parameters with M fixed at 0.9 and seagrass values fixed at the projections for a given year (1990–2060). At each projection time-step y, fishing mortality was numerically estimated using Baranov's catch equation, with catch at time-step y estimated as $\hat{C}_y^{(n)} = (\hat{A}_y^{(n)} + \hat{J}_y^{(n)})u$. The final iteration of the simulation (i.e. 100) was used as the equilibrium population. Simulations indicated that populations typically stabilized after 10-20 iterations, and thus the additional 80 iterations were used as a precaution to ensure stability. For each seagrass estimate in a given year and each exploitation rate, we then extracted the posterior median equilibrium catch and 80% CIs. This procedure was repeated for all three seagrass scenarios (i.e. "no climate change", "nutrient reduction", and "no further reduction"). The exploitation rate corresponding with the maximum equilibrium catch (i.e. the peak of the posterior median curve) was taken to be the exploitation rate at MSY. The distribution of C_{MSY} corresponding to the exploitation rate at MSY was then plotted for all years and all future scenarios. For all mathematical formulas and detailed descriptions of MSY calculations, including conceptual figures, see Appendix D.4 and Fig D4.

4.3 Results

4.3.1 Model selection

The best fitting model was g_3 (Table 4.2), which posited juvenile blue crab density dependence as a function of density-weighted *Z. marina* cover, and corresponded to an ELPD_{LFO} value 26 units lower than the next-best model, Model g_5. Moreover, the standard error of the pairwise 1-SAP ELPD differences between models g_3 and g_5 was 7.04 (i.e. $\Delta_{\text{ELPD}} > 1.96 \times SE_{\Delta_{ELPD}}$), indicating that Model g_3 had superior predictive performance. Hence, we chose Model g_3 as the best-performing model. Notably, predictive performance of all models including seagrass predictors was substantially higher than the base model (g_1) which did not include seagrass effects. Hereafter, inferences are based on model g_3. Posterior distributions of juvenile and adult states for all years are depicted in Fig. 4.4.

Table 4.2: Model selection results (rounded to two decimal places) from five Bayesian state-space models (g_k) expressing juvenile density dependence as a function of various seagrass cover configurations. Models are presented in order of complexity. ELPD_{LFO}: the estimated log-pointwise density calculated from 1-SAP LFO-CV (Equation 4.3; Δ_{ELPD}: the relative difference between the ELPD of any model and the best model in the set; $\text{SE}_{\Delta_{\text{ELPD}}}$: standard error for the pairwise differences in ELPD between the best model and any given model. The values corresponding to the selected model (g_3) are presented in bold font.

Model: Density-dependence structure	**ELPD_{LFO}**	**Δ_{ELPD}**	**$\text{SE}_{\Delta_{\text{ELPD}}}$**
g_1: $\beta_t = e^{\gamma_0}$	-1734.12	184.28	26.25
g_2: $\beta_t = e^{\gamma_0 + \gamma_1 \hat{G}_t}$	-1653.79	103.95	18.13
g_3: $\beta_t = e^{\gamma_0 + \gamma_2 \hat{\xi}_{zt}}$	**-1549.84**	**0.00**	**0.00**
g_4: $\beta_t = e^{\gamma_0 + \gamma_3 \hat{\xi}_{rt}}$	-1600.04	50.20	8.69
g_5: $\beta_t = e^{\gamma_0 + \gamma_4 \hat{\xi}_{zt} + \gamma_5 \hat{\xi}_{rt}}$	-1576.32	26.48	7.04

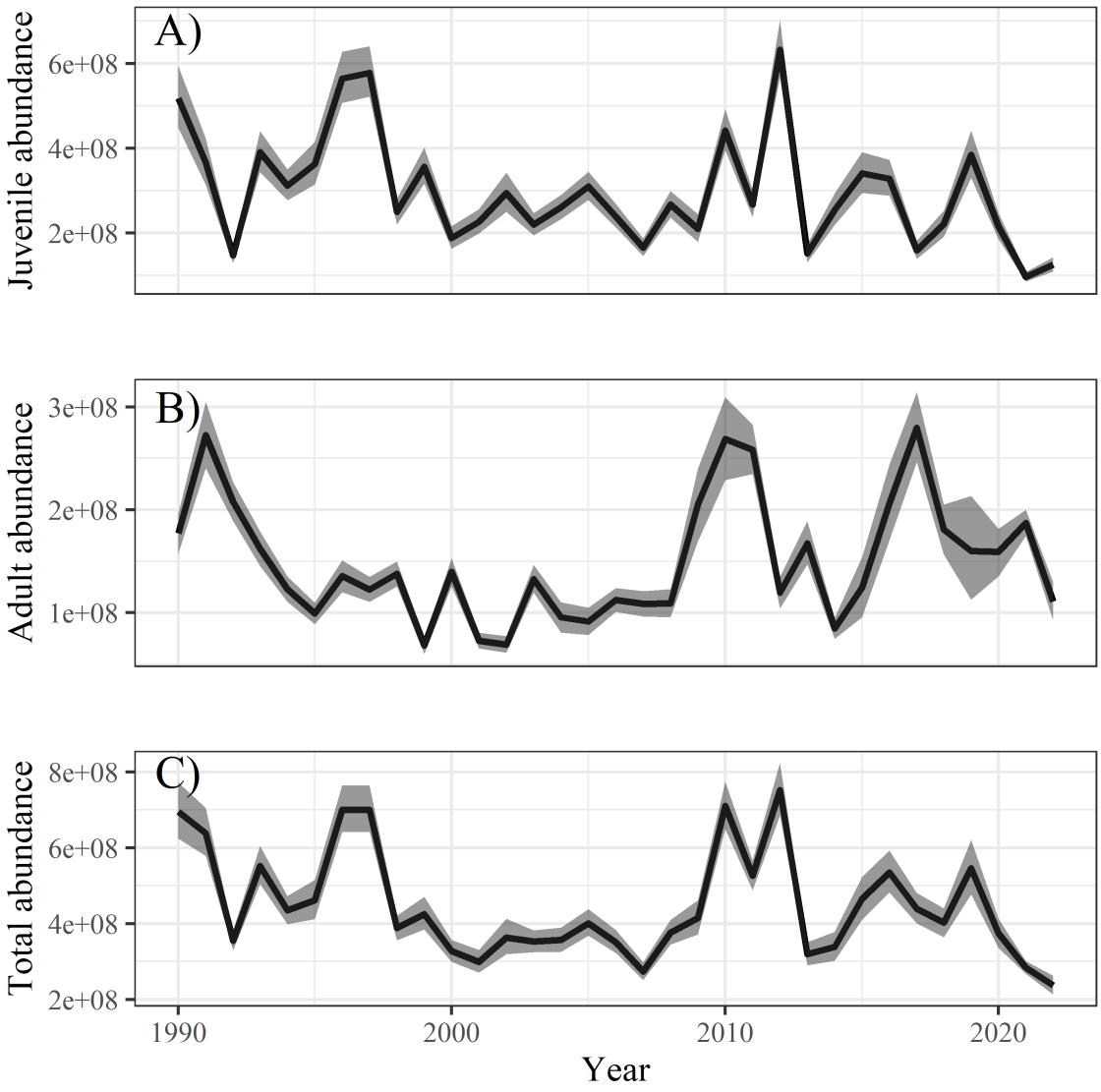

Figure 4.4: Posterior median (black line) and 80% CIs (grey bands) of population states (A: juveniles; B: adults; C: juveniles and adults combined) from Model g_3.

4.3.2 Goodness of fit

Comparisons between posterior predictive intervals and withheld values from the Model g_3 indicated that this model reliably predicted future values. The 80% and 95% posterior

prediction intervals from model g_3 contained 75.7% and 95.9% of withheld observations across indices of abundance, respectively (Fig. 4.5). In addition, estimated catch fell well within 80% Bayesian credible intervals, although catch estimates later in the time series were consistently higher than observed catch, signaling potential, if mild, biases (Fig. D1).

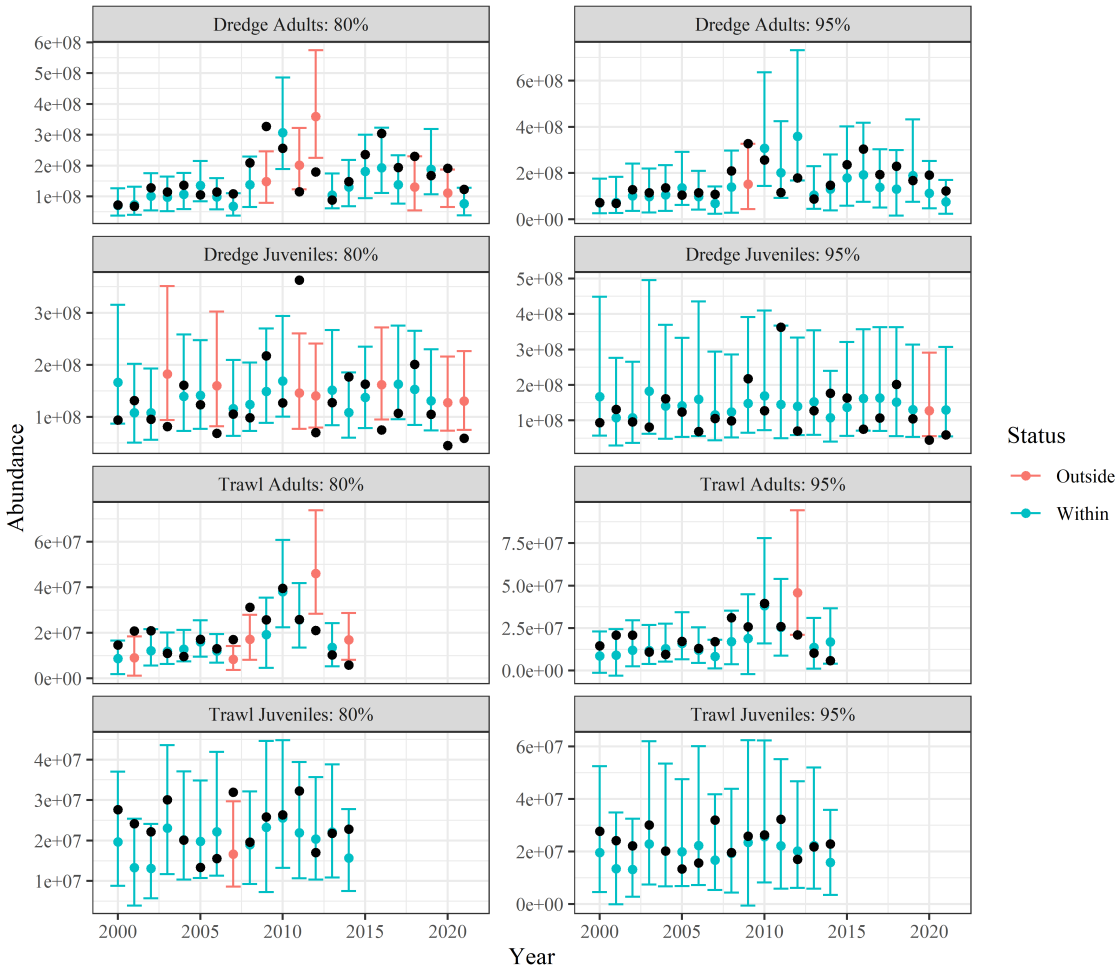

Figure 4.5: Leave-future-out cross validation results for Model g_3. Plot labels denote the index of abundance and posterior prediction confidence level. Colored points (blue or red) denote posterior predictive medians, while error bars denote 80% or 95% CIs (see plot labels). Red error bars indicate an observed value is outside the prediction interval, while blue bars indicate an observed value is within the prediction interval. Black dots depict observed indices of abundance for a given year. Trawl survey values after 2014 are not included in any model or CV because of gear and vessel changes beginning in 2015 (See Section 4.2.4.1).

4.3.3 Recruitment parameters

Population-level recruitment parameters estimated by Model g_3 include α, γ_0, and γ_2 (Tables 4.1 and 4.3). Juvenile carrying capacity is estimated as $K_t = \frac{\alpha}{\beta_t} = \frac{\alpha}{e^{\gamma_0 + \gamma_2 \hat{\xi}_{zt}}}$ using a Beverton-Holt stock-recruit relationship with time-varying density-dependence. In the absence of any *Z. marina* cover (i.e. holding $\hat{\xi}_{zt}$ at 0), posterior median juvenile blue crab carrying capacity of Chesapeake Bay is estimated at 2.9×10^8 (80% CI: 1.9×10^8 to 4.7×10^8). Meanwhile, the posterior distribution of γ_2, the effect of *Z. marina* on juvenile density-dependence, was negative and its 80% CI did not contain 0, indicating that increases in density-weighted *Z. marina* cover decreased the strength of density dependence (β_t) and therefore increased carrying capacity (Table 4.3 and Fig. 4.6).

Table 4.3: Parameter descriptions and posterior median and 80% CIs for model g_3.

Parameter	Description	10%	50%	90%
α	ln Beverton-Holt productivity parameter	5.15	9.81	22.09
γ_0	Seagrass-independent Beverton-Holt density-dependence parameter	-17.74	-16.83	-15.88
γ_2	Coefficients relating density-weighted seagrass cover (see Table 4.1 for details) to Beverton-Holt density-dependence	-0.18	-0.10	-0.02
D	Effect of dredge fishery (operation in 1990-2008 only)	1.00	1.11	1.23
q_{JD}	WDS juvenile catchability coefficient	0.43	0.47	0.51
q_{JV}	VIMS Trawl Survey juvenile catchability coefficient	0.06	0.07	0.08
q_{AV}	VIMS Trawl Survey adult catchability coefficient	0.12	0.13	0.13
σ_J	Juvenile process error sd	0.36	0.42	0.50
σ_A	Adult process error sd	0.40	0.48	0.58

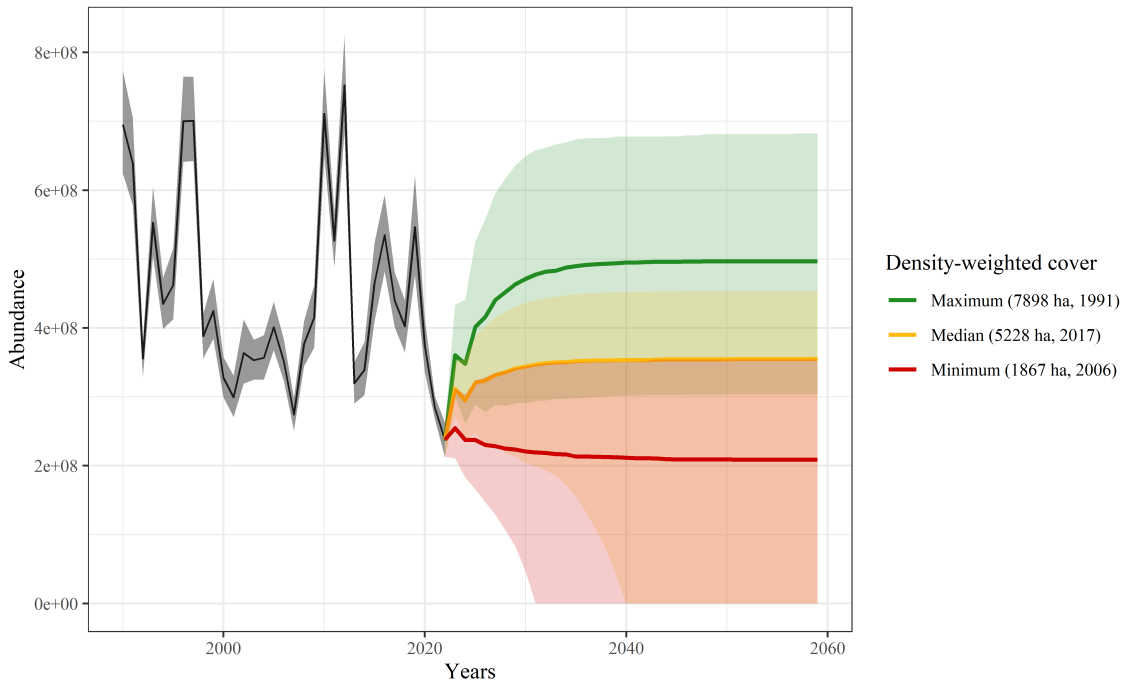

Figure 4.6: Conditional counterfactual projections of total blue crab abundance (adults and juveniles combined for each year; $J_t + A_t$) under three density-weighted *Z. marina* cover values. The black lines and grey bands denote conditional posterior median total blue crab abundance and 80% CI, respectively for years 1990–2022. Meanwhile, colored lines and bands denote posterior predictive median population trajectories and 80% CIs under different fixed *Z. marina* cover: maximum observed cover (green), median observed cover (yellow), and minimum observed cover (red). For details, see Appendix D.1.

4.3.4 Projection-based MSY

Using estimates from Model g_3, and seagrass projections through 2060, we conditionally projected C_{MSY} and corresponding uncertainty for all years (past and future) under each seagrass management scenario. Density-weighted cover of *Z. marina*, the environmental covariate included in Model g_3, dropped precipitously in 2019 and is not expected to reach pre-2019 coverage even under the most optimistic seagrass scenario (Fig. 4.7A) [68]. Consequently, our C_{MSY} estimates (i.e. conditional posterior predictive median and 80% CI)

derived based on mean density-weighted *Z. marina* cover by the VIMS SAV Program were all approximately equal to C_{MSY} estimates between 2004 and 2008 when density-weighted *Z. marina* cover was at similarly low levels (Fig. 4.7B).

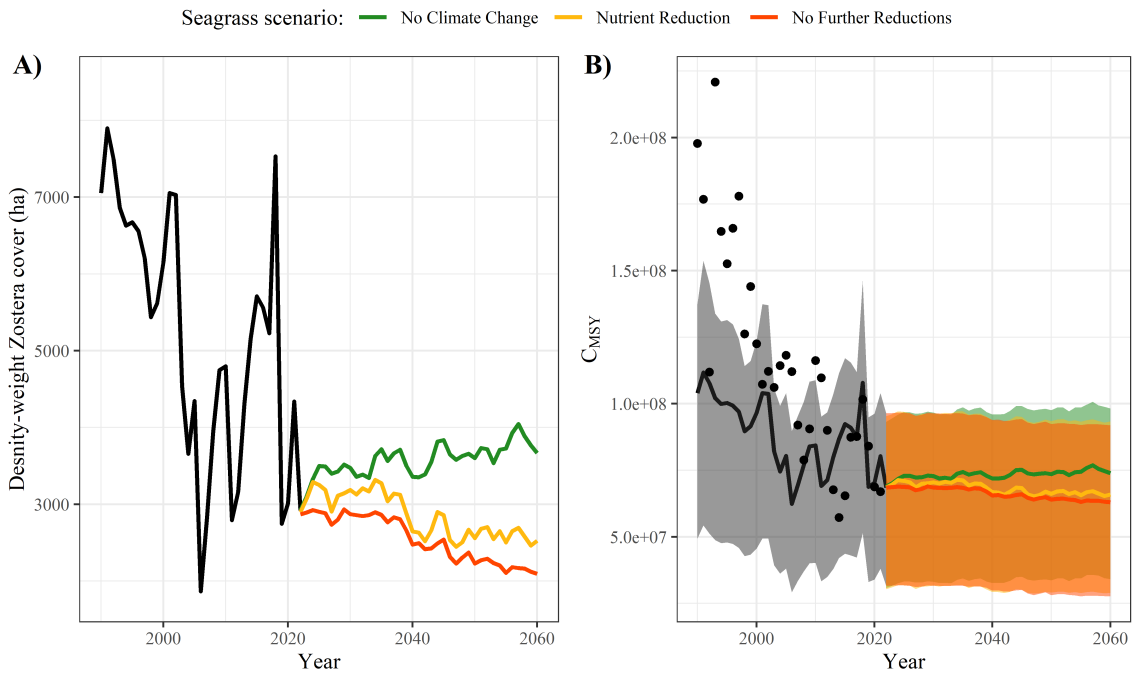

Figure 4.7: Time series of A) past and projected density-weighted mean cover of *Z. marina* by the VIMS SAV Program and B) our estimates and projections for C_{MSY}. For A), density-weighted mean cover of *Z. marina* of observed (black) and projected scenarios for no climate change (green), nutrient reduction (yellow) and no further reductions (red). For B), conditional C_{MSY} posterior median (lines) and 80% CI (shaded regions) are based on past (grey) and future (green: no climate change; yellow: nutrient reduction; red: no further reduction) density-weighted *Z. marina* cover estimates in A). Points in B) depict reported female total catch C_t for each year 1990 to 2022.

Comparisons of past projection-based C_{MSY} values to reported catches (C_t, see equation 4.2 and Section 4.2.5) were generally consistent with the blue crab population trajectory over time (Figs. 4.4 and 4.7). Reported catch generally exceeded C_{MSY} in years prior to 2010, particularly prior to 2000. However, after 2010 almost all reported female catches

were near or below median C_{MSY} (Fig. 4.7B). This broadly corresponded with the estimated population trajectory for total female blue crab populations, which declined from 1990 to 2008 and began increasing in 2009 (Fig. 4.4C). Meanwhile, projection-based C_{MSY} under different future scenarios of density-weighted *Z. marina* were generally consistent with one another due to the relative similarity in projected density-weighted *Z. marina* (Fig. 4.7A). The estimated C_{MSY} in 2060 under the "no climate change" scenario was only marginally higher than the other two scenarios (73 million individuals vs 65 and 63 million individuals in 2060) and confidence intervals overlapped substantially, indicating relative statistical equivalence.

Finally, comparisons of C_{MSY} projections between models g_3 and g_1 (the base model) demonstrated the benefit of including seagrass covariates into future projections. As model g_1 did not include time-varying MSY coefficients, the C_{MSY} derived from Model g_1 for all future years considered was static (conditional posterior median: 116 million individuals year^{-1}; 80% CI: 75 to 138 million individuals year^{-1}). Although the conditional posterior inference for this C_{MSY} was comparable to that from Model g_3 in the early part of the time series (i.e. 1990-2000), they were considerably higher than the highest C_{MSY} posterior distribution produced from Model g_3 future projections ("no climate change" in 2060; conditional posterior median: 74 million individuals year^{-1}; 80% CI: 34 to 98 million individuals year^{-1}). These results suggest that exclusion of density-weighted *Z. marina* cover resulted in conditional median projections for C_{MSY} which were 150% higher and may substantially overestimate sustainable harvest.

4.4 Discussion

In this study, we carried out a model-based assessment of the quantitative value of seagrass distribution on blue crab population dynamics in Chesapeake Bay, which should also be relevant to other blue crab populations along its geographic range. Our findings indicate that 1) inferences for blue crab population states are improved when incorporating seagrass cover as an environmental covariate, 2) blue crab population dynamics are presently more responsive to density-weighted *Z. marina* cover than to that of *R. maritima*, and 3) future *Z. marina* projections under all three scenarios (no climate change, nutrient reduction, no further reductions) suggest general declines in both population abundance and C_{MSY} relative to past values. Hence, these findings enhance our basic understanding of the importance of nursery habitats for exploited marine and estuarine species [139, 188, 16, 102] and rigorously express how declines in nursery habitat quality and quantity impact commercially exploited fisheries.

4.4.1 Seagrass-specific effects

Density-weighted *Z. marina* cover reduced the strength of juvenile blue crab density dependence and increased juvenile carrying capacity in Chesapeake Bay. Inclusion of seagrass covariates improved predictive performance relative to the seagrass-independent base model in all cases, although Model g_3, which included only density-weighted *Z. marina* cover as the sole environmental covariate, exhibited superior predictive performance relative to both the base model and other candidate seagrass models.

Correspondence between juvenile blue crab density dependent regulation and density-weighted *Z. marina* cover as opposed to either *R. maritima* or seagrass generally is potentially due to 1) structural characteristics of *Z. marina* and *R. maritima*, 2) differences

in temporal persistence of these two species, and 3) spatial distribution of *Z. marina* relative to that of *R. maritima*. First, *R. maritima* is characterized by short, thin, rod-like shoots, compared to longer, thicker, strap-like leaves characteristic of *Z. marina* [11, 136, 80, 33]. Thus, *Z. marina* shoots and canopy structure may provide superior refuge quality to juvenile blue crabs [134]. Second, although faunal densities are comparable between the two species in Chesapeake Bay [135, 55], *R. maritima* blades only occupy the water column for 10 to 30% of the year; considerably less than that of *Z. marina*, which occupies the water column 80% of the year [136]. Moreover, *R. maritima* is an ephemeral species reliant on sexual reproduction and known for substantial fluctuations in annual cover [24]. Hence, differences in annual persistence of *R. maritima* may hinder the development of complex communities typically associated with the perennial nature of *Z. marina* [33]. In simpler terms, the seasonal decline of *R. maritima* may prevent the formation of diverse and long-lasting habitats, unlike the more persistent *Z. marina*, which allows for the establishment of more intricate ecological communities [68]. Finally, juvenile blue crabs may be more responsive to distributions of *Z. marina* due to the spatial position of this species in Chesapeake Bay. *Z. marina* remains the dominant seagrass in lower Chesapeake Bay, while *R. maritima* primarily occurs farther from the mouth of Chesapeake Bay in lower salinity environments [68]. Meanwhile, blue crab postlarvae re-enter the Bay through the mouth and rapidly settle into the first structurally complex habitat available – usually lower Bay SAV [201]. Moreover, the stenohaline nature of blue crab postlarvae may limit extensive penetration into relatively fresh middle and upper Chesapeake Bay waters. For example, blue crab postlarvae were found in consistently higher densities in the lower York River ($\approx$ 50 km from Chesapeake Bay mouth) relative to Tangier Sound ($\approx$ 104 km from Chesapeake Bay mouth) [214]. Taken together, the structural complexity, phenology, and spatial position of *Z. marina* provide superior nursery quality compared to

R. maritima.

4.4.2 Implications for blue crab management

Conditional posterior predictive inferences for maximum sustainable yield from both historic and projected density-weighted *Z. marina* cover facilitated useful insights for blue crab management. First, the degree of coherence between reported catches and estimated C_{MSY} from 1990 to 2022 lends insight to blue crab population trajectories. Extensive blue crab population declines from 1990–2008 corresponded with substantial divergences in reported catch and estimated C_{MSY}, particularly from 1990–2000, However, following management changes enacted in 2008, reported catch fell within C_{MSY} confidence intervals. Higher relative population estimates after this time period could reflect the correspondence between reported catch and estimated C_{MSY}. However, in recent years (i.e 2020–2022), both juvenile and adult abundances have fallen notably [22]. These declines appear to coincide with dramatic losses in density-weighted *Z. marina* cover between 2018 (7535 ha) and 2019–2022 (2746–4338 ha) [68]. Hence, discrepancies between reported catch and C_{MSY}, coupled with recent *Z. marina* cover trajectories, could explain observed changes in blue crab population dynamics well.

Unfortunately, *Z. marina* cover is expected to continue declining relative to historic extents even under the most opportunistic scenarios. Unlike *R. maritima*, *Z. marina* is far more sensitive to thermal stress [151]. *Z. marina* currently experiences temperature-induced stress in summer months, giving rise to severe episodic die-offs followed by limited recovery [156, 151, 137]. This species is expected to continue to decline in abundance and distribution in Chesapeake Bay as summer temperatures rise; a direct result of climate change [137, 68]. Summer temperatures are already sufficiently high relative to historic norms that, even under the “no climate change” scenario in [68], long-term *Z. marina*

projections remain far lower than the 1990–2022 values (conditional posterior median value under 3667 ha of density-weighted cover in “no climate change” vs 5228 ha cover observed in time series). Hence, although counterfactual projections demonstrate the value of *Z. marina* cover to blue crab population dynamics, the low contrast in density-weighted cover trajectories correspond to comparable blue crab population trajectories.

Traditionally, population dynamics models have focused on single-species applications primarily concerned with fishing pressure and population vital rates. Although it is widely understood that population vital rates are influenced by environmental processes, vital rates in traditional models are usually assumed static across space and time and unresponsive to fluctuations in environmental variables. This stationarity assumption, although questionable, could be justified in the past because of relatively limited directional anthropogenic influence on environmental variables, and thus stochastic perturbations in environmental variables could be accounted for with the use of random process error. However, anthropogenic pressures have led to multiple unprecedented directional changes in numerous environmental variables. Hence, variation in environmental processes – and corresponding influences on fisheries population dynamics – is increasingly deterministic and directional. As a consequence, ignoring influential environmental processes is increasingly untenable. Comparisons in C_{MSY} projections between our best performing model and our seagrass-independent base model highlighted the benefit of including environmental covariates and the peril of their continued exclusion. First, evidence from cross-validation exercises illustrated the improved performance of Model g_3 relative to Model g_1, irrespective of C_{MSY}. Second, although C_{MSY} estimates from models g_1 and g_3 were more comparable in past years –particularly prior to 2000, C_{MSY} estimates derived from Model g_1 were noticeably higher than those produced from Model g_3 in future years when *Z. marina* cover is projected to be considerably lower than past estimates. This suggests that management advice from

Model g_1 may substantially overestimate sustainable harvest in future scenarios in which *Z. marina* is much lower than historical values. Consequently, although C_{MSY} estimates under various seagrass management scenarios were similar due to the physiology of *Z. marina*, the projections remain notably more conservative relative to estimates from models not considering *Z. marina* cover.

4.4.3 Caveats and future work

A major caveat of this study is the confounding of *Z. marina* and *R. maritima* with spatial position within Chesapeake Bay. Currently, *Z. marina* remains the dominant seagrass species in the lower Bay, while *R. maritima* is the dominant species in the middle and upper portions of Chesapeake Bay. While we believe the superior refuge value of *Z. marina* to blue crabs as evidenced in our model is a function of both seagrass physiology and spatial position, we acknowledge that the relative importance of *R. maritima* may change as this species replaces extirpated *Z. marina* in the lower Bay. As a result, we stress that our results might be improved by using more granular spatial delineations such as density-weighted seagrass species extents in upper, middle, and lower Chesapeake Bay as an initial means of delineating effects of seagrass species and spatial position.

The impacts of habitat declines on population dynamics can be either mitigated or intensified as a result of changes in other habitats, highlighting the importance of considering multiple habitats when evaluating nursery status. For example, fringing salt marsh habitat is gaining recognition as an intermediate nursery for larger (i.e. 15 to 60 mm CW) juvenile blue crabs and potentially as an alternative primary nursery for smaller ($\leq$15 mm CW) juveniles in areas where seagrass meadows are sparse or absent [86, 82, 81, 81]. Ideally, the effects of multiple habitats on species' population dynamics should be assessed together to determine nursery status. We were unable to include additional habitats such as salt

marsh area or salt marsh edge in the present study due to model non-convergence, which likely stems from 1) low temporal contrast in salt marsh habitat due to historic and current marsh migration compensating salt marsh losses [183][1] and/or more likely 2) the absence of an additional, unmeasured juvenile state in our data required to delineate habitat effects of salt marsh and seagrass habitat. Although evidence strongly suggests that smallest and most vulnerable juvenile blue crabs utilize seagrass meadows as a primary nursery habitat [154, 164, 105, 171, 14], juveniles larger than 15 mm CW appear to utilize structured and unstructured salt marsh habitat [105, 81, 81]. It is possible that the increased survival of the most vulnerable and most abundant juvenile stages conferred by seagrass provides a stronger signal that that of salt marsh or other structured habitats, or that the substantially greater aerial cover of seagrass relative to other habitats provides a clearer signal. Isolating potential effects of salt marsh or other structured habitats on juvenile population dynamics (here $\leq$60 mm CW) may require assessment of small ($\leq$15 mm CW) juvenile abundance in addition to the states assessed by the dredge and trawl survey. Unfortunately, no survey in Chesapeake Bay currently exists that samples juvenile blue crabs of that size class in shallow-water structured habitats due to logistical limitations. Moreover, postlarvae re-invade estuaries in sporadic waves between July and November in Chesapeake Bay [148, 214], such that multiple cohorts move through seagrass and other structurally complex habitats within a given year. Hence, accounting for multiple nursery habitats used throughout blue crab ontogeny may require a monthly time-step instead of the annual time step in the present study. Future models operating at finer-scale temporal resolutions with additional juvenile states may substantially improve our understanding of the effects of multiple habitats on juvenile population dynamics. Finally, our C_{MSY} projections were based on conditional posterior predictive inference, whereby state equations were

[1]We were able to make inference on marsh habitat in Chapter 1 due to high spatial contrast in the data

regarded as perfect representations of nature. Although such projections are in line with simulation studies in literature [131, 169], we acknowledge that unconditional posterior predictive simulation studies would yield uninformative projections beyond 2023 (i.e. one year into the future) due to the multiplicative nature of process errors compounded over time.

4.4.4 Relevance

The sustainable management of fisheries requires considering the crucial role of nursery habitats and incorporating ecosystem considerations. Neglecting the value of nursery habitats can result in habitat management failures, leading to the loss of critical habitats and reduced population productivity. By expanding population modeling approaches and rigorously linking habitat availability to fisheries production, we can gain valuable insights for effective fisheries management. Moreover, fisheries management necessitates the use of brief forecasts for stock performance, highlighting the necessity for techniques that can integrate the impact of covariates on recruitment when their influence is significant. The high correspondence between the nominal 1-SAP 80% and 95% posterior intervals and the observed proportion of withheld values captured within those intervals suggests that our best-performing model is a useful forecasting tool for at least the following year, although the multiplicative process error structure may make posterior predictions farther into the future considerably more uncertain.

Our study on the blue crab stock in Chesapeake Bay also exemplifies the interdependence between nursery habitat management and fisheries management, emphasizing the importance of considering these factors for long-term sustainability. Seagrass habitat has long been the focus of conservation [150, 151, 156, 137, 96, 68], and the importance of seagrass as a nursery habitat to blue crabs is well known [103]. However, before this study,

the relative quantitative value of a specific parcel of seagrass to blue crab populations at broad spatial scales remained unclear. Hence our findings can be used to incorporate seagrass habitat availability into stock assessments [117] and management decisions, enhance Integrated Ecosystem Assessments (IEAs) [97], and inform Ecosystem Status Reports, all of which facilitate movement towards ecosystem-based fisheries management (EBFM) [99, 145, 40]. High-quality scientific information detailing the relationships among fishery species and their essential habitats is a fundamental element in EBFM [160]. Hence, our results provide a high-quality EBFM product [160] concentrated on Chesapeake Bay to accurately measure vital nursery habitats and their effects on blue crab population dynamics in this system. It is our hope that our approach and associated findings will provide managers of the multi-state Chesapeake Bay blue crab fishery—the Chesapeake Bay Stock Assessment Committee (CBSAC)—with tactical, and actionable, management advice [108].

Appendix A

Chapter 1

A.1 More on predictor variables

Unstructured habitat constitutes the majority of available shallow habitat in Chesapeake Bay, but varies considerably in food availability and predation refuge [105]. Evidence suggested unstructured mud may serve as an alternative nursery for juveniles where structurally complex habitat is unavailable due to relatively abundant alternative prey and potential for juveniles to bury deep in the soft substrate [119, 168]. Thus, in the earliest exploratory models, we had included mean percent mud composition of substrates in each section-year as a continuous covariate, in addition to those presented in Table 1.1. However, 80% credible intervals for the corresponding regression coefficient of this variable consistently included 0, and inclusion of the variable did not otherwise change inference results of the initial models. In contrast, the other variables, such as seagrass, management status, and predator abundance, were always kept in our models regardless of their statistical importance in explaining juvenile blue crab abundance, due to their implications on large-scale blue crab population management. Because percent mud composition did not carry the same implications with respect to management, it was excluded as a variable of interest

in all models presented in this article.

A.2 Defining areal units

Note that despite the arbitrary nature of areal unit definitions in practice, the one we employed in our work here did not meaningfully influence our results, or bias, our inference. In fact, initially, we explored numerous areal unit configurations when aggregating spatially random trawls. Alternative configurations included dividing each tributary into i) ten sections whose lengths were tributary dependent, ii) sections based on morphologically meaningful characteristics (e.g., branching structures and choke points), and iii) sections $\sim$2km in length along the tributary axis. In all cases, parameter estimates from models were practically identical. The final areal unit configuration was chosen based on the high number of areal units per year produced, and only a single section-year had 0 trawl tows.

A.3 Model validation and predictive performance

Cross validation (CV) is a robust, generic method to adjudicate between competing statistical models. Unlike information theoretic criteria (e.g., AIC, BIC, DIC), cross validation assesses predictive performance directly by separating the data in a part that is used for fitting (i.e., training set) and another used to assess predictive adequacy (i.e., test set). Cross validation preference goes to the model that best predicts the out-of-sample test set withheld.

Cross validation is helpful in determining relative model generalizability. In a Bayesian CV framework, prediction intervals are computed using the posterior predictive distributions of the excluded values in the test set based on posterior distributions of model parameters to simulate the training set. Generalizability is determined based on the observed coverage, i.e., the proportion of excluded values which are successfully captured by their respective

prediction intervals.

We used 80% prediction intervals to infer model performance of our suite of candidate models. Models yielding an observed coverage differing greatly from the nominal Bayesian predictive credible level of 80% may indicate underfitting/overfitting. Cross validation results from Models 1, 2, 3a, and 3b, all indicated underfitting (being less complex than Model 4) and poor predictive performance. In contrast, posterior prediction intervals of Model 4 contained 81% of excluded data ($n = 36$), indicating overall superior predictive performance relative to all other candidate models. Hence, we selected Model 4 as the model which best represents our observed data as well as the most generalizable model.

In contrast with simpler models, Model 4 is characterized by greater uncertainty in posterior distributions of predictor coefficients as well as posterior predictive credible intervals used in cross validation (Figs. 4.5 and C4). This is a frequent characteristic of models with increasing complexity. Complex models (with a larger number of unknown model parameters) lead to more uncertainty in the inference, whereas simpler models which are inadequate in capturing latent dependence processes would give incorrect inference, irrespective of the amount of uncertainty.

A.4 Chapter 1 Supplementary figures

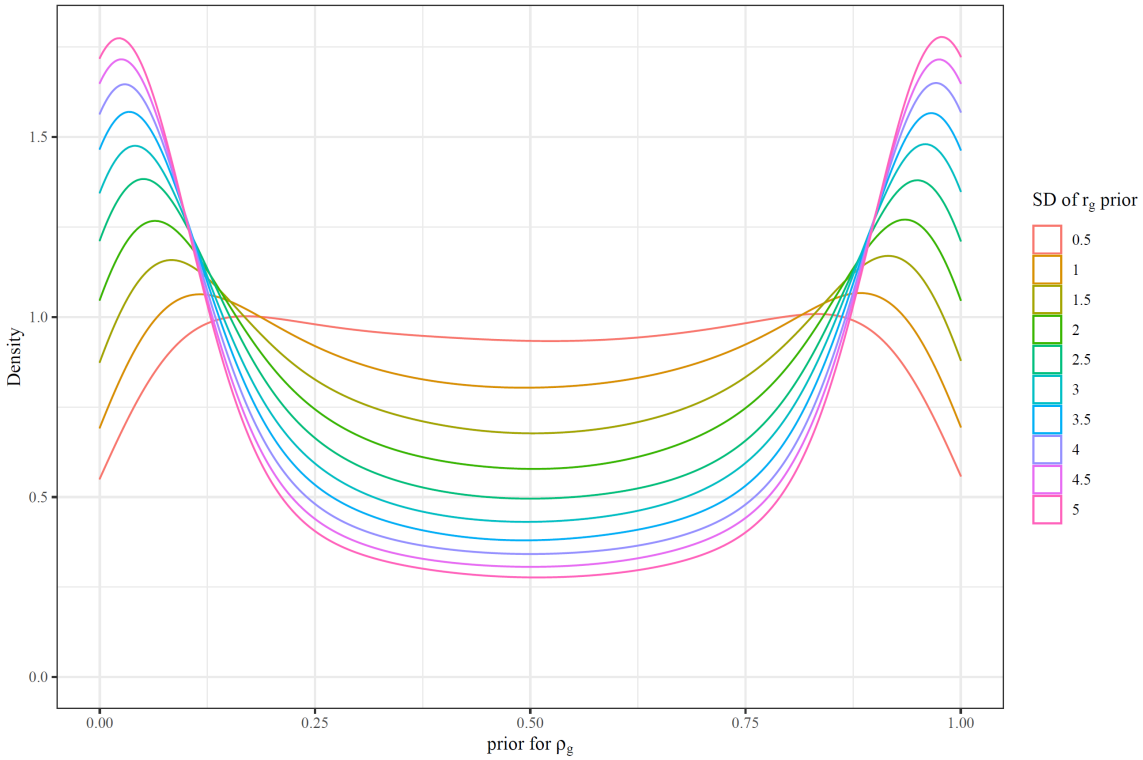

Figure A1: Marginal prior distributions of ρ_g with increasing standard deviations of the normally distributed prior for r_g (whose mean is 0), and a prior distribution of $U(0,1)$ for P. The marginal prior distribution for ρ_g is approximately $U(0,1)$ when a $N(0,0.25)$ is imposed on r_g. Thus, constraining the prior for r_g to a relatively narrow distribution results in a diffuse marginal prior for ρ_g.

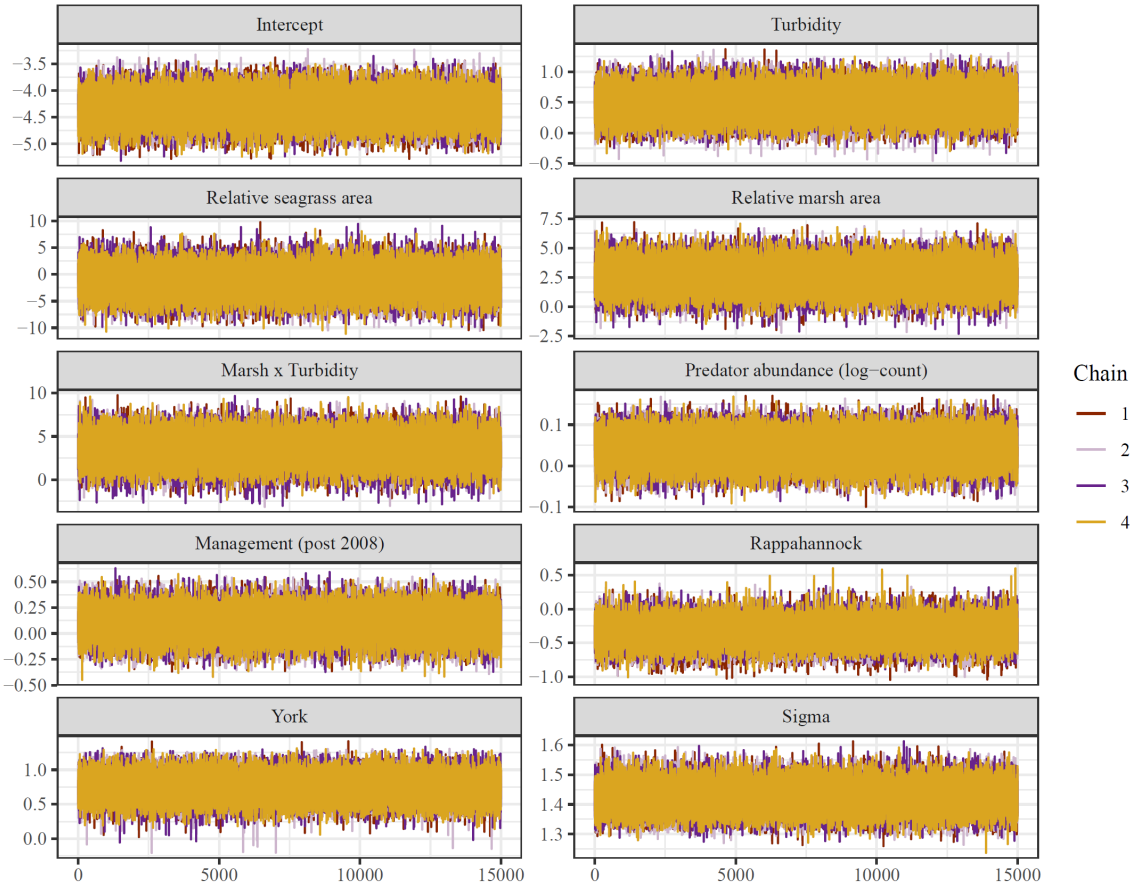

Figure A2: A set of trace plots for Model 4 parameters illustrating sampled values of each regression coefficient and σ_Φ per chain throughout the post burn-in iterations. Visual inspection of trace plots is used to evaluate convergence and mixing of the chains.

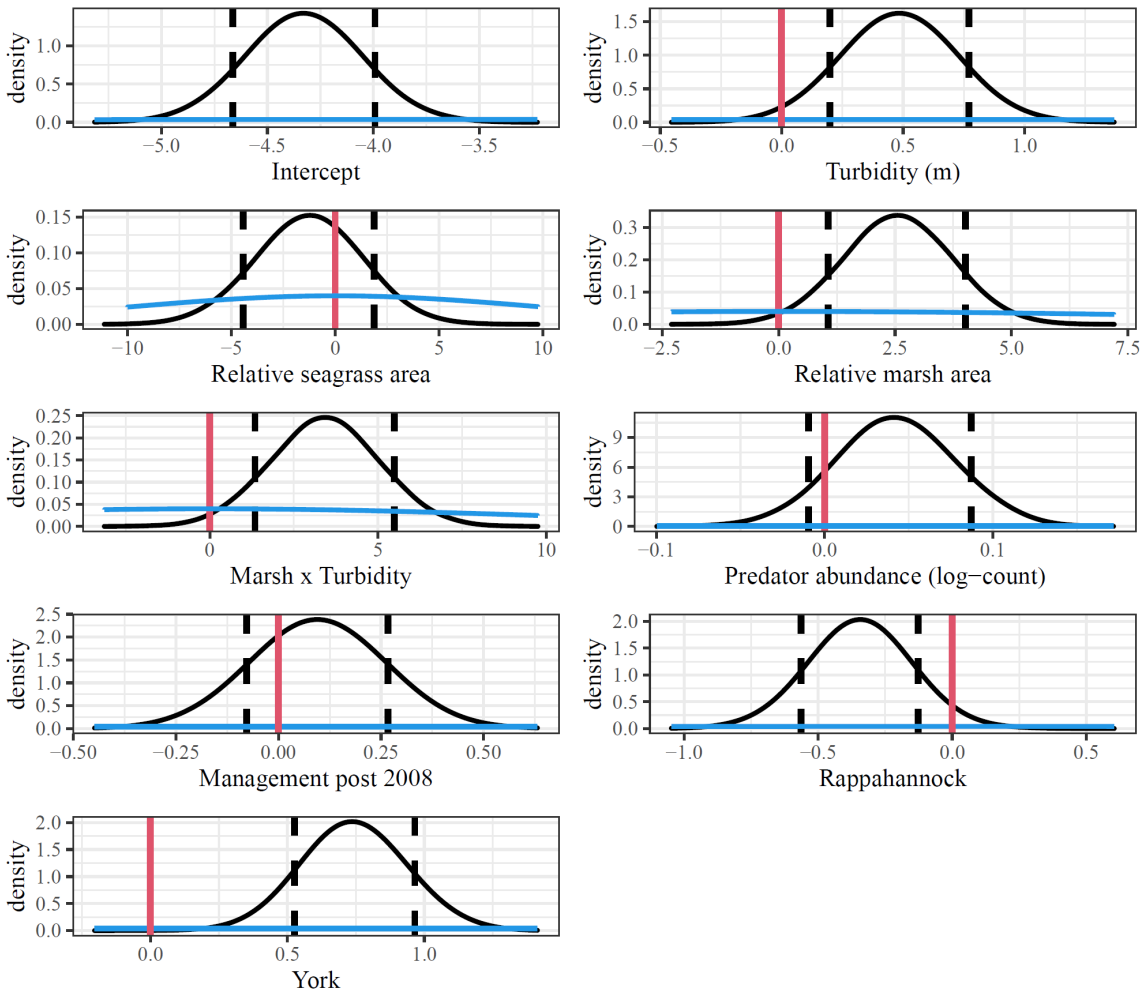

Figure A3: Posterior distributions (black) and prior distributions (blue) of regression coefficients from Model 4; dashed black lines denote 80% credible intervals, while solid red lines denote 0

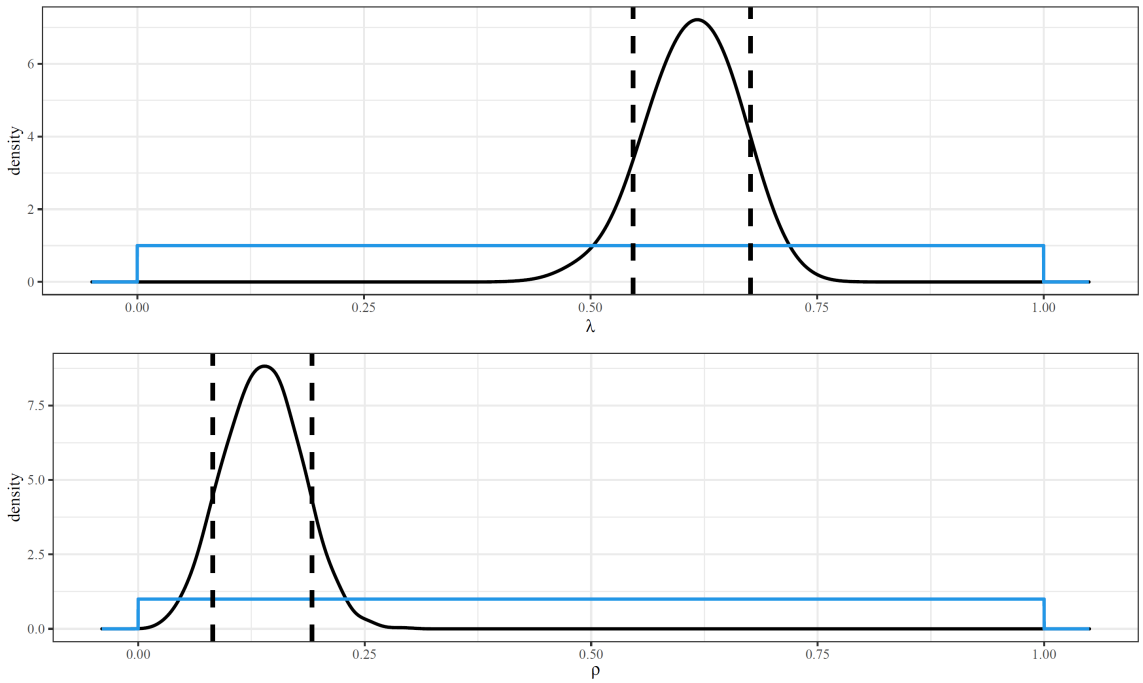

Figure A4: Posterior distributions (black) and prior distributions (blue) of autocorrelation parameters λ (spatial) and ρ (temporal) from Model 4; dashed black lines denote 80% credible intervals. Leave-future-out cross validation of Models 1–4 showed that the non-separable spatiotemporal dependence structure of Model 4 was necessary for good predictive performance, despite the small ρ.

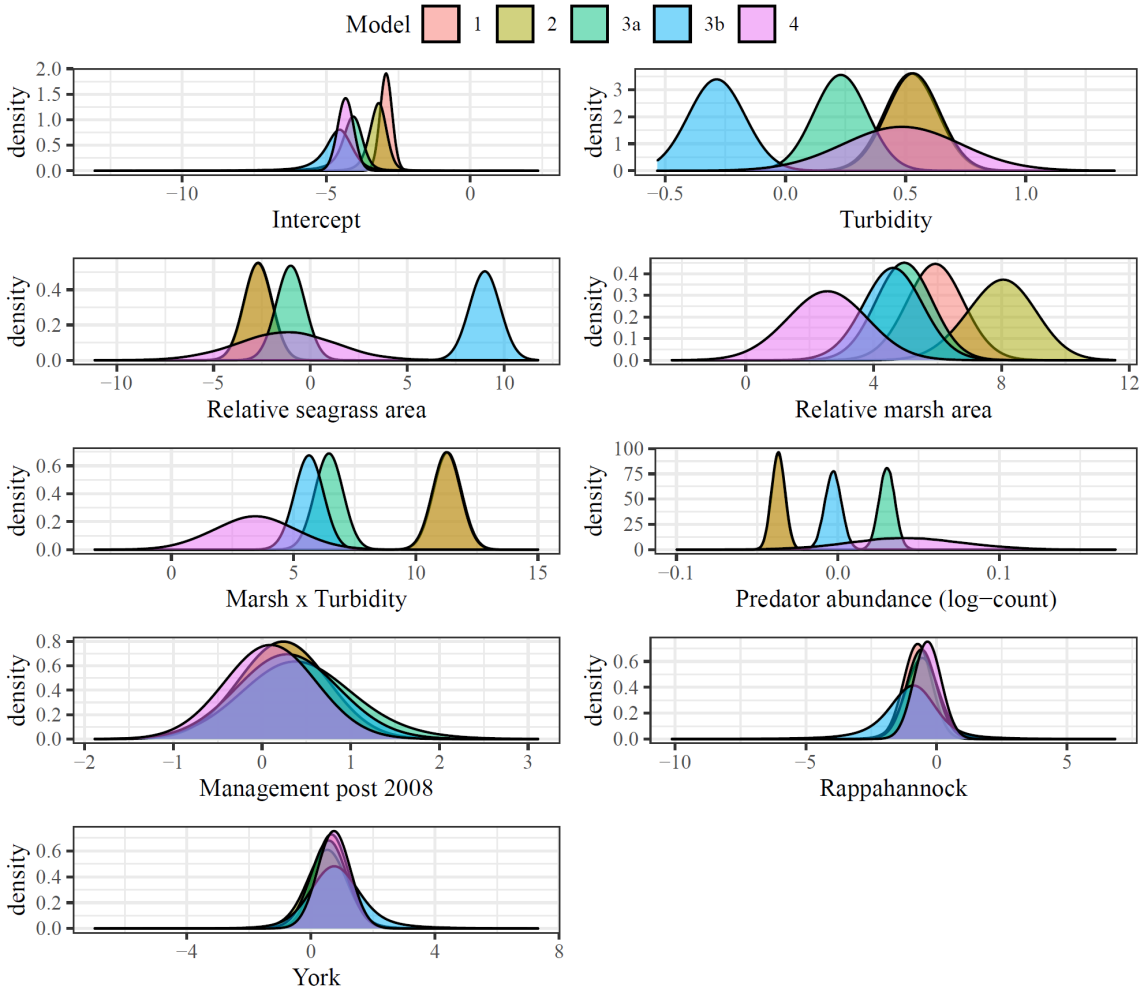

Figure A5: Posterior distributions of regression coefficients from Models 1-4.

Appendix B

Chapter 2

B.1 Logical framework

$\mathbf{g_1}$: Abundance is a function of habitat and turbidity. Structurally complex habitats harbor higher densities of juvenile blue crabs relative to unstructured habitats. Hence, relative to sand habitat, juvenile blue crab density is higher seagrass, SME, and SDH [154, 66, 86, 45, 82]. Meanwhile, high local turbidity increases juvenile abundance through both bottom-up [187, 186] and potentially top-down [146, 4] mechanisms (see methods in [82] for more details).

$\mathbf{g_2}$: Abundance is a function of habitat, turbidity, and an interaction between habitat and turbidity. Here, the effect of turbidity is dependent on a particular habitat. Whereas seagrass meadows are absent from high-turbidity areas due to light requirements, extensive salt marshes and unstructured sand habitats occur in both high- and low-turbidity regions of the tributaries. Turbidity may therefore modify the effectiveness of these habitats as nurseries for juvenile crabs by decreasing predatory foraging efficiency through both low visibility (turbidity) and structural impediments (in SME or SDH; [4, 82]).

$\mathbf{g_3}$: Abundance is a function of habitat, turbidity and spatial position. Recruitment in a given location is dependent on postlarval supply [8, 58, 192]. Blue crab postlarvae enter tributaries from the mouth (i.e. downriver), and decline with distance upriver along the tributary axis as they encounter suitable habitat and settle [201]. Hence, we expected habitats positioned closer to the mouth of the river would be associated with higher juvenile abundances due to proximity to postlarval supply.

$\mathbf{g_4}$: Abundance is a function of habitat, turbidity, spatial position, and an interaction between habitat and spatial position. Environmental conditions vary substantially along tributary axes [165]. Latent variables influencing juvenile abundance may inconsistently affect habitats. As a consequence, the effects of spatial position are habitat-specific [191, 140].

$\mathbf{g_5}$: Abundance is a function of habitat, turbidity, spatial position, and an interaction between habitat and turbidity [82].

$\mathbf{g_6}$: Abundance is a function of habitat, turbidity, spatial position, an interaction between habitat and spatial position, and an interaction between habitat and turbidity. Additional environmental variables other than turbidity may augment habitat suitability at different spatial positions, such as salinity [165] and/or food availability [186].

B.2 Prior distributions for gear efficiency

As different sampling methods were employed for the four habitat types, gear efficiency estimates were required to scale abundance estimates for each sample. Efficiency of the

suction sampling methodology is estimated at 0.88 [154]. Meanwhile, pilot efficiency tests of the modified flume net design using marked blue crabs in fall of 2020 indicated an estimated efficiency of 0.92 $\pm$ 0.02. Finally, juvenile blue crab depletion experiments for benthic scrape gear suggested efficiency between 0.21 and 0.45 [170]. However, benthic scrapes used here differed slightly in that they did not include iron teeth, which may decrease efficiency.

We constructed normally distributed prior distributions for each gear type based on estimates from literature and observed data and subsequently applied a log-transformation to relate prior estimates of efficiency to the model scale. For flume traps, the prior distribution was ln $N(0.92, 0.02)$ which has a mean of-0.083 and standard deviation of 0.02. Similarly, for scrape estimates, we assumed the mean efficiency was 0.33 (average of 0.45 and 0.21) and a standard deviation of 0.12 to yield a prior of ln $N(0.33, 0.12)$ which has a mean of -1.2 and standard deviation of 0.18. Finally, for suction sampling, average efficiency is 0.88 [154], although uncertainty estimates were not supplied in literature. Here, we assumed an efficiency of 0.02 similar to uncertainty in flume traps and applied a prior of ln $N(0.88, 0.02)$ which has a mean of -0.13 and standard deviation of 0.02.

B.3 Chapter 2 Supplemental Tables

Table B1: Data summaries of crab carapace widths (CW) and physicochemical variables.

	Temperature (°C)	Salinity	Secchi (cm)	DO (mg/L)	CW (mm)
Min	17.30	2.66	8.20	3.90	1.00
10%	19.90	6.06	30.00	6.28	6.40
50%	24.10	17.56	78.00	7.63	12.90
90%	28.90	19.46	128.41	8.77	25.28
Max	30.90	20.32	183.00	11.37	135.10

Table B2: Table displaying the number of samples for each habitat by trip. Five of the total 144 samples were expunged due to missing predictor values (i.e. Secchi disk depth) in seagrass (two samples) and SDH (three samples)

Habitat	Trip 1	Trip 2	Trip 3	Trip 4	Total
SME	0	6	6	6	18
SDH	15	18	18	0	51
Seagrass	4	6	6	0	16
Sand	18	18	18	0	54

B.4 Chapter 2 Supplementary figures

Figure B1: Images of flume net in multiple stages of deployment: **a)** depicts a flume net set up at slack flood tide; **b)** denotes flume net collected at slack ebb tide; and **c)** denotes flume in non-deployment stage with net walls down and end removed when net is not in use. When not in use, enclosures will remain on site with the net walls folded and staked into the ground and the end removed, facilitating movement of animals throughout marsh habitat. Prior to use, walls of the flume nets will be rapidly erected to contain all animals occupying the habitat at the time of sampling.

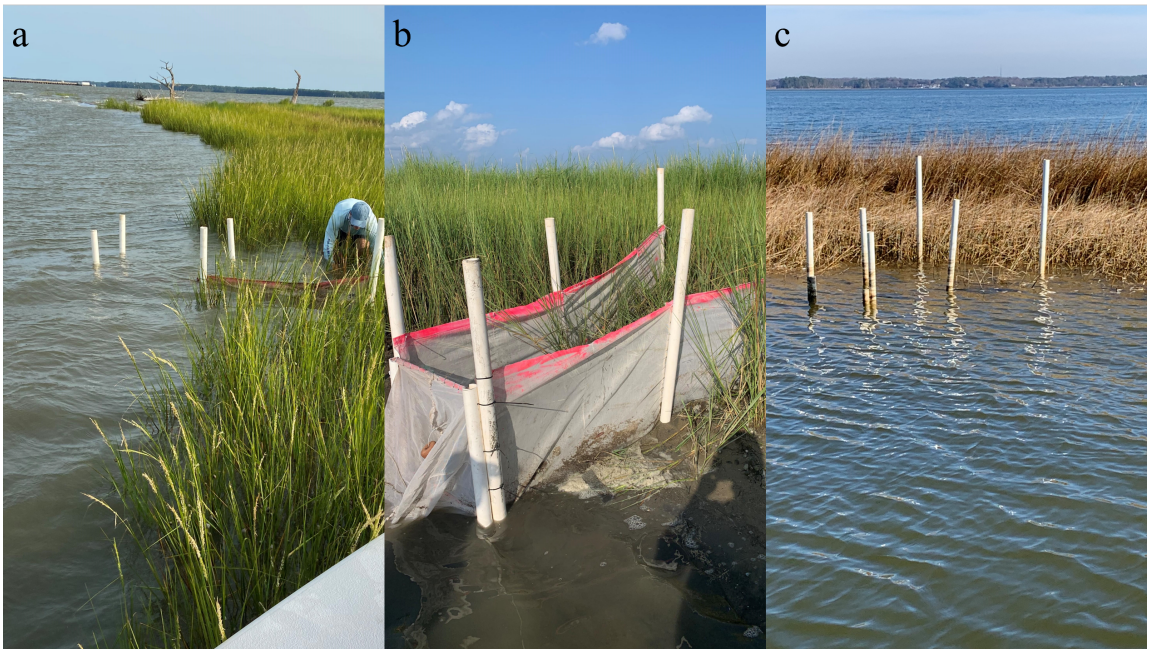

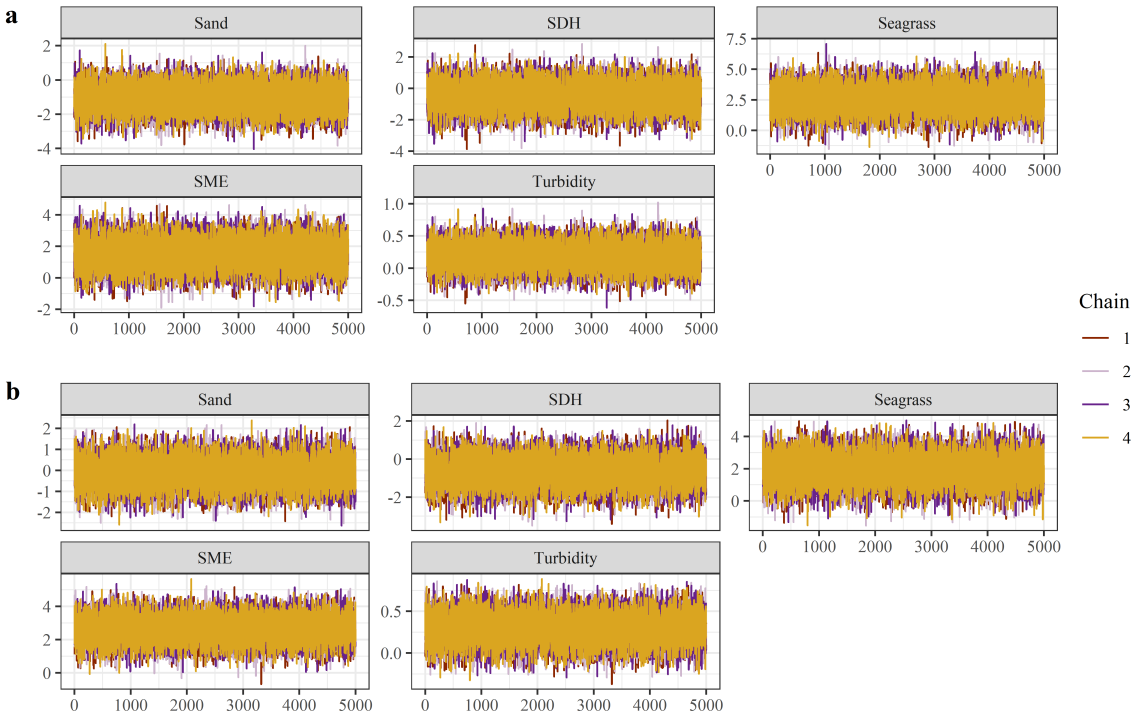

Figure B2: A set of trace plots for model g_1 parameters illustrating sampled values of each regression coefficients per chain throughout the post-warmup/adaptive phase iterations. Visual inspection of trace plots is used to evaluate convergence and mixing of the chains.

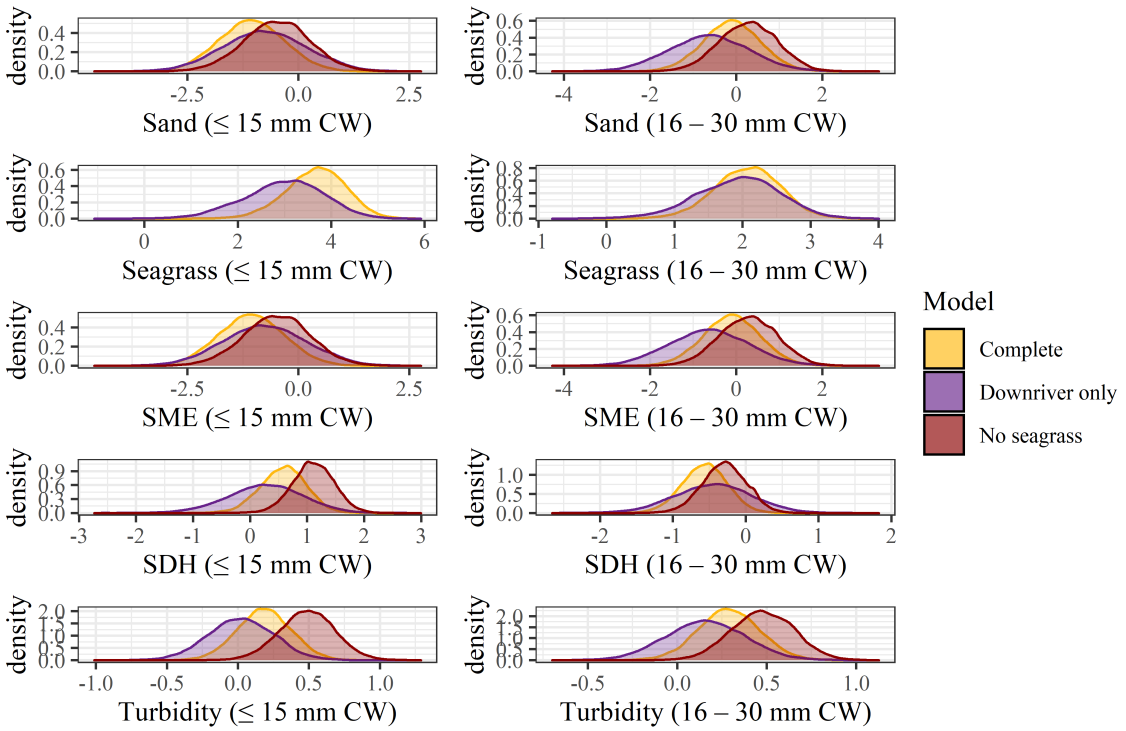

Figure B3: Posterior distributions from the selected model g_1 using the complete data set (Complete), and subsets of the data using only the downriver stratum (Downriver only) and without seagrass (No seagrass). Distributions were largely consistent across models, indicating inferences on the complete data set were robust.

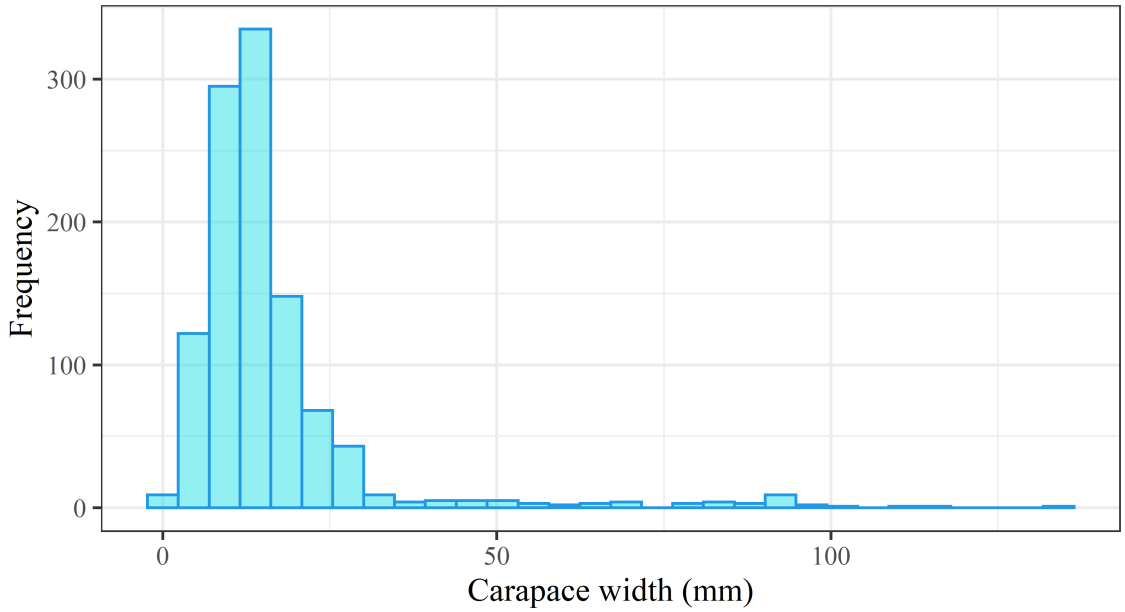

Figure B4: Histogram of all crab carapace wdiths (mm) caught in Fall 2020 recruitment period.

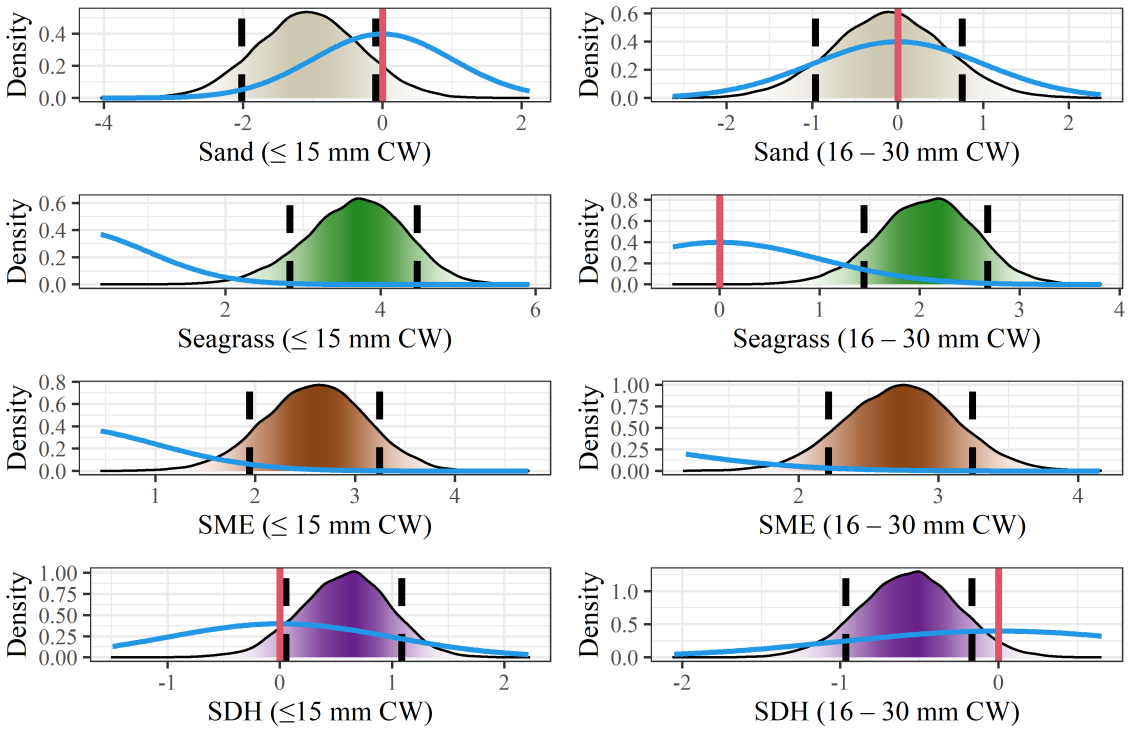

Figure B5: Conditional posterior distributions of mean habitat abundances (conditioned on holding random effects and ln turbidity at 0) from model g_1 for both small (≤ 15 mm CW; left column) and large (16–30 mm CW; right column) size classes. Dashed black lines denote 80% Bayesian confidence intervals, while red lines (where present) denote 0. Blue lines depict prior distributions. Depicted values are on the model (log) scale.

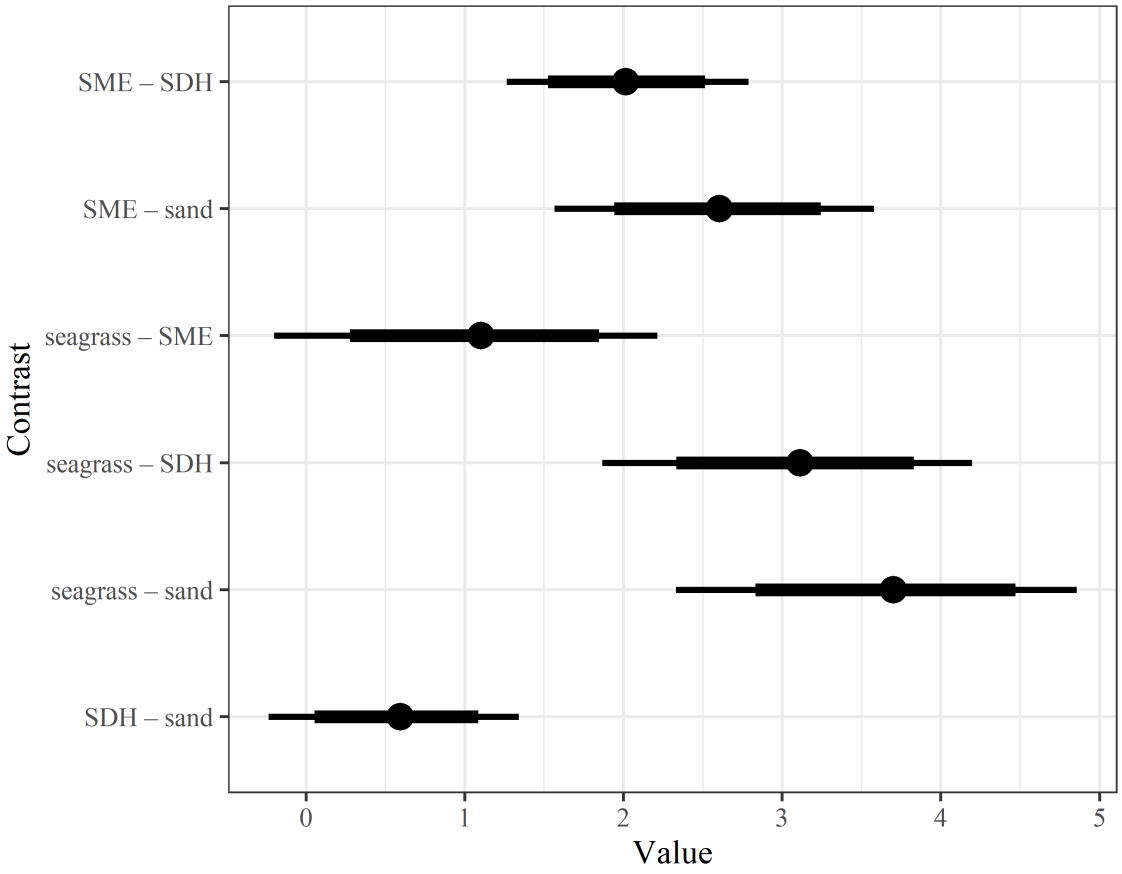

Figure B6: Linear contrast statements (see Section 3.5) depicting differences in expected juvenile blue crab abundance for the small size class from Model g_1. Dots denote mean difference in expected values, while thick bars represent 80% Bayesian CIS and thin bars denote 95% Bayesian CIS. Depicted values are on the model (log) scale.

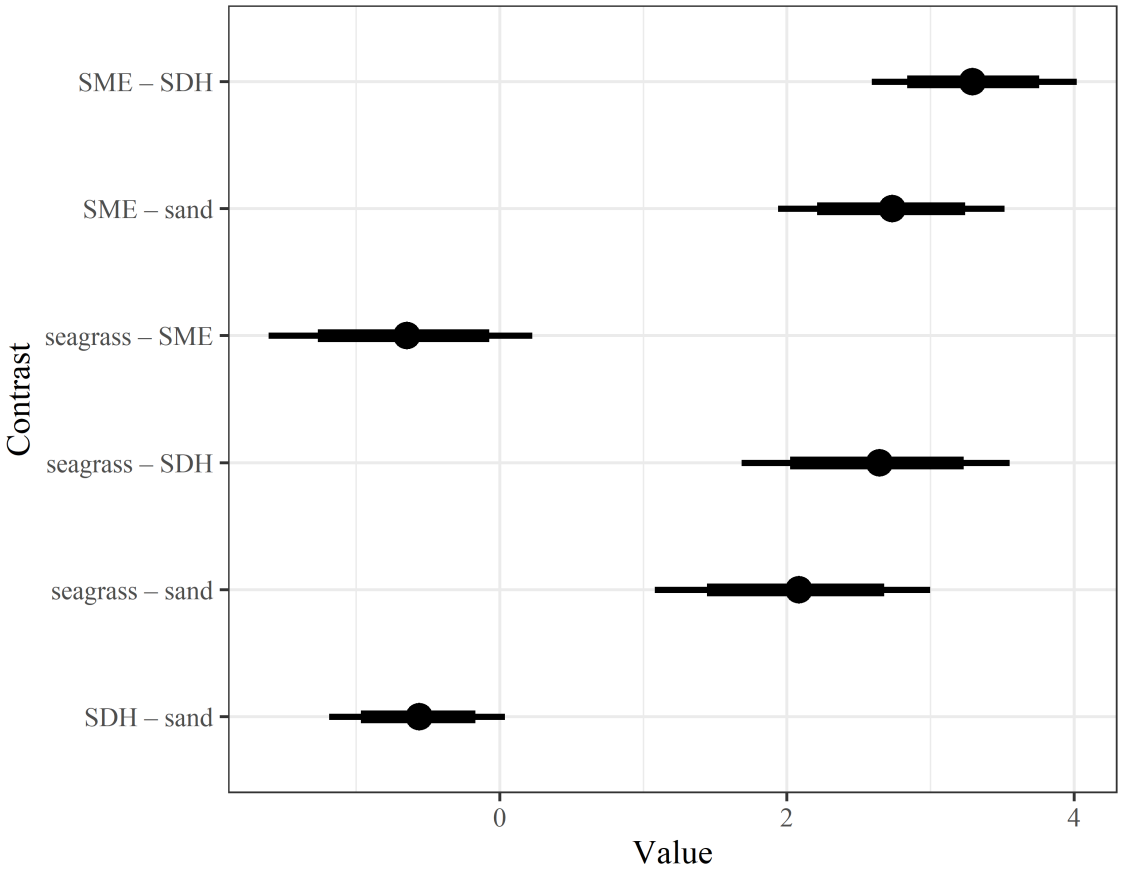

Figure B7: Linear contrast statements (see Section 3.5) depicting differences in expected juvenile blue crab abundance for the large size class from Model g_1. Dots denote mean difference in expected values, while thick bars represent 80% Bayesian CIS and thin bars denote 95% Bayesian CIS. Depicted values are on the model (log) scale.

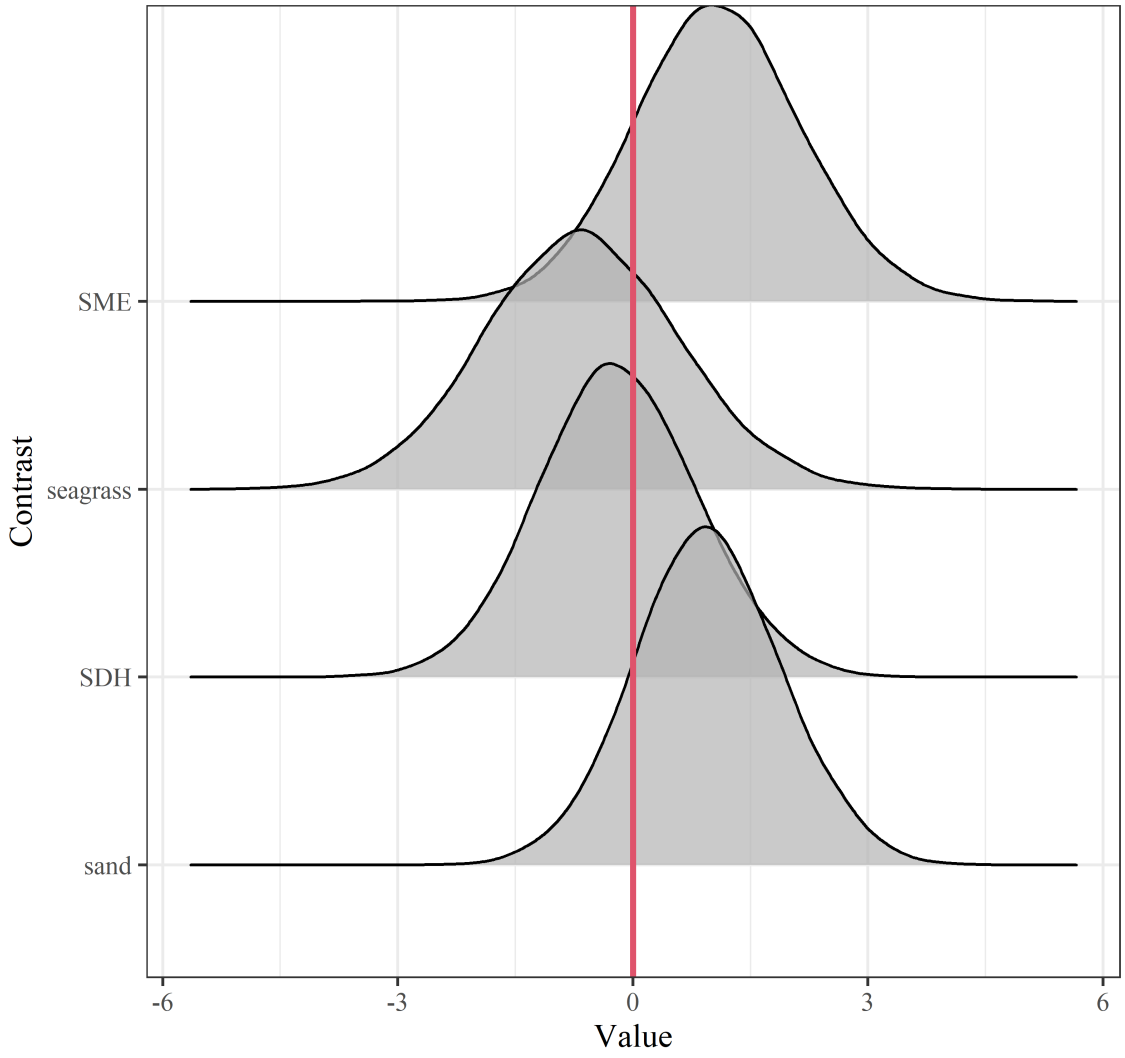

Figure B8: Posterior distributions of within-habitat linear contrasts (see Section 3.5) depicting differences in expected juvenile blue crab abundance for small and large size class from Model g_1. Positive values indicate increases in expected abundance as animals move from $\leq$15 to 16–30 mm, while negative values indicate decreases in expected abundance. Depicted values are on the model (log) scale.

Appendix C

Chapter 3

C.1 Predictor justification

C.1.1 Habitat

Inference on nursery habitat quality with respect to juvenile blue crab abundance and survival was the over-arching objective of this study. Structurally complex habitats harbor higher densities of juvenile blue crabs relative to unstructured habitats due to higher food availability and superior refuge quality [154, 105, 103, 88, 171, 82, 81]. Hence, relative to sand, we expected higher juvenile blue crab densities in seagrass and SME [154, 66, 86, 45, 82, 81]. Moreover structurally complex habitats provide higher refuge quality to small prey through the substantial number of interstitial spaces between biogenic structures such as shoots and rhizomes [76, 155, 88, 123]. Hence, we expected higher survival in structurally complex seagrass and SME relative to sand [110, 4, 14]. However, not all structure provides equally beneficial refuge. For example, smaller interstitial spaces of seagrass shoots may provide superior refuge quality to juveniles relative to the larger spaces characteristic of salt marsh shoots [155]. Moreover, most habitats encompass areas both with and without structural complexity or otherwise spatially vary in the degree

of structure they afford (e.g. patchiness; [76, 77, 105]). Hence, in the survival model we considered ”structured” and ”unstructured” treatments in each habitat (see section 3.2.3.3 for details). We expected high survival in structured components of seagrass and SME and comparatively low survival in adjacent, unstructured portions.

C.1.2 Turbidity

Multiple studies have noted positive correlations between blue crab abundance and turbidity [82, 81]. Two potential mechanisms may engender these observed patterns. First high turbidity is associated with increased juvenile abundance through both bottom-up controls [187]. The thin-shelled baltic clam *Macoma Baltica* is a preferred prey item of juvenile blue crabs [187, 186] which aggregates near estuarine turbidity maxima and may attract juveniles [187, 186, 105]. Second, turbidity may provide juvenile blue crabs with protection from visual predators [32, 113] and from predation [146, 78, 74] through a reduction in light intensity. Upriver unstructured habitat is turbid, whereas similar habitat downriver has lower turbidity, such that upriver unstructured habitat can also serve as an effective nursery [105, 186]. Hence, observed patterns between juvenile blue crab abundance and turbidity at regional scales may be a proxy for patterns between juvenile and potentially top-down [146, 4] mechanisms (see methods in [82] for more details). Hence, we expected turbidity would be positively associated with juvenile blue crab abundance and juvenile blue crab survival.

C.1.3 Stratum

Aside from turbidity, abundance may be influenced by spatial position through spatially correlated, unobserved variables. Hence, stratum was included in our abundance model to avoid confounding variation as well as to assess the effect of spatial orientation. Moreover,

habitats in different spatial locations along the river axis may harbor different predator guilds, such that inference on impacts of structure among habitats may be confounded by unmeasured effects of differing predator communities and abundances (i.e. predation pressure; [165, 105]). Thus, we included stratum as a categorical fixed-effect in our abundance model and a habitat-stratum variable (i.e. an interaction) in our survival model.

C.1.4 Megalopae

Juvenile abundance is initially dictated by megalopae supply [43]. Although post-settlement dynamics of early juvenile blue crabs are strongly density-dependent at local scales [46, 172], early juvenile abundances may be limited by megalopae supply when juvenile populations are relatively low [46, 66, 65]. Megalopae abundance was not expected to affect juvenile blue crab survival, and thus was not included as a predictor in our survival model.

C.1.5 Carapace width

Juvenile blue crab habitat utilization changes through ontology [105, 103, 81]. Smaller juveniles are vulnerable to a larger suite of predators than larger juveniles which achieve a size refuge from smaller foraging species [105]. We therefore included carapace width as a continuous covariate in our survival model. Carapace width was not included as a predictor in our abundance model because we instead chose to include three separate size classes as response variables.

C.1.6 Month

Juvenile blue crab survival fluctuates seasonally. Juvenile blue crab survival is highest in late spring and late fall months, and lowest in summer [73]. Seasonal variation in

survival is likely influenced by seasonal predator abundances. For example, red drum *Sciaenops ocellatus*, and striped bass *Morone saxatilis* both consume juvenile blue crabs at high rates [138, 70, 103]. Abundances of these species fluctuate seasonally in the North Atlantic estuaries as animals utilize estuaries in during early life stages and spawning in summer and early fall [47, 178]. Hence, we included month as a categorical variable in the survival model. In contrast, juvenile blue crab abundances were sampled only within the fall recruitment period and exploratory data analysis did not indicate substantial fluctuations with month or trip. As a result, month was only included in the survival model.

C.2 Statistical treatment of continuous variables

Both megalopae abundance and turbidity values were transformed prior to inclusion in abundance models. Megalopae in a given location must enter the river through the mouth, and as a result megalopae abundances generally decline with distance upriver as megalopae encounter suitable habitat and settle out of suspension [201]. We therefore expect a log-linear relationship between local juvenile blue crab abundance and megalopae abundance, where increases in megalopae abundance at low levels have larger positive effects on juvenile blue crab abundance than at higher levels, as post-settlement processes dominate when megalopae supply exceeds the carrying capacity of a system [66, 197, 103]. The natural log of megalopae plus a constant ($M = \ln(\text{Megalopae} + 1)$) to avoid infinite values when (Megalopae $= 0$) was therefore used in lieu of the raw variable. Moreover, as new recruits require time to grow to a size which could be detected by our gear, we used $\ln(\text{Megalopae} + 1)$ abundances lagged by four weeks as a predictor for local juvenile abundance.

Similarly, a natural log transformation was applied to turbidity measurements. Log-turbidity was defined as the natural log transformation of Secchi-disk depth, multiplied by -1

($T = -\ln$ Secchi). The natural log transformation was applied based on the understanding that a threshold exists in water transparency. Assuming that effects of turbidity on juvenile abundance reflect refuge from visually oriented predators (top-down control), small changes in water transparency when water is relatively clear are not expected to substantially affect juvenile abundance as much as small changes in water transparency when water is cloudy (e.g. predation rates by Summer Flounder on mysid shrimp; [78]). Alternatively, if associations between juvenile abundance and turbidity are related to elevated food availability near the estuarine turbidity maximum, juveniles would presumably remain more sensitive to fluctuations in turbidity at high values compared to clearer waters. Multiplying the variable by -1 facilitates inference on turbidity, instead of water transparency (inverse).

C.3 Tethering methodology details

Tethering involved attaching 30 cm monofilament fishing line to the crab's carapace with cyanoacrylate glue. The other end of the line was tied to a stake pushed into the sediment; the stake was tied to a location pole 1 m from the crab to minimize effects of artificial structures that could attract predators to the tethered crab. Tethered crabs were allowed to acclimate in laboratory aquaria for 24 h prior to placement in the field.

Prior to field experiments, pilot experiments were used to determine probability of escape (i.e., crabs un-tethering themselves) and potential changes in behavior. In April (i.e. when predation is negligible) [177, 133] five crabs were tethered in two locations (n = 10) and checked daily. In the absence of predation, juvenile crabs remained on tethers for over a week and were able to bury themselves in sediment. We replicated this procedure in lab conditions with 10 additional crabs observed daily for 10 d. Here, only one crab escaped its tether on day eight. Since crabs in our field experiments were deployed for approximately 24 h, we concluded that the number of crabs removed due to escape was negligible.

Predation is evident by a missing crab and either pieces of carapace remaining on the line, chewed pieces of tape and monofilament line, or cut monofilament lines [164, 77, 105]. Although uncommon (i.e., $<$ 10% of all instances), some tethers were excluded from analysis because the crab molted and only the exoskeleton remained on the tether. However, this was apparent upon retrieval due to the intact molt remaining on the monofilament line. These features were used to distinguish predation from molting in the field experiments. Molts were subsequently recorded and excluded from analysis.

C.3.1 Treatment-specific bias

Tethering can introduce treatment-specific bias in survival [162]. For example, tethered crabs may experience lower survival in structurally complex habitats such as seagrass and SME as a result of entanglement, but would not experience the same reduction in survival in sand, such that relative survival rates could not be compared between these habitats. Alternatively, variation in escape behaviors (e.g., crypsis in structurally complex habitat vs. fleeing in sand) may also introduce bias. Extensive work from previous studies examining treatment-specific biases of tethering juvenile crabs in seagrass, SME, and sand have not found interactions between tethering and habitat [164, 76, 105, 123], therefore, we assumed there was no treatment-specific bias in our experiments, which used similar tethering methods and habitats as those in previous studies.

C.4 Chapter 3 Supplementary Tables

Table C1: Summary table displaying the number of samples for each habitat by stratum and field study.

Area	**Megalopae**		**Abundance**			**Survival**	
	Shore	SME	Seagrass	Sand	SME	Seagrass	Sand
Downriver	4	3	6	3	2	2	2
Midriver	3	3	NA	3	2	NA	2
Upriver	3	3	NA	3	2	NA	2
Total	10	9	6	9	6	2	6

Table C2: Linear contrast statements depicting differences in expected juvenile blue crab survival (π_{cond}) among habitat-strata combinations. Dots denote mean difference in expected values, while thick bars represent 80% Bayesian CIS and thin bars denote 95% Bayesian CIS. The red vertical line denotes 0. Depicted values are on the model (logit) scale. Relevant contrasts are defined as those which exclude 0 with their 80% CI. Only contrasts which exclude 0 within their 80% CI are included here for brevity.

Contrast		Lower 80% CI	Estimate	Upper 80% CI	Relevant
Downriver sand	Downriver SME structure	-1.47	-0.58	0.26	
Downriver sand	Downriver SME unstructured	-0.31	0.60	1.46	
Downriver sand	Downriver seagrass structure	-3.07	-2.19	-1.32	*
Downriver sand	Downriver seagrass unstructured	0.40	1.37	2.27	*
Downriver sand	Midriver sand	-1.27	-0.32	0.57	
Downriver sand	Midriver SME structure	-2.62	-1.69	-0.76	*
Downriver sand	Midriver SME unstructured	-1.27	-0.35	0.57	
Downriver sand	Upriver sand	-1.24	-0.24	0.68	
Downriver sand	Upriver SME structure	-3.02	-2.06	-1.08	*
Downriver sand	Upriver SME unstructured	-1.33	-0.38	0.56	
Downriver SME structure	Downriver SME unstructured	0.70	1.19	1.65	*
Downriver SME structure	Downriver seagrass structure	-2.41	-1.61	-0.80	*
Downriver SME structure	Downriver seagrass unstructured	1.09	1.95	2.82	*
Downriver SME structure	Midriver sand	-0.54	0.27	1.20	
Downriver SME structure	Midriver SME structure	-1.97	-1.09	-0.22	*
Downriver SME structure	Midriver SME unstructured	-0.61	0.24	1.11	
Downriver SME structure	Upriver sand	-0.52	0.35	1.33	
Downriver SME structure	Upriver SME structure	-2.40	-1.47	-0.52	*
Downriver SME structure	Upriver SME unstructured	-0.75	0.22	1.08	
Downriver SME unstructured	Downriver seagrass structure	-3.62	-2.80	-1.97	*
Downriver SME unstructured	Downriver seagrass unstructured	-0.12	0.76	1.66	
Downriver SME unstructured	Midriver sand	-1.81	-0.92	-0.02	*
Downriver SME unstructured	Midriver SME structure	-3.16	-2.29	-1.37	*
Downriver SME unstructured	Midriver SME unstructured	-1.90	-0.96	-0.11	*
Downriver SME unstructured	Upriver sand	-1.83	-0.85	0.09	
Downriver SME unstructured	Upriver SME structure	-3.65	-2.66	-1.71	*
Downriver SME unstructured	Upriver SME unstructured	-1.96	-0.98	-0.06	*
Downriver seagrass structure	Downriver seagrass unstructured	2.97	3.56	4.09	*
Downriver seagrass structure	Midriver sand	1.02	1.87	2.78	*
Downriver seagrass structure	Midriver SME structure	-0.38	0.51	1.40	
Downriver seagrass structure	Midriver SME unstructured	0.95	1.84	2.73	*
Downriver seagrass structure	Upriver sand	1.02	1.96	2.94	*
Downriver seagrass structure	Upriver SME structure	-0.88	0.14	1.04	
Downriver seagrass structure	Upriver SME unstructured	0.85	1.82	2.72	*
Downriver seagrass unstructured	Midriver sand	-2.63	-1.68	-0.76	*
Downriver seagrass unstructured	Midriver SME structure	-4.01	-3.06	-2.12	*
Downriver seagrass unstructured	Midriver SME unstructured	-2.62	-1.72	-0.74	*
Downriver seagrass unstructured	Upriver sand	-2.64	-1.61	-0.66	*
Downriver seagrass unstructured	Upriver SME structure	-4.45	-3.42	-2.44	*
Downriver seagrass unstructured	Upriver SME unstructured	-2.78	-1.74	-0.81	*
Midriver sand	Midriver SME structure	-2.26	-1.37	-0.53	*
Midriver sand	Midriver SME unstructured	-0.89	-0.04	0.83	
Midriver sand	Upriver sand	-0.80	0.08	0.98	
Midriver sand	Upriver SME structure	-2.63	-1.74	-0.80	*
Midriver sand	Upriver SME unstructured	-0.96	-0.06	0.81	
Midriver SME structure	Midriver SME unstructured	0.83	1.33	1.82	*
Midriver SME structure	Upriver sand	0.58	1.44	2.30	*
Midriver SME structure	Upriver SME structure	-1.24	-0.37	0.53	
Midriver SME structure	Upriver SME unstructured	0.48	1.31	2.18	*
Midriver SME unstructured	Upriver sand	-0.74	0.11	0.95	
Midriver SME unstructured	Upriver SME structure	-2.56	-1.70	-0.82	*
Midriver SME unstructured	Upriver SME unstructured	-0.86	-0.02	0.82	
Upriver sand	Upriver SME structure	-2.69	-1.82	-0.96	*
Upriver sand	Upriver SME unstructured	-0.97	-0.13	0.69	
Upriver SME structure	Upriver SME unstructured	0.16	1.68	2.17	*

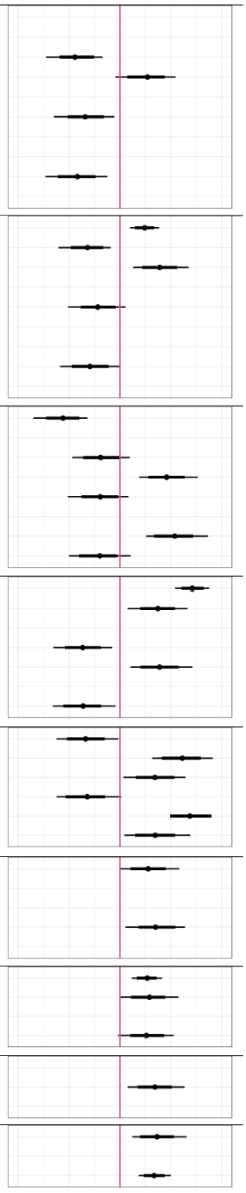

C.5 Chapter 3 Supplementary figures

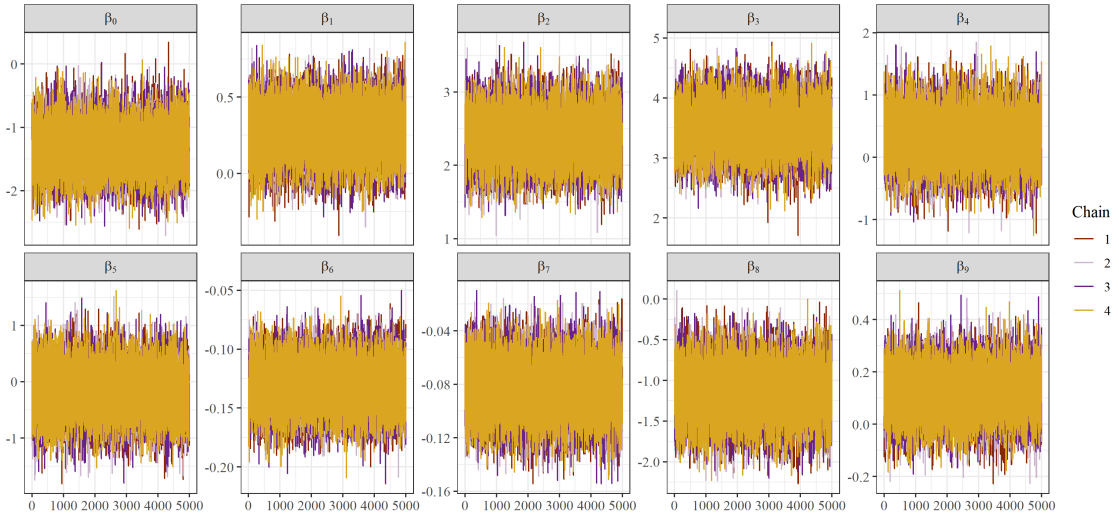

Figure C1: A set of trace plots for abundance model regression parameters for small ($\leq$15 mm) size class illustrating sampled values of each regression coefficients per chain throughout the post-warmup/adaptive phase iterations. Visual inspection of trace plots is used to evaluate convergence and mixing of the chains. See Table 3.3 for details on abundance model predictor coefficients.

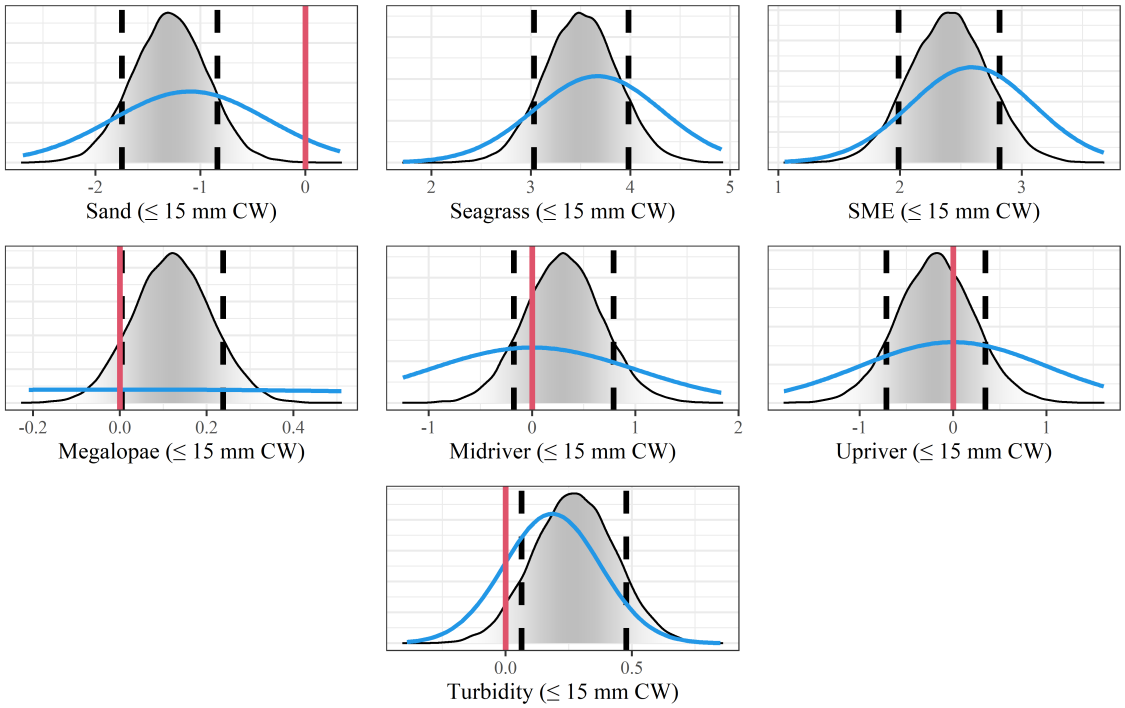

Figure C2: Posterior distributions (grey) and prior distributions (blue) of regression coefficients for small (≤15 mm CW) juvenile blue crabs derived from the abundance model; dashed black lines denote 80% credible intervals, while solid red lines denote 0.

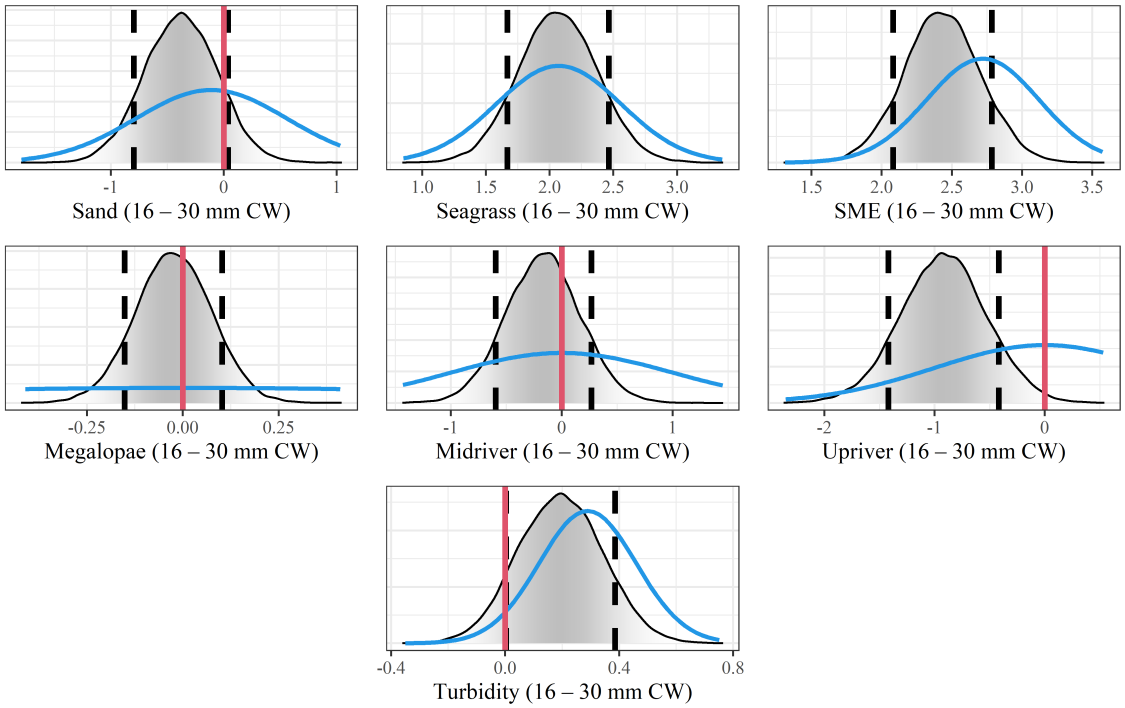

Figure C3: Posterior distributions (grey) and prior distributions (blue) of regression coefficients for medium (16–30 mm CW) juvenile blue crabs derived from the abundance model; dashed black lines denote 80% credible intervals, while solid red lines denote 0.

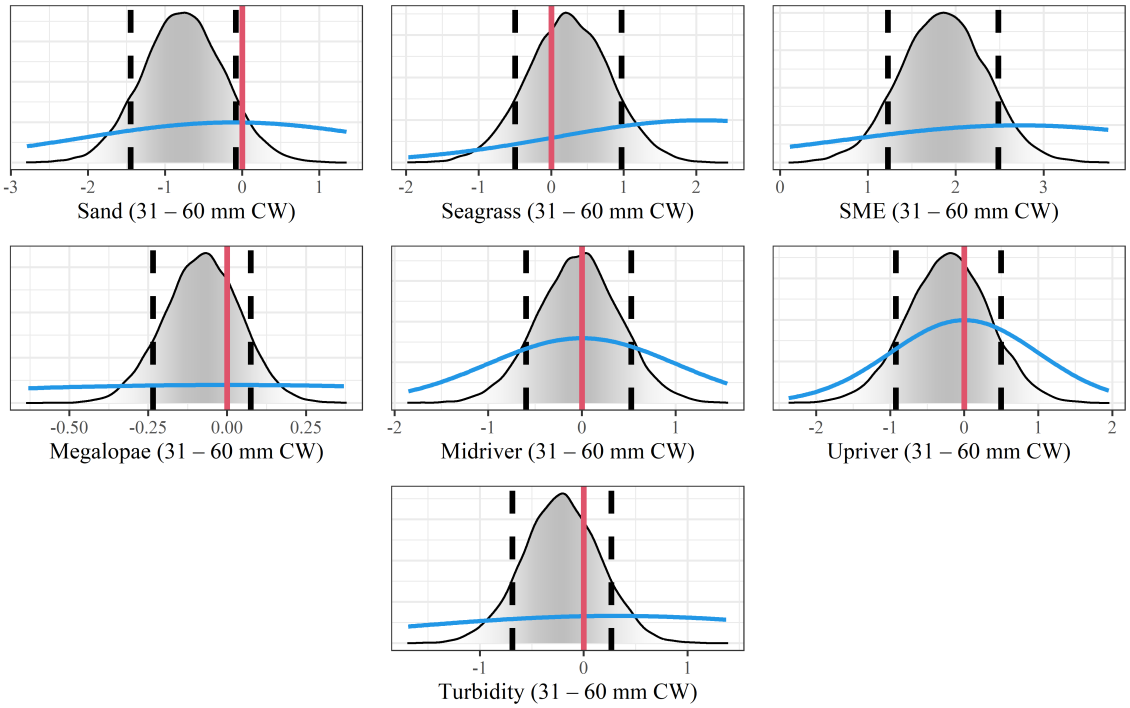

Figure C4: Posterior distributions (grey) and prior distributions (blue) of regression coefficients for large (31–60 mm CW) juvenile blue crabs derived from the abundance model; dashed black lines denote 80% credible intervals, while solid red lines denote 0.

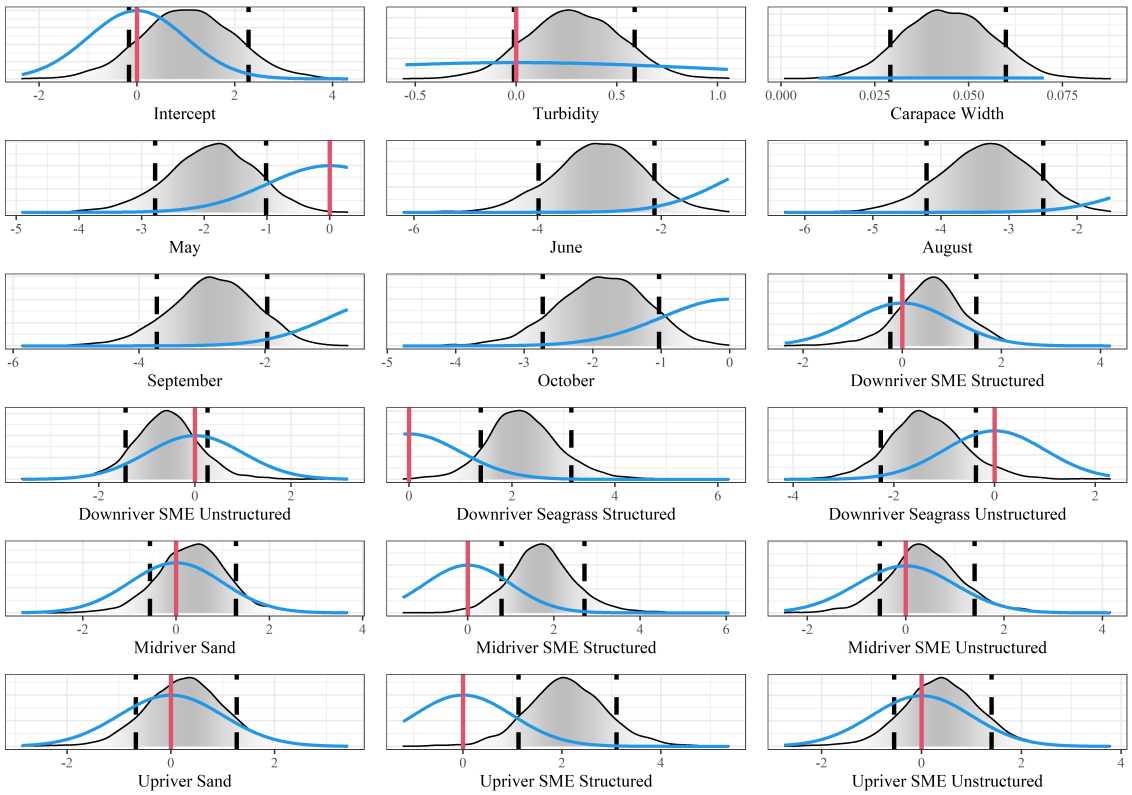

Figure C5: Posterior distributions (grey) and prior distributions (blue) of regression coefficients derived from the survival model; dashed black lines denote 80% credible intervals, while solid red lines denote 0.

Figure C6: Linear contrast statements depicting differences in expected juvenile blue crab survival among months. Dots denote mean difference in expected values, while thick bars represent 80% Bayesian CIs and thin bars denote 95% Bayesian CIs. The red vertical line denotes 0. Depicted values are on the model (logit) scale.

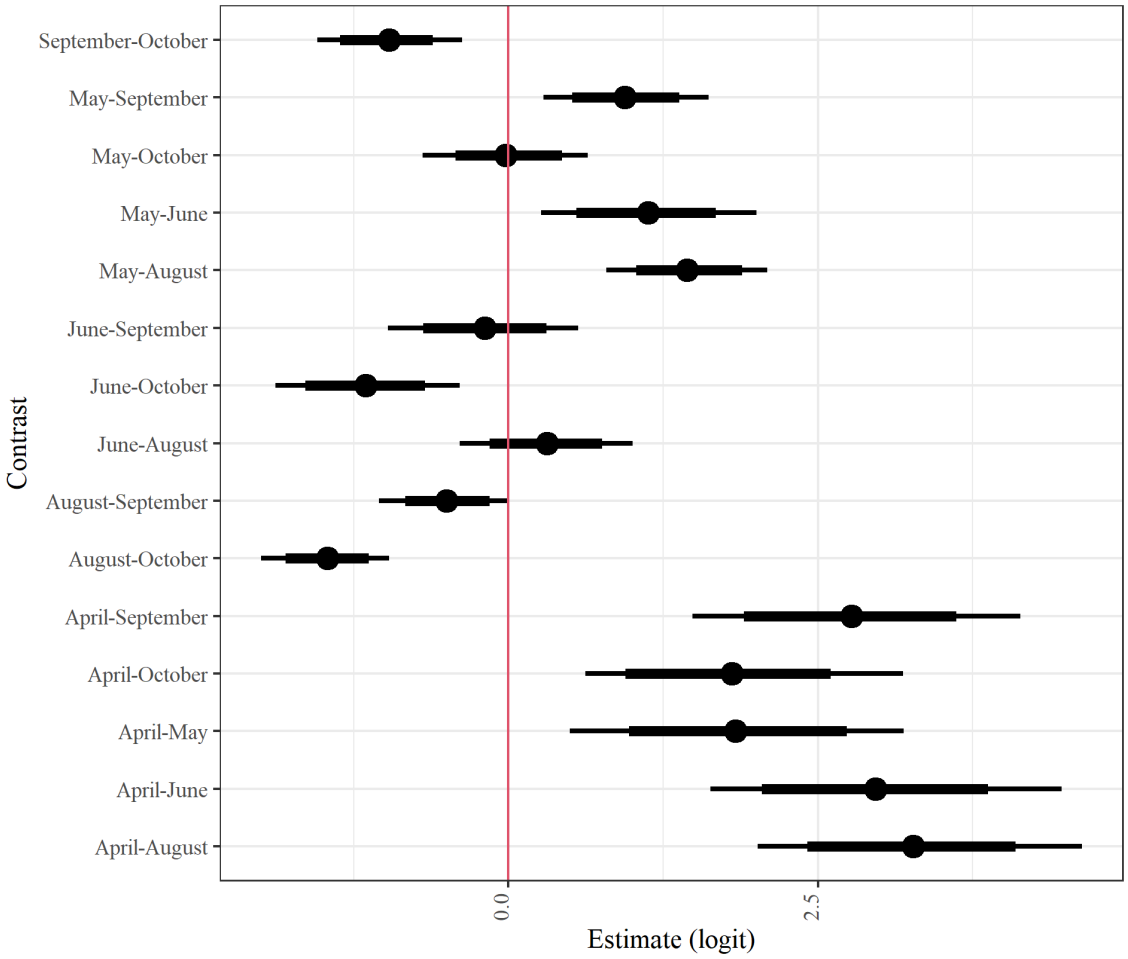

Appendix D

Chapter 4

D.1 Density-weighted seagrass means

Density-weighted mean seagrass cover for *Z. marina* and *R. maritima* were calculated using the following procedure. Species-specific total area for each density index $s = 1, 2, 3, 4$ for each observed year were supplied by [68]. For each year $t = 1990, ..., 2022$, we used the following weighted-sum equations to generate density-weighted mean values $\hat{\xi}_{gt}$ for each species-complex g (where $g = z, r,$ and m for *Z. marina*, *R. maritima* and mixed beds, respectively) and density index s:

$$\hat{\xi}_{gt} = \sum_{s=1}^{4} d_s \hat{\eta}_{gts} + \frac{1}{2} \sum_{s=1}^{4} d_s \hat{\eta}_{mts}$$

where d_s refers to the weight associated with a given density index s (i.e. 0.05, 0.25, 0.55, and 0.85), and $\hat{\eta}_{gts}$ refers to the area of species-complex g of density index s in year t. Mixed-beds are a combination of *Z. marina* and *R. maritima*. In absence of an obvious classification scheme, we divided the density-weighted area of $\sum_{s=1}^{4} d_s \hat{\eta}_{mts}$ by two and

added the corresponding value to $\sum_{s=1}^{4} d_s \hat{\eta}_{zts}$ and $\sum_{s=1}^{4} d_s \hat{\eta}_{rts}$. Finally, for models using total density-weighted seagrass cover $\hat{G}_t$, we took $\hat{G}_t = \hat{\xi}_{rt} + \hat{\xi}_{zt}$.

D.2 Prior distributions

We employed informative prior distributions on all parameters using a combination of exploratory data analysis, literature, and expert judgement. To facilitate parameter estimation, we specified log-normal prior distributions for most parameters. The exceptions were process error terms and coefficients influencing density-dependence as well as γ_0 and γ, which were already practically on the ln scale due to the log-linear relationship between γ_0 and γ and β_t (Equation 4.2). To obtain a reasonable initial estimate for VIMS Trawl Survey adult catchability q_{AV}, we used least squares regression of $\hat{O}_{AVt}$ on $\hat{O}_{ADt}$ and fixed the intercept at 0, which resulted in a slope estimate of 0.124. We subsequently specified a prior mean of $\ln(0.124) = -2.08$ and prior standard deviation of 0.5 for $\ln q_{AV}$ to allow allocation of prior probability for catchability coefficient values between 0 and 1 (i.e. the minimum and maximum values for catchability). Meanwhile, in accordance with estimates of juvenile WDS catchability from [170], we specified a prior for $\ln q_{JD}$ as $N(0.2, 0.02)$ which has a mean of -1.61 and standard deviation of 0.1. Similar to adult VIMS Trawl Survey catchability, to specify a reasonable prior distribution for q_{JV}, we used least-squares regression $\hat{O}_{JVt}$ on $\frac{\hat{O}_{JDt}}{0.2}$ and fixed the intercept at 0 – the mean *a priori* catchability of WDS juveniles being 0.2 [170]. This yielded a slope estimate of 0.03. We used a prior mean of $\ln(0.03) = -3.52$ and prior standard deviation of 1 that yielded a plausible prior for q_{JV} values between 0 and 1. These values were deemed reasonable in lieu of an obviously better method to estimate catchability given the data and prior information available.

Prior distributions for Beverton-Holt stock-recruit parameters were derived from fitting the function using least-squares regression of $\hat{O}_{JDt}$ on $\hat{O}_{ADt-1}$. Natural-log transformations

were applied to the resulting estimates for α and β (5 and 1×10^{-8}, respectively), and used to center prior distributions for $\ln \alpha$ and γ_0 (i.e. density dependence without considering seagrass effects, exponentiated in the model structure to estimate β). We specified prior standard deviations for $\ln \alpha$ and γ_0 as 1 and 2, respectively, resulting in a plausible prior range of parameter values for each term (0 to 60 for α and 0 to 6×10^{-6} for e^{γ_0}). Finally, for models with seagrass coefficients (i.e. models 2–5, Table 4.1), we specified priors for γ centered at 0 with a standard deviation of 1 to constrain the effects of seagrass covariates such that resulting prior range of β_t remained plausible.

For time-varying fishing mortality F_t, we specified a prior distribution $\ln F_t \sim N(-0.3, 0.3)$. This centered values of F_t at 0.74 and allocated prior probability to values of F_t ranging from 0 to 2.5, which was considered relatively diffuse compared to estimated ranges of fishing mortality from previous work [124, 125, 131, 126, 169]. The winter dredge fishery operated from December to March in years prior to 2009. Unpublished data suggested that dredge fishery mortality as high as 28% (*R. Lipcius pers comm*). Given that the fishery only operated for one third of the year, we assigned a normally distributed prior of D_o centered at 1 with a standard deviation of 0.1 (i.e. 1 + 0.28/3). Finally, for lack of an obvious prior distribution for process error terms, we assigned diffuse exponential prior distributions with a mean of 10 for σ_J and σ_A.

D.3 Conditional counterfactual projections

Conditional counterfactual plots were made by projecting the population outwards from $t = 2022$ conditioned on fixing catch and density-weighted *Z. marina* cover and holding process error at 0. For the n^{th} posterior draw (from the inferences of models g_1 and g_3) in the k^{th} seagrass conditional counterfactual scenario, the set of projection equations are as follows:

$$\hat{J}^{(n)}_{2022} = J^{(n)}_{2022} \tag{D.1}$$

$$\hat{A}^{(n)}_{2022} = A^{(n)}_{2022}$$

$$\hat{J}^{(n)}_{t} = \frac{\alpha^{(n)}\hat{A}^{(n)}_{t-1}}{1 + e^{\gamma^{(n)}_0 + \gamma^{(n)}_2 Z_k \hat{A}^{(n)}_{t-1}}} \text{ for } t = 2023, ..., 2060$$

$$\hat{A}^{(n)}_{t} = (\hat{A}^{(n)}_{t-1} + \hat{J}^{(n)}_{t-1})e^{-(\hat{F}^{(n)}_{t-1}+M)} \text{ for } t = 2023, ..., 2060$$

$\hat{F}^{(n)}_t$ is such that $\hat{C} = \frac{\hat{F}^{(n)}_t}{\hat{F}^{(n)}_t + M}\big(1 - e^{-(\hat{F}^{(n)}_t + M)}\big)(\hat{A}^{(n)}_t + \hat{J}^{(n)}_t)$ for $t = 2023, ..., 2060$

That is, we first set starting values for juvenile and adults states at the entire posterior distributions for adults and juveniles in 2022 ($\hat{J}_{2022}$ and $\hat{A}_{2022}$). Next, we fixed catch at reported harvest (i.e. $\hat{C}$) from 2022: 67 million individuals). We then fixed density-weighted *Z. marina* cover (here denoted Z_k in equation D.1) to values observed from 1990–2022 for all years 2023–2060, where $k = 1$ for minimum observed cover, $k = 2$ for median observed cover, and $k = 3$ for maximum observed cover. Finally, using fixed catch $\hat{C}$, projected juvenile and adult states ($\hat{J}_t$ and $\hat{A}_t$), Baranov's catch equation, and the bisection method, we numerically estimated $\hat{F}_t$ and projected the states forward to the next time-step. The resulting conditional posterior projections at each time-step are presented in Fig. 4.6B for all years after 2022. Note that the superscript (n) for state projections is due to their dependence on $\hat{J}^{(n)}_{2022}$ and $\hat{A}^{(n)}_{2022}$,

D.4 MSY projections

Conditional posterior inference for C_{MSY} based on annual density-weighted *Z. marina* values is as follows. First, starting values for the unfished population (A_1 and J_1, respectively) were set to 500 million individuals each, constituting a reasonably high 'unfished' population.

Second, for each year t (both past and future), the observed (past) or projected (future) density-weighted *Z. marina* values were held constant at their estimated or projected values ($\hat{\xi}_{zt}$, see Appendix D.1). Note that here t still denotes a given year for which MSY is estimated, while y refers to time-steps within a single projection used to estimate C_{MSY} for year t. Next, for each posterior draw n in year t, we ran the population projections for each exploitation rate (in equal increments of 0.05) $u = 0.0, 0.05, 0.1, \ldots, 1$ from time-steps $y = 1, \ldots, 100$. For each exploitation rate u in projection time-step y, catch was calculated as $\hat{C}_y^{(n)} = (\hat{A}_y^{(n)} + \hat{J}_y^{(n)})u$. We subsequently numerically solved for $\hat{F}_y^{(n)}$ using the bisection method and Baranov's catch equation to project the population forward to the next time-step $y+1$. Note that $\hat{J}_y^{(n)}, \hat{A}_y^{(n)}$ and $\hat{F}_y^{(n)}$ for $y > 1$ are scan-dependent because they are functions of the n^{th} scan of model coefficients (i.e. $\alpha^{(n)}, \gamma_0^{(n)}, \gamma_2^{(n)}, D_o^{(n)}$). That is:

$$\hat{J}_{y=1} = 5 \times 10^8 \tag{D.2}$$

$$\hat{A}_{y=1} = 5 \times 10^8$$

$$\hat{J}_y^{(n)} = \frac{\alpha^{(n)} \hat{A}_{y-1}^{(n)}}{1 + e^{\gamma_0^{(n)} + \gamma_2^{(n)} \hat{\xi}_{zt}} \hat{A}_{y-1}^{(n)}} \text{ for } y > 1$$

$$\hat{A}_y^{(n)} = (\hat{A}_{y-1}^{(n)} + \hat{J}_{y-1}^{(n)}) e^{-(\hat{F}_{y-1}^{(n)} + M)} \text{ for } y > 1$$

$\hat{F}_y^{(n)}$ is such that $= (\hat{A}_y + \hat{J}_y)u = \dfrac{\frac{\hat{F}_y^{(n)}}{\hat{F}_y^{(n)} + M}\left(1 - e^{-(\hat{F}_y^{(n)} + M)}\right)(\hat{A}_y^{(n)} + \hat{J}_y^{(n)})}{D_t^{(n)}}$

$$D_t^{(n)} = D_o^{(n)} \text{ if } t = 1990, 1991, ..., 2008$$

$$D_t^{(n)} = 1 \text{ if } t = 2009, 2010, ..., 2060$$

For each posterior draw n in year t, the exploitation rate u corresponding with the maximum equilibrium catch (i.e. the peak of the n^{th} curve) was taken to be the exploitation

rate at MSY at $y = 100$ (Fig. D4A). The posterior distribution of C_{MSY} corresponding to the exploitation rate at MSY was then plotted based on posterior draws in all past years and future scenarios (Figs. D4A and D4B).

D.5 Chapter 4 Supplemental tables

Table D1: Parameter descriptions and prior distributions for all models.

Parameter	Description	Prior distribution
ln α	ln Beverton-Holt productivity parameter	$N(1.54, 1)$
γ_0	Seagrass-independent Beverton-Holt density-dependence parameter	$N(-18.4, 2)$
γ	Coefficients relating density-weighted seagrass cover (see Table 4.1 for details) to Beverton-Holt density-dependence	$N(0, 1)$
D_o	Effect of dredge fishery (operation in 1990-2008 only)	$N(1, 0.1)$
ln $q_{J,D}$	ln WDS juvenile catchability coefficient	$N(-1.5, 0.1)$
ln $q_{J,V}$	ln VIMS Trawl Survey juvenile catchability coefficient	$N(-3.53, 0.1)$
ln $q_{A,V}$	ln VIMS Trawl Survey adult catchability coefficient	$N(-2.09, 0.1)$
σ_J	Juvenile process error sd	$exp(10)$
σ_A	Adult process error sd	$exp(10)$

D.6 Chapter 4 Supplemental figures

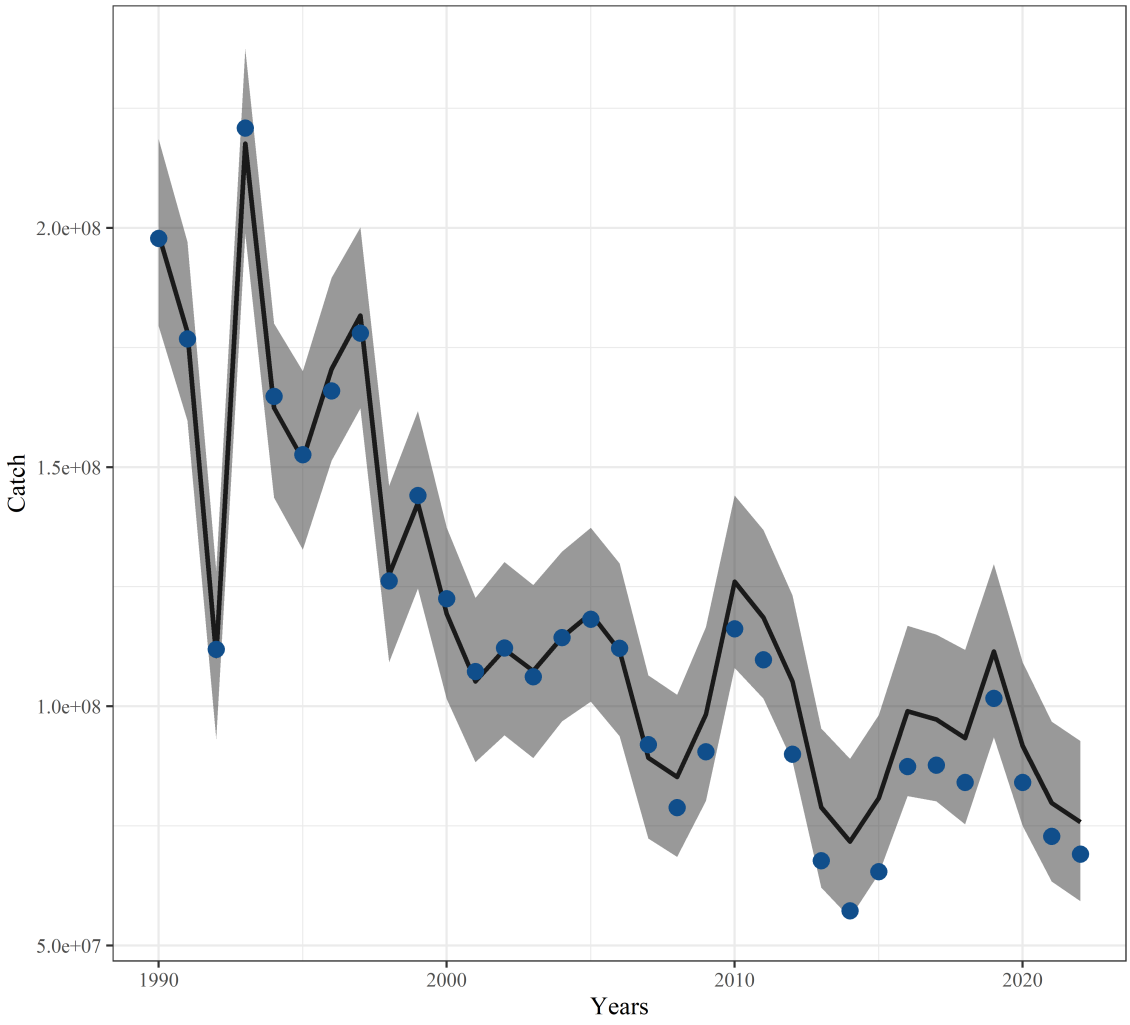

Figure D1: Comparison of reported and modeled mean catches from the best-performing model (g_3). The black line and grey regions depict posterior median and 80% CI for modeled mean catch (see equation 4.2), while blue dots depict reported catch. In all cases, reported catch C_t fell within 80% CI for modeled mean catch.

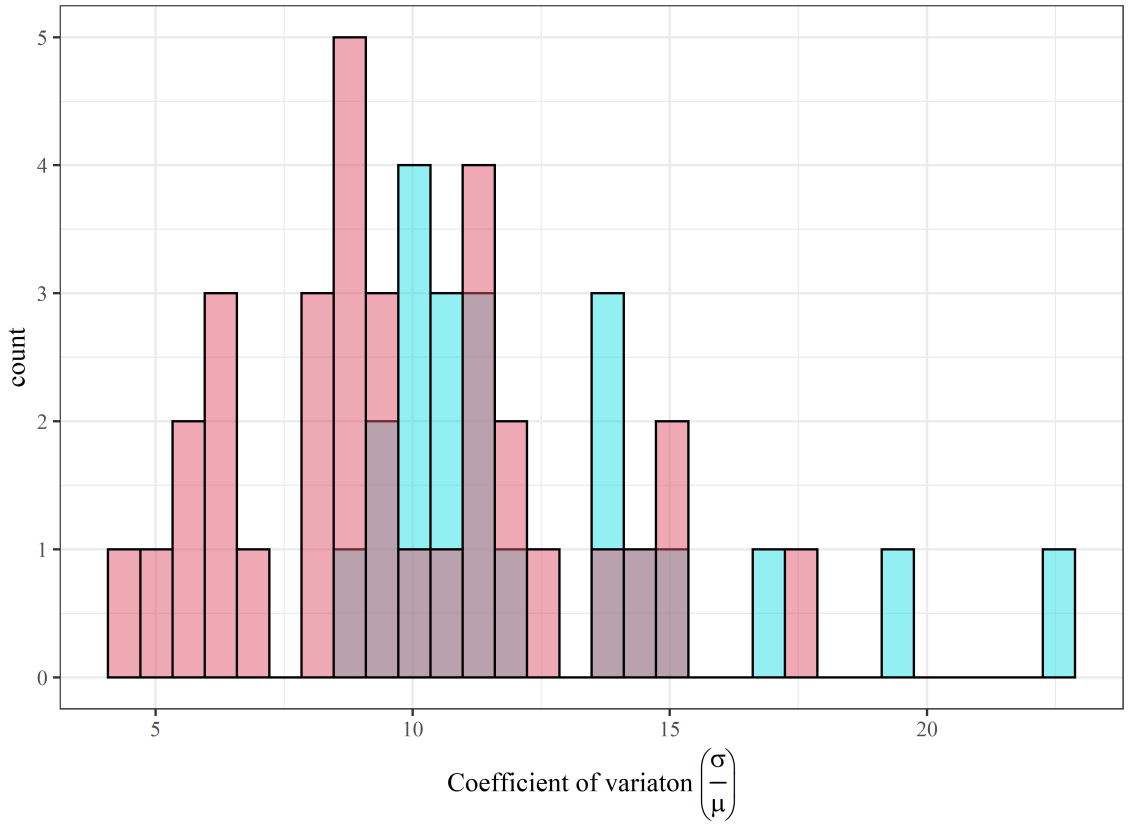

Figure D2: Histogram of coefficients of variation on catch from the most recent blue crab benchmark stock assessment [126] from 1990 to 2010 (blue) and values specified in the present study (red).

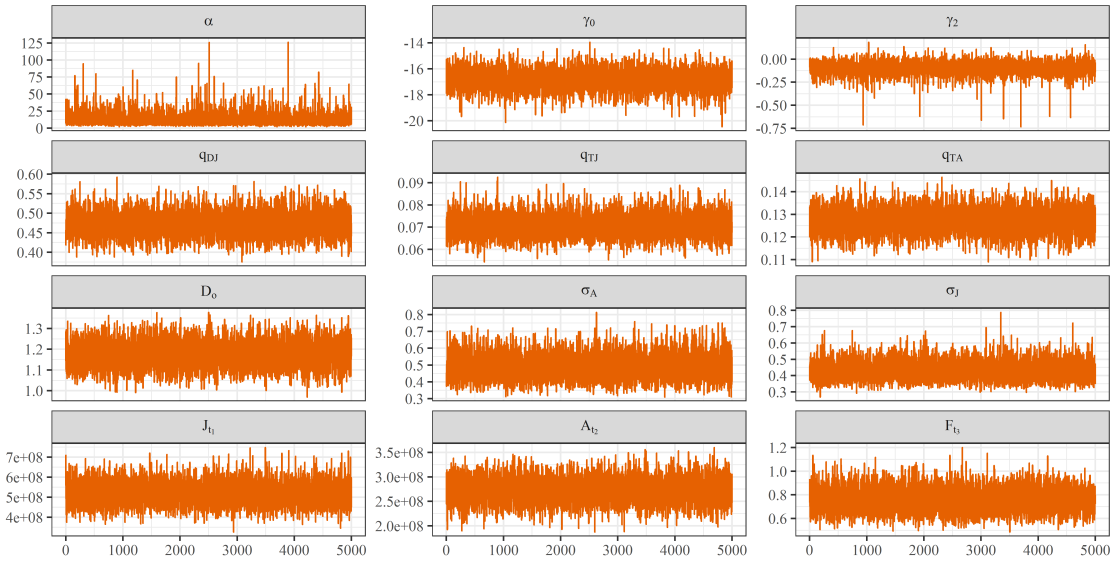

Figure D3: A set of trace plots for non-temporal parameters (panels 1–9) and temporal (panels 10–12) for selected years ($t = 1, 2,$ and 3) in Model g_3 illustrating sampled posterior values throughout the post-warmup/adaptive phase iterations. Visual inspection of trace plots is used to evaluate convergence and mixing of the Markov chains.

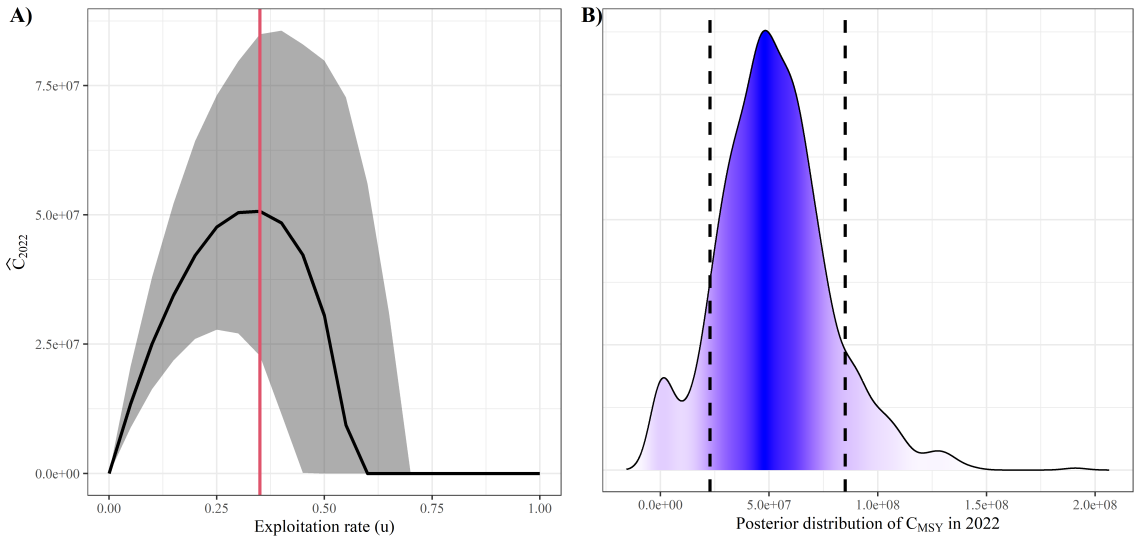

Figure D4: Plots displaying C_{MSY} estimation for year 2022. Plot A) depicts the conditional posterior distribution of $\hat{C}_y$ for year 2022 (black line and shaded region denote posterior median and 80% CIs, respectively) derived from equation D.2 as a function of exploitation rate u. The red line in A) denotes the exploitation rate with the maximum conditional posterior median catch (0.35). Plot B) depicts the conditional posterior distribution of catch corresponding to the exploitation rate with the maximum conditional posterior median catch. Black dashed lines in B) denote 80% CI.

Bibliography

[1] Octavio Aburto-Oropeza, Isaí Dominguez-Guerrero, José Cota-Nieto, and Tomás Plomozo-Lugo. Recruitment and ontogenetic habitat shifts of the yellow snapper (*Lutjanus argentiventris*) in the Gulf of California. *Marine Biology*, 156:2461–2472, 2009.

[2] Aaron J Adams, Craig P Dahlgren, G Todd Kellison, Matthew S Kendall, Craig A Layman, Janet A Ley, Ivan Nagelkerken, and Joseph E Serafy. Nursery function of tropical back-reef systems. *Marine Ecology Progress Series*, 318:287–301, 2006.

[3] William H Aeberhard, Joanna Mills Flemming, and Anders Nielsen. Review of state-space models for fisheries science. *Annual Review of Statistics and Its Application*, 5:215–235, 2018.

[4] MJ Ajemian, S Sohel, and J Mattila. Effects of turbidity and habitat complexity on antipredator behavior of three-spined sticklebacks (*Gasterosteus aculeatus*). *Environmental Biology of Fishes*, 98(1):45–55, 2015.

[5] Eva Amorim, Sandra Ramos, Michael Elliott, and Adriano A Bordalo. Dynamic habitat use of an estuarine nursery seascape: Ontogenetic shifts in habitat suitability of the European flounder (*Platichthys flesus*). *Journal of Experimental Marine Biology and Ecology*, 506:49–60, 2018.

[6] Ronald Baker and Nathan Waltham. Tethering mobile aquatic organisms to measure predation: A renewed call for caution. *Journal of Experimental Marine Biology and Ecology*, 523:151270, 2020.

[7] Fedor I Baranov. *On the question of the biological basis of fisheries*. 1918.

[8] Michael W Beck, Kenneth L Heck, Kenneth W Able, Daniel L Childers, David B Eggleston, Bronwyn M Gillanders, Benjamin Halpern, Cynthia G Hays, Kaho Hoshino, Thomas J Minello, Robert J Orth, Peter F Sheridan, and Michael P Weinstein. The identification, conservation, and management of estuarine and marine nurseries for fish and invertebrates: a better understanding of the habitats that serve as nurseries

for marine species and the factors that create site-specific variability in nursery quality will improve conservation and management of these areas. *Bioscience*, 51(8):633–641, 2001.

[9] Charlotte Berkström, Regina Lindborg, Matilda Thyresson, and Martin Gullström. Assessing connectivity in a tropical embayment: fish migrations and seascape ecology. *Biological Conservation*, 166:43–53, 2013.

[10] Raymond JH Beverton and Sidney J Holt. *On the dynamics of exploited fish populations*, volume 11. Springer Science & Business Media, 2012.

[11] Richard E Bigley and Paul G Harrison. Shoot demography and morphology of *Zostera japonica* and *Ruppia maritima* from British Columbia, Canada. *Aquatic Botany*, 24(1):69–82, 1986.

[12] T Dale Bishop, Harlan L Miller, Randal L Walker, Dorset H Hurley, Theron Menken, and Charles E Tilburg. Blue crab (*Callinectes sapidus Rathbun*, 1896) settlement at three Georgia (USA) estuarine sites. *Estuaries and coasts*, 33(3):688–698, 2010.

[13] Derrick C Blackmon and David B Eggleston. Factors influencing planktonic, post-settlement dispersal of early juvenile blue crabs (*Callinectes sapidus* Rathbun). *Journal of Experimental Marine Biology and Ecology*, 257(2):183–203, 2001.

[14] Amanda M Bromilow and Romuald N Lipcius. Mechanisms governing ontogenetic habitat shifts: role of trade-offs, predation, and cannibalism for the blue crab. *Marine Ecology Progress Series*, 584:145–159, 2017.

[15] Amanda Marie Bromilow. *Juvenile blue crab survival in nursery habitats: predator identification and predation impacts in Chesapeake Bay*. PhD thesis, Virginia Institute of Marine Science, William & Mary, 2017.

[16] Christopher J Brown, Andrew Broadley, Maria F Adame, Trevor A Branch, Mischa P Turschwell, and Rod M Connolly. The assessment of fishery status depends on fish habitats. *Fish and Fisheries*, 20(1):1–14, 2019.

[17] Alida Bundy, Johanna J Heymans, Lyne Morissette, and Claude Savenkoff. Seals, cod and forage fish: a comparative exploration of variations in the theme of stock collapse and ecosystem change in four Northwest Atlantic ecosystems. *Progress in Oceanography*, 81(1-4):188–206, 2009.

[18] Paul-Christian Bürkner, Jonah Gabry, and Aki Vehtari. Approximate leave-future-out cross-validation for Bayesian time series models. *Journal of Statistical Computation and Simulation*, 90(14):2499–2523, 2020.

[19] Paul-Christian Bürkner, Jonah Gabry, and Aki Vehtari. Efficient leave-one-out cross-validation for Bayesian non-factorized normal and Student-t models. *Computational Statistics*, 36(2):1243–1261, 2021.

[20] Noel G Cadigan. A state-space stock assessment model for northern cod, including under-reported catches and variable natural mortality rates. *Canadian Journal of Fisheries and Aquatic Sciences*, 73(2):296–308, 2015.

[21] Edward V Camp, Kai Lorenzen, and Matthew D Taylor. Impacts of habitat repair on a spatially complex fishery. *Estuarine, Coastal and Shelf Science*, 244:106102, 2020.

[22] CBSAC. 2022 Chesapeake Bay Blue Crab Advisory Report. Technical report, Chesapeake Bay Stock Assessment Committee, 2022.

[23] GS Chiu, EA Lehmann, and JC Bowden. A spatial modelling approach for the blending and error characterization of remotely sensed soil moisture products. *Journal of Environmental Statistics*, 4(9):1–17, 2013.

[24] Hyun Jung Cho, Patrick Biber, and Cristina Nica. The rise of *Ruppia* in seagrass beds: changes in coastal environment and research needs. *Handbook on environmental quality*, pages 1–15, 2009.

[25] G Cicchetti and RJ Diaz. Types of salt marsh edge and export of trophic energy from marshes to deeper habitats. In *Concepts and controversies in tidal marsh ecology*, Michael P Weinstein and Daniel A Kreeger, editors, pages 535–564. Kluwer, 2000.

[26] Giancarlo Cicchetti. *Habitat use, secondary production, and trophic export by salt marsh nekton in shallow waters*. PhD thesis, The College of William and Mary, 1998.

[27] Benjamin Ciotti, Elliot Brown, Fancesco Colloca, Olivier Le Pape, Alexander C Hyman, Romuald N Lipcius, Rochelle Seitz, Margaret Maathuis, Suzanne Poiesz, Kenny Rose, Daniele Ventura, and Karen van de Wolfshaar. Measuring the quality of nursery habitats for juvenile fish and invertebrates: perspectives from 50 years of research. in prep.

[28] Kelton L Clark, Gregory M Ruiz, and Anson H Hines. Diel variation in predator abundance, predation risk and prey distribution in shallow-water estuarine habitats. *Journal of Experimental Marine Biology and Ecology*, 287(1):37–55, 2003.

[29] William B Cronin. Volumetric, areal, and tidal statistics of the Chesapeake Bay estuary and its tributaries. *Chesapeake Bay Institute, The Johns Hopkins University. Baltimore, Maryland.*, Special Report 20, 1971.

[30] Larry B Crowder and William E Cooper. Habitat structural complexity and the interaction between bluegills and their prey. *Ecology*, 63(6):1802–1813, 1982.

[31] Larry B Crowder, Deborah D Squires, and James A Rice. Nonadditive effects of terrestrial and aquatic predators on juvenile estuarine fish. *Ecology*, 78(6):1796–1804, 1997.

[32] DP Cyrus and SJM Blaber. The influence of turbidity on juvenile marine fish in the estuaries of Natal, South Africa. *Continental Shelf Research*, 7(11-12):1411–1416, 1987.

[33] Nicholas James Da Silva. *Impact of Submerged Aquatic Vegetation (Zostera marina and Ruppia maritima) on Habitat Parameters and Macroinvertebrate Community Composition within an Urbanized Coastal Lagoon*. California State University, Long Beach, 2020.

[34] Craig P Dahlgren and David B Eggleston. Ecological processes underlying ontogenetic habitat shifts in a coral reef fish. *Ecology*, 81(8):2227–2240, 2000.

[35] Craig P Dahlgren, G Todd Kellison, Aaron J Adams, Bronwyn M Gillanders, Matthew S Kendall, Craig A Layman, Janet A Ley, Ivan Nagelkerken, and Joseph E Serafy. Marine nurseries and effective juvenile habitats: concepts and applications. *Marine Ecology Progress Series*, 312:291–295, 2006.

[36] Jana LD Davis, Alicia C Young-Williams, Anson H Hines, and Oded Zmora. Comparing two types of internal tags in juvenile blue crabs. *Fisheries Research*, 67(3):265–274, 2004.

[37] Jana LD Davis, Alicia C Young-Williams, Anson H Hines, and Yonathan Zohar. Assessing the potential for stock enhancement in the case of the Chesapeake Bay blue crab (*Callinectes sapidus*). *Canadian Journal of Fisheries and Aquatic Sciences*, 62(1):109–122, 2005.

[38] Paula de la Barra, Martin W Skov, Peter J Lawrence, Juan I Schiaffi, and Jan G Hiddink. Tidal water exchange drives fish and crustacean abundances in salt marshes. *Marine Ecology Progress Series*, 694:61–72, 2022.

[39] Richard B Deriso, Mark N Maunder, and Walter H Pearson. Incorporating covariates into fisheries stock assessment models with application to pacific herring. *Ecological Applications*, 18(5):1270–1286, 2008.

[40] Tara E Dolan, Wesley S Patrick, and Jason S Link. Delineating the continuum of marine ecosystem-based management: a us fisheries reference point perspective. *ICES Journal of Marine Science*, 73(4):1042–1050, 2016.

[41] Martijn Dorenbosch, Monique GG Grol, A de Groene, Gerard van der Velde, and Ivan Nagelkerken. Piscivore assemblages and predation pressure affect relative

safety of some back-reef habitats for juvenile fish in a Caribbean bay. *Marine Ecology Progress Series*, 379:181–196, 2009.

[42] David B Eggleston, Geoffrey W Bell, and Allison D Amavisca. Interactive effects of episodic hypoxia and cannibalism on juvenile blue crab mortality. *Journal of Experimental Marine Biology and Ecology*, 325(1):18–26, 2005.

[43] CE Epifanio. Biology of larvae. *The Blue Crab, Callinectes sapidus. Maryland Sea Grant, College Park, MD*, pages 513–533, 2007.

[44] Charles E Epifanio. Early life history of the blue crab *Callinectes sapidus*: a review. *Journal of Shellfish Research*, 38(1):1–22, 2019.

[45] Lisa L Etherington and David B Eggleston. Large-scale blue crab recruitment: linking postlarval transport, post-settlement planktonic dispersal, and multiple nursery habitats. *Marine Ecology Progress Series*, 204:179–198, 2000.

[46] Lisa L Etherington, David B Eggleston, and William T Stockhausen. Partitioning loss rates of early juvenile blue crabs from seagrass habitats into mortality and emigration. *Bulletin of Marine Science*, 72(2):371–391, 2003.

[47] Joseph J Facendola. *Predation by Sub-adult Red Drum (Sciaenops Ocellatus), on Juvenile Blue Crabs (Callinectes Sapidus): Estimation of Daily Ration and Seasonal Variation in the Contribution of Blue Crab to the Diet*. PhD thesis, University of North Carolina Wilmington, 2010.

[48] Katherine C Filippino, Todd A Egerton, William S Hunley, and Margaret R Mulholland. The influence of storms on water quality and phytoplankton dynamics in the tidal James River. *Estuaries and Coasts*, 40(1):80–94, 2017.

[49] H Carlton Fitz and Richard G Wiegert. Utilization of the intertidal zone of a salt marsh by the blue crab Callinectes sapidus: density, return frequency, and feeding habits. *Marine Ecology Progress Series*, pages 249–260, 1991.

[50] Steven J Fleischman, Matthew J Catalano, Robert A Clark, and David R Bernard. An age-structured state-space stock–recruit model for Pacific salmon (*Oncorhynchus spp.*). *Canadian Journal of Fisheries and Aquatic Sciences*, 70(3):401–414, 2013.

[51] F Joel Fodrie and Lisa A Levin. Linking juvenile habitat utilization to population dynamics of California halibut. *Limnology and Oceanography*, 53(2):799–812, 2008.

[52] F Joel Fodrie, Lisa A Levin, and Andrew J Lucas. Use of population fitness to evaluate the nursery function of juvenile habitats. *Marine Ecology Progress Series*, 385:39–49, 2009.

[53] Graham E Forrester and Stephen E Swearer. Trace elements in otoliths indicate the use of open-coast versus bay nursery habitats by juvenile California halibut. *Marine Ecology Progress Series*, 241:201–213, 2002.

[54] Douglas F Fraser and Edward E Emmons. Behavioral response of blacknose dace (*Rhinichthys atratulus*) to varying densities of predatory creek chub (*Semotilus atromaculatus*). *Canadian Journal of Fisheries and Aquatic Sciences*, 41(2):364–370, 1984.

[55] Emily French and Kenneth Moore. Canopy Functions of *R. maritima* and *Z. marina* in the Chesapeake Bay. *Frontiers in Marine Science*, 5:461, 2018.

[56] A Gelman, JB Carlin, HS Stern, DB Dunson, A Vehtari, and BD Rubin. *Bayesian Data Analysis. 3rd edition*. Chapman & Hall/CRC, 2013.

[57] Andrew Gelman, Daniel Lee, and Jiqiang Guo. Stan: a probabilistic programming language for Bayesian inference and optimization. *Journal of Educational and Behavioral Statistics*, 40(5):530–543, 2015.

[58] Bronwyn M Gillanders, Kenneth W Able, Jennifer A Brown, David B Eggleston, and Peter F Sheridan. Evidence of connectivity between juvenile and adult habitats for mobile marine fauna: an important component of nurseries. *Marine Ecology Progress Series*, 247:281–295, 2003.

[59] Kim Graham. A review of the biology and management of blue catfish. In *Catfish 2000: proceedings of the international ictalurid symposium. American Fisheries Society, Symposium*, volume 24, pages 37–49, 1999.

[60] Arnaud Grüss, Kenneth A Rose, James Simons, Cameron H Ainsworth, Elizabeth A Babcock, David D Chagaris, Kim De Mutsert, John Froeschke, Peter Himchak, Isaac C Kaplan, Halie O'Farrell, and Manuel J Zetina Rejon. Recommendations on the use of ecosystem modeling for informing ecosystem-based fisheries management and restoration outcomes in the Gulf of Mexico. *Marine and Coastal Fisheries*, 9(1):281–295, 2017.

[61] Vincent Guillory and Megan Elliot. A review of blue crab predators. *Proceedings of the Blue Crab Mortality Symposium*, 90:69–83, 2001.

[62] Benjamin S Halpern, Catherine Longo, Courtney Scarborough, Darren Hardy, Benjamin D Best, Scott C Doney, Steven K Katona, Karen L McLeod, Andrew A Rosenberg, and Jameal F Samhouri. Assessing the health of the us west coast with a regional-scale application of the ocean health index. *Plos One*, 9(6):e98995, 2014.

[63] Michael J Hansen, T Douglas Beard Jr, and Daniel B Hayes. Sampling and experimental design. *Analysis and interpretation of freshwater fisheries data. American Fisheries Society, Bethesda, Maryland*, pages 51–120, 2007.

[64] Kenneth L Heck and Timothy A Thoman. The nursery role of seagrass meadows in the upper and lower reaches of the chesapeake bay. *Estuaries*, 7:70–92, 1984.

[65] Kenneth L Heck Jr and Patricia M Spitzer. Post settlement mortality of juvenile blue crabs: patterns and processes. In *Proceedings of the Blue Crab Mortality Symposium*, volume 90, pages 18–27. Gulf States Marine Fisheries Commission, Ocean Springs, MS, 2001.

[66] KL Heck Jr, LD Coen, and SG Morgan. Pre-and post-settlement factors as determinants of juvenile blue crab *Callinectes sapidus* abundance: results from the north-central Gulf of Mexico. *Marine Ecology Progress Series*, 222:163–176, 2001.

[67] KL Heck Jr, G Hays, and Robert J Orth. Critical evaluation of the nursery role hypothesis for seagrass meadows. *Marine Ecology Progress Series*, 253:123–136, 2003.

[68] Marc J S Hensel, Christopher J Partick, Robert J Orth, David J Wilcox, William C Dennison, Cassie Gurbisz, Mike J Hannam, Brooke Landry, Ken Moore, Rebecca R Murphy, Jeremy Testa, and Jonathan S Lefcheck. Rise of *Ruppia* in Chesapeake Bay: Climate-change driven turnover of foundation species creates new threats and management opportunities. *Proceedings of the National Academy of Sciences*, 120(23):e2220678120, 2023.

[69] David A Hewitt, Debra M Lambert, John M Hoenig, Romuald N Lipcius, David B Bunnell, and Thomas J Miller. Direct and indirect estimates of natural mortality for Chesapeake Bay blue crab. *Transactions of the American Fisheries Society*, 136(4):1030–1040, 2007.

[70] Anson H Hines. Ecology of juvenile and adult blue crabs. *The Blue Crab Callinectes sapidus. Maryland Sea Grant College, College Park, Maryland*, pages 565–654, 2007.

[71] Anson H Hines, Eric G Johnson, Alicia C Young, Robert Aguilar, Margaret A Kramer, Michael Goodison, Oded Zmora, and Yonathan Zohar. Release strategies for estuarine species with complex migratory life cycles: stock enhancement of Chesapeake blue crabs (*Callinectes sapidus*). *Reviews in Fisheries Science*, 16(1-3):175–185, 2008.

[72] Anson H Hines, Romuald N Lipcius, and A Mark Haddon. Population dynamics and habitat partitioning by size, sex, and molt stage of blue crabs callinectes sapidus in a

subestuary of central chesapeake bay. *Marine Ecology Progress Series*, 36(1):55–64, 1987.

[73] Anson H Hines and Gregory M Ruiz. Temporal variation in juvenile blue crab mortality: nearshore shallows and cannibalism in Chesapeake Bay. *Bulletin of Marine Science*, 57(3):884–901, 1995.

[74] Andrij Z Horodysky, Richard W Brill, Eric J Warrant, John A Musick, and Robert J Latour. Comparative visual function in four piscivorous fishes inhabiting Chesapeake Bay. *Journal of Experimental Biology*, 213(10):1751–1761, 2010.

[75] Kevin A Hovel and Mark S Fonseca. Influence of seagrass landscape structure on the juvenile blue crab habitat-survival function. *Marine Ecology Progress Series*, 300:179–191, 2005.

[76] Kevin A Hovel and Romuald N Lipcius. Habitat fragmentation in a seagrass landscape: patch size and complexity control blue crab survival. *Ecology*, 82(7):1814–1829, 2001.

[77] Kevin A Hovel and Romuald N Lipcius. Effects of seagrass habitat fragmentation on juvenile blue crab survival and abundance. *Journal of Experimental Marine Biology and Ecology*, 271(1):75–98, 2002.

[78] Ursula A Howson. *Nursery habitat quality for juvenile paralichthyid flounders: Experiemental analyses of the effects of physicochemical parameters*. PhD thesis, University of Delaware, 2000.

[79] Ursula A Howson, Timothy E Targett, Paul A Grecay, and Patrick M Gaffney. Foraging by estuarine juveniles of two *paralichthyid* flounders: experimental analyses of the effects of light level, turbidity, and prey type. *Marine Ecology Progress Series*, 695:139–156, 2022.

[80] A Randall Hughes, Susan L Williams, Carlos M Duarte, Kenneth L Heck Jr, and Michelle Waycott. Associations of concern: declining seagrasses and threatened dependent species. *Frontiers in Ecology and the Environment*, 7(5):242–246, 2009.

[81] A Challen Hyman, Grace Chiu, Micheal Seebo, Alison Smith, Gabrielle Saluta, and Romuald Lipcius. Ontogenetic patterns in juvenile blue crab density: Effects of habitat and turbidity in a chesapeake bay tributary. *bioRxiv*, pages 2023–06, 2023.

[82] A Challen Hyman, Grace S Chiu, Mary C Fabrizio, and Romuald N Lipcius. Spatiotemporal modeling of nursery habitat using bayesian inference: Environmental drivers of juvenile blue crab abundance. *Frontiers in Marine Science*, 9:834990, 2022.

[83] Robert E Isdell, Donna Marie Bilkovic, Amanda G Guthrie, Molly M Mitchell, Randolph M Chambers, Matthias Leu, and Carl Hershner. Living shorelines achieve functional equivalence to natural fringe marshes across multiple ecological metrics. *PeerJ*, 9:e11815, 2021.

[84] Paul R Jivoff and Kenneth W Able. Evaluating salt marsh restoration in Delaware Bay: the response of blue crabs, *Callinectes sapidus*, at former salt hay farms. *Estuaries*, 26(3):709–719, 2003.

[85] David S Johnson. Beautiful swimmers attack at low tide. *Ecology*, pages ecy–3787, 2022.

[86] Eric G Johnson and David B Eggleston. Population density, survival and movement of blue crabs in estuarine salt marsh nurseries. *Marine Ecology Progress Series*, 407:135–147, 2010.

[87] Cora A Johnston and Olivia N Caretti. Mangrove expansion into temperate marshes alters habitat quality for recruiting *Callinectes spp. Marine Ecology Progress Series*, 573:1–14, 2017.

[88] Cora Ann Johnston and Romuald N Lipcius. Exotic macroalga *Gracilaria vermiculophylla* provides superior nursery habitat for native blue crab in Chesapeake Bay. *Marine Ecology Progress Series*, 467:137–146, 2012.

[89] David L Jones, John F Walter, Elizabeth N Brooks, and Joseph E Serafy. Connectivity through ontogeny: fish population linkages among mangrove and coral reef habitats. *Marine Ecology Progress Series*, 401:245–258, 2010.

[90] Daniel K Kimura and David A Somerton. Review of statistical aspects of survey sampling for marine fisheries. *Reviews in Fisheries Science*, 14(3):245–283, 2006.

[91] Matthew L Kirwan and J Patrick Megonigal. Tidal wetland stability in the face of human impacts and sea-level rise. *Nature*, 504(7478):53–60, 2013.

[92] John K Kruschke. Bayesian analysis reporting guidelines. *Nature Human Behaviour*, 5(10):1282–1291, 2021.

[93] Allbert Kuo, Maynard M Nichols, and James Lewis. *Modeling sediment movement in the turbidity maximum of an estuary*. Virginia Water Resources Research Center, 1978.

[94] Debra M Lambert, Romuald N Lipcius, and John M Hoenig. Assessing effectiveness of the blue crab spawning stock sanctuary in Chesapeake Bay using tag-return methodology. *Marine Ecology Progress Series*, 321:215–225, 2006.

[95] Jonathan S Lefcheck, Brent B Hughes, Andrew J Johnson, Bruce W Pfirrmann, Douglas B Rasher, Ashley R Smyth, Bethany L Williams, Michael W Beck, and Robert J Orth. Are coastal habitats important nurseries? A meta-analysis. *Conservation Letters*, 12(4):e12645, 2019.

[96] Jonathan S Lefcheck, Robert J Orth, William C Dennison, David J Wilcox, Rebecca R Murphy, Jennifer Keisman, Cassie Gurbisz, Michael Hannam, J Brooke Landry, Kenneth A Moore, et al. Long-term nutrient reductions lead to the unprecedented recovery of a temperate coastal region. *Proceedings of the National Academy of Sciences*, 115(14):3658–3662, 2018.

[97] Phillip S Levin, Michael J Fogarty, Steven A Murawski, and David Fluharty. Integrated ecosystem assessments: developing the scientific basis for ecosystem-based management of the ocean. *PLoS Biol*, 7(1):e1000014, 2009.

[98] Jing Lin and Albert Y Kuo. A model study of turbidity maxima in the York River Estuary, Virginia. *Estuaries*, 26(5):1269–1280, 2003.

[99] Jason S Link. What does ecosystem-based fisheries management mean. *Fisheries*, 27(4):18–21, 2002.

[100] RL Lipcius. Chesapeake Bay Blue Crab Advisory Report. *Annual report to the Virginia Marine Resources Commission. Virginia Institute of Marine Science, Gloucester Point, VA.*, 2020.

[101] RL Lipcius. Chesapeake Bay Blue Crab Advisory Report. *Annual report to the Virginia Marine Resources Commission. Virginia Institute of Marine Science, Gloucester Point, VA.*, 2022.

[102] Romuald N Lipcius, David B Eggleston, F Joel Fodrie, Jaap Van Der Meer, Kenneth A Rose, Rita P Vasconcelos, and Karen E Van De Wolfshaar. Modeling quantitative value of habitats for marine and estuarine populations. *Frontiers in Marine Science*, 6:280, 2019.

[103] Romuald N Lipcius, David B Eggleston, Kenneth L Heck Jr, Rochelle D Seitz, and J van Montrans. Post-settlement abundance, survival, and growth of postlarvae and young juvenile blue crabs in nursery habitats. *The Blue Crab Callinectes sapidus. Maryland Sea Grant College, College Park, Maryland*, pages 535–564, 2007.

[104] Romuald N Lipcius, Rochelle D Seitz, William J Goldsborough, Marcel M Montane, and William T Stockhausen. A deepwater dispersal corridor for adult female blue crabs in Chesapeake Bay. *Kruse GH and*, 8:643–666, 2001.

[105] Romuald N Lipcius, Rochelle D Seitz, Michael S Seebo, and Duamed Colón-Carrión. Density, abundance and survival of the blue crab in seagrass and unstructured salt marsh nurseries of Chesapeake Bay. *Journal of Experimental Marine Biology and Ecology*, 319(1-2):69–80, 2005.

[106] Romuald N Lipcius and William T Stockhausen. Concurrent decline of the spawning stock, recruitment, larval abundance, and size of the blue crab *Callinectes sapidus* in Chesapeake Bay. *Marine Ecology Progress Series*, 226:45–61, 2002.

[107] Romuald N Lipcius, William T Stockhausen, Rochelle D Seitz, and Patrick J Geer. Spatial dynamics and value of a marine protected area and corridor for the blue crab spawning stock in Chesapeake Bay. *Bulletin of Marine Science*, 72(2):453–469, 2003.

[108] Camino Liquete, Núria Cid, Denis Lanzanova, Bruna Grizzetti, and Arnaud Reynaud. Perspectives on the link between ecosystem services and biodiversity: the assessment of the nursery function. *Ecological Indicators*, 63:249–257, 2016.

[109] Steven Y Litvin, Michael P Weinstein, Marcus Sheaves, and Ivan Nagelkerken. What makes nearshore habitats nurseries for nekton? An emerging view of the nursery role hypothesis. *Estuaries and Coasts*, 41(6):1539–1550, 2018.

[110] W Christopher Long, Andrew J Sellers, and Anson H Hines. Mechanism by which coarse woody debris affects predation and community structure in Chesapeake Bay. *Journal of Experimental Marine Biology and Ecology*, 446:297–305, 2013.

[111] Blandina R Lugendo, Annelies Pronker, Ilse Cornelissen, Arjan De Groene, Ivan Nagelkerken, Martijn Dorenbosch, Gerard Van der Velde, and Yunus D Mgaya. Habitat utilisation by juveniles of commercially important fish species in a marine embayment in zanzibar, tanzania. *Aquatic Living Resources*, 18(2):149–158, 2005.

[112] Marc Mangel, Alec D MacCall, Jon Brodziak, EJ Dick, Robyn E Forrest, Roxanna Pourzand, and Stephen Ralston. A perspective on steepness, reference points, and stock assessment. *Canadian Journal of Fisheries and Aquatic Sciences*, 70(6):930–940, 2013.

[113] Guy SA Marley, Amy E Deacon, Dawn AT Phillip, and Andrew J Lawrence. Mangrove or mudflat: prioritizing fish habitat for conservation in a turbid tropical estuary. *Estuarine, Coastal and Shelf Science*, 240:106788, 2020.

[114] Mark N Maunder and Richard B Deriso. A state–space multistage life cycle model to evaluate population impacts in the presence of density dependence: illustrated with application to delta smelt (hyposmesus transpacificus). *Canadian Journal of Fisheries and Aquatic Sciences*, 68(7):1285–1306, 2011.

[115] Richard McElreath. *Statistical rethinking: a Bayesian course with examples in R and Stan*. Chapman and Hall/CRC, 2018.

[116] Carole C McIvor and William E Odum. The flume net: a quantitative method for sampling fishes and macrocrustaceans on tidal marsh surfaces. *Estuaries*, 9(3):219–224, 1986.

[117] MDNR. Stock assessment update of blue crab in Chesapeake Bay. Technical report, Maryland Department of Natural Resources, Annapolis, Maryland, March 2019.

[118] Milad Memarzadeh, Gregory L Britten, Boris Worm, and Carl Boettiger. Rebuilding global fisheries under uncertainty. *Proceedings of the National Academy of Sciences*, 116(32):15985–15990, 2019.

[119] David J Mense and Elizabeth L Wenner. Distribution and abundance of early life history stages of the blue crab, *Callinectes sapidus*, in tidal marsh creeks near Charleston, South Carolina. *Estuaries*, 12(3):157–168, 1989.

[120] Karen S Metcalf and Romuald N Lipcius. Relationship of habitat and spatial scale with physiological state and settlement of blue crab postlarvae in Chesapeake Bay. *Marine Ecology Progress Series*, 82:143, 1992.

[121] Karen S Metcalf, Jacques Van Montfrans, Romuald N Lipcius, and Robert J Orth. Settlement indices for blue crab megalopae in the York River, Virginia: temporal relationships and statistical efficiency. *Bulletin of Marine Science*, 57(3):781–792, 1995.

[122] Catherine GJ Michielsens, Murdoch K McAllister, Sakari Kuikka, Tapani Pakarinen, Lars Karlsson, Atso Romakkaniemi, Ingemar Perä, and Samu Mäntyniemi. A bayesian state space mark recapture model to estimate exploitation rates in mixed-stock fisheries. *Canadian Journal of Fisheries and Aquatic Sciences*, 63(2):321–334, 2006.

[123] Cole R Miller, Alexander C Hyman, Daniel Shi, and Romuald N Lipcius. Test of treatment-specific bias in simulated marsh with juvenile blue crab *Callinectes sapidus*. *In prep*, 2023.

[124] Thomas J Miller. Matrix-based modeling of blue crab population dynamics with applications to the Chesapeake Bay. *Estuaries*, 24(4):535–544, 2001.

[125] Thomas J Miller. Incorporating space into models of the Chesapeake Bay blue crab population. *Bulletin of Marine Science*, 72(2):567–588, 2003.

[126] Thomas J Miller, Michael J Wilberg, A R Colton, G R Davis, A Sharov, Romulad N Lipcius, Gina M Ralph, Eric G Johnson, and A G Kaufman. Stock assessment of blue

crab in chesapeake bay. *Final Report to NOAA Chesapeake Bay Office, Technical Report*, pages TS–614–11, 2011.

[127] Timothy J Miller, Jonathan A Hare, and Larry A Alade. A state-space approach to incorporating environmental effects on recruitment in an age-structured assessment model with an application to southern new england yellowtail flounder. *Canadian Journal of Fisheries and Aquatic Sciences*, 73(8):1261–1270, 2016.

[128] Thomas J Minello, Kenneth W Able, Michael P Weinstein, and Cynthia G Hays. Salt marshes as nurseries for nekton: testing hypotheses on density, growth and survival through meta-analysis. *Marine Ecology Progress Series*, 246:39–59, 2003.

[129] Thomas J Minello, Lawrence P Rozas, and Ronald Baker. Geographic variability in salt marsh flooding patterns may affect nursery value for fishery species. *Estuaries and Coasts*, 35(2):501–514, 2012.

[130] Jonathon D Mintz, Romuald N Lipcius, David B Eggleston, and Michael S Seebo. Survival of juvenile Caribbean spiny lobster: effects of shelter size, geographic location and conspecific abundance. *Marine Ecology Progress Series*, pages 255–266, 1994.

[131] Toni Mizerek, Helen M Regan, and Kevin A Hovel. Seagrass habitat loss and fragmentation influence management strategies for a blue crab *Callinectes sapidus* fishery. *Marine Ecology Progress Series*, 427:247–257, 2011.

[132] Kirt E Moody. Predators of juvenile blue crabs outside of refuge habitats in lower Chesapeake Bay. *Estuaries*, 26(3):759–764, 2003.

[133] Kirt Edward Moody. *Predation on juvenile blue crabs, Callinectes sapidus Rathbun, in lower Chesapeake Bay: patterns, predators, and potential impacts*. The College of William and Mary, 1994.

[134] Althea FP Moore and J Emmett Duffy. Foundation species identity and trophic complexity affect experimental seagrass communities. *Marine Ecology Progress Series*, 556:105–121, 2016.

[135] Cordelia Moore, Jeffrey C Drazen, Ben T Radford, Christopher Kelley, and Stephen J Newman. Improving essential fish habitat designation to support sustainable ecosystem-based fisheries management. *Marine Policy*, 69:32–41, 2016.

[136] Kenneth A Moore. Influence of seagrasses on water quality in shallow regions of the lower Chesapeake Bay. *Journal of Coastal Research*, (10045):162–178, 2009.

[137] Kenneth A Moore, Erin C Shields, and David B Parrish. Impacts of varying estuarine temperature and light conditions on *Zostera marina* (eelgrass) and its interactions with *Ruppia maritima* (widgeongrass). *Estuaries and Coasts*, 37(1):20–30, 2014.

[138] Thomas C Mosca III, Paul J Rudershausen, and Rom Lipcius. Do striped bass and blue crab abundances correlate in chesapeake bay? *Virginia Journal of Science*, 46(4):249, 1995.

[139] MSA. Magnuson–stevens fishery conservation and management act. Technical report, National Oceanic and Atmospheric Administration, Department of Commerce, 2007.

[140] Ivan Nagelkerken, Marcus Sheaves, Ronald Baker, and Rod M Connolly. The seascape nursery: a novel spatial approach to identify and manage nurseries for coastal marine fauna. *Fish and Fisheries*, 16(2):362–371, 2015.

[141] Yohei Nakamura, Keisuke Hirota, Takuro Shibuno, and Yoshiro Watanabe. Variability in nursery function of tropical seagrass beds during fish ontogeny: timing of ontogenetic habitat shift. *Marine biology*, 159(6):1305–1315, 2012.

[142] Maynard M Nichols and Galen Thompson. Development of the turbidity maximum in a coastal plain estuary. 1973.

[143] NMFS. Marine fisheries habitat assessment improvement plan: report of the National Marine Fisheries Service Habitat Assessment Improvement Plan Team. Technical report, National Oceanic and Atmospheric Administration, 2010.

[144] NOAA. National oceanic and atmospheric administration, 2023. landings. 2023.

[145] NOAA Chesapeake Bay Fisheries Ecosystem Advisory Panel. Fisheries Ecosystem Planning for the Chesapeake Bay, Trends in Fisheries Science and Management. Technical report, American Fisheries Society, 2006.

[146] W John O'Brien, Norman A Slade, and Gary L Vinyard. Apparent size as the determinant of prey selection by bluegill sunfish (*Lepomis macrochirus*). *Ecology*, 57(6):1304–1310, 1976.

[147] Matthew B Ogburn, Kenneth C Stuck, Richard W Heard, Shiao Y Wang, and Richard B Forward Jr. Seasonal variability in morphology of blue crab, *Callinectes sapidus*, megalopae and early juvenile stage crabs, and distinguishing characteristics among co-occurring *Portunidae*. *Journal of Crustacean Biology*, 31(1):106–113, 2011.

[148] Eugene J Olmi III, Jacques van Montfrans, Romuald N Lipcius, Robert J Orth, and Phillip W Sadler. Variation in planktonic availability and settlement of blue crab megalopae in the York River, Virginia. *Bulletin of Marine Science*, 46(1):230–243, 1990.

[149] Angeleen M Olson, Margot Hessing-Lewis, Dana Haggarty, and Francis Juanes. Nearshore seascape connectivity enhances seagrass meadow nursery function. *Ecological Applications*, 29(5):e01897, 2019.

[150] Robert J Orth, Tim JB Carruthers, William C Dennison, Carlos M Duarte, James W Fourqurean, Kenneth L Heck, A Randall Hughes, Gary A Kendrick, W Judson Kenworthy, Suzanne Olyarnik, et al. A global crisis for seagrass ecosystems. *Bioscience*, 56(12):987–996, 2006.

[151] Robert J Orth, Scott R Marion, Kenneth A Moore, and David J Wilcox. Eelgrass (*Zostera marina* L.) in the Chesapeake Bay region of mid-Atlantic coast of the USA: challenges in conservation and restoration. *Estuaries and Coasts*, 33:139–150, 2010.

[152] Robert J Orth and Kenneth A Moore. Seasonal and year-to-year variations in the growth of zostera marina l.(eelgrass) in the lower chesapeake bay. *Aquatic Botany*, 24(4):335–341, 1986.

[153] Robert J Orth and Kenneth A Moore. Distribution of *Zostera marina* L. and *Ruppia maritima* L. sensu lato along depth gradients in the lower Chesapeake Bay, USA. *Aquatic Botany*, 32(3):291–305, 1988.

[154] Robert J Orth and Jacques van Montfrans. Utilization of a seagrass meadow and tidal marsh creek by blue crabs *Callinectes sapidus*. Seasonal and annual variations in abundance with emphasis on post-settlement juveniles. *Marine Ecology Progress Series*, 41:283, 1987.

[155] Robert J Orth and Jacques van Montfrans. Habitat quality and prey size as determinants of survival in post-larval and early juvenile instars of the blue crab *Callinectes sapidus*. *Marine Ecology Progress Series*, 231:205–213, 2002.

[156] Robert J Orth, Michael R Williams, Scott R Marion, David J Wilcox, Tim JB Carruthers, Kenneth A Moore, W Michael Kemp, William C Dennison, Nancy Rybicki, Peter Bergstrom, and Richard A Batiuk. Long-term trends in submersed aquatic vegetation (SAV) in Chesapeake Bay, USA, related to water quality. *Estuaries and Coasts*, 33(5):1144–1163, 2010.

[157] Renee A Pardieck, Robert J Orth, Robert J Diaz, and Romuald N Lipcius. Ontogenetic changes in habitat use by postlarvae and young juveniles of the blue crab. *Marine Ecology Progress Series*, 186:227–238, 1999.

[158] Christopher J Patrick, Donald E Weller, Robert J Orth, David J Wilcox, and Michael P Hannam. Land use and salinity drive changes in SAV abundance and community composition. *Estuaries and Coasts*, 41(1):85–100, 2018.

[159] Eileen Perkins-Visser, Thomas G Wolcott, and Donna L Wolcott. Nursery role of seagrass beds: enhanced growth of juvenile blue crabs (*Callinectes sapidus Rathbun*). *Journal of Experimental Marine Biology and Ecology*, 198(2):155–173, 1996.

[160] Rebecca Peters, Anthony R Marshak, Margaret M Brady, Stephen K Brown, Kenric Osgood, Correign Greene, Vincent Guida, Matthew Johnson, Todd Kellison, Robert McConnaughey, Tom Nojiand Michael Parke, Chris Rooper, Waldo Wakefield, and Mary Yoklavich. Habitat science is a fundamental element in an ecosystem-based fisheries management framework: an update to the Marine Fisheries Habitat Assessment Improvement Plan. 2018.

[161] Bradley J Peterson, Kip R Thompson, James H Cowan Jr, and Kenneth L Heck Jr. Comparison of predation pressure in temperate and subtropical seagrass habitats based on chronographic tethering. *Marine Ecology Progress Series*, 224:77–85, 2001.

[162] Charles H Peterson and Robert Black. An experimentalist's challenge: when artifacts of intervention interact with treatments. *Marine Ecology Progress Series*, pages 289–297, 1994.

[163] Charles H Peterson and Romuald N Lipcius. Conceptual progress towards predicting quantitative ecosystem benefits of ecological restorations. *Marine Ecology Progress Series*, 264:297–307, 2003.

[164] Adele J Pile, Romuald N Lipcius, Jacques van Montfrans, and Robert J Orth. Density-dependent settler-recruit-juvenile relationships in blue crabs. *Ecological Monographs*, 66(3):277–300, 1996.

[165] Martin H Posey, Troy D Alphin, Heather Harwell, and Bryan Allen. Importance of low salinity areas for juvenile blue crabs, *Callinectes sapidus Rathbun*, in river-dominated estuaries of southeastern United States. *Journal of Experimental Marine Biology and Ecology*, 319(1-2):81–100, 2005.

[166] André E Punt, Teresa A'mar, Nicholas A Bond, Douglas S Butterworth, Carryn L de Moor, José AA De Oliveira, Melissa A Haltuch, Anne B Hollowed, and Cody Szuwalski. Fisheries management under climate and environmental uncertainty: control rules and performance simulation. *ICES Journal of Marine Science*, 71(8):2208–2220, 2014.

[167] R Core Team. *R: A Language and Environment for Statistical Computing*. R Foundation for Statistical Computing, Vienna, Austria, 2022.

[168] Chet F Rakocinski, Harriet M Perry, Michael A Abney, and Kirsten M Larsen. Soft-sediment recruitment dynamics of early blue crab stages in Mississippi Sound. *Bulletin of Marine Science*, 72(2):393–408, 2003.

[169] Gina Ralph. *Quantification of Nursery Habitats for Blue Crabs in Chesapeake Bay*. PhD thesis, Virginia Institute of Marine Science, William & Mary, 2014.

[170] Gina M Ralph and Romuald N Lipcius. Critical habitats and stock assessment: age-specific bias in the chesapeake bay blue crab population survey. *Transactions of the American Fisheries Society*, 143(4):889–898, 2014.

[171] Gina M Ralph, Rochelle D Seitz, Robert J Orth, Kathleen E Knick, and Romuald N Lipcius. Broad-scale association between seagrass cover and juvenile blue crab density in Chesapeake Bay. *Marine Ecology Progress Series*, 488:51–63, 2013.

[172] Nathalie B Reyns and David B Eggleston. Environmentally-controlled, density-dependent secondary dispersal in a local estuarine crab population. *Oecologia*, 140(2):280–288, 2004.

[173] Nathalie B Reyns, David B Eggleston, and Richard Jr A Luettich. Secondary dispersal of early juvenile blue crabs within a wind-driven estuary. *Limnology and Oceanography*, 51(5):1982–1995, 2006.

[174] Sébastien Rochette, Olivier Le Pape, Joel Vigneau, and Etienne Rivot. A hierarchical bayesian model for embedding larval drift and habitat models in integrated life cycles for exploited fish. *Ecological Applications*, 23(7):1659–1676, 2013.

[175] Lawrence P Rozas and Thomas J Minello. Nekton use of salt marsh, seagrass, and nonvegetated habitats in a south Texas (USA) estuary. *Bulletin of marine science*, 63(3):481–501, 1998.

[176] Paul J Rudershausen, Jeffery H Merrell, and Jeffrey A Buckel. Factors Influencing Colonization and Survival of Juvenile Blue Crabs *Callinectes sapidus* in Southeastern US Tidal Creeks. *Diversity*, 13(10):491, 2021.

[177] Gregory M Ruiz, Anson H Hines, and Martin H Posey. Shallow water as a refuge habitat for fish and crustaceans in non-vegetated estuaries: an example from Chesapeake Bay. *Marine Ecology Progress Series*, pages 1–16, 1993.

[178] Roger A Rulifson and Michael J Dadswell. Life history and population characteristics of striped bass in Atlantic Canada. *Transactions of the American Fisheries Society*, 124(4):477–507, 1995.

[179] Alastair Rushworth, Duncan Lee, and Richard Mitchell. A spatio-temporal model for estimating the long-term effects of air pollution on respiratory hospital admissions in Greater London. *Spatial and spatio-temporal epidemiology*, 10:29–38, 2014.

[180] Clifford H Ryer, Jacques van Montfrans, and Kurt E Moody. Cannibalism, refugia and the molting blue crab. *Marine Ecology Progress Series*, 147:77–85, 1997.

[181] Lawrence P Sanford, Steven E Suttles, and Jeffrey P Halka. Reconsidering the physics of the Chesapeake Bay estuarine turbidity maximum. *Estuaries*, 24(5):655–669, 2001.

[182] Frederick S Scharf, Francis Juanes, and Rodney A Rountree. Predator size-prey size relationships of marine fish predators: interspecific variation and effects of ontogeny and body size on trophic-niche breadth. *Marine Ecology Progress Series*, 208:229–248, 2000.

[183] Nathalie W Schieder, David C Walters, and Matthew L Kirwan. Massive upland to wetland conversion compensated for historical marsh loss in Chesapeake Bay, USA. *Estuaries and Coasts*, 41:940–951, 2018.

[184] Joseph D Schmitt, Brandon K Peoples, Aaron J Bunch, Leandro Castello, and Donald J Orth. Modeling the predation dynamics of invasive blue catfish (*Ictalurus furcatus*) in Chesapeake Bay. 2019.

[185] Rochelle D Seitz, Romuald N Lipcius, NH Olmstead, Michael S Seebo, and Debra M Lambert. Influence of shallow-water habitats and shoreline development on abundance, biomass, and diversity of benthic prey and predators in Chesapeake Bay. *Marine Ecology Progress Series*, 326:11–27, 2006.

[186] Rochelle D Seitz, Romuald N Lipcius, and Michael S Seebo. Food availability and growth of the blue crab in seagrass and unvegetated nurseries of Chesapeake Bay. *Journal of Experimental Marine Biology and Ecology*, 319(1-2):57–68, 2005.

[187] Rochelle D Seitz, Romuald N Lipcius, William T Stockhausen, Kristen A Delano, Michael S Seebo, and Paul D Gerdes. Potential bottom-up control of blue crab distribution at various spatial scales. *Bulletin of Marine Science*, 72(2):471–490, 2003.

[188] Rochelle D Seitz, Håkan Wennhage, Ulf Bergström, Romuald N Lipcius, and Tom Ysebaert. Ecological value of coastal habitats for commercially and ecologically important species. *ICES Journal of Marine Science*, 71(3):648–665, 2014.

[189] Lennah M Shakeri, Kelly M Darnell, Tim JB Carruthers, and M Zachary Darnell. Blue crab abundance and survival in a fragmenting coastal marsh system. *Estuaries and Coasts*, 43(6):1545–1555, 2020.

[190] AF Sharov, JH Vølstad, GR Davis, BK Davis, RN Lipcius, and MM Montane. Abundance and exploitation rate of the blue crab (*Callinectes sapidus*) in Chesapeake Bay. *Bulletin of Marine Science*, 72(2):543–565, 2003.

[191] Marcus Sheaves, Ronald Baker, Ivan Nagelkerken, and Rod M Connolly. True value of estuarine and coastal nurseries for fish: incorporating complexity and dynamics. *Estuaries and Coasts*, 38(2):401–414, 2015.

[192] Marcus Sheaves, Ronnie Baker, and Ross Johnston. Marine nurseries and effective juvenile habitats: an alternative view. *Marine Ecology Progress Series*, 318:303–306, 2006.

[193] Brian R Silliman, Edwin D Grosholz, and Mark D Bertness. *Human impacts on salt marshes: a global perspective*. Univ of California Press, 2009.

[194] Tuomas Sivula, Måns Magnusson, Asael Alonzo Matamoros, and Aki Vehtari. Uncertainty in bayesian leave-one-out cross-validation based model comparison. *arXiv preprint arXiv:2008.10296*, 2020.

[195] Timothy M Smith, Jeremy S Hindell, Gregory P Jenkins, Rod M Connolly, and Michael J Keough. Edge effects in patchy seagrass landscapes: the role of predation in determining fish distribution. *Journal of Experimental Marine Biology and Ecology*, 399(1):8–16, 2011.

[196] Leonard A Smock, Anne B Wright, and Arthur C Benke. Atlantic coast rivers of the southeastern United States. *Rivers of North America*, 72:122, 2005.

[197] Patricia M Spitzer, Kenneth L Heck, and John F Valentine. Then and now: a comparison of patterns in blue crab post-larval abundance and post-settlement mortality during the early and late 1990s in the mobile bay system. *Bulletin of Marine Science*, 72(2):435–452, 2003.

[198] Stan Development Team. RStan: the R interface to Stan, 2020. R package version 2.21.2.

[199] Stan Development Team. The Stan Core Library, 2022. Version 2.32.

[200] Robert S Steneck and Daniel Pauly. Fishing through the anthropocene. *Current Biology*, 29(19):R987–R992, 2019.

[201] William T Stockhausen and Romuald N Lipcius. Simulated effects of seagrass loss and restoration on settlement and recruitment of blue crab postlarvae and juveniles in the York River, Chesapeake Bay. *Bulletin of marine science*, 72(2):409–422, 2003.

[202] Zhenming Su and Randall M Peterman. Performance of a bayesian state-space model of semelparous species for stock-recruitment data subject to measurement error. *Ecological Modelling*, 224(1):76–89, 2012.

[203] Göran Sundblad, Ulf Bergström, Alfred Sandström, and Peter Eklöv. Nursery habitat availability limits adult stock sizes of predatory coastal fish. *ICES Journal of Marine Science*, 71(3):672–680, 2014.

[204] Douglas P Swain, Ian D Jonsen, James E Simon, and Ransom A Myers. Assessing threats to species at risk using stage-structured state–space models: mortality trends in skate populations. *Ecological Applications*, 19(5):1347–1364, 2009.

[205] JL Thomas, RJ Zimmerman, and TJ Minello. Abundance patterns of juvenile blue crabs (*Callinectes sapidus*) in nursery habitats of two Texas bays. *Bulletin of Marine Science*, 46(1):115–125, 1990.

[206] TD Tuckey and MC Fabrizio. Estimating relative juvenile abundance of ecologically important finfish in the Virginia portion of Chesapeake Bay. project. *Annual report to the Virginia Marine Resources Commission. Virginia Institute of Marine Science, Gloucester Point, VA.*, 2020.

[207] TD Tuckey and MC Fabrizio. Estimating relative juvenile abundance of ecologically important finfish in the Virginia portion of Chesapeake Bay. *Annual report to the Virginia Marine Resources Commission. Virginia Institute of Marine Science, Gloucester Point, VA.*, 2022.

[208] RK Turner and GC Daily. The ecosystem services framework and natural capital conservation. *Environmental and resource economics*, 39(1):25–35, 2008.

[209] Stephanie J Turner, SF Thrush, JE Hewitt, VJ Cummings, and G Funnell. Fishing impacts and the degradation or loss of habitat structure. *Fisheries Management and Ecology*, 6(5):401–420, 1999.

[210] AJ Underwood, MG Chapman, and SD Connell. Observations in ecology: you can't make progress on processes without understanding the patterns. *Journal of Experimental Marine Biology and Ecology*, 250(1-2):97–115, 2000.

[211] Mark C Urban. The growth–predation risk trade-off under a growing gape-limited predation threat. *Ecology*, 88(10):2587–2597, 2007.

[212] Karen E. Van de Wolfshaar, I Tulp, H Wennhage, and JG Støttrup. Modelling population effects of juvenile offshore fish displacement towards adult habitat. *Marine Ecology Progress Series*, 540:193–201, 2015.

[213] Willard A Van Engel. The blue crab and its fishery in chesapeake bay. part 1. reproduction, early development, growth and migration. *Commercial fisheries review*, 20(6):6, 1958.

[214] Jacques Van Montfrans, Charles E Epifanio, David M Knott, Romuald N Lipcius, David J Mense, Karen S Metcalf, Eugene J Olmi III, Robert J Orth, Martin H Posey, Elizabeth L Wenner, and Terry L West. Settlement of blue crab postlarvae in Western North Atlantic Estuaries. *Bulletin of Marine Science*, 57(3):834–854, 1995.

[215] Jacques van Montfrans, Clifford H Ryer, and Robert J Orth. Substrate selection by blue crab *Callinectes sapidus* megalopae and first juvenile instars. *Marine Ecology Progress Series*, 260:209–217, 2003.

[216] Rita P Vasconcelos, David B Eggleston, Olivier Le Pape, and Ingrid Tulp. Patterns and processes of habitat-specific demographic variability in exploited marine species. *ICES Journal of Marine Science*, 71(3):638–647, 2014.

[217] Aki Vehtari, Andrew Gelman, and Jonah Gabry. Practical Bayesian model evaluation using leave-one-out cross-validation and WAIC. *Statistics and Computing*, 27(5):1413–1432, 2017.

[218] Jay M Ver Hoef, Erin E Peterson, Mevin B Hooten, Ephraim M Hanks, and Marie-Josèe Fortin. Spatial autoregressive models for statistical inference from ecological data. *Ecological Monographs*, 88(1):36–59, 2018.

[219] Erin P Voigt and David B Eggleston. Spatial variation in nursery habitat use by juvenile blue crabs in a shallow, wind-driven estuary. *Estuaries and Coasts*, pages 1–15, 2022.

[220] Lance A Waller, Bradley P Carlin, Hong Xia, and Alan E Gelfand. Hierarchical spatio-temporal mapping of disease rates. *Journal of the American Statistical association*, 92(438):607–617, 1997.

[221] Sumio Watanabe. A widely applicable Bayesian information criterion. *The Journal of Machine Learning Research*, 14(1):867–897, 2013.

[222] James M Welch, Dan Rittschof, Traci M Bullock, and Richard B Forward Jr. Effects of chemical cues on settlement behavior of blue crab *Callinectes sapidus* postlarvae. *Marine Ecology Progress Series*, 154:143–153, 1997.

[223] Earl E Werner and James F Gilliam. The ontogenetic niche and species interactions in size-structured populations. *Annual review of ecology and systematics*, 15:393–425, 1984.

[224] KA Wilson, KL Heck Jr, and KW Able. Juvenile blue crab, callinectes sapidus, survival: an evaluation of eelgrass, zostera marina, as refuge. *Fishery Bulletin*, 85(1):53–58, 1987.

[225] Kristen L Wilson and Heike K Lotze. Climate change projections reveal range shifts of eelgrass *Zostera marina* in the northwest atlantic. *Marine Ecology Progress Series*, 620:47–62, 2019.

[226] Melisa C Wong and Michael Dowd. A model framework to determine the production potential of fish derived from coastal habitats for use in habitat restoration. *Estuaries and Coasts*, 39(6):1785–1800, 2016.

[227] Megan Woods. *Juvenile Blue Crab (Callinectes sapidus) Response to Altered Nursery Habitat*. PhD thesis, Virginia Institute of Marine Science, William & Mary, 2017.

[228] Megan A Woods and Romuald N Lipcius. Non-native red alga *Gracilaria vermiculophylla* compensates for seagrass loss as blue crab nursery habitat in the emerging Chesapeake Bay ecosystem. *PloS One*, 17(5):e0267880, 2022.

[229] Boris Worm, Edward B Barbier, Nicola Beaumont, J Emmett Duffy, Carl Folke, Benjamin S Halpern, Jeremy BC Jackson, Heike K Lotze, Fiorenza Micheli, Stephen R Palumbi, et al. Impacts of biodiversity loss on ocean ecosystem services. *science*, 314(5800):787–790, 2006.

[230] Amanda Bridgette Wrona. *Determining movement patterns and habitat use of blue crabs (Callinectes sapidus Rathbun) in a Georgia saltmarsh estuary with the use of ultrasonic telemetry and a geographic information system (GIS)*. PhD thesis, uga, 2004.

[231] Hao Yu, Yan Jiao, Zhenming Su, and Kevin Reid. Performance comparison of traditional sampling designs and adaptive sampling designs for fishery-independent surveys: a simulation study. *Fisheries Research*, 113(1):173–181, 2012.

[232] Roger J Zimmerman, Thomas J Minello, and Lawrence P Rozas. Salt marsh linkages to productivity of penaeid shrimps and blue crabs in the northern gulf of mexico. pages 293–314, 2000.

[233] Philine SE zu Ermgassen, Bryan DeAngelis, Jonathan R Gair, Sophus zu Ermgassen, Ronald Baker, Andre Daniels, Timothy C MacDonald, Kara Meckley, Sean Powers, Marta Ribera, Lawrence P Rozas, and Jonathan H Grabowski. Estimating and applying fish and invertebrate density and production enhancement from seagrass, salt marsh edge, and oyster reef nursery habitats in the Gulf of Mexico. *Estuaries and Coasts*, pages 1–16, 2021.

[234] Philine SE Zu Ermgassen, Jonathan H Grabowski, Jonathan R Gair, and Sean P Powers. Quantifying fish and mobile invertebrate production from a threatened nursery habitat. *Journal of Applied Ecology*, 53(2):596–606, 2016.